

IDENTIFYING LOW-MASS MEMBERS OF NEARBY STAR CLUSTERS USING
PROPER MOTION & COLOR SELECTION

A DISSERTATION SUBMITTED TO THE GRADUATE DIVISION OF THE
UNIVERSITY OF HAWAI'I IN PARTIAL FULFILLMENT
OF THE REQUIREMENTS FOR THE DEGREE OF

DOCTOR OF PHILOSOPHY

IN

ASTRONOMY

AUGUST 2011

By

Mark A. Pitts

Dissertation Committee:

Eugene Magnier, Chairperson

Michael Liu

Roberto Méndez

John Rayner

Bo Reipurth

John Learned

We certify that we have read this dissertation and that, in our opinion, it is satisfactory in scope and quality as a dissertation for the degree of Doctor of Philosophy in Astronomy.

DISSERTATION COMMITTEE

Chairperson

©Copyright 2011

by

Mark A. Pitts

To my beloved father,

Dr. Ronald E. Pitts (1949-2008),

himself a noted astronomer and the first person to show me the beauty of the heavens.

Acknowledgments

I wish to thank the National Science Foundation for the funding of this research under grant AST 0709460. The United States Air Force also provided funding under the AFRL Cooperative Agreement FA9451-06-2-0338. I thank George Herbig for sharing his knowledge about the earliest proper motion studies of the Taurus region. This work was made possible by the data pipeline software developed primarily for the Pan-STARRS-1 telescope and associated survey programs. My appreciation goes to the graduate student and post-doc communities of the UH Institute for Astronomy for their camaraderie and support during my dissertation work. Much gratitude goes to my dissertation committee for their scrutiny and constructive feedback on this project, as well as their timely attendance of many update meetings over the years. Last but not least, I wish to extend my deep appreciation to the native peoples of the Hawaiian Islands. It is with their cooperation and support in generously sharing their sacred mountains that astronomers have access to some of the world's best ground-based observing facilities.

Abstract

I present a combined kinematic and photometric search for new, low-mass ($m \leq 0.2M_{\odot}$) members of nearby ($d < 300$ pc) star clusters. Using both proper motion and color criteria, a total of 33 low-mass objects have been newly recognized as members of the Taurus, Praesepe, and Pleiades clusters. In addition, 18 potential cluster members are noted, and 4 members are recovered from previous member searches. Multi-epoch imaging was performed using *i*-band Megacam observations unique to this study, combined with archival CFH telescope data in the optical *I* and *Z* bands. Near-infrared detections were also acquired from the 2MASS survey. The imaging data were processed using the Pan-STARRS IPP data pipeline software in order to provide high-precision relative astrometry, from which proper motions were extracted. Low-resolution, near-infrared spectroscopy from the IRTF telescope gives confirmation on the membership status of the selected candidates. The addition of proper motion criteria to complement the often-used color selection allows for a more effective identification of low-mass cluster members whose broadband spectral features are similar to the bulk of galactic field objects lying along the line-of-sight. Culling the candidates using proper motion also significantly reduces the amount of candidates that require spectroscopic follow-up, even in the NIR color-space with the highest levels of field contamination. Comparison of the search results to a galactic field model by Robin et al. (2003) provides strong evidence that brighter member candidates in Taurus ($i < 17$) found to be of mid-M spectral types are highly likely to be cluster members rather than field dwarfs. While the addition of new members to the Praesepe and Pleiades clusters are minor compared to the current known population, there is suggestive evidence that the mass function of Taurus is significantly lacking in mid-M dwarfs, and in fact may actually resemble the mass functions of other similarly-aged clusters. The successful application of this search technique using the IPP software is significant, as the Pan-STARRS survey program is conducting regular imaging of 75% of the total sky over the next 3-4 years.

Table of Contents

Acknowledgments	v
Abstract	vi
List of Tables	ix
List of Figures	x
1 Introduction	1
1.1 Low-Mass Objects	1
1.2 Observational Benefits & Challenges of Cluster Studies	2
1.3 Previous Cluster Member Searches	5
1.3.1 Taurus	5
1.3.2 Praesepe & The Pleiades	5
1.4 Aims of this Study	6
2 Multi-Epoch Imaging	8
2.1 Queued Megacam Observations	8
2.1.1 Taurus	8
2.1.2 Praesepe & The Pleiades	9
2.2 Archival Data	11
2.3 The Pan-STARRS IPP	11
3 Candidate Selection	13
3.1 Quality Criteria	13
3.2 Proper Motion Criteria	14
3.2.1 Taurus	14
3.2.2 Praesepe & The Pleiades	14
3.3 Color Criteria	16
3.3.1 Taurus	16
3.3.2 Praesepe & The Pleiades	20
4 Spectroscopic Follow-Up	23
4.1 SpeX Observations	23
4.2 SED Fitting	24
4.3 Spectral Indices	25
5 Field Contamination	48
5.1 Galactic Field Model	48
5.2 Properties of Contaminants	49
5.2.1 Taurus	49
5.2.2 Praesepe & The Pleiades	53
5.3 The Overabundance of “Mid-M” Candidates	57

6	Discussion	66
6.1	Properties of Identified Members	66
6.2	Properties of Identified Non-Members	71
6.3	Properties of Previously Claimed Members	74
7	Conclusions	94
A	Previously Claimed Low-Mass Cluster Members	96
B	SED Fitting Results of Member Candidates	162
C	Spectroscopic Follow-Up Observing Logs	175
	References	182

List of Tables

<u>Table</u>	<u>Page</u>
2.1 Megacam/CFH12K Observations	9
4.1 Newly Recognized Taurus Members	30
4.2 Contaminants & Undetermined Candidates (Taurus)	32
4.3 Newly Recognized Praesepe Members	37
4.4 Contaminants & Undetermined Candidates (Praesepe)	39
4.5 Newly Recognized Pleiades Members	42
4.6 Contaminants & Undetermined Candidates (Pleiades)	44
5.1 M-Type Candidates Selected	63
5.2 Early-Type Contaminants Selected	64
6.1 Previously Claimed Members of Taurus	77
6.2 Previously Claimed Members of Praesepe	81
6.3 Previously Claimed Members of the Pleiades	91
A.1 Previously Claimed Low-Mass Taurus Members	98
A.2 Previously Claimed Low-Mass Praesepe Members	115
A.3 Previously Claimed Low-Mass Pleiades Members	150
C.1 Taurus Follow-Up Observations	175
C.2 Praesepe Follow-Up Observations	179
C.3 Pleiades Follow-Up Observations	180

List of Figures

<u>Figure</u>	<u>Page</u>
2.1 Image Pointings (Taurus)	10
2.2 Astrometry Residuals (Taurus)	12
3.1 Proper Motions in the Direction of Taurus	15
3.2 Proper Motions in the Direction of Praesepe	17
3.3 Proper Motions in the Direction of the Pleiades	18
3.4 $(i - J)$ Color-Magnitude Diagram (Taurus)	19
3.5 $(i - J)$ Color-Magnitude Diagram (Praesepe)	21
3.6 $(i - J)$ Color-Magnitude Diagram (Pleiades)	22
4.1 SED Fitting Examples	26
4.2 Spectral Index Measurements (SED Library vs. Taurus Candidates)	28
4.3 Candidate Proper Motions (Taurus)	36
4.4 Spectral Index Measurements (Praesepe Candidates)	40
4.5 Candidate Proper Motions & Colors (Praesepe)	41
4.6 Spectral Index Measurements (Pleiades Candidates)	45
4.7 Candidate Proper Motions & Colors (Pleiades)	46
4.8 Spectral Index Measurements (Field Objects)	47
5.1 Field Model Distances (Taurus)	50
5.2 Field Model Distances (Praesepe)	51
5.3 Field Model Distances (Pleiades)	52
5.4 $(i - J)$ Colors (Model vs. Taurus Data)	54
5.5 Selected Model Population (Taurus)	55
5.6 Selected M-Type Field Objects (Taurus)	56
5.7 $(i - J)$ Colors (Model vs. Praesepe Data)	58
5.8 $(i - J)$ Colors (Model vs. Pleiades Data)	59
5.9 Selected Model Population (Praesepe)	60
5.10 Selected Model Population (Pleiades)	61
5.11 Spectral Type vs. i (Taurus)	65
6.1 $(i - J)/(J - K)$ Color-Color Diagram (Taurus)	68
6.2 $(i - J)/(J - K)$ Color-Color Diagram (Praesepe)	69
6.3 $(i - J)/(J - K)$ Color-Color Diagram (Pleiades)	70

6.4	Member Population vs. SpT (Taurus)	72
6.5	Taurus Low-Mass IMF	73
B.1	SED Best-Fit Results (Taurus Candidates 000-011)	163
B.2	SED Best-Fit Results (Taurus Candidates 012-023)	164
B.3	SED Best-Fit Results (Taurus Candidates 024-035)	165
B.4	SED Best-Fit Results (Taurus Candidates 036-119)	166
B.5	SED Best-Fit Results (Taurus Candidates 120-131)	167
B.6	SED Best-Fit Results (Taurus Candidates 132-192)	168
B.7	SED Best-Fit Results (Taurus Candidates 193-203)	169
B.8	SED Best-Fit Results (Praesepe Candidates 091-102)	170
B.9	SED Best-Fit Results (Praesepe Candidates 103-114)	171
B.10	SED Best-Fit Results (Pleiades Candidates 063-086)	172
B.11	SED Best-Fit Results (Pleiades Candidates 087-181)	173
B.12	SED Best-Fit Results (Pleiades Candidates 182-183)	174

Chapter 1

Introduction

1.1 Low-Mass Objects

The focus of this work is on low-mass objects, hereafter defined as stellar or stellar-like objects with mass $m \leq 0.2M_{\odot}$. This definition includes both very-low-mass (VLM) stars and brown dwarfs. The latter are differentiated from the former by being unable to reach the core temperature required for sustained hydrogen burning (~ 3 million K), and therefore will never reach the stellar main sequence. However, as the observable properties of both VLM stars and brown dwarfs appear to form a smooth continuum across the minimum hydrogen burning mass at $\sim 0.075M_{\odot}$ (Kirkpatrick, 2005), their distinction is not informative to this particular study, and is largely ignored hereafter. It should also be emphasized that mass is not a property directly observable via the methodology used in this study. Instead, the proxy of spectral type is utilized, which is measured by classifying the broad shape of an object’s spectral energy distribution (SED). The physical characteristics that determine spectral type include the emitting object’s atmospheric composition, surface gravity, and surface temperature. For the objects of interest in this work (i.e., low-mass cluster members), spectral types are typically in the range of M0-M9, which correspond to surface temperatures of $\sim 4000 - 3000$ K.

The significance of low-mass objects within the field of astrophysics stems from both their numerical majority within the Galaxy ($\sim 70\%$), as well as their ability to test theories of stellar formation. The mass function of the galactic field has been measured to peak around early-to-mid M-types, which corresponds to a mass of $0.1 - 0.2M_{\odot}$ at the typical age of the galactic population (\sim few Gyr, Chabrier, 2003). This majority is due partly to the lingering presence of low-mass objects within the field from multiple epochs of galactic star formation. The low-mass population includes the longest “living” stars, with VLM stars existing on the main sequence up

to three orders of magnitude longer than Sun-like stars. However, it also appears that galactic star formation is most efficient at such masses given both theoretical simulations of star formation (Bate, 2009) and empirical measurements of cluster mass functions (Thies & Kroupa, 2007). Thus, it becomes important to identify and characterize these objects in order to better understand the primary stellar component of the Galaxy.

In addition to dominating the number density, low-mass objects also represent the lowest extreme of star formation within the Galaxy. There have been several proposed mechanisms to create low-mass objects, including lower scale star-like formation (Bonnell, Clark, & Bate, 2008), massive circumstellar disc fragmentation (Stamatellos, Hubber, & Whitworth, 2007), and dynamical ejection during close encounters between young stellar systems (Reipurth & Clarke, 2001). Models of these formation theories can produce testable properties such as the shape of the initial mass function (IMF) of a star-forming region (e.g., see Figure 6 in Bate, 2009), the spatial distribution of objects within the star-forming region (Morau & Clarke, 2005), or unique dynamical signatures of the forming population (Boudreault & Bailer-Jones, 2009). Observations of such properties within the low-mass population of a star-forming region can then favor one or more mechanism as being dominant in the formation of low-mass objects. A statistically significant accounting of the complete low-mass population of a cluster is thus vital in determining which formation mechanism plays the largest role in producing the Galaxy's most common stellar and stellar-like constituents.

1.2 Observational Benefits & Challenges of Cluster Studies

There are several observational advantages when searching for low-mass objects within clusters. By their very nature, star clusters have a higher density of low-mass objects per square degree of sky than the galactic field. This results in fewer pointings in order to detect a similar amount of sources when compared to field surveys. In addition, the membership of a cluster is believed to be approximately coeval. In other words, all members are believed to have formed at about the same time and thus have a common age. This implies that more easily observable properties such as brightness and spectral type can serve as proxies for mass, with fainter and later-type cluster members corresponding to smaller-mass objects. This property conveniently avoids the mass-age degeneracy that is present when low-mass objects from multiple formation epochs are included in the same sample. Objects within clusters are also younger than the bulk of the surrounding field population. For those cluster members that are still pre-main sequence, their radii are larger than main-sequence dwarfs of similar mass. In this way cluster members will be intrinsically brighter

and easier to detect than field dwarfs at a given mass and distance. For “young” clusters ($t \leq 10$ Myr), a comparatively small amount of dynamical evolution has occurred, meaning that its members are still close to the location of their formation. Within such clusters, it is more appropriate to associate the spatial location of members with the environment that formed them. Minimal dynamical evolution also implies that the motions of the members through the Galaxy are still very close to that of the parent molecular cloud that formed them. This results in cluster members having similar motion to one another when compared to the field. This property in particular is a key part of the search technique utilized here and is discussed further below.

The observational challenges of correctly identifying low-mass cluster members involve both adequately detecting the objects at typical cluster distances and extinctions, as well as removing photometric and spectroscopic confusion with unassociated objects along the line-of-sight to the cluster. Within a given cluster population, the low-mass members are fainter (i.e., have smaller radii and cooler surface temperatures) than those of higher mass. Thus, while larger telescopes (10m-class) can conduct narrow and deep observations to find the lowest-mass objects at the distances of most galactic clusters ($d > 100$ pc), detecting such objects within wider and shallower surveys can push the limits of current instrumentation. In addition, members of young clusters will often have their light extinguished by intervening cluster gas and dust. As this extinction also results in the reddening of the emergent light, cluster surveys based primarily on optical data can be insensitive to the lowest-mass members. Only since the late 1990s have large-format infrared cameras become available to perform sizable imaging surveys for these objects. This is a crucial advancement, as the near-infrared (NIR) region of the spectrum is where such relatively cool VLM stars and brown dwarfs peak in their spectral energy distribution. Many diagnostic spectral features of these objects thus far recognized are also located in the NIR region, including absorption features sensitive to physical properties such as effective temperature and surface gravity. The opacity of the Earth’s atmosphere at such wavelengths restricts the most sensitive NIR observations to being conducted from extremely dry, high-altitude observatories (e.g., Mauna Kea, Hawaii).

In addition to the difficulty in detecting these objects, there is often confusion between bona fide low-mass members and unassociated objects lying along the line-of-sight. Such ambiguity is caused by the similarity of broadband NIR colors between: 1) low-mass cluster members, 2) interloping dwarfs in the local field, and 3) distant, reddened background giants. A common method used in previous cluster member searches has been to generate a list of candidates via broadband optical/NIR color selection. Low-mass cluster members, due to their cool temperatures, possess redder optical/NIR colors than the bulk of galactic objects. Cuts to the candidate lists are thus made

by eliminating from further consideration objects bluer than a chosen value, often one that varies with magnitude and is based upon a stellar evolutionary model. The membership of the remaining candidates is then confirmed or rejected using their observed optical or NIR spectra. The works of Briceño et al. (2002), Guieu et al. (2006), and Luhman (2006) provide informative examples of this methodology. The spectra of low-mass objects contain both temperature and gravity sensitive features, primarily due to molecules such as VO , metal hydrides, and water. Since low-mass members of young clusters are still contracting in size as they approach the main-sequence, their youthful nature can be inferred by an intermediate surface gravity¹. However, such follow-up spectroscopy for M-type objects within large cluster surveys can be very time-consuming and exacerbated by high contamination from nonmember objects if preceded only by photometric selection. This contamination is greater within the M0-M6 spectral type range than for later types, whose intrinsically redder colors distinguish them more unambiguously from the bulk of the galactic population. In addition, while obtaining lower-resolution spectra is more time-efficient, the NIR spectra of early-to-mid M field dwarfs are very similar in shape to those of young M-type cluster members at $R \sim 100 - 1000$. Given these observational challenges, and with the current high interest in sub-stellar cluster members, searches over the past decade have largely focused on objects with spectral types of around M6 or later, though the mass functions of clusters have been measured to peak in the early-to-mid-M range (Luhman et al., 2003; Thies & Kroupa, 2007).

A viable alternative to this “color-only” screening method is to complement the photometric selection with additional proper motion criteria. Examples of previous work using this approach in cluster member searches include Adams et al. (2002), Bihain et al. (2005), and Casewell et al. (2007). The motions of foreground objects are dominated by the galactic flow (i.e., the proper motion caused by the differential orbital motion of the Sun around the Galaxy as compared to other stars). Distant background objects should have little or no detectable proper motion at all over the time period of a typical proper motion study (\sim few–10 yr). Cluster members, on the other hand, will tend to congregate about a common proper motion vector (see Figure 3.2). In this work, I apply proper motion selection to a search of low-mass member candidates within the clusters of Taurus, Praesepe, and the Pleiades in order to identify new early-to-mid M-type members and determine how the member detection efficiency is improved for such objects over color-only selection methods.

¹An “intermediate” surface gravity measurement being between the typical values of giants ($\log(g) \sim 3$) and dwarfs ($\log(g) \sim 5$) in units of cm/s^2

1.3 Previous Cluster Member Searches

1.3.1 Taurus

Being nearby ($d = 141.5 \pm 2.8$ pc, Loinard et al., 2005), populous ($N_{mem} > 300$, Luhman et al., 2006), and young ($t \sim 1 - 3$ Myr, Kraus & Hillenbrand, 2009), the Taurus star-forming region has already been extensively searched for low-mass members. The first published search for Taurus members with proper motion measurements was carried out by Jones & Herbig (1979) using photographic plates. Their work was later expanded upon by Hartmann et al. (1991), whose list of newly-found Taurus members included mostly mid-M objects. In the decades that have followed, proper motion searches have benefited from the transition to digital detectors in both the optical and the NIR. While some studies have used space-based telescopes for candidate selection in the X-ray (Scelsi et al., 2008) and the mid-IR (Luhman et al., 2006; Rebull et al., 2010), the majority of Taurus member searches have relied on broadband optical/NIR color selection from ground-based data. Both the Two-Micron All-Sky Survey (2MASS) and the Sloan Digital Sky Survey (SDSS) have contributed significantly to these searches due to their large coverage on the sky, and much of the previous literature makes use of their photometric measurements. In these studies, evidence of Taurus member status may include: 1) the detection of $H\alpha$ in emission as an indicator of on-going accretion (Muzerolle et al., 2005), 2) the detection of Li absorption as an indicator of youth (Sestito, Palla, & Randich, 2008), 3) spectral indices that measure gravity-sensitive absorption features in the optical and NIR (Briceño et al., 2002; Luhman, 2006), and/or 4) SED fits to empirical data of previously-confirmed member spectra (Guieu et al., 2006). All of these status indicators are designed to show that the candidates are youthful, and thus it is implied that they are most likely to be a part of the newly-formed cluster population rather than that of the (much older) field. The mean member selection efficiency² of previous Taurus studies for M-type objects is on the order of 30%, typically increasing with studies that focus on later spectral types, but decreasing as the candidate sample size becomes larger.

1.3.2 Praesepe & The Pleiades

Unlike Taurus, the Praesepe and Pleiades clusters have been found to have a substantially different proper motion from that of the surrounding field. Because of this, sizable proper motion searches for low-mass members have been previously carried out (for examples, see Kraus &

²We define “efficiency” here to simply mean the number of confirmed low-mass cluster members compared to the total number of candidates that were followed-up with spectroscopy.

Hillenbrand, 2007; Lodiéu et al., 2007). Most searches have combined these proper motion measurements with optical colors to select member candidates. While some studies have performed follow-up spectroscopy work (e.g., Adams et al., 2002), many objects remain only proper-motion selected candidates. Praesepe is a relatively old cluster ($t \sim 600$ Myr) with a large membership ($N_{mem} \sim 1000$) and a similar distance as Taurus ($d \sim 170$ pc, Kraus & Hillenbrand, 2007). Jones & Stauffer (1991) and Hambly et al. (1995) were the first to identify M-type cluster members near the cluster center, while subsequent studies have probed out to larger radii. Such a spatial extent for member searches is needed because of the cluster’s advanced age, which will have allowed some of the low-mass population (only loosely bound gravitationally) to travel far from the cluster interior. The Pleiades is an intermediate-age cluster ($t \sim 120$ Myr) at a distance of ~ 130 pc (Bihain et al., 2006). It also has on the order of 1000 members, and objects as late as early-to-mid L type have been identified as member candidates. These two clusters were chosen along with Taurus in order to provide a significant spread in both age and cluster environment in order to better determine how such factors affect the search methodology used in this work.

1.4 Aims of this Study

The software written for the Pan-STARRS Image Processing Pipeline (IPP, Magnier, Kaiser, & Chambers, 2006) has been designed in part to quickly produce large amounts of photometric and astrometric measurements. As the Pan-STARRS survey program³ (Kaiser et al., 2010; Kaiser, Tonry, & Luppino, 2000) includes the “3-Pi Survey”, which will image 75% of the total sky at regular intervals from 2010 to (at least) 2013, this study seeks to verify that the IPP software can in fact be practically utilized to conduct a photometric and kinematic low-mass cluster member search. Such a search can be extended to lower masses and larger cluster distances as both the time and photometric depth of the survey increases. With this eventuality in mind, the primary aims for this study are as follows:

1. To utilize the Pan-STARRS IPP software in conducting a member search of nearby star clusters using a combination of proper motion and color criteria
2. To establish the strengths and limitations of this search technique when specifically applied to low-mass members at the distances of the nearest star-forming regions

³<http://pan-starrs.ifa.hawaii.edu/public/>

3. To determine the primary sources of contamination that produce false positives, and how the contamination is influenced by the cluster's motion and environment
4. To examine the properties of previously claimed cluster members that do not pass the selection criteria
5. To determine if and how the newly identified cluster members impact the currently established mass functions of the clusters

Chapter 2 describes the imaging data obtained over multiple epochs in order to generate the proper motion measurements and gives a brief overview of the analysis performed on the image data by the IPP. The chosen membership criteria based on both proper motion and color are described in Chapter 3. In Chapter 4, the success of the search method is verified via NIR spectroscopic follow-up on a subset of the member candidates. The effects of contamination from the galactic field are discussed in Chapter 5. Results from all three clusters are discussed in Chapter 6. Lastly, the conclusions of this study are summarized in Chapter 7.

Chapter 2

Multi-Epoch Imaging

In order to apply both proper motion and color selection to the clusters of interest, photometric observations are required. Given the limited time of the study and the distance of the clusters, it was necessary to include previous imaging data that was publically available and covers both a similar field-of-view and similar photometric bands. To acquire useful proper motion measurements, new image fields obtained for the study were placed to overlap the older archival fields. Using previous image data provides a long enough time baseline so that proper motion candidates can be extracted from all three clusters.

2.1 Queued Megacam Observations

2.1.1 Taurus

A portion of the Taurus star-forming region was observed in 2006 using 2 hours of Queued Service Observing (QSO) time for the Megacam wide-field camera mounted on the Canada-France-Hawaii Telescope (CFHT), located on Mauna Kea, Hawaii. The observations are summarized in Table 2.1. The field-of-view of Megacam ($\sim 1.0 \text{ deg}^2$) allowed coverage of about 10% of the projected cluster area within a manageable number of pointings given the large size of Taurus on the sky ($\sim 220 \text{ deg}^2$, Luhman, 2006). Since the focus of this work is on the bulk kinematics of the low-mass cluster members, area was chosen over depth in the observation strategy, covering $\sim 20 \text{ deg}^2$ in the i -band. Both 10- and 90-second exposures were taken in order to cover many magnitudes in i at which low-mass objects would be detected at the distance of Taurus. The resulting range of sensitivity is $i_{AB} \sim 14.5 - 20.5$. Saturation at the 10-sec exposures determines the bright limit, while the faint limit is set by 25σ detections at the 90-sec exposures. Such detections correspond to the minimal signal-to-noise required by the IPP for accurate relative astrometry measurements.

Given the depth of this survey, the main sequence is detectable at the distance of Taurus down to spectral types as late as $\sim M9$ (assuming zero extinction). At the young age of Taurus, its low-mass members will still be contracting towards the main sequence, and will thus be intrinsically brighter, potentially allowing the detection of early-L members. At 1 – 3 Myr, evolutionary models such as those from Chabrier et al. (2000) predict the stellar/substellar boundary to be $\sim M6$ (Guieu et al., 2006), so both VLM stars and high-mass BDs can be detected. As the images were taken in the optical, areas of highest extinction were avoided where source counts would be significantly reduced (see Figure 2.1). The i -band was chosen as the best compromise between instrument sensitivity and the red colors of the target objects.

Table 2.1: Megacam/CFH12K Observations

Epoch	Inst	# Images	Filters	$t_{exp}(s)$	References
Taurus					
pre-2003	CFH12K	215	I, Z	6 – 360	CADC ¹ , Martín et al. (2001)
2003 – 2005	CFH12K/MC	381	i, z, I, Z	5 – 360	CADC, Guieu et al. (2006)
2006	MC	110	i	10 – 90	This Work
Praesepe					
pre-2003	CFH12K/MC	61	z, I, Z	2 – 720	CADC
2006 – 2007	MC	59	i	5 – 300	This Work
Pleiades					
pre-2003	CFH12K	168	I, Z	10 – 360	CADC
2006 – 2007	MC	36	i	5 – 300	This Work

2.1.2 Praesepe & The Pleiades

A similar observing strategy was used for both Praesepe and the Pleiades. The amount of extinction along the line of sight towards both clusters was found to be negligible when checking

¹<http://www3.cadc-ccda.hia-ihp.nrc-cnrc.gc.ca/cadc/>

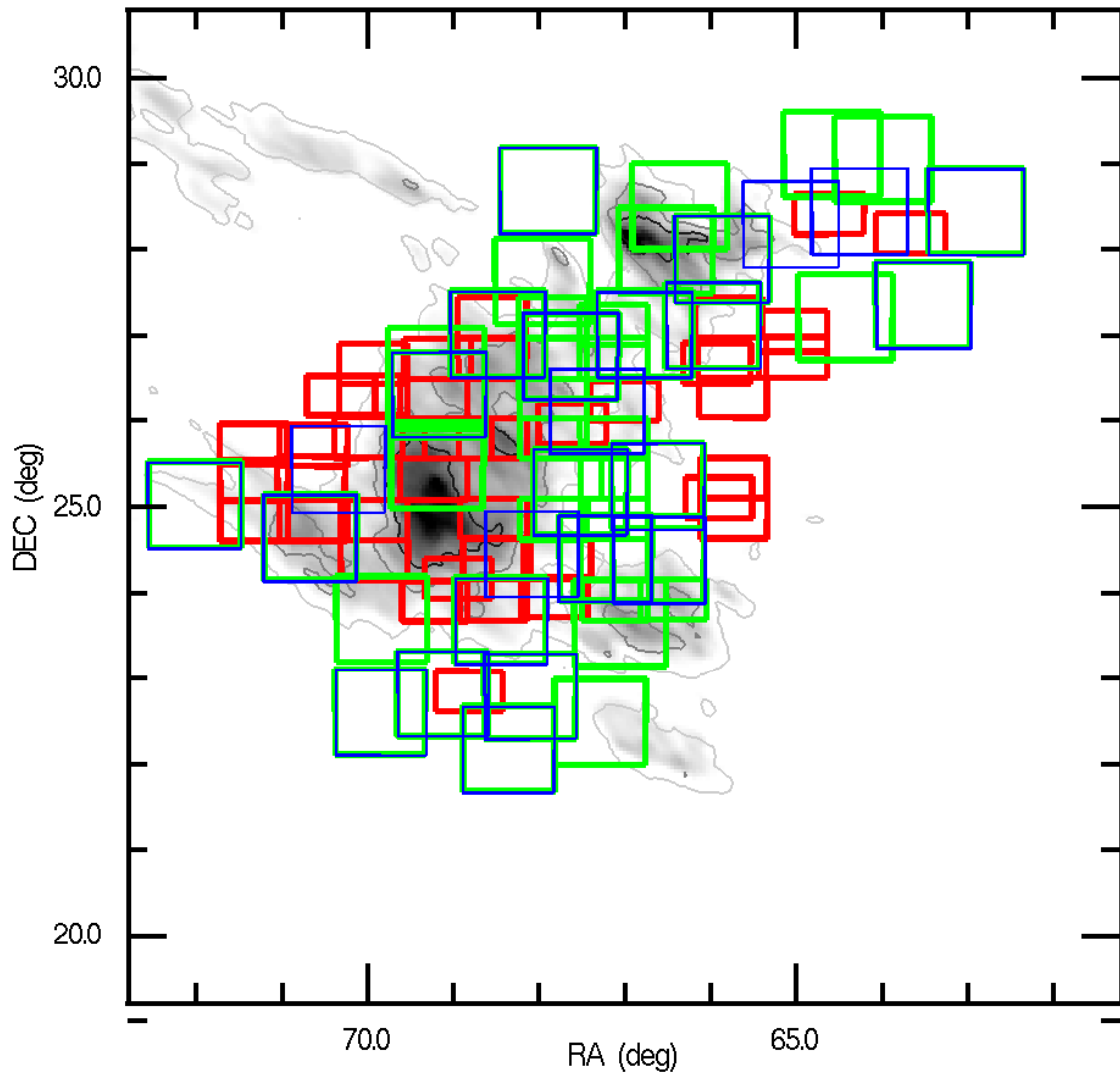


Figure 2.1 The locations of the 2006 Megacam pointings for the Taurus cluster on the plane of the sky (blue), along with the extracted archival data from the 2003 – 2005 (green) and pre-2003 (red) epochs. All the 2006 fields overlap at least one pointing from the 2003 – 2005 epoch. The A_V image and contours are taken from Schlegel, Finkbeiner, & Davis (1998), and mark 1.0, 1.5, and 2.0 magnitudes of extinction.

their positions in the A_V maps from Schlegel, Finkbeiner, & Davis (1998). Eight square degrees were covered in Praesepe and cover most of the cluster’s spatial extent. Five square degrees were observed of the Pleiades, with pointings designed to avoid the brightest cluster members that could cause large saturation effects on the detector. The range in exposure time for both clusters was 5 to 300 seconds. The longer exposure times compared to Taurus were used to make sure objects of a similar mass range were detected in these clusters, whose members are older by an order of magnitude.

2.2 Archival Data

The 2006/2007 Megacam observations were chosen to overlap previous pointings in the i -band from Megacam, as well as the I - and Z -bands from CFH12K (see Figure 2.1 for image overlaps in Taurus). These archival observations span the time period of 2001-2005, and were retrieved from the Canadian Astronomy Data Center (CADC) archive⁴. In order to provide NIR photometry to complement our optical data, we obtained 2MASS J , H , and K_s detections lying within our Megacam pointings. These NIR detections were associated with those from Megacam using a matching radius of 1 arcsec. For the purposes of this study, all archived and 2MASS photometry was converted to AB magnitudes (i.e., a zero-point shift), as this is the photometric system used by Megacam. Since the 2MASS data were taken circa 1999, it provides us with an approximate 7-year total baseline for our proper motion measurements. This long baseline serves to offset the larger positional inaccuracies of 2MASS (~ 70 mas) compared to the Megacam/CFH12K data (~ 18 mas, see below). Taurus possesses three epochs of optical imaging (pre-2003, 2003-2005, and 2006), while Praesepe and the Pleiades have two epochs (pre-2003 and 2006/2007).

2.3 The Pan-STARRS IPP

While the Megacam and CFH12K images were detrended (i.e., corrected using bias, dark, and flat frames) using the CFHT’s standard Elixir routines (Magnier & Cuillandre, 2004), the photometry and astrometry presented here were produced using the Pan-STARRS IPP. In brief, the *PSPhot* program determines an analytical model of the point-spread function (PSF) for each image using the brighter (but unsaturated) stars within the field-of-view. Detections are flagged as point sources or extended sources based on a comparison of each object’s shape with that of the

⁴<http://www3.cadc-ccda.hia-ihp.nrc-cnrc.gc.ca/cadc/>

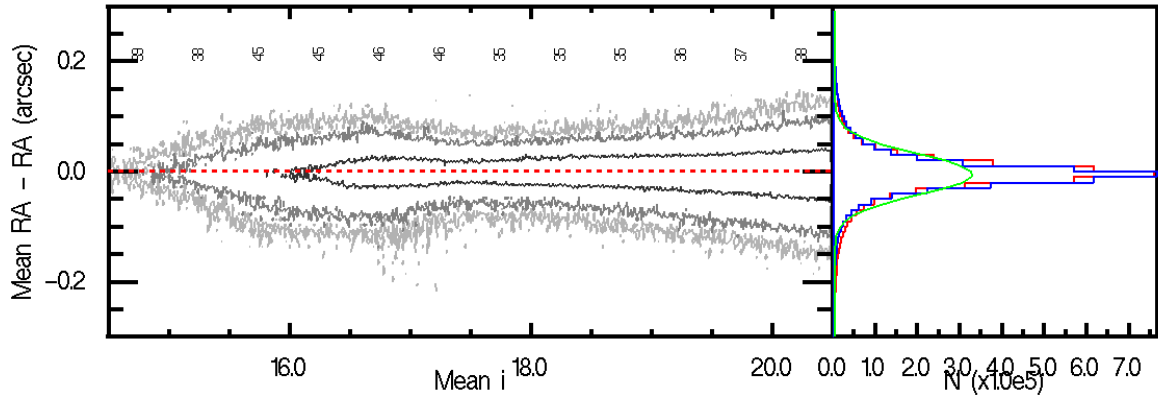


Figure 2.2 *Left*: The RA position residuals from the Pan-STARRS IPP as a function of i magnitude. Contour levels are at 50, 100, and 500 measurements per bin ($0.01 \text{ mag} \times 0.01 \text{ arcsec}$). The numbers listed across the top of the figure display how the RMS (in units of mas) changes as a function of i . The DEC position residuals have a similar spread and are not displayed for reasons of clarity. *Right*: A histogram of the RA (red) and DEC (blue) position residuals across all i magnitudes. They are fit to a Gaussian distribution (green) with $\sigma = 37 \text{ mas}$.

PSF model. Astrometry for each image was performed by the *PSAstro* program by comparing the centroid positions of the objects in each epoch calculated from the PSF models. The resulting measurements from the IPP were then ingested into an installation of the in-house Desktop Virtual Observatory (DVO) software package. The DVO program *addstar* then associates multiple detections to a common source using the aforementioned 1-arcsec matching radius. Relative astrometry was performed using the DVO program *relastro*. The positions are fit to a linear function of time and the proper motions of objects are calculated as $\mu_\alpha \cos(\delta)$ and μ_δ . Given that the bulk proper motion for Taurus is $\sim 20 \text{ mas/yr}$, a 7-yr baseline results in a shift in the member positions on the sky of 140 mas across the three epochs. This motion is quite detectable given our astrometric residuals from the CFH12K and Megacam data (see Figure 2.2). The bulk proper motions of Praesepe and the Pleiades are even larger. Across the i magnitude range of interest, the measured relative positions in Taurus are typically accurate to within $\pm 18 \text{ mas}$, with the most accurate astrometry occurring for objects with $i \sim 17.5$. The lack of a 2003-2005 epoch for Praesepe and the Pleiades results in a slight increase in the position residuals, averaging ± 23 and $\pm 18 \text{ mas}$, respectively.

Chapter 3

Candidate Selection

With the imaging survey completed, the detected objects can be culled using both photometric and kinematic criteria. In the first level of selection, only well-detected objects are considered in order to minimize false positives caused by spurious events and large measurement errors. From this dataset (hereafter, the “quality” data), objects are excluded from further consideration if their motion in the plane of the sky is not consistent with that of the previously established low-mass population of the cluster. Lastly, objects are retained only if their $(i - J)$ color falls above the cluster’s modeled main sequence (i.e., redder than the main sequence at a given i magnitude), and thus are likely to be youthful cluster members still contracting from their initial formation within the molecular cloud. All three selections presented serve to significantly reduce the number of member candidates that must be followed up with more time-intensive spectroscopy. In this way, the vast majority of false positives are removed from further consideration as cluster members.

3.1 Quality Criteria

The DVO software can be used to extract or reject objects that satisfy user-defined criteria. In the first round of selection, objects were excluded that had less than a minimum number of detections (< 5) in order to remove cosmic rays and other spurious events. To avoid saturation effects and still extract objects with well-measured astrometry, objects were also required to have a mean measured magnitude of $i = 14.5 - 20.5$. Remaining candidates possessed non-zero proper motions (> 0.001 mas/yr), as well as photometric and astrometric errors smaller than 0.3 mag and 10 mas, respectively. These error limits were chosen to eliminate objects that might be scattered into or out of our proper motion and color criteria via random measurement error. From the Taurus data, $\sim 80,000$ member candidates were selected as well-detected from an initial population of 9

million measured objects. Similar selections applied to Praesepe and the Pleiades produced initial candidate pools of ~ 7000 and ~ 9000 objects, respectively.

3.2 Proper Motion Criteria

3.2.1 Taurus

In order to examine the kinematic properties of previously claimed cluster members, a database was compiled from the literature containing over 2,300 objects (see Appendix A), ~ 400 of which show evidence of being associated with Taurus. A total of 32 of these members fall within the Taurus imaging fields, are well-detected within the dataset, and have a measurable proper motion using the IPP. These member positions were matched with those of the IPP’s astrometric measurements (given an association radius of 1 arcsec). The median measured proper motion for these previously claimed members is $\mu_\alpha \cos(\delta) = 7.68$ mas/yr and $\mu_\delta = -15.56$ mas/yr. Half of these claimed members are tightly congregated as one would expect for a cluster population. The mean motion of these members is $\mu_\alpha \cos(\delta) = 11.50 \pm 1.15$ mas/yr and $\mu_\delta = -16.55 \pm 1.02$ mas/yr. For comparison, a detailed kinematic study of 127 pre-main sequence members of Taurus by Bertout & Genova (2006) yielded mean values of $\mu_\alpha \cos(\delta) = 8.20 \pm 1.28$ mas/yr and $\mu_\delta = -20.82 \pm 1.23$ mas/yr. With the astrometric accuracy of the measurements as stated above, all objects were kept as candidates if their proper motion was within 10 mas/yr of the calculated mean value (see Figure 3.1). This encloses the proper motion variations due to the intrinsic velocity dispersion of the cluster members. At the distance of Taurus, a typical cluster velocity dispersion of ~ 5 km/s (Bertout & Genova, 2006) equates to 7 mas/yr. The proper motion restriction left $\sim 4,000$ candidates whose motion in the plane of the sky matches that of the currently known low-mass population of Taurus.

3.2.2 Praesepe & The Pleiades

Out of 452 previously claimed low-mass members of Praesepe, 118 passed the quality cut. The median proper motion of this subset is $\mu_\alpha \cos(\delta) = -30.85$ mas/yr and $\mu_\delta = -8.39$ mas/yr. However, as can be seen in Figure 3.2, these proper motions consist both of a tightly congregated population as well as a widely-scattered halo. When only the compact population is considered, the mean proper motion of the Praesepe members is $\mu_\alpha \cos(\delta) = -32.67 \pm 0.51$ mas/yr and $\mu_\delta = -9.32 \pm 0.53$ mas/yr. The work by van Leeuwen (2009) using Hipparcos data on 24 established Praesepe members yielded a proper motion measurement for the cluster of $\mu_\alpha \cos(\delta) = -35.81$

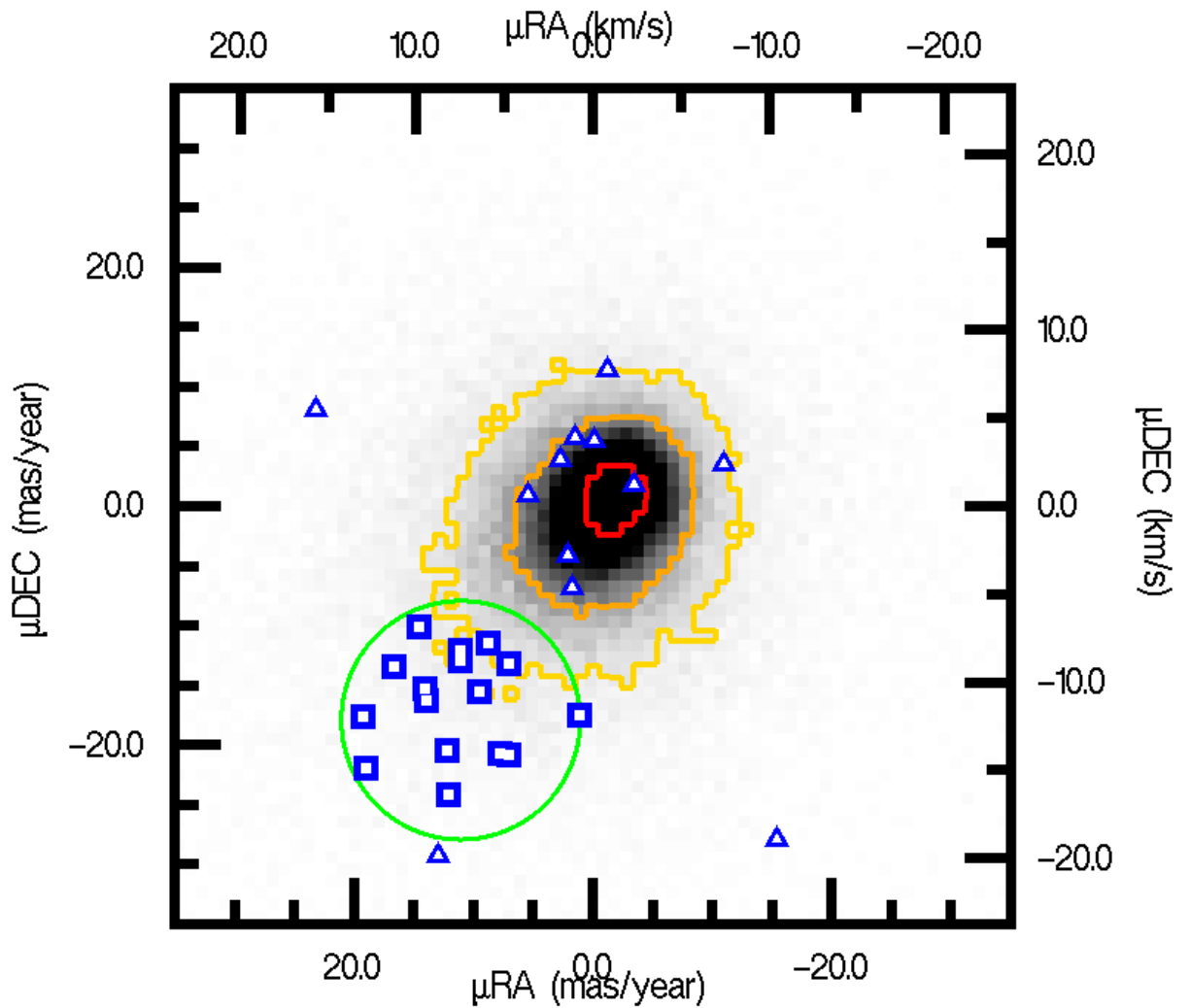


Figure 3.1 A vector-point diagram of the Taurus proper motion measurements, displaying a binned image of all the objects that passed the “quality” data cut. Contour levels are at 25 (yellow), 100 (orange), and 500 (red) objects per bin (1.0×1.0 mas/yr). The blue boxes (triangles) mark the proper motions of previously claimed members of Taurus that passed (did not pass) our kinematic cut. The top and right axes show the velocity of the objects within the plane of the sky when assumed to be at the distance of the cluster. The green circle marks the selection region.

mas/yr and $\mu_\delta = -12.85$ mas/yr. Like Taurus, all member candidates were kept if their motion was within 10 mas/yr of the calculated mean value. For 111 previously claimed low-mass members of the Pleiades that fall within the Megacam fields of this work, 26 passed our quality cut. Nearly all of these members cluster about a mean proper motion of $\mu_\alpha \cos(\delta) = 19.82 \pm 1.31$ mas/yr and $\mu_\delta = -43.30 \pm 0.95$ mas/yr. The proper motion search by Lodieu et al. (2007) cites a cluster proper motion value of $\mu_\alpha \cos(\delta) = 19.15$ mas/yr and $\mu_\delta = -45.72$ mas/yr. Because the spread in proper motions of the Pleiades members is slightly larger than those of the other two clusters, a wider selection radius of 17 mas/yr was used. The proper motion restriction selected out 154 member candidates for Praesepe and 114 candidates for the Pleiades. It can be clearly seen in the vector-point diagrams for these clusters (Figures 3.2 and 3.3) that Praesepe and the Pleiades are much more separated from the bulk of the galactic field than the Taurus cluster.

3.3 Color Criteria

3.3.1 Taurus

The evolutionary models of Baraffe et al. (1998) and Chabrier et al. (2000) (hereafter, BC models) provide cluster isochrones that can be compared with color measurements. An $(i - J)$ vs. i color-magnitude diagram of the Taurus data is shown in Figure 3.4. Objects were permitted to remain member candidates if they lie above a 5-Myr isochrone, despite the fact that Taurus objects would likely be closer to a redder, 1-3 Myr isochrone. As evolutionary models are uncertain within the low-mass regime, it was decided that it was preferable to risk allowing nonmembers into the sample rather than exclude true members whose colors are slightly bluer than the models predict. This cut provided the final list of 250 low-mass member candidates (a mean density of ~ 10 candidates per square degree of the 2006-epoch Taurus imaging).

Sixteen previously-claimed members of Taurus are recovered as member candidates, out of a possible 32 that landed in our field-of-view and passed the quality data cut. The majority of those members that were not selected have a proper motion lying outside the 10 mas/yr selection radius. This suggests that a significant number of claimed Taurus members have a disparate motion compared to the rest of the cluster. It remains to be determined whether this disparity is caused by inaccurate astrometry, nearby nebulosity, binary motion, the claimed members being part of a sub-population within the Taurus cloud, or the objects belonging to a separate young population along the line-of-sight. The disparate members are discussed in more detail in Chapter 6. All but two of

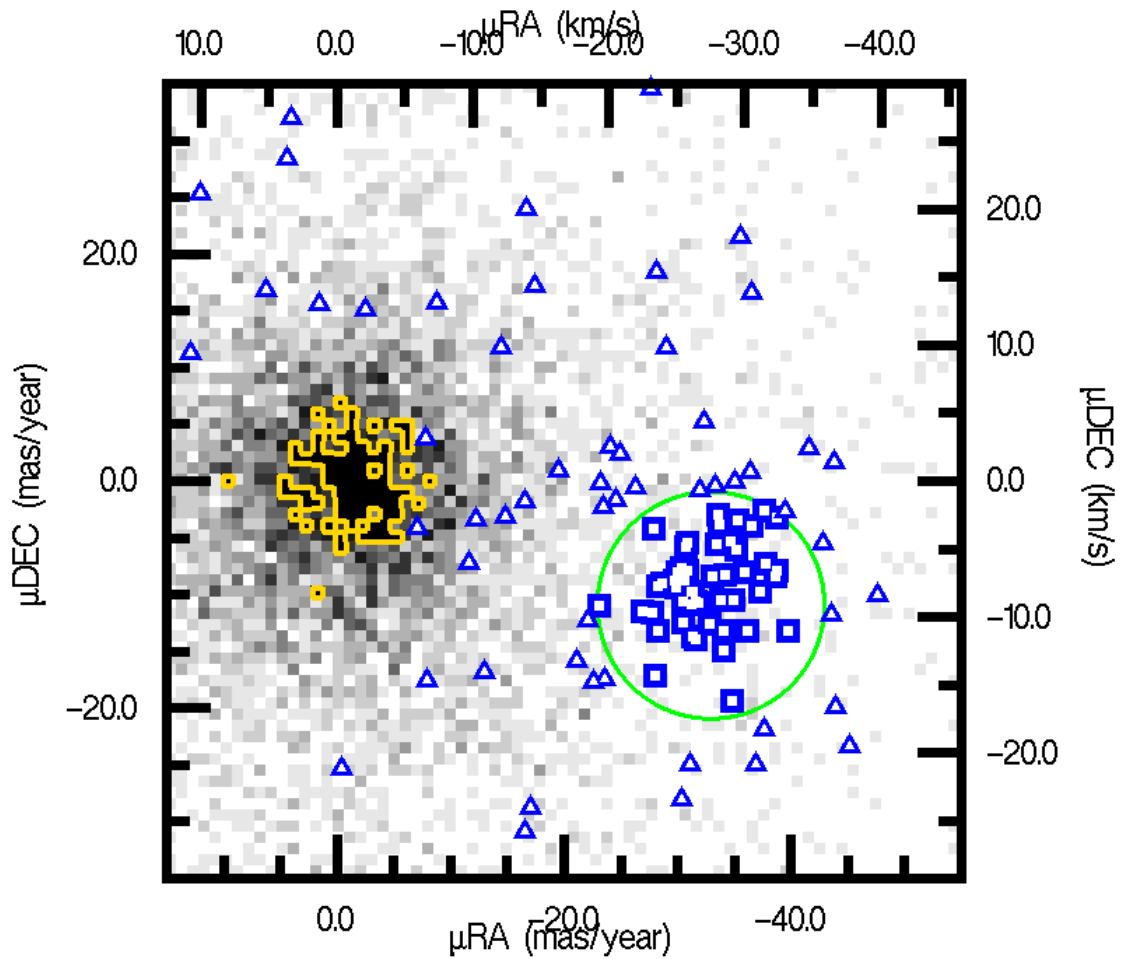


Figure 3.2 A similar diagram as Figure 3.1 displaying the Praesepe proper motion measurements. The contour (yellow) encloses the region with > 10 objects per bin. Note the population of previously-claimed cluster members clustered in the lower-right of the figure ($\sim 60\%$ of the total sample) as compared to the widely scattered halo. The green circle marks the selection region.

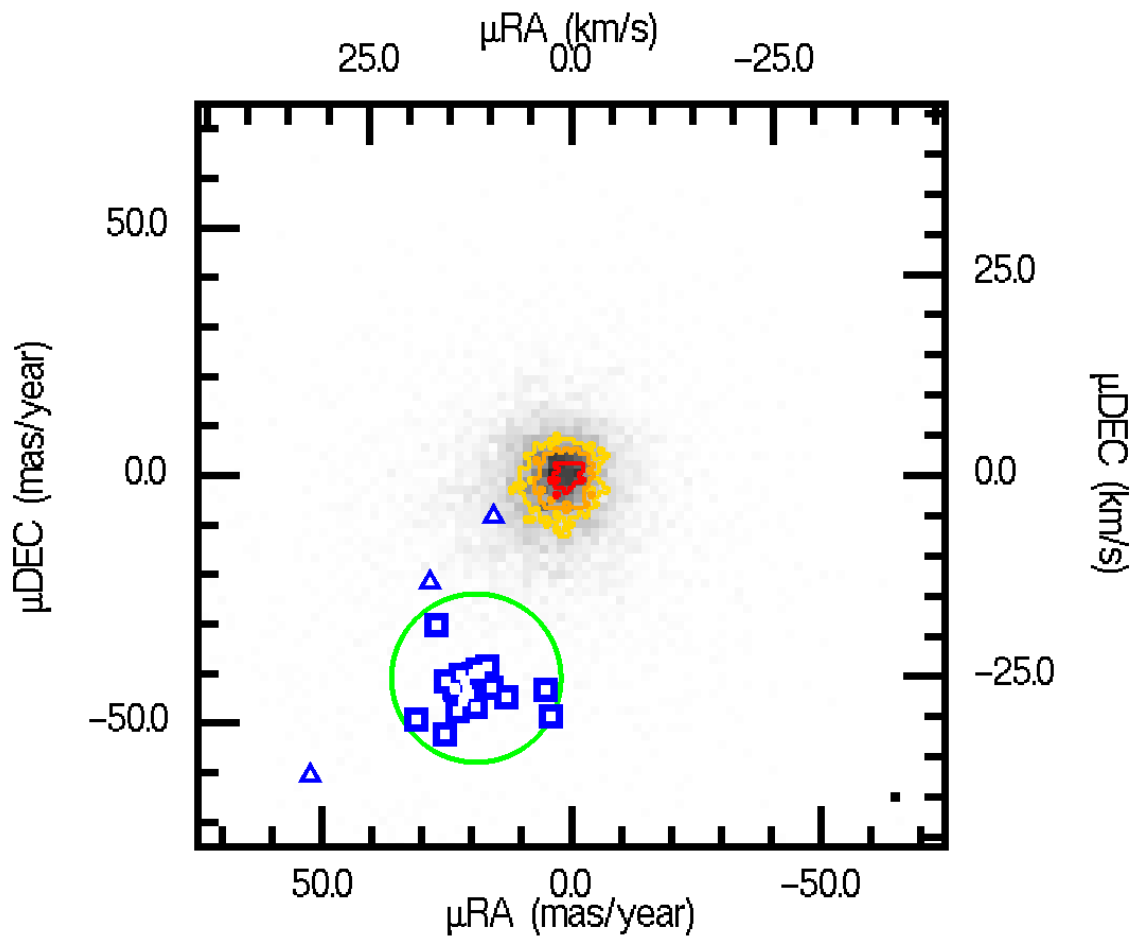


Figure 3.3 A similar diagram as Figure 3.1 displaying the Pleiades proper motion measurements. Contour levels are at 10 (yellow), 20 (orange), and 50 (red) objects per bin. Almost all previous members with IPP-measured proper motions lie within the selection region (green).

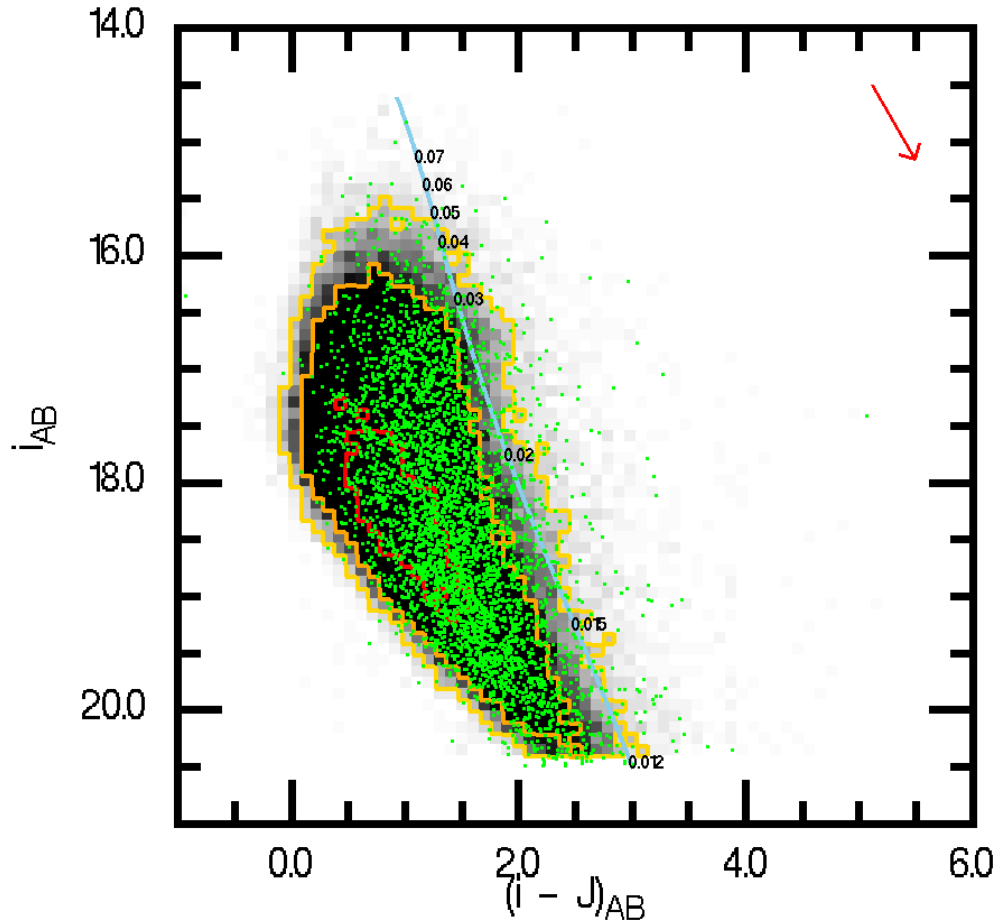


Figure 3.4 An $(i - J)$ vs. i color-magnitude diagram (CMD) of the Taurus data. The contours show 10 (yellow), 50 (orange), and 250 (red) objects per bin (0.1×0.1 mag) of the quality data. Green dots are objects that passed the proper motion criteria. The light-blue line shows the 5-Myr Taurus isochrone based on the BC models, along with the locations of masses at that age and distance of the cluster in units of M_{\odot} . The red arrow shows the $A_V = 1$ reddening vector based on the extinction law by Fitzpatrick (1985).

these claimed members pass the color cut, which is consistent with these objects being identified largely through broadband color selection.

It should be noted that during the first round of spectroscopic follow-up in 2007 (discussed in Chapter 4), a more simplistic astrometric measurement method was used in calculating the proper motions. This method involved treating one epoch (i.e., the 2006 images) as a fixed reference of object positions. The updated method as of 2008 allows all of the epochs to float and converge to a solution over a series of iterations. This change of method yielded smaller astrometric residuals by a factor of ~ 2 . We also used a crude approximation for the isochrones of the BC models when performing the color cut in 2007. This has since been replaced by a better fitting, higher-order function. The correction now excludes several Taurus member candidates that were later found via spectroscopy to be early-type field objects.

3.3.2 Praesepe & The Pleiades

A 500-Myr isochrone was used for color selection within the much older Praesepe cluster (600 Myr). Roughly 60% of the previously-claimed low-mass membership with IPP-measured proper motions are recovered in this study as member candidates. Given that the majority of Praesepe members have been identified by their proper motion, this significant fraction of widely scattered objects begs further study (see Chapter 6). Virtually all claimed cluster members pass the $(i - J)$ color selection. Given the 120 Myr age of the Pleiades, a 100-Myr isochrone was used to select color candidates. All but two of the 26 well-measured objects matched to Pleiades members are also recovered as member candidates for this study and pass color selection.

An effect of cluster environment (i.e., cluster distance from the galactic plane) can be seen in the asymmetry across the model isochrone of objects that pass the proper motion criteria. In Taurus, which lies closer to the bulk of the galactic field in proper motion space, a much greater fraction of the proper motion candidates lies blueward of the isochrone (see green dots in Figure 3.1). The exact opposite is true for Praesepe and the Pleiades, both of whom are very distinctive from the field in their bulk motion. This demonstrates in a very clear, visual way why clusters kinematically separated from the field can benefit from proper motion selection more than color selection when attempting to remove nonmember contamination. Yet, as explained below, the properties of both the cluster and the field can combine to weed out contaminants even in cases like Taurus where kinematic contamination is high.

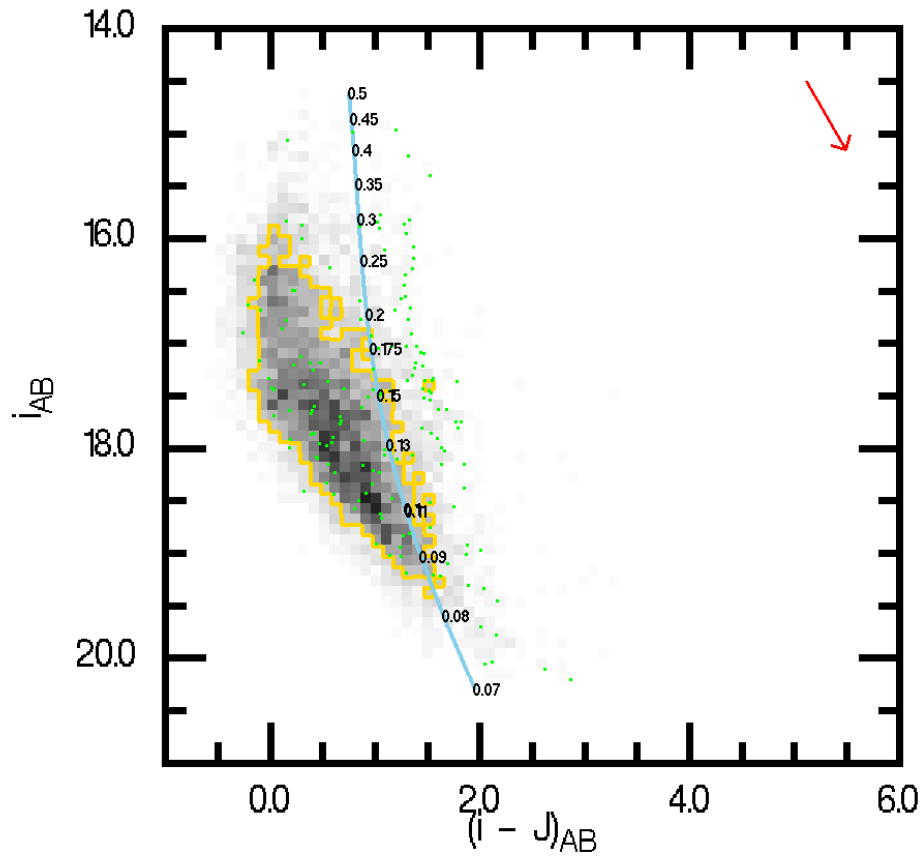


Figure 3.5 Similar CMD as in Figure 3.4 for the Praesepe data. The yellow contour encloses the region with > 10 objects per bin. A 500-Myr isochrone is overlaid (light-blue line).

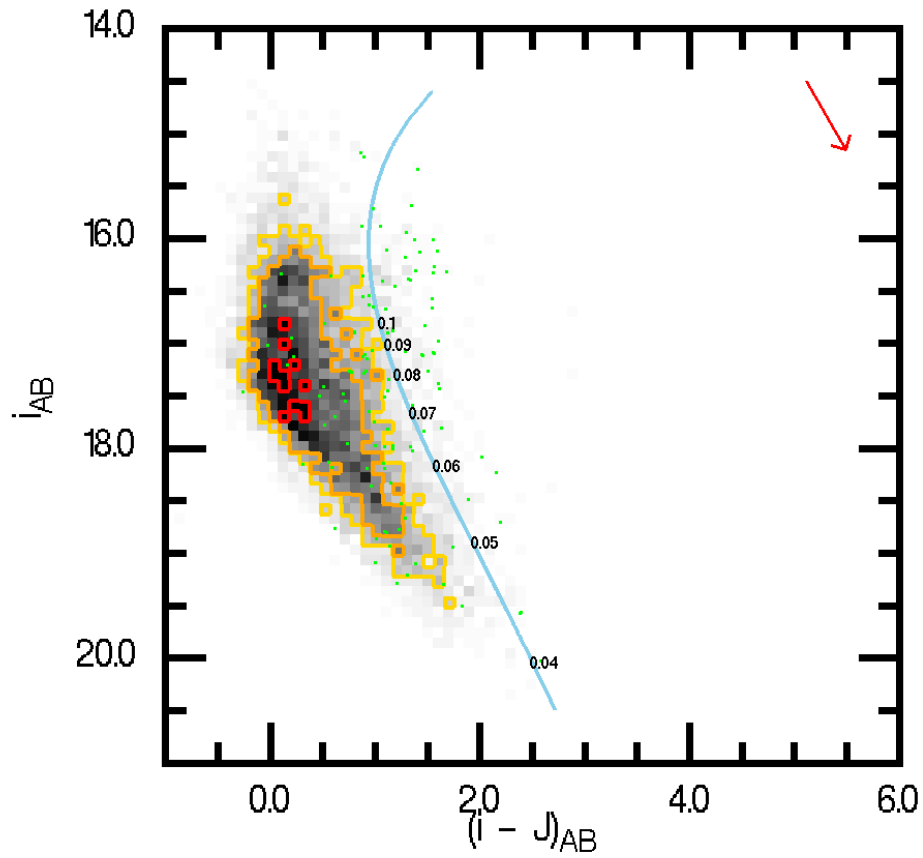


Figure 3.6 Similar CMD as in Figure 3.4 for the Pleiades data. The contours mark 10 (yellow), 20 (orange), and 50 (red) objects per bin. A 100-Myr isochrone is overlaid (light-blue line).

Chapter 4

Spectroscopic Follow-Up

Spectroscopy provides some of the most unambiguous confirmation of a candidate's membership status. Both temperature and gravity sensitive spectral features are present within the NIR region for low-mass objects. The overall shape of the SED provides the object's spectral type (a proxy for surface temperature). The relative depth of water and FeH absorption lines in the J and K bands compared to the continuum are highly sensitive to pressure (and thus, surface gravity) for objects of M and L type. By showing that a member candidate is cool and has an intermediate surface gravity between those of giants and dwarfs, it can be inferred that the candidate is youthful compared to the field population, and is thus likely a member of the more youthful cluster population.

4.1 SpeX Observations

NIR spectroscopic follow-up was performed on a subset of the selected member candidates for all three clusters. Preference was given to candidates with redder ($i - J$) colors and with $J < 17$. The color preference is due to the general trend of cluster members having redder colors at a given magnitude than the older field objects. Brighter objects were observed first so that higher resolution spectra could be obtained in a reasonable amount of integration time (≤ 25 min per object). The SpeX instrument (Rayner et al., 2003) mounted on NASA's Infrared Telescope Facility (IRTF) located on Mauna Kea, Hawaii was utilized to measure the NIR spectra for 134 of the 369 member candidates selected. Ninety-four of the brighter candidates (i.e., those with a J magnitude brighter than 14-16 depending on weather conditions) were observed using the short cross-dispersed (SXD) mode ($R \sim 1000$) with a typical exposure time of ≤ 12 minutes per object. The other 40 candidates were observed using the prism mode ($R \sim 100$). Both modes cover the NIR region of

0.8-2.5 microns. The data reduction was performed using the Spextool software package⁵ (Cushing, Vacca, & Rayner, 2004; Vacca, Cushing, & Rayner, 2003) with the settings commonly applied to point sources.

4.2 SED Fitting

To determine the spectral types of the candidates, the candidate spectra were fitted to empirical templates of known spectral type and surface gravity. A NIR spectral library was compiled of 296 objects spanning a broad range of spectral types (O-T) from three online sources: the Pickles Spectral Library⁶ (Pickles, 1998), the IRTF Spectral Library⁷ (Rayner, Cushing, & Vacca, 2009), and the SpeX Prism Library⁸. Of these, 186 spectra are within the K-L spectral type range, and include field dwarfs, giants, and youthful objects of intermediate surface gravity taken from other nearby clusters (e.g., ρ Ophiuchi and IC 348). The templates or the targets were then Gaussian smoothed as needed (depending on which spectrum had a lower resolution) so that they could be directly compared. A least- χ^2 fit was performed for each target spectrum using the library templates, with multiple iterations performed to test the effect of measurement error. The full 0.8-2.5 micron range was used for the fitting, excluding the heavy telluric absorption separating the *J*, *H*, and *K* bands (see Figure 4.1). Due to the significant extinction that can be present in and around clusters (and the Taurus region in particular), the amount of reddening in the fit was allowed to be a free parameter. The extinction law from Fitzpatrick (1985) was applied over a range of $A_V = 0 - 10$ for each fitting attempt.

Of the 83 Taurus member candidates followed-up with spectroscopy, 14 were best-fit to cluster M-type templates, while the majority of the remaining candidates were fit to either M-type field dwarfs or G/K-type giants (Figure 4.1). The fitting results for the Taurus candidates are summarized in Tables 4.1 and 4.2. Twenty-four candidates from Praesepe were followed-up with SpeX and yielded another 14 best-fits to cluster templates. Out of the 27 candidates with spectra from the Pleiades, 10 were fit to cluster member templates. The majority of non-cluster template fits from both Praesepe and the Pleiades were to M-type field dwarfs. Most of the candidates fit to cluster templates from all three clusters have spectral types in the M3-M6 range, which is consistent with the follow-up strategy of giving priority to brighter candidates. Tables 4.3 through 4.6 list the

⁵<http://irtfweb.ifa.hawaii.edu/~spex/SpeX.pdf>

⁶<http://www.ifa.hawaii.edu/users/pickles/AJP/hilib.html>

⁷<http://irtfweb.ifa.hawaii.edu/~spex/WebLibrary/index.html>

⁸<http://web.mit.edu/ajb/www/browndwarfs/spexprism/library.html>

fitting results for Praesepe and the Pleiades. See Appendix B for a complete listing of the best-fit results for all of the followed-up member candidates.

To determine the accuracy of this SED-fitting method, the spectral library underwent a self-test by fitting the templates and dis-allowing the spectra to match themselves. The library templates were also allowed to be reddened in the same manner as the data. It was found that 73% of the K- to L-type templates were matched to another template of similar luminosity type (i.e., field dwarf, giant, or cluster member) within ± 1 sub-type and an additional 21% matched within ± 2 sub-types, showing the fitting to be robust within the spectral type range associated with low-mass cluster members. Repeated fits were performed on the member candidates with random Gaussian errors added into the spectra at each iteration corresponding to the signal-to-noise of the data. However, this approach did not yield any alternate spectral type fits for our candidates, suggesting that measurement errors do not dominate the SED-fitting results.

To test the potential effect of the data reduction on the fitting, the faintest Taurus candidate targets ($J \sim 17$) were reduced in two ways: 1) extracting each spectrum measurement separately, and 2) pre-combining the spectra measurements using the median before extraction. For 9 of these 19 faint objects (47%), there was no difference in the fitted template between both reduction strategies. Another 2 objects had a spectral type discrepancy of ≤ 1 subtype, which is within the aforementioned fitting errors. Of the more significant differences, 3 differed by 4-5 spectral subtypes and 4 were discrepant between G and K/M types. This is likely due to the shape of the J-band, which changes significantly within these spectra between the two reduction methods. As these objects are faintest in the J-band, the median-combined versions are considered to be more accurate, as the individual extractions are noisier in appearance. The last discrepancy was in the gravity of an early M object (either young or dwarf-like). As discussed in the following section, the gravity-sensitive features are less distinct in early-mid M types compared with late-M types, so this discrepancy is not surprising.

4.3 Spectral Indices

In addition to fitting the overall SED, a complementary method of classifying the candidates is to use previously developed NIR spectral indices that are specifically designed to distinguish objects either by spectral type or surface gravity. From Allers et al. (2007), a temperature-sensitive index was chosen based on water absorption (given as H_2O), along with a gravity-dependent sodium index (Na). Both indices are located within the J-band. Another three temperature indices were

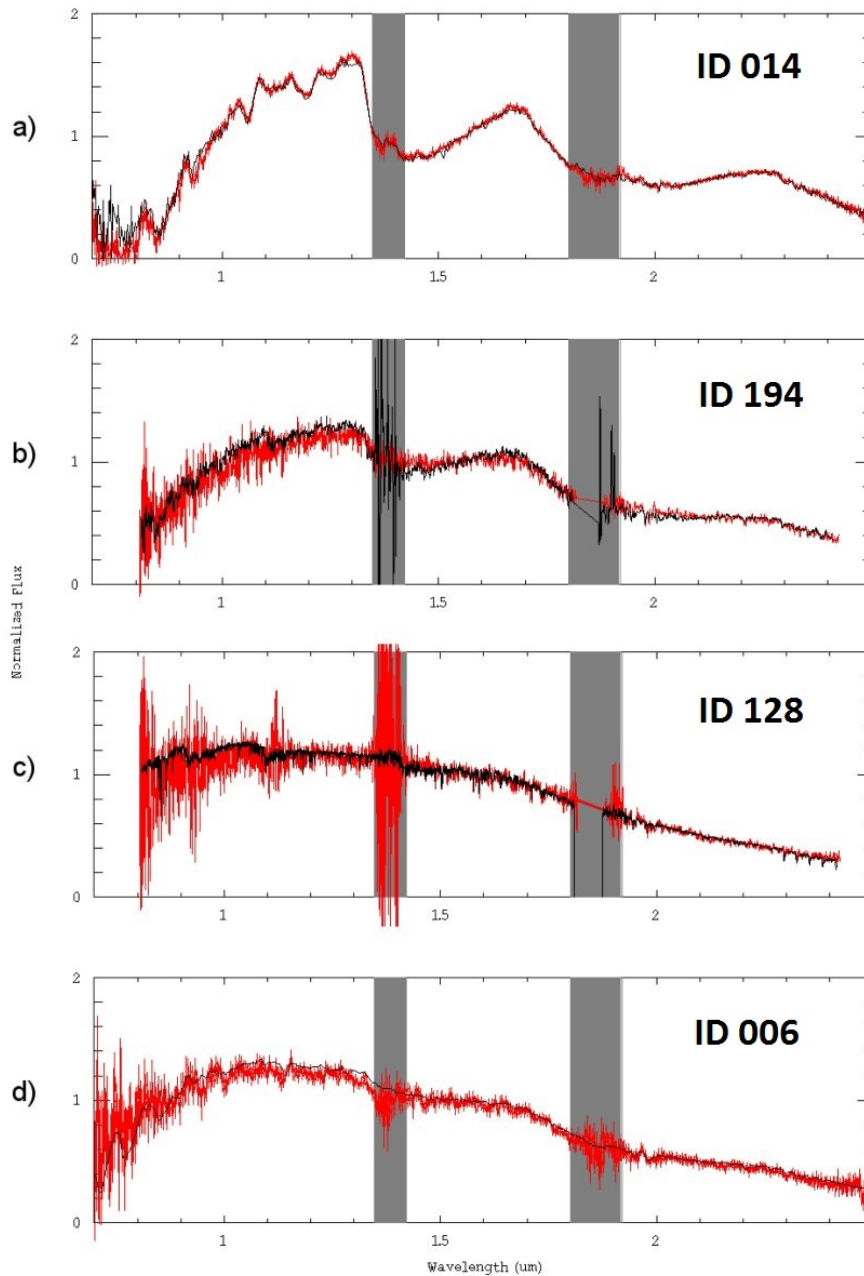


Figure 4.1 Four examples of fitting the member candidates (red) to spectral library templates (black). The gray areas mark the locations of the most significant telluric absorption between the J , H , and K bands. The best fits are: *a*) a recovered late-M Taurus member, *b*) a newly-identified mid-M Taurus member, *c*) a background K giant, and *d*) a mid-M field dwarf. See Tables 4.1 and 4.2 for fitting information, and see Appendix B for a full listing of the SED best-fit results.

taken from Slesnick, Hillenbrand, & Carpenter (2004), labeled as H_2O-1 , H_2O-2 , and FeH . H_2O-1 and FeH are also measured in the J -band, while H_2O-2 lies in the K -band. As with the spectral fitting, we performed an initial test of the spectral index accuracy by measuring our library templates. The H_2O index accurately measures late-M to mid-L objects within 1 subtype, while results outside this range become more degenerate. The H_2O-1 index provides the broadest range of spectral typing objects, but also has a systematic trend towards underestimating the spectral type. It is worthy of note that all giants but those with the latest M-types are separated from the dwarfs and young cluster objects by having a H_2O-1 calculated spectral type $\leq M0$. The H_2O-2 and FeH indices behave similarly to the H_2O-1 index, with the giants separated out by having the lowest index values. As opposed to H_2O-1 however, they tend to overestimate the spectral types across the M range. The mean spectral type calculated from these four temperature-sensitive indices allows us to assign spectral types to $\geq M3$ objects accurate to ± 1 subtype. Using the Na index, mid-to-late M objects separate based on their surface gravity. The majority of field dwarfs (80%) have an Na index greater than 1.05, while most giants and cluster members (92%) have an index less than or equal to this value (Figure 4.2). Earlier type objects of various gravities remain mixed, however. As expected from the SED-fitting, there is more ambiguity at early-M spectral types, while the agreement between SED-fitting and spectral index grows towards mid-to-late M types. This analysis provides added confidence that those candidates that have been SED-fit to mid- or late-M cluster member templates are in fact young, and thus are likely cluster members.

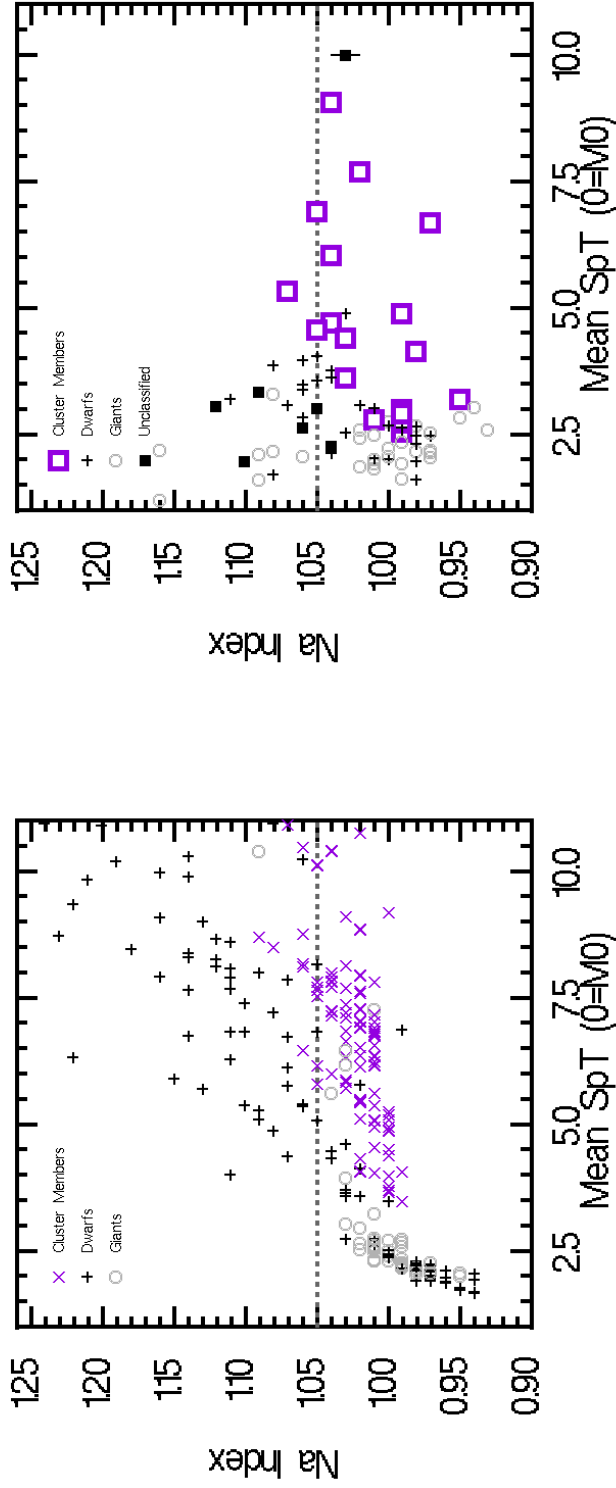


Figure 4.2 *Left:* The measured surface gravity sensitive Na index versus the mean calculated spectral type for the spectral library. Violet X's are cluster members, black crosses indicate field dwarfs, and gray circles denote giants. The dotted gray line shows the cut used in this study to distinguish between objects with higher surface gravity (dwarfs) and those with lower surface gravity (giants and cluster members). *Right:* The same measurements for the Taurus follow-up candidates, where the symbols correspond to the final status of each candidate as determined by both the SED fits and spectral index measurements. The filled black squares denote unclassified candidates. The black barred box on the far right shows the median value of the index measurement errors. The median spectral type measurement error is smaller than the point size.

Taking into account both the SED fitting and the spectral index measurements, the status of the followed-up Taurus candidates is concluded in Tables 4.1 and 4.2. Twelve candidates are reported to be newly identified low-mass Taurus members, 4 to be potential members, and another 4 to be recovered members from previous Taurus studies. The proper motions and colors of the follow-up targets are displayed in Figure 4.3. Thirteen Praesepe candidates are newly recognized as members, along with 5 potential members (Table 4.3). The remaining candidates likely to be background objects are listed in Table 4.4. For the Pleiades, 8 new members have been identified, and another nine candidates are listed as potential cluster members (Table 4.5). Candidates likely to be unassociated with the Pleiades are listed in Table 4.6. The proper motions and colors of the Praesepe and Pleiades candidates followed-up with spectroscopy are shown in Figures 4.5 and 4.7, respectively.

Table 4.1: Newly Recognized Taurus Members

ID	RA ¹	DEC ¹	χ^2 Fit ²	A_V ³	SpT ⁴	$\Delta N a^5$	i_{AB}	$(i - J)_{AB}$	$(J - K)_{AB}$	$\mu_\alpha \cos(\delta)^6$	μ_δ^6	Status
186	04:10:46.61	+28:17:21.0	M3 yng ⁸	5.25	M4	0.01	19.880	3.220	1.079	5	-26	Mem
000	04:10:56.37	+28:15:08.1	M3 yng	5.00	M3	-0.06	18.285	2.062	0.413	18	-11	Mem
129	04:14:54.34	+26:51:18.6	M3.5 V	1.00	M5	-0.06	16.190	1.774	0.024	9	-18	Mem
009	04:21:30.62	+28:21:40.7	M5.25 yng	2.00	M6	-0.01	17.952	3.199	0.738	14	-16	Rec Mem
200	04:23:26.77	+26:40:15.0	M3 yng	10.00	M3.5	-0.06	20.370	3.391	1.720	12	-10	Mem
012	04:24:43.20	+28:02:09.6	M3 yng	1.50	M3.5	-0.02	18.012	1.830	0.350	13	-3	Mem
014	04:26:30.51	+24:43:55.8	M9.25 yng	2.00	M9	-0.01	19.035	3.439	0.317	12	-21	Rec Mem
015	04:27:45.30	+23:57:25.2	M7.5 yng	1.75	M8	-0.03	19.042	3.179	0.293	9	-16	Rec Mem
135	04:28:06.21	+24:27:33.3	Poor Fit ⁹	...	M4.5	0.00	17.815	2.403	0.694	13	-15	Pot Mem
024	04:30:34.37	+28:48:51.7	Poor Fit	...	M3	-0.04	17.037	1.454	0.103	15	-22	Pot Mem
025	04:31:26.11	+27:03:19.8	M6 yng	1.25	M7	0.00	18.906	3.148	0.427	19	-18	Rec Mem
027	04:31:42.50	+23:29:40.5	Poor Fit	...	M3	-0.06	18.318	2.601	1.133	22	-8	Pot Mem
028	04:31:53.82	+24:54:49.8	Poor Fit	...	M3.5	-0.1	17.045	1.410	0.091	15	-15	Pot Mem
199	04:32:04.48	+21:42:19.0	M5 yng	0.25	M5	0.02	16.044	1.914	-0.041	4	-12	Mem
032	04:34:15.85	+22:50:37.9	M7.75 yng	2.25	M7	-0.08	18.430	3.760	0.940	12	-7	Mem
033	04:34:36.52	+26:49:40.3	M5.25 yng	1.25	M4	-0.07	16.723	2.498	0.619	Mem
191	04:39:56.42	+25:34:07.0	M3 yng	6.75	M3.5	-0.06	19.812	3.294	1.101	6	-11	Mem
194	04:42:12.06	+25:04:28.4	M5 yng	1.50	M4.5	-0.02	17.482	2.344	0.391	17	-18	Mem

Table 4.1 (cont'd)

ID	RA ¹	DEC ¹	χ^2 Fit ²	A_V ³	SpT ⁴	$\Delta N a$ ⁵	i_{AB}	$(i - J)_{AB}$	$(J - K)_{AB}$	$\mu_\alpha \cos(\delta)$ ⁶	μ_δ ⁶	Status	7
127	04:44:00.27	+24:19:37.5	M5 yng	1.00	M5	-0.01	16.916	1.978	0.180	13	-14	Mem	
042	04:47:13.73	+25:01:04.5	M5 V	0.25	M5	-0.02	16.996	1.782	0.019	Mem	

¹Position in J2000 coordinates²Spectral type based on χ^2 fitting³Reddening based on χ^2 fitting⁴Spectral type based on measured spectral indices⁵ $\Delta N a = \text{Na Index} - 1.05$ ⁶Proper Motion in units of mas/yr⁷Mem=New Cluster Member; Pot Mem=Potential Cluster Member; Rec Mem=Recovered Cluster Member⁸yng = fit to a cluster member template⁹SED fitting did not yield a good fit to a library template

Table 4.2: Contaminants & Undetermined Candidates (Taurus)

ID	RA ¹	DEC ¹	χ^2 Fit ²	A_V ³	SpT ⁴	$\Delta N a^5$	i_{AB}	$(i - J)_{AB}$	$(J - K)_{AB}$	$\mu_\alpha \cos(\delta)^6$	μ_δ^6	Status ⁷
187	04:10:54.64	+28:41:41.8	Poor Fit ⁸	...	<M	-0.04	16.568	2.284	0.559	6	-11	Gnt
001	04:11:15.38	+28:31:47.9	Poor Fit	...	<M	0.11	17.807	2.451	0.658	22	2	Unknown
002	04:11:15.81	+28:19:48.7	K7 V	3.75	M3	-0.06	17.112	1.665	0.382	47	-32	Dwf
003	04:11:27.57	+28:44:12.7	M4 V	3.00	M3.5	0.01	18.356	2.039	0.320	12	-11	Dwf
004	04:12:47.23	+28:33:38.0	M2.5 V	2.50	M4	-0.01	17.053	1.719	0.250	14	-17	Dwf
196	04:13:06.34	+28:26:02.9	M0.5 V	5.00	M3	-0.02	16.997	2.362	0.759	7	-25	Dwf
005	04:13:06.36	+28:12:05.6	K2 III	5.75	M3	-0.03	17.498	2.114	0.709	7	-17	Gnt
006	04:15:10.72	+27:38:09.1	M4 V	2.00	M3	0.02	17.311	1.527	0.183	14	-16	Dwf
007	04:15:28.24	+27:26:36.3	Poor Fit	...	M3	-0.1	18.113	3.213	-2.068	16	-14	Gnt
197	04:17:31.00	+28:14:19.5	Poor Fit	...	<M	-0.04	17.269	2.527	0.604	19	-20	Gnt
198	04:17:45.63	+28:46:14.1	K7 V	5.25	<M	-0.07	16.913	2.194	0.637	15	-10	Dwf
008	04:21:47.01	+26:59:32.1	K7 V	2.25	<M	-0.01	16.797	1.405	0.154	73	27	Dwf
010	04:23:42.06	+28:10:52.8	K2 III	5.00	M3	-0.04	18.399	2.033	0.521	30	-24	Gnt
011	04:23:54.35	+27:39:40.2	M0.5 V	2.75	M3	-0.06	17.050	1.776	0.322	16	-18	Dwf
013	04:25:22.14	+27:25:12.2	K7 V	5.00	M3	-0.07	18.153	2.154	0.550	6	-17	Dwf
201	04:26:01.22	+27:10:45.2	K1 III	9.75	<M	-0.08	19.883	3.251	1.252	7	-13	Gnt
133	04:26:56.84	+24:46:34.7	Poor Fit	...	<M	-0.01	16.987	1.692	0.409	10	-13	Unknown
134	04:28:05.38	+24:32:34.5	F7 III	6.00	<M	-0.08	16.804	1.643	0.262	9	-16	Gnt

Table 4.2 (cont'd)

ID	RA ¹	DEC ¹	χ^2 Fit ²	A_V ³	SpT ⁴	$\Delta N a^5$	i_{AB}	$(i - J)_{AB}$	$(J - K)_{AB}$	$\mu_\alpha \cos(\delta)^6$	μ_δ^6	Status ⁷
016	04:28:25.49	+27:12:18.1	K0 III	5.00	<M	-0.08	18.494	2.115	0.726	6	-4	Gnt
136	04:28:27.10	+25:29:03.5	Poor Fit	...	M3	0.01	16.474	1.484	0.091	5	-19	Unknown
017	04:28:38.45	+24:29:39.4	K2 III	4.50	M3	-0.05	17.751	2.226	0.770	10	-20	Gnt
018	04:28:49.91	+24:31:42.1	K2 III	4.50	<M	0.04	17.410	2.009	0.539	19	-26	Gnt
019	04:28:52.48	+24:59:58.1	M2.5 V	2.75	M4	0.00	17.463	1.942	0.352	10	-11	Dwf
020	04:29:24.01	+24:46:06.9	M1 V	3.50	M3	-0.07	17.375	1.904	0.406	Dwf
188	04:29:30.24	+26:58:27.7	Poor Fit	...	M3.75	0.03	17.412	5.075	2.326	13	-9	Dwf
021	04:29:31.01	+25:17:52.9	F5 V	1.00	<M	-0.08	16.906	1.653	0.025	9	-2	Dwf
022	04:29:58.88	+24:22:21.8	Poor Fit	...	<M	0.04	16.536	1.616	0.207	26	-37	Unknown
023	04:30:06.85	+26:19:57.2	K1 III	2.00	<M	-0.06	17.060	1.056	0.149	18	-22	Gnt
115	04:31:34.26	+24:09:08.3	F7 III	7.00	<M	-0.06	15.505	1.883	0.424	16	-20	Gnt
026	04:31:40.00	+27:05:32.8	G4 III	5.50	<M	-0.04	16.719	2.091	0.391	2	5	Gnt
202	04:31:41.92	+24:41:07.6	Poor Fit	...	<M	-0.05	17.705	2.271	0.605	4	-22	Gnt
118	04:31:55.44	+26:35:00.6	K4 V	4.00	<M	-0.05	16.435	1.485	0.216	10	-13	Gnt
029	04:32:41.70	+28:12:02.9	M2.5 V	2.00	M3	-0.05	17.122	1.624	0.187	9	-22	Dwf
203	04:32:52.80	+24:47:33.8	Poor Fit	...	<M	-0.03	16.443	2.040	0.591	21	-19	Gnt
030	04:32:54.98	+22:25:34.2	M2.5 V	1.75	M4	0.03	16.811	1.577	0.230	27	-20	Dwf
116	04:33:21.42	+24:16:14.6	Poor Fit	...	M4	0.00	17.022	1.631	0.287	14	-13	Dwf
117	04:33:49.96	+22:30:16.9	Poor Fit	...	M4	-0.01	16.857	1.735	-0.019	8	-15	Dwf

Table 4.2 (cont'd)

ID	RA ¹	DEC ¹	χ^2 Fit ²	A_V ³	SpT ⁴	$\Delta N a^5$	i_{AB}	$(i - J)_{AB}$	$(J - K)_{AB}$	$\mu_\alpha \cos(\delta)^6$	μ_δ^6	Status ⁷
031	04:34:08.13	+22:48:05.9	K3 III	10.00	<M	0.11	19.521	3.384	1.617	-8	-9	Gnt
189	04:34:36.45	+27:04:56.1	K3 III	7.50	<M	-0.06	17.169	2.838	0.923	7	-12	Gnt
119	04:34:54.87	+26:19:32.5	K7 V	4.25	M3	0.01	16.911	1.885	0.481	6	-17	Dwf
034	04:35:15.49	+26:18:08.2	K2 III	4.25	M3	-0.11	16.698	1.921	0.412	10	-36	Gnt
190	04:35:36.91	+26:40:18.2	M2 V	4.75	M3.5	0.01	17.505	2.244	0.522	6	-13	Dwf
035	04:35:39.56	+27:05:43.8	Poor Fit	...	<M	0.05	17.542	2.642	-0.609	7	-22	Unknown
036	04:37:05.36	+26:22:03.7	G5 III	6.25	<M	-0.03	17.592	2.192	0.561	9	-25	Gnt
120	04:37:20.93	+26:10:08.4	K4 V	6.25	<M	0.03	17.631	2.190	0.514	7	-19	Dwf
125	04:37:21.86	+23:11:50.6	K4 V	2.75	<M	-0.06	15.993	1.601	0.223	6	-16	Dwf
121	04:37:39.60	+25:15:58.3	G6 III	5.00	<M	-0.04	17.037	1.921	0.416	9	-17	Gnt
195	04:38:19.69	+26:30:40.0	K1 III	6.50	<M	-0.05	16.841	2.244	0.598	20	-23	Gnt
037	04:38:20.31	+26:30:47.9	G8 III	7.00	<M	0.03	16.841	2.244	0.598	20	-23	Gnt
038	04:38:38.99	+26:47:06.3	Poor Fit	...	<M	-0.12	16.645	1.689	0.204	4	-15	Unknown
192	04:41:15.42	+25:22:24.7	F5 V	9.50	<M	-0.07	16.772	3.051	0.922	3	-18	Dwf
193	04:41:17.92	+25:21:28.2	G4 V	10.00	<M	-0.04	20.330	3.674	1.398	2	-13	Dwf
122	04:41:27.52	+24:47:35.3	M2.5 V	2.75	M3.5	0.06	16.657	1.772	0.341	13	-21	Dwf
126	04:41:36.71	+24:20:01.2	K4 V	3.00	M3.25	-0.03	16.885	1.655	0.266	16	-16	Dwf
039	04:41:36.91	+24:19:53.6	M2.5 V	1.75	M3	-0.04	16.885	1.655	0.266	16	-16	Dwf
123	04:41:49.70	+25:16:44.2	K7 V	6.75	<M	-0.07	17.877	2.424	0.751	6	-20	Dwf

Table 4.2 (cont'd)

ID	RA ¹	DEC ¹	χ^2 Fit ²	A_V ³	SpT ⁴	$\Delta N a$ ⁵	i_{AB}	$(i - J)_{AB}$	$(J - K)_{AB}$	$\mu_\alpha \cos(\delta)$ ⁶	μ_δ ⁶	Status ⁷
124	04:42:02.84	+24:59:34.5	K4 V	3.75	<M	-0.07	16.453	1.587	0.168	10	-14	Dwf
040	04:43:03.27	+24:23:40.5	Poor Fit	...	<M	-0.08	16.545	1.405	0.202	Unknown
128	04:45:50.83	+24:57:14.7	K2 III	2.75	<M	-0.07	16.095	1.546	0.278	16	-20	Gnt
130	04:46:47.66	+25:06:02.9	K2 III	4.75	M3.25	0.07	17.409	2.114	0.474	14	-15	Unknown
041	04:46:48.08	+25:05:48.1	Poor Fit	...	M3	0.00	17.409	2.114	0.474	14	-15	Dwf
131	04:46:50.95	+24:58:04.8	Poor Fit	...	M3.5	0.04	17.322	1.918	0.337	16	-17	Dwf
132	04:48:10.94	+25:26:00.1	K1 III	5.50	<M	0.01	17.200	1.973	0.357	0.011	-22	Gnt

¹Position in J2000 coordinates²Spectral type based on χ^2 fitting³Reddening based on χ^2 fitting⁴Spectral type based on measured spectral indices⁵ $\Delta N a = \text{Na Index} - 1.05$ ⁶Proper Motion in units of mas/yr⁷Dwf=Field Dwarf; Gnt=Background Giant; Unknown=Status Cannot Be Determined⁸SED fitting did not yield a good fit to a library template

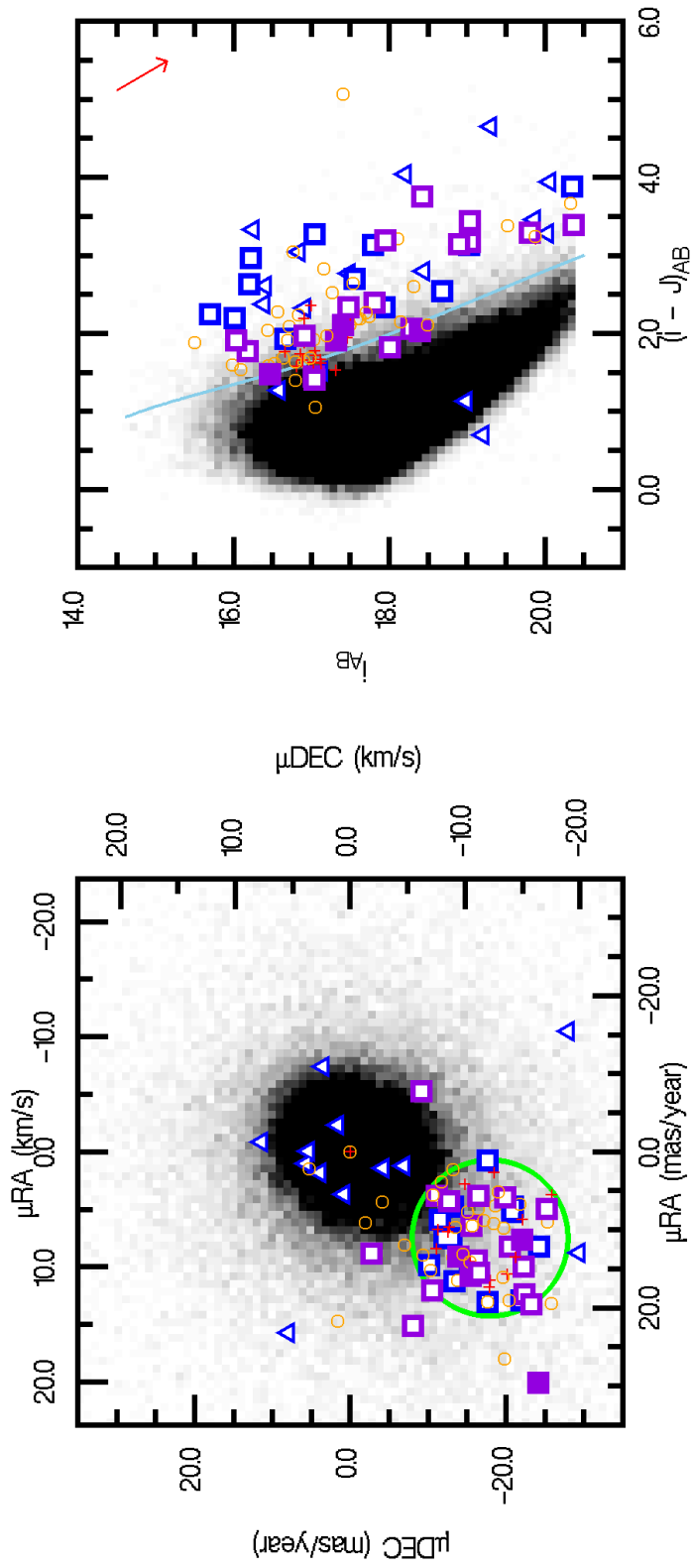


Figure 4.3 *Left*: Same as Figure 3.1 with plotted follow-up candidates. Blue boxes (triangles) mark previously claimed cluster members that passed (failed) the proper motion criteria. Violet boxes are claimed in this work as Taurus members, red crosses are M field dwarfs, and orange circles are objects with spectral types $< M$. *Right*: Same as Figure 3.4, with plotted follow-up candidates. The candidates blueward of the isochrone and/or outside of the PM cut are from a previous fitting to the BC models and a previous astrometric solution, respectively (see Chapter 3).

Table 4.3: Newly Recognized Praesepe Members

ID	RA ¹	DEC ¹	χ^2 Fit ²	A_V^3	SpT ⁴	$\Delta N a^5$	i_{AB}	$(i - J)_{AB}$	$(J - K)_{AB}$	$\mu_\alpha \cos(\delta)^6$	μ_δ^6	Status
111	08:33:02.96	+19:07:41.3	M3.5 yng ⁸	0.50	M4	-0.05	17.516	0.939	-0.133	-30	-15	Mem
112	08:33:57.12	+19:10:09.4	M4.25 yng	0.25	M3.5	-0.07	17.251	0.985	-0.041	-34	-14	Mem
113	08:34:54.98	+19:33:24.3	Poor Fit ⁹	...	M4	-0.06	17.486	1.066	-0.273	-29	-10	Pot Mem
114	08:35:12.15	+19:11:43.9	M3 yng	1.50	M3	-0.05	16.596	0.856	-0.055	-36	-10	Mem
105	08:36:22.25	+20:11:12.3	M3.5 yng	1.50	M4	-0.04	17.032	1.306	-0.072	-29	-9	Mem
106	08:36:36.43	+20:26:53.8	M3.25 yng	1.00	M4	-0.02	18.102	1.216	-0.273	-36	-20	Mem
107	08:36:38.19	+20:21:37.8	M3 yng	1.25	M3	-0.06	17.493	1.047	0.100	-32	-8	Mem
108	08:38:27.98	+20:07:36.8	M2 V	0.25	M3	-0.08	17.049	1.031	-0.095	-38	-13	Pot Mem
093	08:39:07.95	+19:11:13.4	Poor Fit	...	M4	-0.02	18.068	1.091	-0.157	-38	-6	Pot Mem
109	08:39:20.02	+20:01:29.2	M4.75 yng	1.00	M5.5	-0.03	18.387	1.850	0.080	-27	-14	Mem
094	08:39:31.98	+19:57:12.3	M4.25 yng	2.50	M5	-0.1	17.435	1.462	0.057	-31	-17	Mem
095	08:39:39.09	+19:48:10.8	M4.25 yng	1.25	M4	-0.05	18.971	2.013	-0.134	-37	-17	Mem
110	08:39:43.98	+20:08:40.8	M3.25 yng	1.00	M3	-0.04	16.774	0.866	-0.070	-24	-14	Mem
098	08:40:36.67	+19:36:25.3	M4.25 yng	0.75	M4	-0.03	18.064	1.360	-0.035	-30	-11	Mem
099	08:40:39.11	+19:40:13.9	M4.5 yng	0.75	M4	-0.04	17.354	1.307	-0.135	-33	-6	Mem
100	08:40:43.43	+19:13:32.8	M4 yng	0.25	<M	-0.02	17.446	0.990	-0.420	-28	-17	Pot Mem
102	08:40:57.50	+19:26:50.3	M4.25 yng	0.75	M4.5	-0.02	17.857	1.542	-0.008	-34	-9	Mem
104	08:44:49.51	+20:10:56.2	M5 V	0.75	M5	-0.08	18.558	1.753	-0.063	-32	-11	Pot Mem

Table 4.3 (cont'd)

ID	RA ¹	DEC ¹	χ^2 Fit ²	A_V ³	SpT ⁴	ΔNa ⁵	i_{AB}	$(i - J)_{AB}$	$(J - K)_{AB}$	$\mu_\alpha \cos(\delta)$ ⁶	μ_δ ⁶	Status	7
----	-----------------	------------------	---------------------------	--------------------	------------------	--------------------------	----------	----------------	----------------	--	---------------------------	--------	---

¹Position in J2000 coordinates²Spectral type based on χ^2 fitting³Reddening based on χ^2 fitting⁴Spectral type based on measured spectral indices⁵ $\Delta Na = Na \text{ Index} - 1.05$ ⁶Proper Motion in units of mas/yr⁷Mem=New Cluster Member; Pot Mem=Potential Cluster Member⁸ying = fit to a cluster member template⁹SED fitting did not yield a good fit to a library template

Table 4.4: Contaminants & Undetermined Candidates (Praesepe)

ID	RA ¹	DEC ¹	χ^2 Fit ²	A_V ³	SpT ⁴	$\Delta N a$ ⁵	i_{AB}	$(i - J)_{AB}$	$(J - K)_{AB}$	$\mu_\alpha \cos(\delta)$ ⁶	μ_δ ⁶	Status ⁷
103	08:36:18.61	+20:31:40.6	G4 III	2.00	<M	-0.05	17.617	0.873	-0.101	-25	-7	Gnt
091	08:38:14.52	+19:52:29.0	Poor Fit ⁸	...	<M	-0.04	15.910	1.048	-0.196	-34	-4	Unknown
092	08:38:56.53	+19:50:59.6	G8 III	1.50	M4	-0.03	16.286	0.568	-0.152	-27	-10	Unknown
096	08:40:06.90	+18:14:55.3	Poor Fit	...	<M	-0.02	18.158	1.633	0.408	-32	-4	Unknown
097	08:40:35.13	+19:49:30.5	M2.5 V	0.25	M3	0.03	15.890	0.862	-0.018	-34	-20	Dwf
101	08:40:51.94	+18:00:59.4	M5 V	0.50	M4	-0.01	17.998	1.634	-0.059	-24	-7	Dwf

¹Position in J2000 coordinates

²Spectral type based on χ^2 fitting

³Reddening based on χ^2 fitting

⁴Spectral type based on measured spectral indices

⁵ $\Delta N a = \text{Na Index} - 1.05$

⁶Proper Motion in units of mas/yr

⁷Dwf=Field Dwarf; Gnt=Background Giant; Unknown=Status Cannot Be Determined

⁸SED fitting did not yield a good fit to a library template

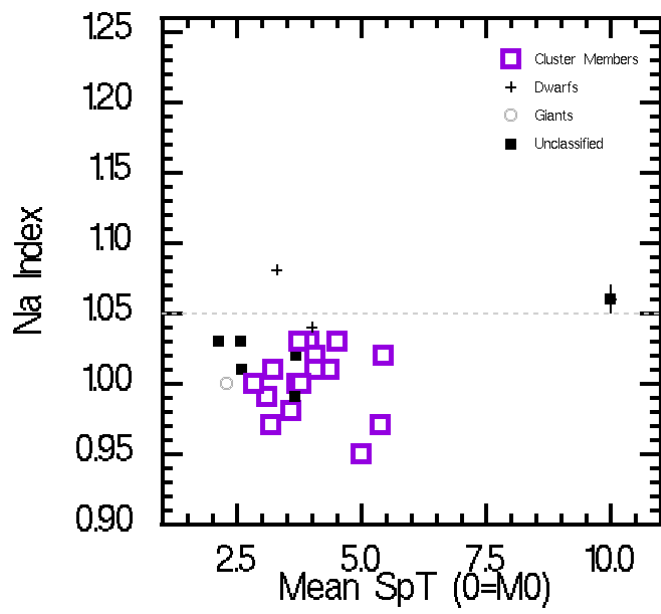


Figure 4.4 Similar plot as Figure 4.2 with Praesepe follow-up candidates.

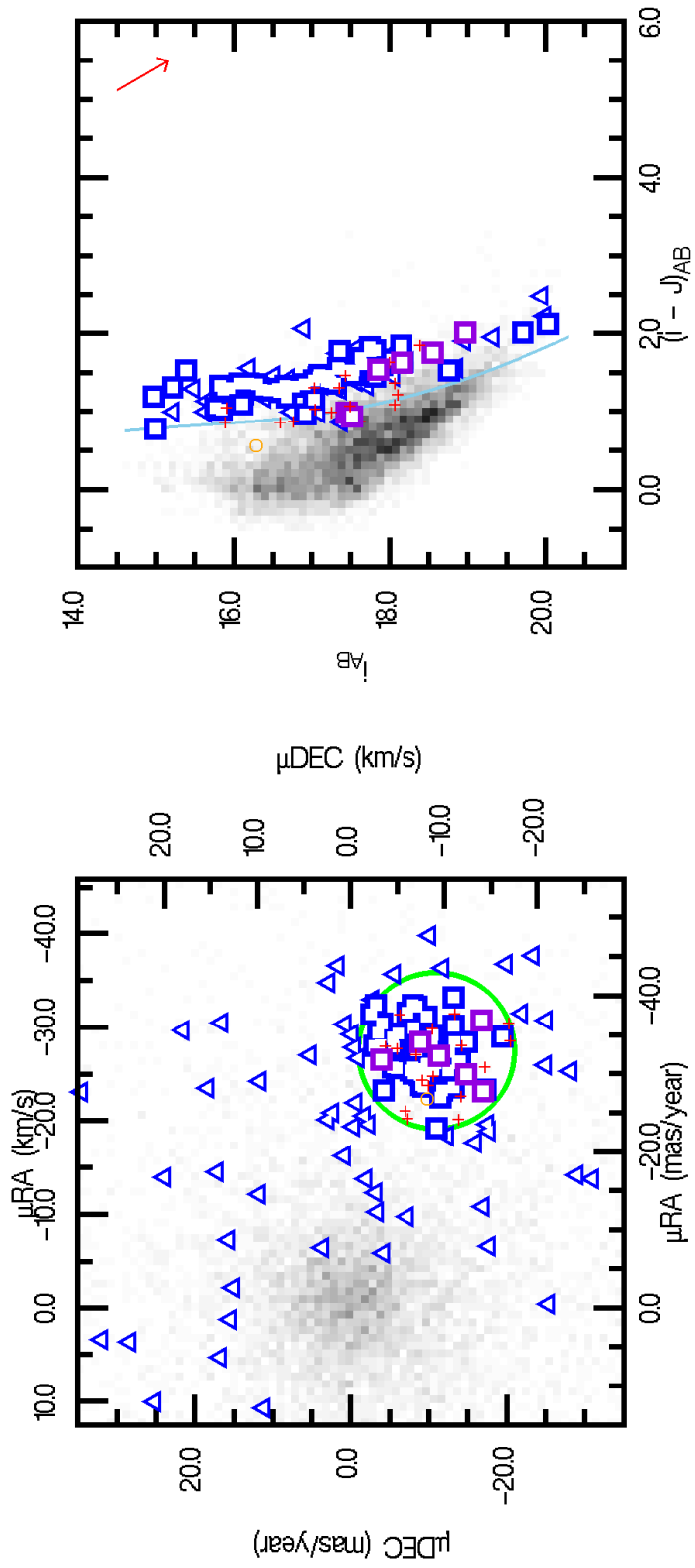


Figure 4.5 Similar follow-up as shown in Figure 4.3 for Praesepe candidates. Follow-up candidates bluerward of the isochrone were selected from a cruder approximation of the isochrone. These candidates were kept in consideration since the Praesepe cluster is believed to be older (i.e., its members have bluer colors) than the 500-Myr isochrone that was used for the color selection.

Table 4.5: Newly Recognized Pleiades Members

ID	RA ¹	DEC ¹	χ^2 Fit ²	A_V ³	SpT ⁴	$\Delta N d^5$	i_{AB}	$(i - J)_{AB}$	$(J - K)_{AB}$	$\mu_\alpha \cos(\delta)^6$	μ_δ^6	Status	7
180	03:44:47.19	+25:27:58.7	M2.5 V	0.50	M3	-0.02	16.111	1.117	-0.037	27	-33	Pot Mem	
063	03:44:52.19	+25:05:17.3	M3.5 V	1.00	M5	-0.01	16.275	1.563	-0.009	13	-46	Pot Mem	
088	03:45:04.77	+26:40:40.4	M5 yng ⁸	0.25	M5	-0.07	16.120	1.595	-0.091	20	-50	Mem	
065	03:45:37.76	+25:16:34.0	M5 yng	0.25	M5	0.04	16.861	1.178	0.025	15	-43	Pot Mem	
182	03:46:06.68	+25:25:02.3	M2.5 V	0.50	M3.5	0.00	15.719	0.990	0.011	21	-29	Pot Mem	
067	03:46:25.85	+26:34:43.2	M5 yng	0.25	M4	0.03	16.016	1.381	-0.090	20	-44	Pot Mem	
068	03:46:33.84	+25:51:41.7	M3.5 V	0.75	M5.5	-0.05	16.012	1.553	-0.067	23	-40	Mem	
069	03:46:57.27	+25:51:47.2	M5 yng	0.25	M5	0.00	17.118	1.461	-0.006	13	-33	Mem	
183	03:46:59.79	+25:48:56.1	M4.25 yng	0.25	M4	-0.07	17.978	1.175	-0.248	9	-33	Mem	
089	03:51:05.39	+26:36:51.0	M4.25 yng	0.75	M4	-0.06	16.985	1.605	0.041	18	-39	Mem	
090	03:51:33.58	+26:38:42.6	Poor Fit ⁹	...	M3.5	-0.03	17.383	1.608	-0.067	25	-39	Pot Mem	
176	03:51:51.69	+23:34:48.3	M5 yng	0.25	M4.5	0.04	16.458	1.197	-0.006	18	-52	Pot Mem	
178	03:53:22.31	+24:03:21.2	M5 yng	0.25	M5	0.06	16.661	1.546	-0.014	5	-35	Pot Mem	
175	03:54:00.74	+24:34:48.7	M4.75 yng	1.00	M5.75	0.00	17.266	1.507	-0.017	27	-33	Mem	
179	03:54:18.27	+23:56:09.3	M2 V	0.75	M3	-0.02	16.411	1.070	-0.092	31	-31	Pot Mem	
181	03:54:27.54	+23:19:14.9	M3.25 yng	2.50	M3	-0.01	18.489	1.890	-0.381	14	-28	Mem	
087	03:55:34.46	+23:58:24.7	M4.5 V	0.25	M4	-0.05	16.385	1.320	-0.079	21	-39	Mem	

Table 4.5 (cont'd)

ID	RA ¹	DEC ¹	χ^2 Fit ²	A_V ³	SpT ⁴	$\Delta N a$ ⁵	i_{AB}	$(i - J)_{AB}$	$(J - K)_{AB}$	$\mu_\alpha \cos(\delta)$ ⁶	μ_δ ⁶	Status	7
----	-----------------	------------------	---------------------------	--------------------	------------------	---------------------------	----------	----------------	----------------	--	---------------------------	--------	---

¹Position in J2000 coordinates

²Spectral type based on χ^2 fitting

³Reddening based on χ^2 fitting

⁴Spectral type based on measured spectral indices

⁵ $\Delta N a = \text{Na Index} - 1.05$

⁶Proper Motion in units of mas/yr

⁷Mem=New Cluster Member; Pot Mem=Potential Cluster Member

⁸ying = fit to a cluster member template

⁹SED fitting did not yield a good fit to a library template

Table 4.6: Contaminants & Undetermined Candidates (Pleiades)

ID	RA ¹	DEC ¹	χ^2 Fit ²	A_V ³	SpT ⁴	$\Delta N a$ ⁵	i_{AB}	$(i - J)_{AB}$	$(J - K)_{AB}$	$\mu_\alpha \cos(\delta)$ ⁶	μ_δ ⁶	Status ⁷
177	03:44:39.50	+25:31:19.9	M4 V	0.75	M4	-0.03	17.993	1.345	-0.234	27	-34	Dwf
064	03:44:55.07	+25:36:27.3	M4.5 V	0.25	M4	0.06	17.593	1.355	0.050	25	-42	Dwf
066	03:46:00.24	+26:20:14.1	M4 V	1.25	M5	0.02	16.573	1.549	-0.041	23	-46	Dwf
174	03:47:44.42	+26:13:22.2	Poor Fit ⁸	...	M4.25	0.02	15.950	1.302	-0.057	30	-42	Dwf
082	03:48:52.82	+25:22:29.6	M3.5 V	0.75	M4	0.08	16.129	1.428	-0.053	13	-41	Dwf
070	03:51:56.18	+24:56:58.5	K4 V	2.00	<M	-0.06	17.151	0.924	-0.102	19	-39	Dwf
084	03:52:02.36	+24:05:32.4	Poor Fit	...	<M	-0.19	17.133	0.885	-0.153	22	-42	Unknown
085	03:52:24.93	+24:14:34.6	G5 III	0.50	M7	-0.01	16.359	0.891	-0.351	12	-39	Unknown
083	03:52:34.54	+24:25:22.4	Poor Fit	...	M3	-0.02	16.890	0.807	-0.137	21	-40	Dwf
086	03:53:55.68	+23:23:43.9	M7 V	0.75	M4.5	0.00	18.233	2.162	0.113	20	-46	Dwf

¹Position in J2000 coordinates

²Spectral type based on χ^2 fitting

³Reddening based on χ^2 fitting

⁴Spectral type based on measured spectral indices

⁵ $\Delta N a = \text{Na Index} - 1.05$

⁶Proper Motion in units of mas/yr

⁷Dwf=Field Dwarf; Gnt=Background Giant; Unknown=Status Cannot Be Determined

⁸SED fitting did not yield a good fit to a library template

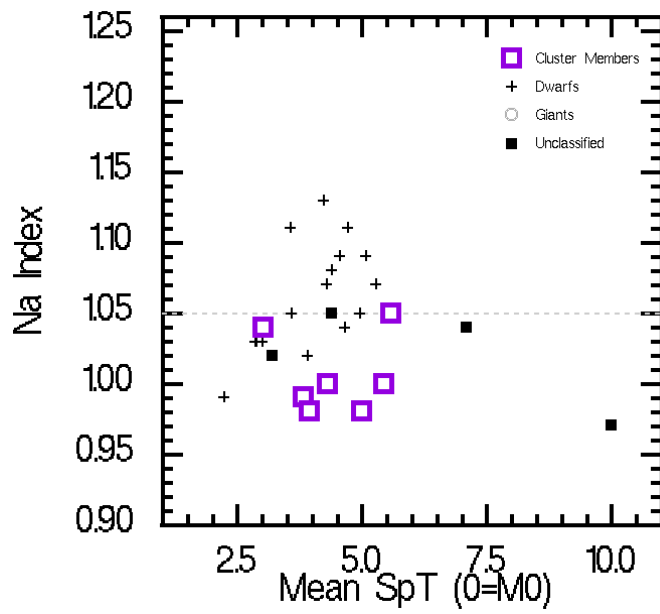


Figure 4.6 Similar plot as Figure 4.2 with Pleiades follow-up candidates.

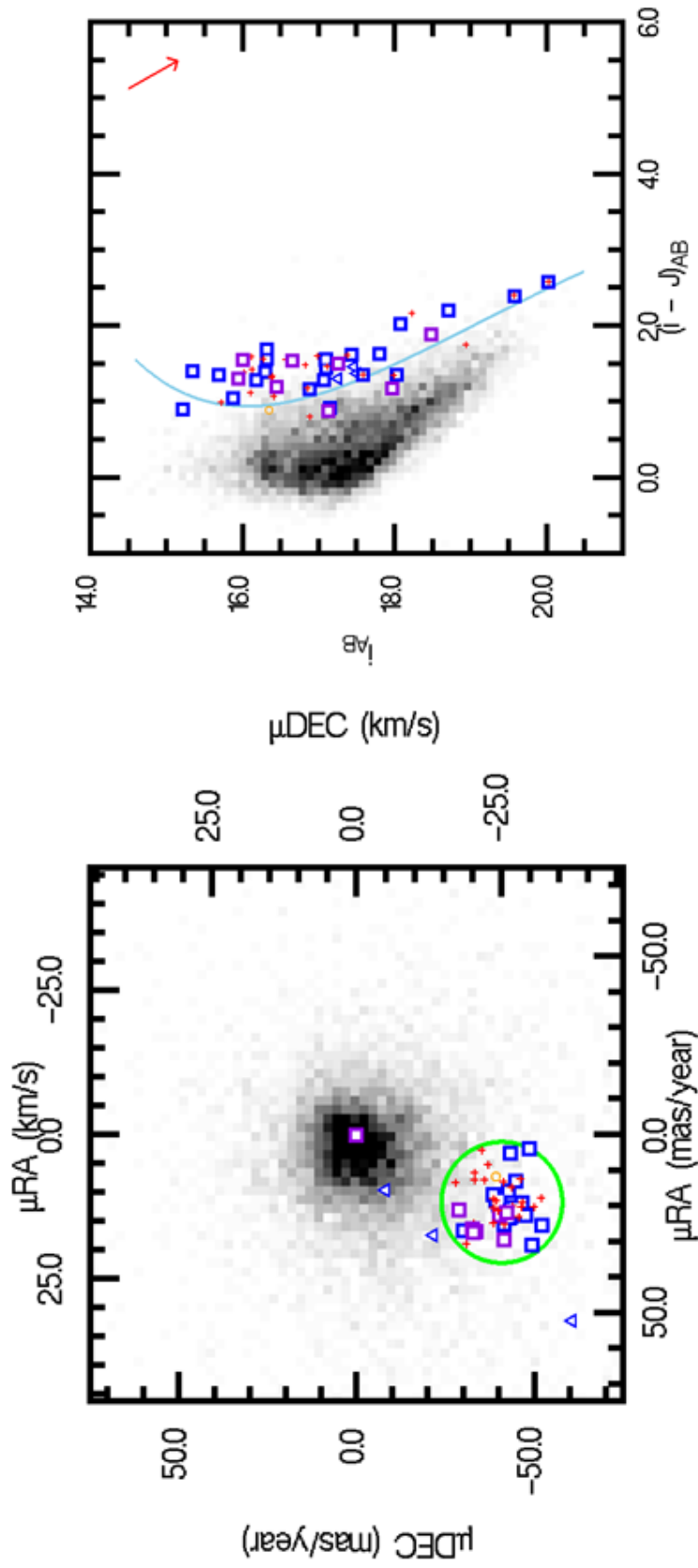


Figure 4.7 Similar follow-up as shown in Figure 4.3 for Pleiades candidates. Follow-up candidates outside of the proper motion selection region and/or blueward of the isochrone were selected from a previous astrometric solution and a cruder approximation of the isochrone. These candidates were kept in consideration since the SED best-fit results were suggestive of membership, and the Pleiades cluster is believed to be slightly older (i.e., its members have bluer colors) than the 120-Myr isochrone that was used for the color selection.

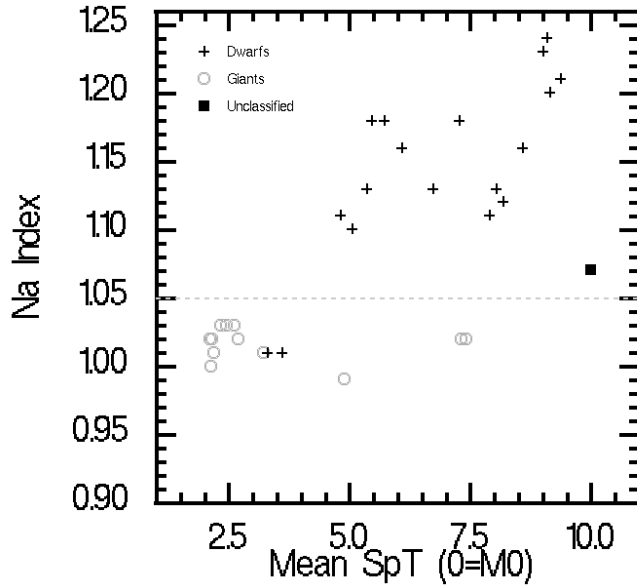


Figure 4.8 Similar plot as Figure 4.2 with known field objects.

As an additional check on the classification scheme, a collection of 29 field dwarfs and giants of known spectral type from Cruz et al. (2007) were observed alongside the cluster member candidates using the same instrument settings and under similar weather conditions. Twenty-five of these field objects had acceptable SED fits to the spectral library, and the agreement with Cruz et al. (2007) was typically within 1.5-2 sub-types. In six of these fits, a dwarf was fit to a cluster template, once again demonstrating how SED fitting at low resolution can sometimes confuse cluster members and field dwarfs within the early-to-mid M types. The spectral index measurements of these field dwarfs confirm the results of the spectral library test (Figure 4.8), with the majority of field dwarfs lying above the 1.05 division for the Na index.

Chapter 5

Field Contamination

As demonstrated by the spectroscopic follow-up, the search technique described in this work is not perfect. A mixture of field dwarfs and background giants were also selected as potential members. To properly place the spectroscopic results in context, it is necessary to adequately account for the field population that is extracted using the aforementioned search criteria. Since an empirical measurement of the entire galactic low-mass population is not practical, a model is required that provides a good indicator of what types of contamination we are preferentially selecting, along with their bulk properties. Not only does such a model characterize the contaminant population, but can also allow for additional means by which to conclude that certain candidates must indeed be cluster members.

5.1 Galactic Field Model

An online query tool⁹ was used that generates a galactic field population along a given line-of-sight based on the model described in Robin et al. (2003). Running the model population through the same kinematic and photometric criteria as the data allows a determination of the population of field objects to which the selection method is most sensitive. The distance distribution of the model objects towards Taurus is shown in Figure 5.1. The proper motion of the Taurus cluster corresponds to that of the galactic field at a distance of $\sim 200 - 900$ pc behind the cluster, so field dwarfs at this distance will be included by our kinematic cut. For Praesepe and the Pleiades, the proper-motion-selected field lies directly behind the cluster at a distance of $\sim 100 - 300$ pc (Figures 5.2 and 5.3). However, unlike Taurus, the latter two clusters have a proper motion different enough from the bulk galactic flow to avoid any contamination at all by background giants. Based

⁹<http://model.obs-besancon.fr/>

on the field model, the vast majority of contaminants within all three clusters will be M-type field dwarfs.

5.2 Properties of Contaminants

5.2.1 Taurus

To verify that the galactic field as detected in the data is accurately reproduced by the model, it must be shown that a vector-point diagram and color-magnitude diagram similar to the data can be constructed from the model. Since the model query tool at the time of access did not include J magnitudes, we fitted a spectral type vs. $(i - J)$ color relation from the work of Kraus & Hillenbrand (2007), who calculated colors from the mean SEDs of objects followed-up spectroscopically from the SDSS survey. This relation applies only to field dwarf colors. However, the model suggests that dwarfs do indeed dominate our contamination when compared to background giants (Figure 5.1). Given the spectral type of each model object, it was assigned an $(i - J)$ color, and then random error was applied based on the i magnitude vs. error relation of the photometric data. While the model does include typical ISM extinction values at the galactic latitude of the clusters ($A_V \leq 0.4$), it does not take into consideration the molecular clouds that lie about regions such as Taurus. Therefore, more realistic A_V values are needed for the model objects, most of which lie behind the clusters. Using the galactic A_V maps from Rowles & Froebrich (2009), a 1-arcmin resolution mean- A_V grid was generated about the Taurus region. The model objects were then assigned a new A_V value given their RA/DEC position, and model objects reddened below our faint limit ($i > 20.5$) were removed from further consideration. Model objects with a given distance less than the measured distance of Taurus were not reddened. Also removed were model objects with $J_{AB} > 18.4$ to simulate the sensitivity limit of the 2MASS photometry. The model was then normalized to the data based on the relative number of data-to-model objects as a function of i magnitude. This normalization varies from 0-24.6%, with a mean value of 11.5%. Model objects were then selected at random based on this normalization factor. If it is assumed that the galactic field model were perfect, then the normalization factor would only be the difference in the total angular coverage between the model and the 2006 Megacam pointings. This scaling factor based on the field-of-view for the data is 18.6%. This suggests that the model over-predicts the number of field contaminants we should detect by at least $\sim 7\%$. As seen in Figure 5.4, the model $(i - J)$ color-magnitude diagram reproduces the broad features found in the data. Under more scrutiny, the

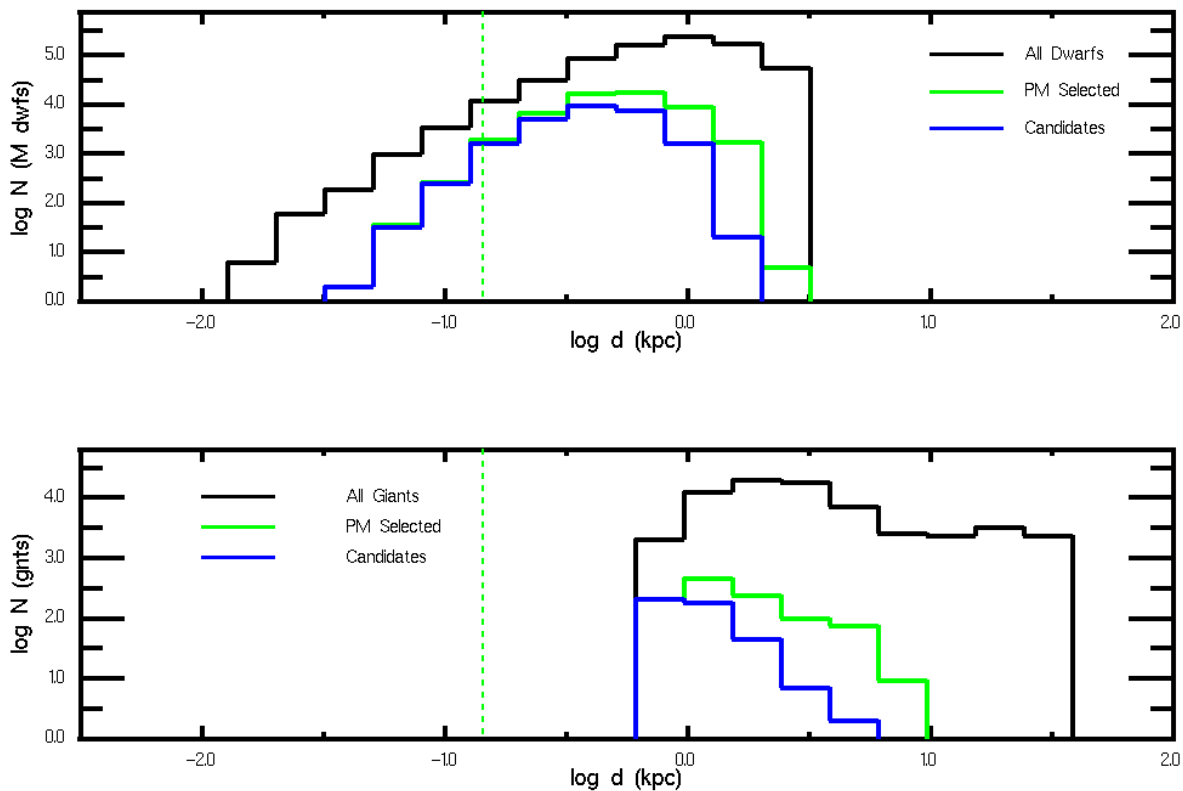


Figure 5.1 *Top*: Distance histogram of the Robin et al. (2003) galactic field population model scaled to the Taurus dataset as a function of i magnitude ($i = 14.5 - 20.5$). The black line includes all field dwarfs, the green line are only those dwarfs that pass the proper motion criteria, and the blue line passes both the kinematic and color criteria for Taurus members (assuming zero extinction). The green dashed line marks the location of Taurus (146 pc). *Bottom*: Distance histogram for the modeled field giants, with the same cuts as those above. The peak of the field population masquerading as Taurus members (the vast majority of which are M dwarfs) lies $\sim 200 - 900$ pc behind the Taurus cluster.

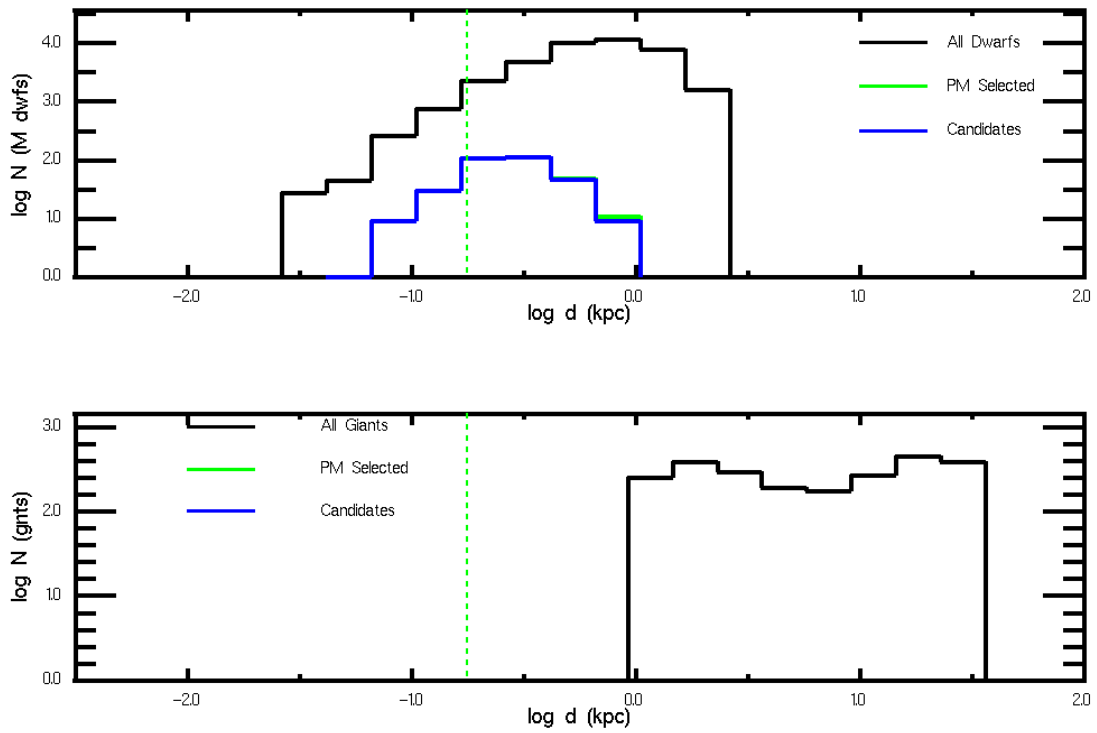


Figure 5.2 Similar as Figure 5.1 for the field in the direction of Praesepe. The cluster lies at a distance of 176 pc. No giants are selected from the field.

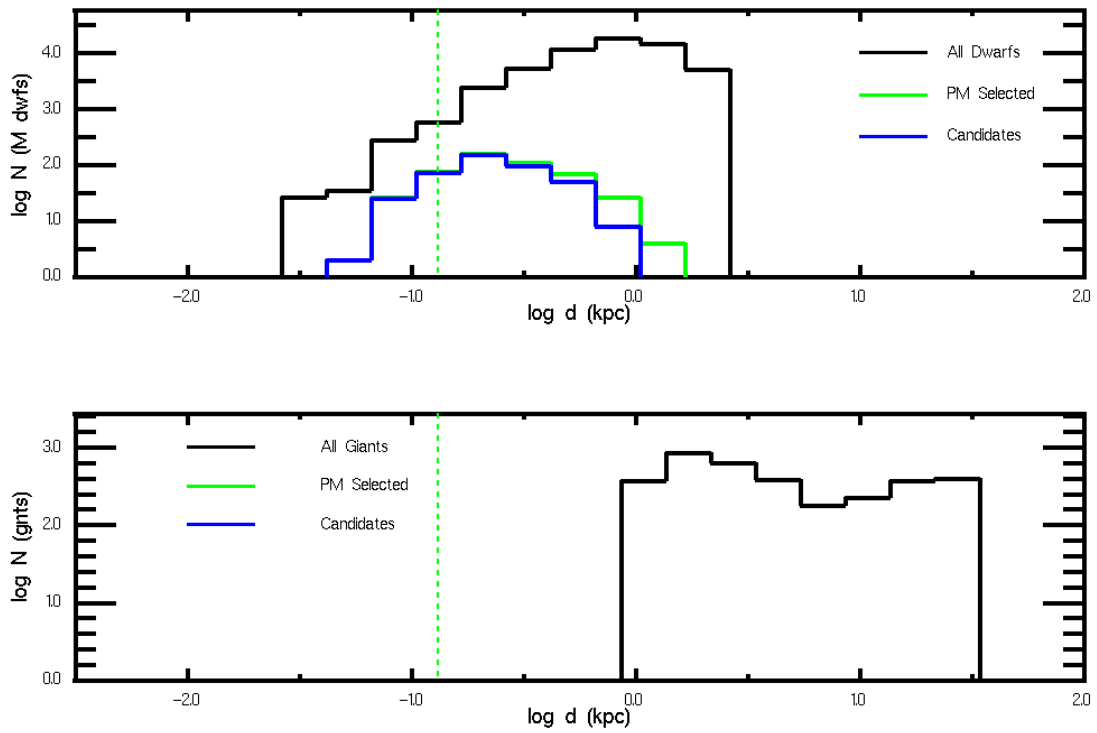


Figure 5.3 Similar as Figure 5.1 for the field in the direction of the Pleiades. The cluster lies at a distance of 130 pc. No giants are selected from the field.

model possesses relatively more objects at the brightest magnitudes and bluest colors, while there are more real data objects around $i \sim 16$ and $(i - J) \sim 1.5$.

With the field model now properly reddened to match the extinction of the Taurus region, the population was run through the same selection criteria as the data. The resulting color-magnitude and vector-point diagrams can be seen in Figure 5.5. The density gradients of candidates across both proper motion and color space appear similar, save for an abundance of fainter, redder objects in the model when compared to the observations. Upon examination, these objects are largely distant early-to-mid M field dwarfs that have been reddened by the Taurus cloud. As seen in Figure 5.6, modeled M0-M2 field dwarfs span the entire i magnitude range of our data, while M3-M4 field dwarfs are less common at $i < 17$. M5-M6 field dwarfs are largely fainter than $i \sim 18$, and the latest M field dwarfs are not selected at magnitudes brighter than $i \sim 19$. To pass the proper motion cut, a contaminating mid-M field dwarf would have to be at a distance of $d > 200$ pc behind Taurus, at which point it would become too faint to be at $i < 17$. Similarly, if the dwarf was close enough to be measured at $i < 17$, its typical proper motion then becomes too discrepant from Taurus to pass the proper motion cut. We can thus conclude with even greater confidence that any of the Taurus member candidates fit to M3-M4 (M5-M6) spectral types and brighter than $i \sim 17(18)$ are indeed cluster members and not line-of-sight field dwarfs.

5.2.2 Praesepe & The Pleiades

The same normalization and random draw method was also performed on the field models corresponding to the positions of Praesepe and the Pleiades. However, both clusters are substantially older than the Taurus region, and most of their residual gas and dust has dispersed. This results in negligible reddening towards both clusters, and our reddening scheme did not substantially affect the final colors of the model objects. The field models for both Praesepe and the Pleiades reproduced our photometric data well, with the ratio of the number density of data objects to model objects being of order unity across all but the bluest colors (see Figures 5.7 and 5.8). Upon inspection of the selected candidates, the data objects appear more tightly concentrated about the cluster motion than the field objects (Figures 5.9 and 5.10). This is a very encouraging indicator that the extracted candidates from the data are cluster members all possessing the same motion as the (now dispersed) molecular cloud that birthed them. By contrast, the field objects about Praesepe appear slightly more concentrated towards the upper-left of the diagram (i.e., towards the zero point on the diagram). Contamination from the field is minimized for these clusters because, unlike Taurus, their motion is very different than that of the surrounding field. It is difficult for any M-type field objects to mimic

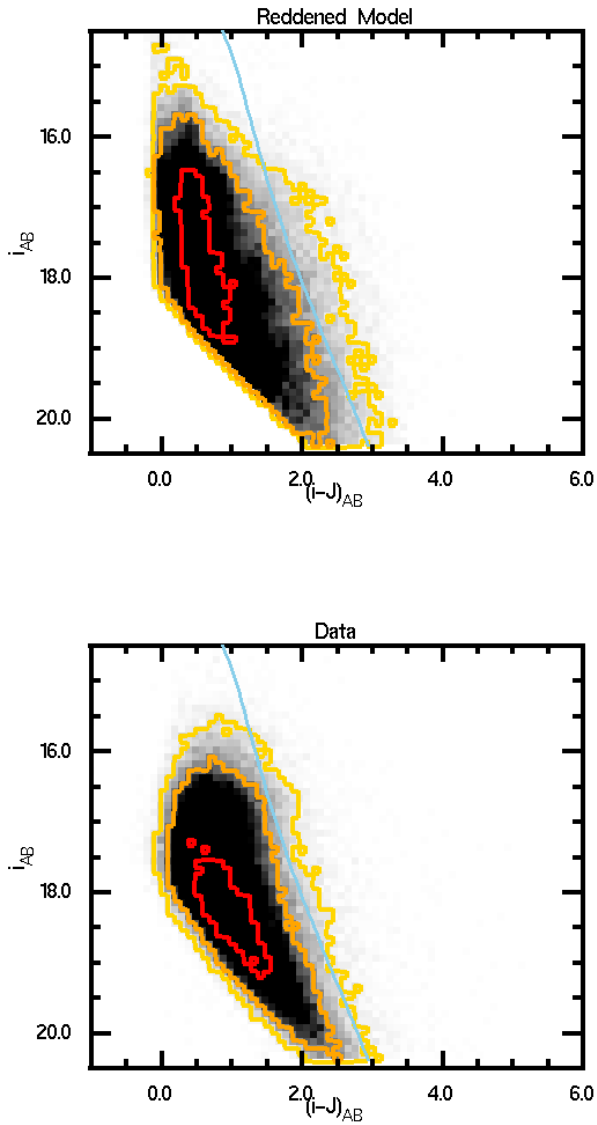


Figure 5.4 A comparison of the $(i - J)$ colors of our Galactic Field model (top) vs. the actual Taurus data (bottom), with the same contours and isochrone as in Figure 3.4. The model over-predicts the number of field objects at the brightest i magnitudes and bluest colors. On the other hand, the data objects are more populous than the model around $i \sim 16$ and $(i - J) \sim 1.5$.

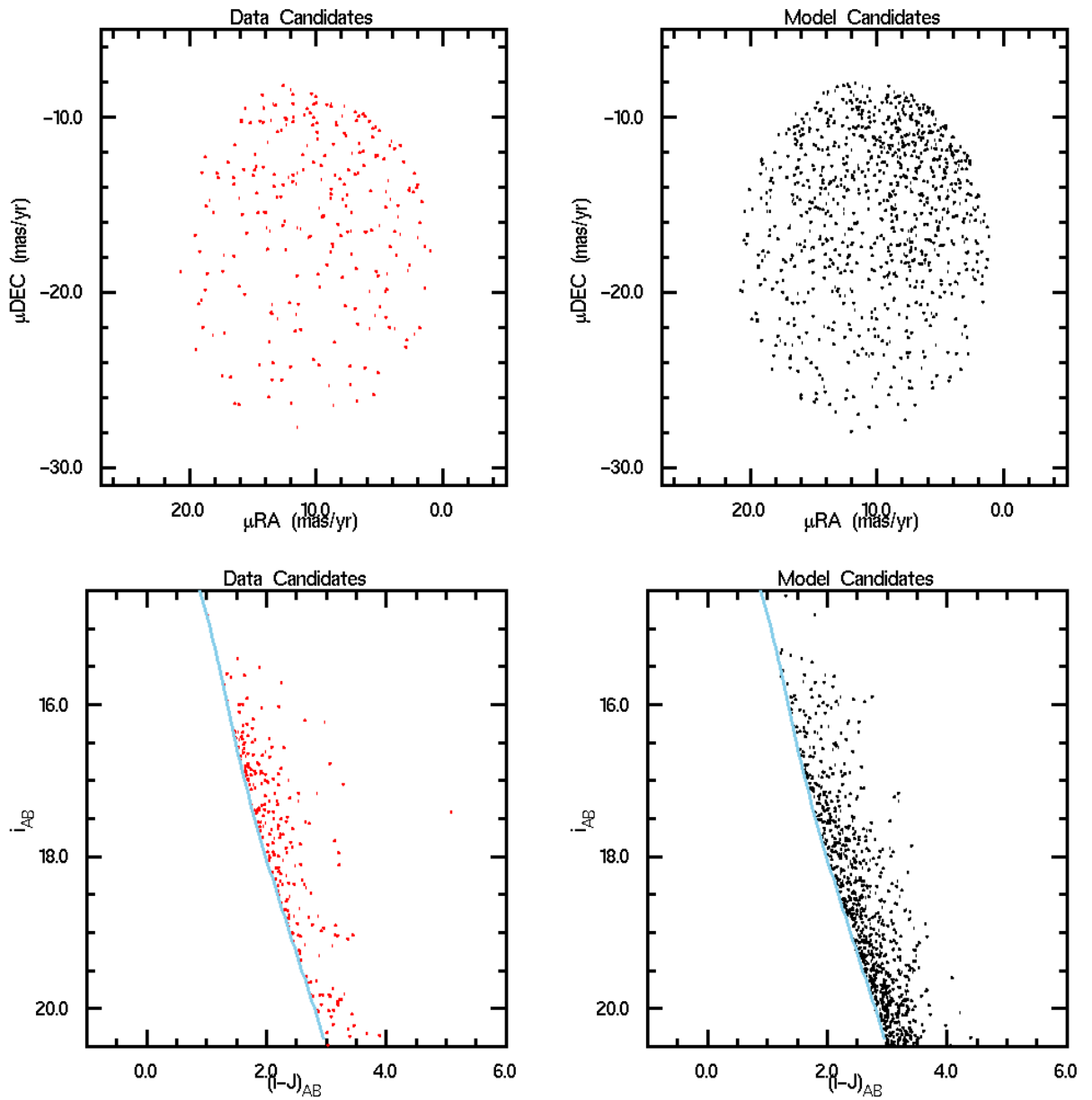


Figure 5.5 The proper motions and colors of the Taurus member candidates (left) and modeled field objects also selected out as candidates (right). The false positives from the galactic field are dominated by reddened early-M dwarfs.

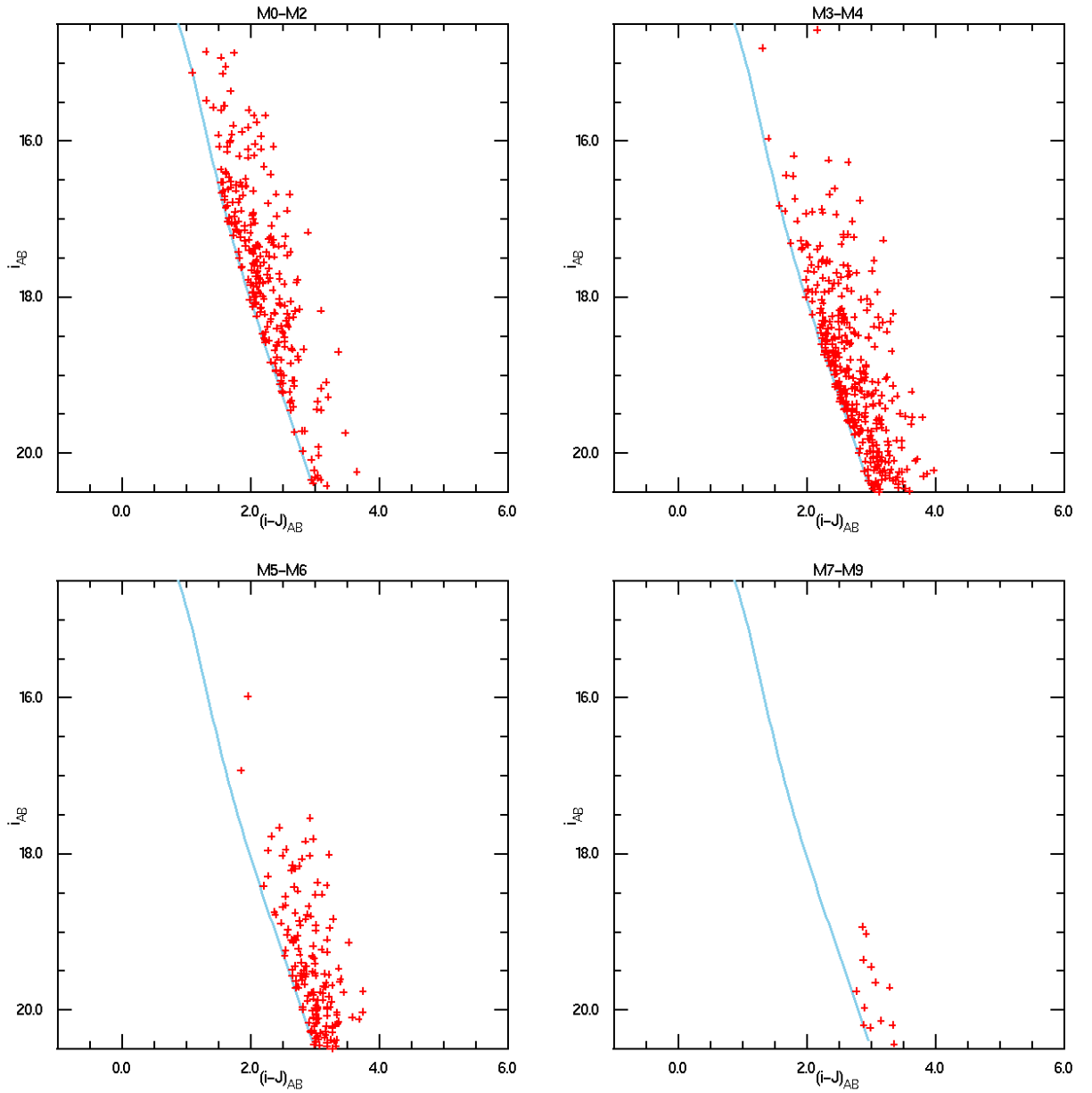


Figure 5.6 The distribution of the modeled M field dwarfs selected as member candidates. The bright limit for the mid-M and late-M field objects is determined not only by their intrinsic brightness, but also by their typical distances behind the Taurus cluster ($\sim 200 - 900$ pc).

this proper motion and yet also pass the color selection and lie within the magnitude limits. Due to the lack of extinction, modeled M0-M2 objects chosen as candidates of either Praesepe or the Pleiades remain clustered at higher i magnitudes ($i \sim 15 - 17$). Similar to Taurus, upper limits in i magnitude for the M3-M9 model candidates are seen. This is due to the fact that all three clusters are contaminated mostly by background M field dwarfs located at distances of several hundred parsecs behind the cluster itself. However, given the larger ages of Praesepe and the Pleiades, finding mid-M member candidates about $i \sim 16$ is not as likely as in Taurus. Members of Praesepe and the Pleiades have had sufficient time to contract towards the main sequence, reducing their apparent magnitude and making them appear much more closer to field objects in color-space. In such cases, it is the kinematic selection that contributes the most in reducing field contamination.

5.3 The Overabundance of “Mid-M” Candidates

The normalized, random draw from the model population was repeated 10,000 times for each cluster in order to determine the mean number of the modeled field objects selected using the proper motion and color criteria. These results are compared along side the various data cuts for M-type objects (Table 5.1), as well as earlier type contaminants (Table 5.2). The spectral types of the data candidates not followed-up with spectroscopy are estimated by using the same spectral type vs. $(i - J)$ relation used to generate the field model J magnitudes. Across all types earlier than M7, the model candidates in Taurus number higher than the data candidates, confirming that a confident claim of cluster membership for early-to-mid M candidates cannot be made solely by using kinematic and color criteria. The numbers of modeled field objects selected compared to the real member candidates for Praesepe and the Pleiades are comparable, which is another indication that the field is being excluded more significantly by the proper motion criteria. In all clusters, the color selection is more effective at ruling out $< M2$ objects as contaminants, while the proper motion cut is more selective at later-type objects. The former effect is caused by the bluer colors of earlier-type objects. The latter trend is due to mid-to-late M objects being intrinsically fainter compared to both earlier-type field dwarfs as well as the younger cluster members, meaning they must be closer to the cluster to be detected within the i magnitude range. However, as mentioned previously, at these closer distances the field objects no longer behave kinematically like the cluster, and will be more likely to fall outside the proper motion selection radius. By plotting the estimated spectral types of all of the Taurus member candidates versus the model spectral types as a function of i magnitude (Figure 5.11), an overabundance of M5-M6 spectral types is indeed present and

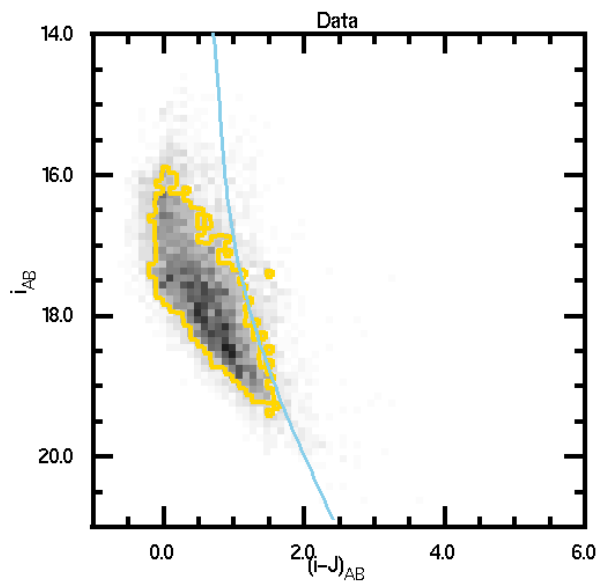
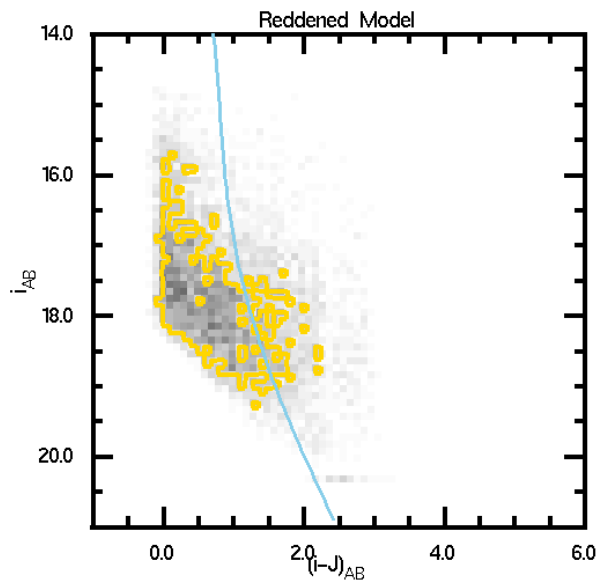


Figure 5.7 A comparison of the $(i-J)$ colors of our galactic field model (top) vs. the actual Praesepe data (bottom), with the same contour and isochrone as in Figure 3.5. The model reproduces the number density of the data across most magnitudes and colors.

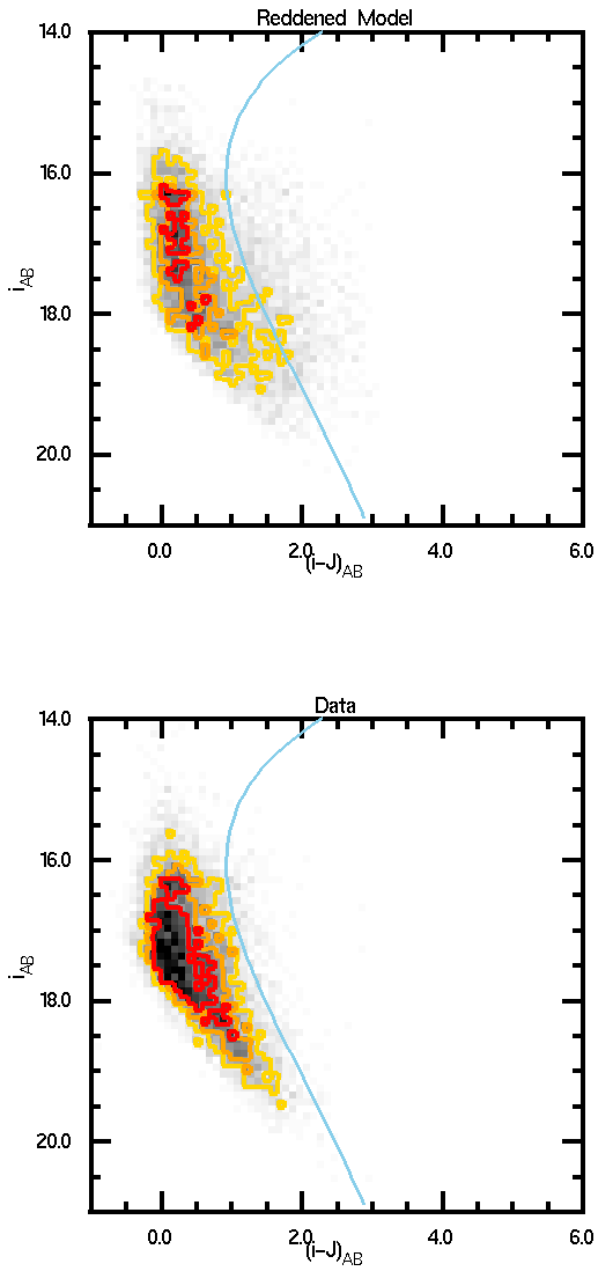


Figure 5.8 A comparison of the $(i - J)$ colors of our galactic field model (top) vs. the actual Pleiades data (bottom), with the same contours and isochrone as in Figure 3.6. The model tends to under-predict the density of objects at blueward colors, but reproduces the data well around the color cut (i.e., the plotted isochrone).

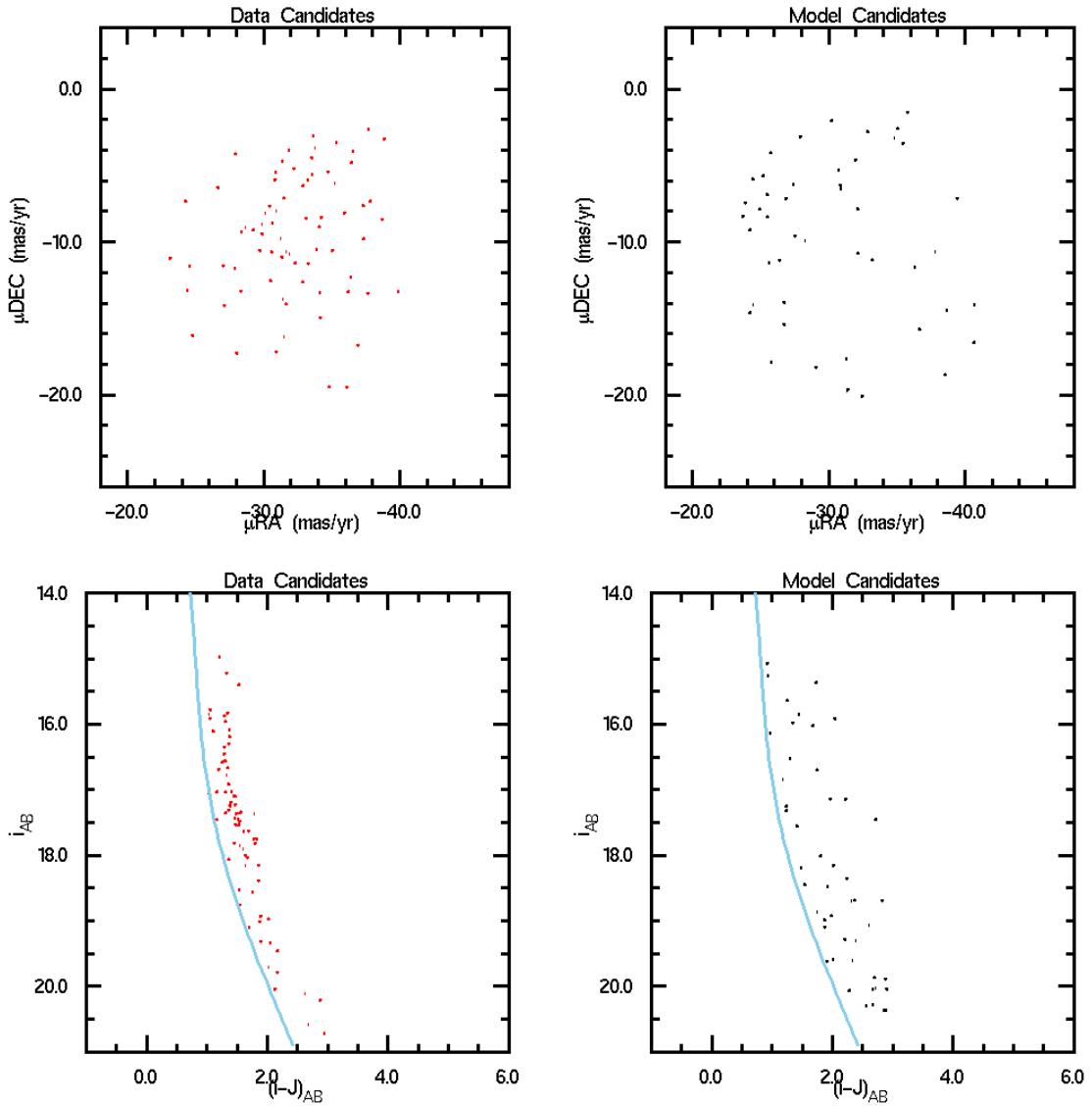


Figure 5.9 The proper motions and colors of our Praesepe member candidates (left) and modeled field objects selected out as candidates (right). Note the apparent over-density of field objects in the upper-left area of the modeled vector-point diagram. This area is in the direction of the origin (i.e., the bulk of the field population) and shows the potential variation of field contamination as a function of proper motion.

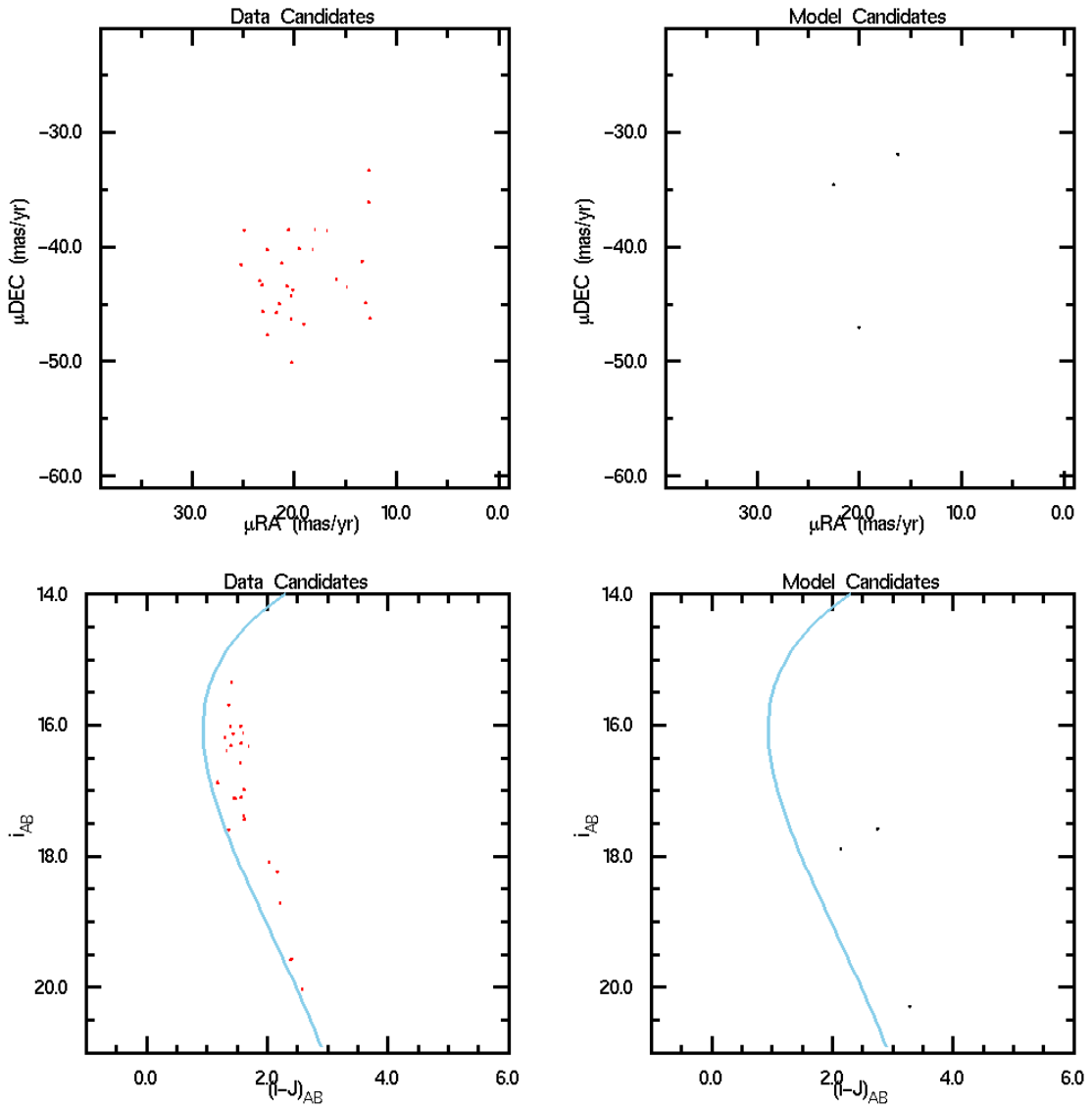


Figure 5.10 The proper motions and colors of our Pleiades member candidates (left) and modeled field objects selected out as candidates (right). Note the highly “clumped” appearance of the data objects in proper motion space.

is centered about $i = 16.5$. These candidates would thus have a higher priority in subsequent spectroscopic follow-up. SED-fits to mid-M spectral types for such candidates would prove highly conclusively that they would indeed be additional cluster members. Three of the brightest Taurus candidates claimed as new members in this work (#127, #129, & #194) are in fact fit to mid-M spectral types and have an i magnitude in this range.

Table 5.1: M-Type Candidates Selected

Candidate Population	M0-M2	M3-M4	M5-M6	M7-M9
Taurus				
Quality Selected ¹	25110	18722	9996	3194
Color Selected ¹	10	340	858	706
PM Selected ¹	879	1148	829	269
Color+PM Selected ¹	1	25	69	70
Color+PM Model ²	263 ± 15	373 ± 24	163 ± 17	15 ± 4
Measured SpT ³	5	21	14	15
Praesepe				
Quality Selected	1770	876	226	29
Color Selected	128	320	171	28
PM Selected	34	44	16	5
Color+PM Selected	9	37	14	4
Color+PM Model	8 ± 3	11 ± 4	13 ± 5	3 ± 2
The Pleiades				
Quality Selected	1678	675	230	19
Color Selected	91	105	55	10
PM Selected	11	16	3	2
Color+PM Selected	2	14	2	2
Color+PM Model	1 ± 1	3 ± 2	3 ± 2	2 ± 2

¹Spectral types are estimated based on the measured ($i - J$) colors

²Model scaled by 0-24.6% based on i magnitude; Listed values are the mean and standard deviation after 10^4 random selections

³The combined total of our candidates with spectroscopic follow-up and the previously claimed Taurus members with measured spectral types that have also been selected as member candidates

Table 5.2: Early-Type Contaminants Selected

Candidate Population	F-Types	G-Types	K-Types
Quality Selected ¹	133	1116	25283
Color Selected ¹	0	0	0
PM Selected ¹	0	7	398
Color+PM Selected ¹	0	0	0
Color+PM Model ²	0	0	45 ± 6
Measured SpT ³	2	5	21
Praesepe			
Quality Selected	340	834	2880
Color Selected	0	0	0
PM Selected	4	10	34
Color+PM Selected	0	0	0
Color+PM Model	0	0	1 ± 1
The Pleiades			
Quality Selected	661	1444	4116
Color Selected	0	0	0
PM Selected	1	2	3
Color+PM Selected	0	0	0
Color+PM Model	0	0	0 ± 1

¹Spectral types are estimated based on the measured ($i - J$) colors

²Model scaled by 0-24.6% based on i magnitude; Listed values are the mean and standard deviation after 10^4 random selections

³The combined total of our candidates with spectroscopic follow-up and the previously claimed Taurus members with measured spectral types that have also been selected as member candidates

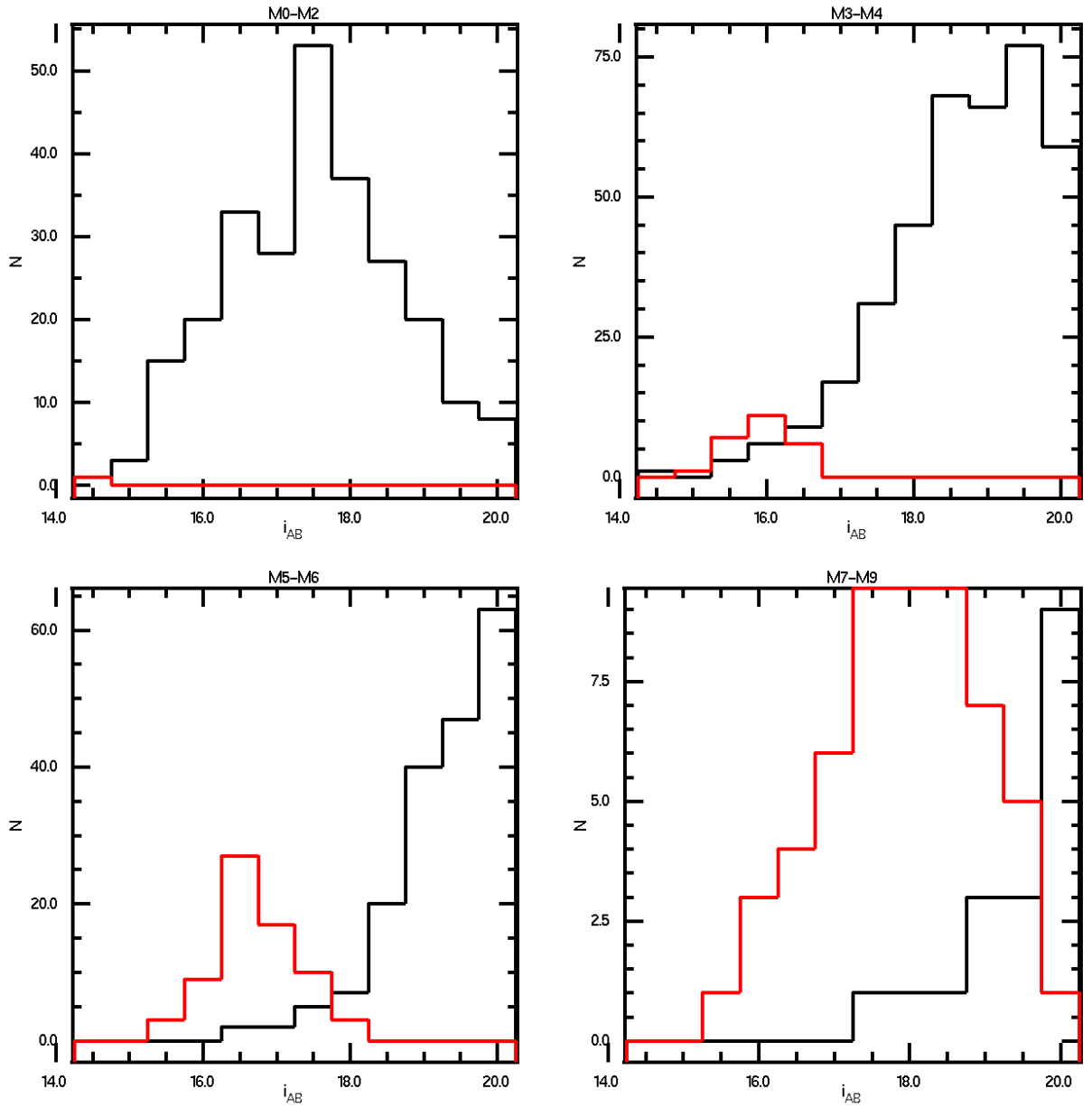


Figure 5.11 Spectral type histograms as a function of i magnitude for the data (red) and the field model (black). The abundance of data objects estimated to have mid-to-late M types and $i \sim 16-18$ suggests a significant amount of Taurus members.

Chapter 6

Discussion

By establishing confidence in the classification of the follow-up candidates and characterizing the sources of contamination from the galactic field, conclusions can now be drawn concerning the effectiveness of the candidate selection, additions to the mass functions of the target clusters, and the status of previously claimed cluster members recovered in the data. Overall, the precision astrometry achieved by the Pan-STARRS IPP on Megacam imaging data has yielded promising returns in the reduction of cluster member candidates from those of color selection alone. It also allows for effective spectroscopic follow-up, especially for kinematically distinct clusters such as Praesepe. On the other hand, the method of using i -band magnitudes for a wide-area survey limits the detectability of both highly embedded sources, as well as the lowest mass members. While at zero extinction it was predicted that objects down to an early-L spectral type could be detected in the youngest target cluster (i.e., Taurus), no such objects were found within the spectroscopic follow-up. However, this is likely due in part to the follow-up strategy itself, which gives preference to brighter candidates.

6.1 Properties of Identified Members

If all the candidates claimed in this work to be cluster members are indeed bona fide, then the follow-up efficiency as defined in Chapter 1 is 19% for Taurus, 54% for Praesepe, and 29% for the Pleiades. All but one of the new cluster members lie within the M3-M5 range, though known Taurus members were recovered as late as M8-M9. In general, the overall confidence of candidate membership increases towards later spectral types where both the SED-fit and spectral index measurements more clearly distinguish cluster members from field objects. However, the kinematic argument stated in Chapter 5 provides additional confidence in the membership of mid-M spectral types if their apparent i magnitudes lie above the majority of the galactic field that is mimicking

the motion of the foreground cluster. Across the spectral type range at which cluster membership can be reasonably determined with this selection method ($\geq M3$), the addition of a kinematic cut to the color criteria results in a reduction of the candidate pools for all three clusters by $\sim 92\%$. This order-of-magnitude reduction in the total number of member candidates allows for more effective spectroscopic follow-up. This is not only accomplished by simply reducing the size of the candidate pool, as the addition of more strenuous color criteria has been applied in previous cluster searches to also achieve such a reduction. Rather, the addition of proper motion criteria enables effective searches within areas of the color-space normally overwhelmed by field contamination. For example, NIR color-selection by Guieu et al. (2006) is more effective at identifying members that are redder than the bulk of field objects. On the other hand, many of our new members are selected at somewhat bluer colors and were not recognized by Guieu et al. (2006) as members despite lying within the color cut (Figure 6.1). Indeed, many of the new members listed in this work across all three clusters lie in NIR regions completely dominated by background objects and would be much more difficult to recognize using color selection alone (Figures 6.1-6.3).

The results of this work provide additional mid-M members to all three clusters. In Taurus, the 11-15 new members represent a 10-13% increase in the known IMF across the M3-M5 range (see Figures 6.4 and 6.5) when compared to the full Taurus membership as reported by Luhman et al. (2009). However, this can be regarded as a lower limit when considering the limited spatial coverage of Taurus in this study. If only Taurus members within the 2006 epoch field-of-view are considered, the IMF contribution of new members increases to 16-21%. Given the above argument for proper motion selected member candidates with $i \sim 16$ and brighter, the contribution can rise even higher with additional spectroscopic follow-up if such candidates are shown to have a mid-M spectral type (i.e., there are ~ 60 Taurus member candidates in this study with these attributes). These results are suggestive that the higher mass turn-over point of the IMF in Taurus as compared to other young clusters as claimed by Luhman et al. (2009) may not be as distinct as previously believed. If there is truly a previously unrecognized (but substantial) population of mid-M objects in the Taurus membership, then the relative abundance of M-type members to earlier-type members becomes more similar to other young clusters such as IC 348 and Chamaeleon I.

Praesepe has on the order of ~ 500 members within the same M3-M5 range as the new members presented here according to Kraus & Hillenbrand (2007). Thus, the new members reported here do not add as significantly to the overall cluster mass function (3-4%). This is due in part to previous extensive studies of Praesepe that have also relied primarily on proper motions to cull their candidates. Boudreault et al. (2010) compared their own calculated mass function of Praesepe with

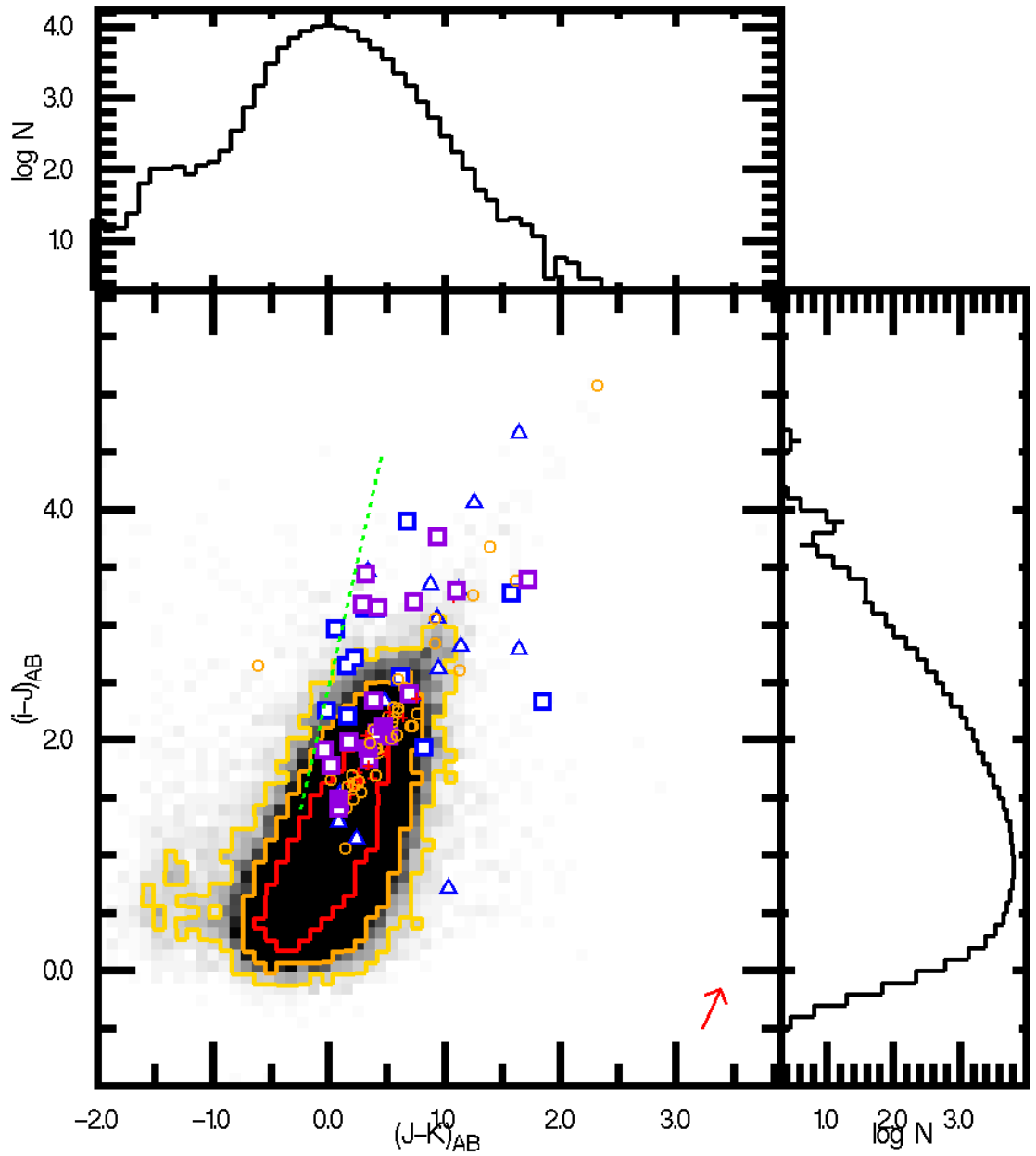


Figure 6.1 An $(i-J)/(J-K_s)$ color-color diagram with the same symbols and labels as Figure 4.3, along with corresponding color histograms. The dashed green line shows the cut made by Guieu et al. (2006) when selecting Taurus member candidates. Slightly less than half of the claimed Taurus members in this work lie in and around the area of highest contamination from the field.

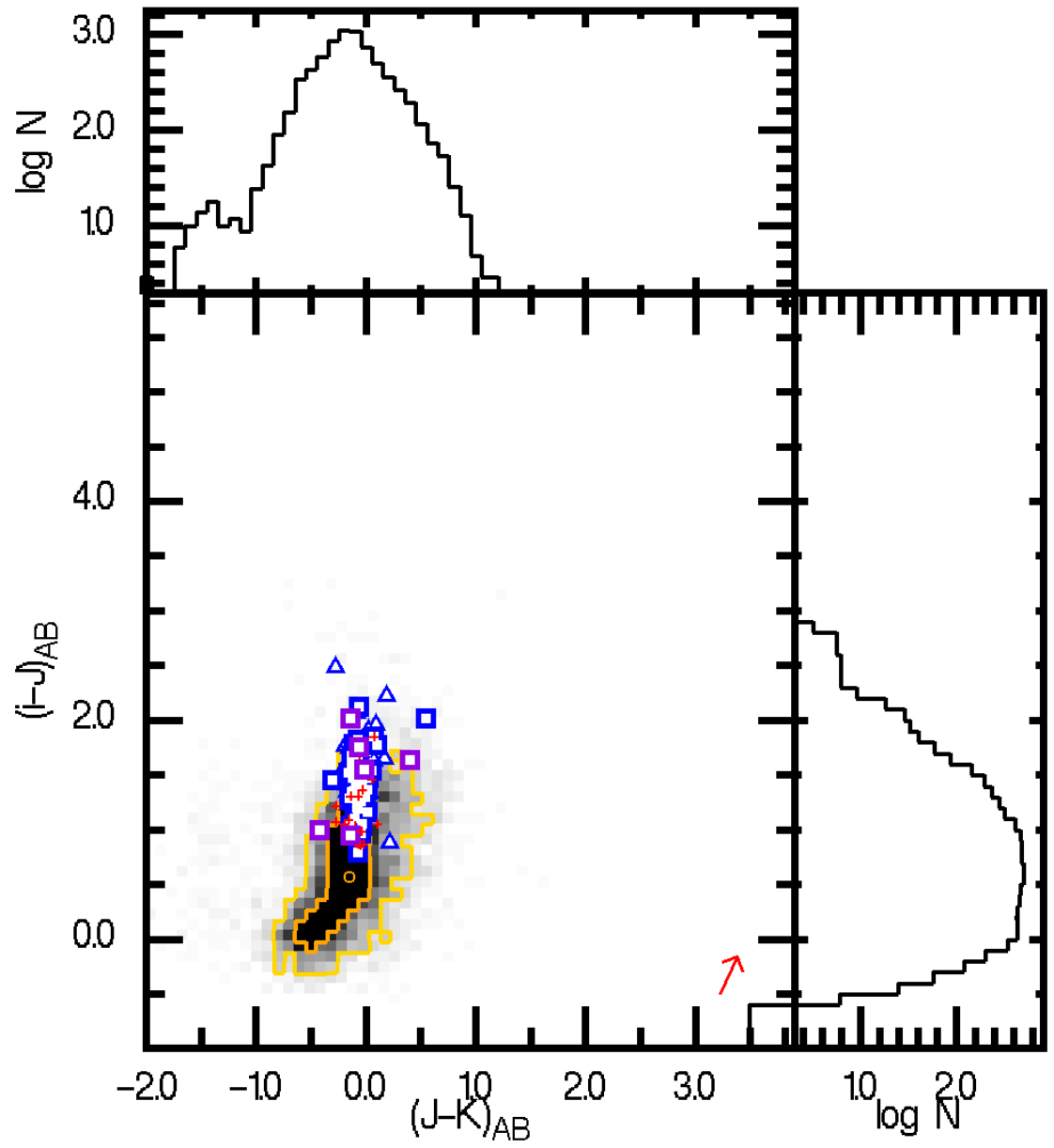


Figure 6.2 An iJK_s color-color diagram of the Praesepe data with the same colors and labels as Figure 4.5, along with corresponding color histograms.

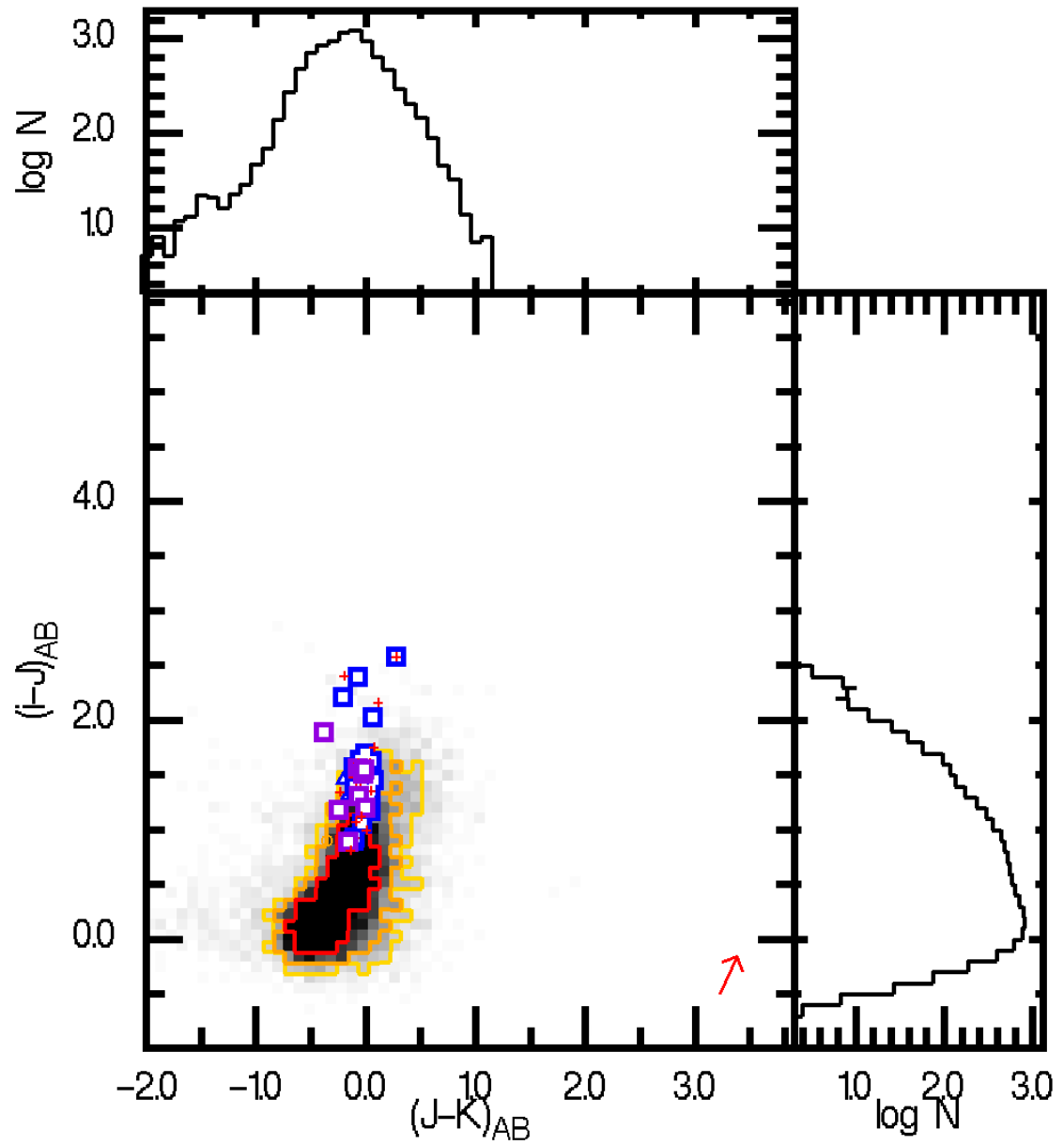


Figure 6.3 An iJK_s color-color diagram of the Pleiades data with the same colors and labels as Figure 4.7, along with corresponding color histograms.

others published from as early as 1995. The majority of these IMFs agree in shape and consistently rise from $0.6M_{\odot}$ to a turn-over at $0.1M_{\odot}$. The new Praesepe members presented in this study congregate about $i \sim 18.5$, which according to the BC models, corresponds to the $0.1M_{\odot}$ peak. Thus, it is not surprising that the relatively few new members identified in this work come from the most numerous part of the cluster population.

The 8-17 new members of the Pleiades also represent a few percent increase of the known cluster population as reported by Lodieu et al. (2007). Their measurement of the cluster IMF peaks about a mass of $0.2M_{\odot}$, and 4 out of the 8 candidates determined here to be confident members have an i magnitude that corresponds to approximately this mass in the BC models. The remaining confident members dwell about the substellar boundary, and some may in fact be high-mass brown dwarfs.

6.2 Properties of Identified Non-Members

While Luhman & Mamajek (2010) have identified background galaxies as the most pervasive contaminant in brown dwarf cluster member searches, within this work it is instead M field dwarfs along the line-of-sight that are contributing the most contamination to the candidate list. This is clear from both the spectroscopic follow-up itself, as well as in the applied galactic field model. The next most common contaminants in both the field model and the follow-up results are background K-type objects that have been reddened (mostly by the Taurus cloud). According to the field model, such K contamination should be rare compared to the M-types. Given the spectral typing errors stated in Chapter 4, many candidates SED-fitted to late-K dwarfs may in fact be early-M field dwarfs. Contaminants fit to the earliest types (i.e., F objects) were included in the very first round of follow-up due to the crude estimation of the Taurus 5-Myr isochrone. The revised fit now excludes most of these candidates as too blue in $(i - J)$ to be selected. As might be expected, the largest percentage of contaminants within a follow-up sample was in Taurus, which lies closest to the bulk galactic population in proper motion space. Because care was taken to exclude known nonmembers from our spectroscopic follow-up, only a single candidate identified here as a Taurus nonmember has been matched to a previous study. Candidate #188 has been confirmed as a background field star by Shenoy et al. (2008). While DVO flags detections as point sources or extended sources, these flags were not utilized when extracting member candidates. It is an additional indication of the precision of the IPP astrometry that at no stage of the analysis have any of the candidates been identified as a background galaxy.

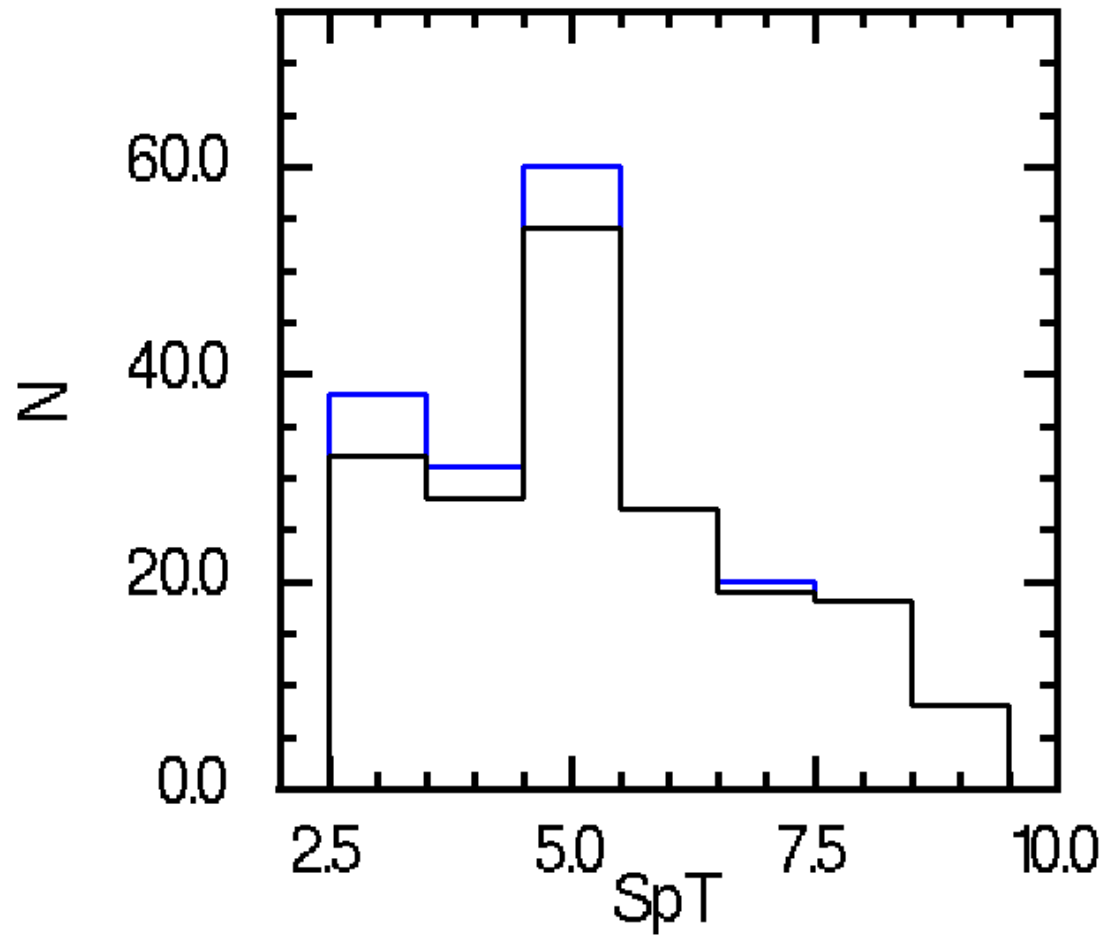


Figure 6.4 The total known membership for Taurus (black) with spectral types M3-M9 from Luhman et al. (2009). The contributions shown can be considered a lower limit, as this study only observed about 10% of the total area of the Taurus cluster, and some of the highest extinction regions were not searched for new members.

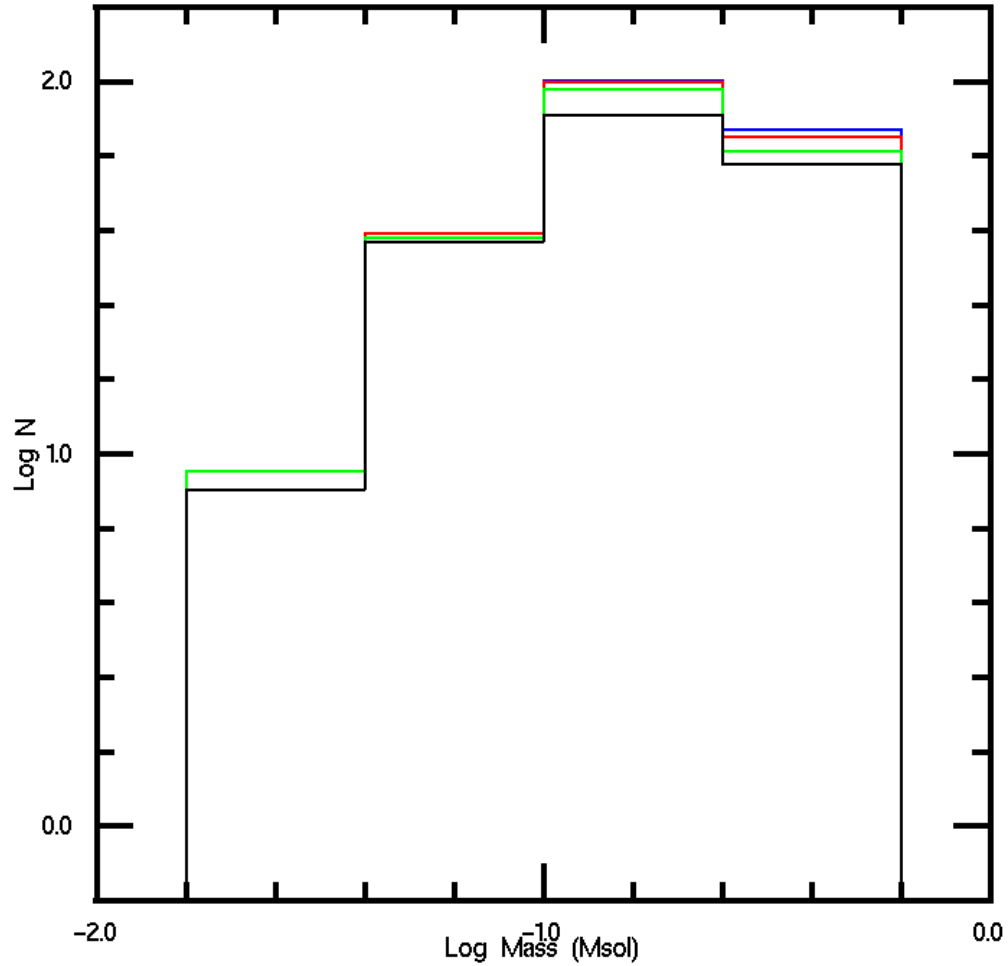


Figure 6.5 The total known IMF for Taurus (black) across the range of masses corresponding to M3-M9 spectral types according to the BC Models (Luhman et al., 2009). The newest contributions by the “A+” member candidates of Rebull et al. (2010) are given by the green histogram. The red histogram marks the new, confident members of this study, while the blue one includes the potential cluster members. According to the literature, the Taurus IMF is believed to be complete for $<M8$ ($m \geq 0.04M_{\odot}$).

6.3 Properties of Previously Claimed Members

A search of the literature for low-mass member searches of Taurus yielded 283 objects in the M spectral type range (Table A.1), of which 212 are M3-M9. For comparison, Luhman et al. (2009) claim 186 Taurus members for this spectral range within their IMF calculations. Given that our 2006 Megacam pointings cover $\sim 10\%$ of the total sky coverage of Taurus, a subset of 121 low-mass members are within the field-of-view of the image data, and 109 are detected on multiple observations ($N_{det} \geq 5$). Due to the range of spectral types and the variable reddening of the Taurus cloud, some of these claimed members are either saturated or too faint to possess robust DVO measurements of their proper motion. Others were only imaged during a single epoch, making a proper motion measurement impossible. Thus, there are 31 previously claimed members that have well-measured proper motions by the DVO software, and 18 of those remain after passing them through the same quality cut as that used for the member candidates of this study. If earlier-type members are included, then this sample increases to 32 known Taurus members. These earlier-type objects also passed the quality data selection, and were used to provide a more robust proper motion measurement for Taurus (as described in Chapter 3). Since proper motion is not thought to be heavily dependent on spectral type when considering a dynamically young cluster, these $\leq M2$ members should not possess a wildly different motion than their fellow, later members.

Sixteen of these claimed members congregate about a common proper motion vector. One additional object is just outside the selection radius. Within the stated errors of the proper motion measurements, this object could also be considered to have a motion reasonably consistent with the cluster, resulting in 17 previously claimed cluster members that pass the proper motion criteria. All but one of these PM-consistent members are listed as members in recent Taurus studies by Luhman et al. (Luhman et al., 2009; Luhman, 2006; Luhman et al., 2006). Evidence of membership consists primarily of the detection of emission lines indicating on-going accretion, as well as spectral index measurements showing an intermediate surface gravity (see Table 6.1). The other proper motion member is noted in Rebull et al. (2010), and is classified as a highly confident result (rank A+) based on mid-IR color selection and optical spectroscopic follow-up. The claimed members who do not have a motion consistent with Taurus fall into two general categories: 1) those with a measured proper motion close to zero (consistent with the distant galactic field), and 2) those with highly discrepant motion (consistent neither with Taurus nor the distant field). Seven members are in the near-zero group, including two listed as well-known cluster members in Luhman et al. (2006): PSC 04154+2823 and V410 X-ray 5a. The remaining objects are listed in Rebull et al. (2010)

as poorer candidates (rank B+ to C-) that still lacked sufficient follow-up to be confident of their member status. In addition, two of these Rebull candidates have extremely blue ($i - J$) colors (see Figure 4.3), casting further doubt on their membership. Thus, these Rebull candidates are likely not to be members of the Taurus cluster. The highly discrepant group consists of 8 objects from the Luhman studies, Rebull et al. (2010), and one from Briceño et al. (2002). Among these odd-behaving objects are KPNO 2, KPNO-Tau 9, IRAS 04166+2706, and IRAS 04264+2433, all of whom are also listed as well-established members. The Rebull objects have high rankings (A+ to B-) and one of them is concluded with high confidence to be a Taurus member. It remains to be seen if the bizarre motions of these objects are due to actual intrinsic velocities of the objects, or the result of factors that can skew the proper motion measurement (e.g., astrometric error, nebulosity, or binary motion). However, if these motions can be confirmed, then either these objects are not true cluster members, or they have had dynamical encounters that have changed their motion significantly when compared the rest of the cluster.

Of the 481 M-type Praesepe members listed in Table A.2, 452 lie within the Megacam field-of-view. Similar to the Taurus results, saturation and single-epoch detections reduce the amount of previously claimed members with well-measured proper motions down to 118 objects. As mentioned in Chapter 3, these objects can be separated into a tightly packed population in proper motion space and a widely scattered halo. Metrics on how consistent these objects are in proper motion with the Praesepe cluster are provided by both Adams et al. (2002) and Kraus & Hillenbrand (2007). The former uses a functional fit to the cluster in proper motion space that gives a probability based on an object’s distance from the mean cluster motion. Significant member candidates are given as having a probability of $p \geq 0.2$. The authors note that their method is sensitive to field contamination due in part to their wide magnitude range of study ($8.5 \leq K_s \leq 15$). Kraus & Hillenbrand (2007) utilize a metric that takes into account both the candidate’s spatial location and proper motion. They describe “high-probability” candidates as having a membership percentage of $P_{mem} \geq 80\%$.

For the Praesepe population matched to objects in this study that are consistent with the bulk cluster motion, the mean probability for membership given by Adams et al. (2002) is $p = 0.463 \pm 0.019$. The same metric for the scattered population is $p = 0.431 \pm 0.028$. Using the Kraus & Hillenbrand (2007) metric, the results for the tightly-packed and halo populations are $P_{mem} = 98.0 \pm 0.5$ and $P_{mem} = 96.9 \pm 0.5$, respectively. While the population also chosen as candidates by this study possesses the higher probability value using both metrics, neither is significantly higher than about 1-sigma from the discrepant population value. For Adams et al.

(2002), this may be caused by the aforementioned field contamination ($\sim 30\%$) mimicking the motion of the cluster. In the case of Kraus & Hillenbrand (2007), their use of a selection radius twice the size of the one used in this study (20 mas/yr) would be more accepting of candidates and assign those within 10 mas/yr of our selection boundary a higher probability. As one might expect, the primary evidence of cluster membership in the literature for these objects is proper motion, although some members possess additional spectroscopic evidence from spectral indices and significant H α emission (see Table 6.2).

A total of 111 previously claimed low-mass members of the Pleiades lie within the Megacam fields of this study (Table A.3), of which 26 have well-measured proper motions. Nearly all are located near the bulk motion of the cluster, and have been identified as members by Bihain et al. (2006) and Lodieu et al. (2007). Both studies cite color and proper motion selection as the primary evidence of membership.

Table 6.1: Previously Claimed Members of Taurus

ID	Other Name(s)	RA ¹	DEC ¹	PM ²	$\mu_{\alpha \cos(\delta)}$ ³	μ_{δ} ³	Evidence ⁴	References ⁵
2231	...	04 18 01.10	+28 35 26.0	No	3	4	<i>MIR(B+), III, BI</i>	REB10
759	J04183203+2831153 PSC04154+2823	04 18 32.03	+28 31 15.3	No	2	-7	Arch	LUH06b
767	J04185115+2814332 KPNO2	04 18 51.15	+28 14 33.2	Yes	7	-21	<i>SED, SI</i>	LUH06a, BRI02
768	J04185147+2820264 KPNO-Tau 2	04 18 51.47	+28 20 26.4	No	-17	-60	Arch	LUH06b, KRA09
769	J04185813+2812234 PSC04158+2805 IRAS04158+2805	04 18 58.13	+28 12 23.4	Yes	13	-29	<i>e, ex, Av, NaK, SI</i>	LUH06a, KRA09
772	J04190197+2822332 V410X-ray5a	04 19 01.97	+28 22 33.2	No	2	-4	Arch	LUH06b, KRA09
777	J04194148+2716070 IRAS04166+2706	04 19 41.48	+27 16 07.0	No	62	-155	<i>e, ex</i>	LUH06a
779	J04214631+2659296 CFHT10	04 21 46.31	+26 59 29.6	Yes	14	-16	<i>Av, NaK</i>	LUH06a, KRA09
780	J04215450+2652315	04 21 54.50	+26 52 31.5	Yes	14	-10	<i>NaK?, SI</i>	LUH06a, KRA09

Table 6.1 (cont'd)

ID	Other Name(s)	RA ¹	DEC ¹	PM ²	$\mu_{\alpha} \cos(\delta)^3$	μ_{δ}^3	Evidence ⁴	References ⁵
2163	J04221568+2657060 XEST 11-078	04 22 15.68	+26 57 06.0	Yes	14	-15	A_V, e, ex, μ	LUH09
	IRAS 04192+2650							
2247	...	04 22 20.90	+26 42 48.0	No	-1	11	$MIR(A), I$	REB10
2251 ⁶	FS116	04 23 50.10	+26 40 06.0	No	5	1	$MIR(C), III$	REB10
792	J04242646+2649503 CFHT9	04 24 26.46	+26 49 50.3	Yes	12	-24	Li, NaK	LUH06a, KRA09
799	J04263055+2443558	04 26 30.55	+24 43 55.8	Yes	12	-21	e, NaK, SI	LUH06a
808	J04274538+2357243 CFHT15	04 27 45.38	+23 57 24.3	Yes	9	-16	NaK	LUH06a
809	J04275730+2619183 IRAS04248+2612	04 27 57.30	+26 19 18.3	No	-16	-28	e, ex, NaK, A_V	LUH06a
812	J04290498+2649073 IRAS04260+2642	04 29 04.98	+26 49 07.3	Yes	9	-12	Arch	LUH06b
2266	2MASX042905172615358	04 29 05.20	+26 15 35.0	No	-11	3	$MIR(B-), II$	REB10
817	J04293008+2439550 IRAS04264+2433	04 29 30.08	+24 39 55.0	No	-15	-84	Arch	LUH06b
821	J04294568+2630468 KPNO5	04 29 45.68	+26 30 46.8	Yes	19	-22	SED, SI, HA	LUH06a, BRI02, KRA09

Table 6.1 (cont'd)

ID	Other Name(s)	RA ¹	DEC ¹	PM ²	$\mu_{\alpha} \cos(\delta)^3$	μ_{δ}^3	Evidence ⁴	References ⁵
	KPNO-Tau 5							
826	J04302365+2359129	04 30 23.65	+23 59 12.9	Yes	8	-21	<i>NaK</i>	LUH06a,KRA09
	CFHT16							
831	J04305171+2441475	04 30 51.71	+24 41 47.5	Yes	17	-13	Arch	LUH06b
	ZZTauIRS							
836	J04312669+2703188	04 31 26.69	+27 03 18.8	Yes	19	-18	<i>NaK</i>	LUH06a,KRA09
	CFHT13							
2280 ⁶	...	04 32 14.60	+22 37 42.0	No	-4	2	<i>MIR(C), flat</i>	REB10
843	J04322329+2403013	04 32 23.29	+24 03 01.3	Yes	1	-17	<i>e, NaK</i>	LUH06a,KRA09
867	J04350850+2311398	04 35 08.50	+23 11 39.8	Yes	11	-13	<i>NaK</i>	LUH06a
	CFHT11							
2073	2M J0435514+224911	04 35 51.43	+22 49 11.9	No	23	8	<i>SED, SI</i>	BRI02,KRA09
	KPNO-Tau-9							
2293	J04355760+2253574	04 35 57.6	+22 53 57.0	Yes	7	-13	<i>MIR(A+), II</i>	REB10
880	J04363893+2258119	04 36 38.93	+22 58 11.9	Yes	11	-12	Arch	LUH06b,BRI02,KRA09
	CFHT3							
	CFHT BD-Tau 3							
2299	...	04 38 01.90	+25 19 26.0	No	13	-55	<i>MIR(A+), II</i>	REB10
2317	...	04 45 57.00	+24 40 42.0	No	0	5	<i>MIR(B-), III</i>	REB10

Table 6.1 (cont'd)

ID	Other Name(s)	RA ¹	DEC ¹	PM ²	$\mu_{\alpha} \cos(\delta)^3$	μ_{δ}^3	Evidence ⁴	References ⁵
2325	...	04 49 13.70	+25 25 49.0	No	1	6	MIR(C-), III	REB10

¹Position in J2000 coordinates²Is the object identified by this work as a proper motion candidate of the cluster?³Proper motion in units of mas/yr⁴ $I/II/III/f_{lat}$ = YSO classification based on Mid-IR SED slope, Arch = Listed as a known Taurus member without explicitly stated evidence, A_V = Source is highly reddened and lies above the zero-age main sequence of Taurus, BI = Objects noted as a possible double source or binary, e = Lines measured in emission, ex = IR excess emission, HA = High $H\alpha$ emission indicative of accretion, Li = Lithium detected in absorption, MIR = Mid-IR bands are suggestive of membership and are ranked A+ (very confident member) to C- (very unlikely member), NaK = NaI and KI lines indicate an intermediate surface gravity, SED = overall SED fit to that of an intermediate gravity object, SI = Spectral indices match those of other intermediate gravity objects⁵REB10 = Rebull et al. (2010), LUH06a = Luhman (2006), LUH06b = Luhman et al. (2006), BRI02 = Briceño et al. (2002), KRA09 = Kraus & Hillenbrand (2009)⁶Object does not pass the $(i - J)$ color criteria

Table 6.2: Previously Claimed Members of Praesepe

ID	Other Name(s)	RA ¹	DEC ¹	PM ²	$\mu_{\alpha \cos(\delta)}^3$	μ_{δ}^3	Evidence ⁴	References ⁵
1026	J08325958+2007149 AD1696	08 32 59.58	+20 07 14.9	No	-28	18	PM	KRAU07
1041	J08332348+2018032 AD1750	08 33 23.48	+20 18 03.2	Yes	-36	-13	PM	KRAU07
1045	J08332821+1843363 HSHJ41	08 33 28.21	+18 43 36.3	No	-64	-38	PM	KRAU07
1048	J08333450+1957059 AD1775	08 33 34.50	+19 57 05.9	No	-15	-3	PM	KRAU07
1067	J08342092+2031444 AD1887	08 34 20.92	+20 31 44.4	No	-15	12	PM	KRAU07
1068	J08342738+1841501 AD1904	08 34 27.38	+18 41 50.1	No	-26	-47	PM	KRAU07
1070	J08343109+2037456 AD1907	08 34 31.09	+20 37 45.6	No	-1	-26	PM	KRAU07
1086	J08351521+1922315 AD1994	08 35 15.21	+19 22 31.5	No	-29	12	PM	KRAU07
1092	J08352430+1925443	08 35 24.30	+19 25 44.3	No	-24	3	PM	KRAU07
1096	J08353613+1931583	08 35 36.13	+19 31 58.3	No	-47	-43	PM	KRAU07

Table 6.2 (cont'd)

ID	Other Name(s)	RA ¹	DEC ¹	PM ²	$\mu_{\alpha} \cos(\delta)^3$	μ_{δ}^3	Evidence ⁴	References ⁵
	HSHJ78							
366	J0835520+201558	08 35 52.07	+20 15 58.8	No	-8	4	SPEC,PM,HA,PHOT	ADAM02
1107	J08355651+2037070 AD2082	08 35 56.51	+20 37 07.0	Yes	-25	-2	PM	KRAU07
367	J0835572+192106	08 35 57.21	+19 21 06.5	No	-23	0	SPEC,PM,HA,PHOT	ADAM02,HAMB95
	HSHJ090							
362	J0835063+195648	08 35 06.34	+19 56 48.0	No	-9	16	SPEC,PM,HA,PHOT	ADAM02,HAMB95
	HSHJ067							
1111	J08360242+1904265	08 36 02.42	+19 04 26.5	No	-20	1	PM	KRAU07
	HSHJ99							
1119	J08360991+1917166 IZ031	08 36 09.91	+19 17 16.6	No	-17	-2	PM	KRAU07
369	J0836016+195731	08 36 01.62	+19 57 31.4	Yes	-21	-16	SPEC,PM,HA,PHOT	ADAM02,HAMB95
	HSHJ095							
1120	J08361083+1941413	08 36 10.83	+19 41 41.3	No	-12	-4	PM	KRAU07
372	J0836161+192240 HSHJ113	08 36 16.16	+19 22 40.7	Yes	-40	-13	SPEC,PM,HA,PHOT	ADAM02,HAMB95
1129	J08362111+1850276 HSHJ118	08 36 21.11	+18 50 27.6	Yes	-24	-2	PM	KRAU07

Table 6.2 (cont'd)

ID	Other Name(s)	RA ¹	DEC ¹	PM ²	$\mu_{\alpha} \cos(\delta)^3$	μ_{δ}^3	Evidence ⁴	References ⁵
598	WFC140	08 36 21.20	+19 38 45.5	No	-7	-4	PM,PHOT	CHAP05
607	WFC204	08 36 29.90	+19 38 37.5	No	13	11	PM,PHOT	CHAP05
377	J0836450+200845	08 36 45.02	+20 08 45.8	No	-17	24	SPEC,PM,HA,PHOT	ADAM02
600	WFC150	08 36 48.06	+19 49 02.2	No	-18	17	PM,PHOT	CHAP05
1168	J08372526+2006350 AD2314	08 37 25.26	+20 06 35.0	No	-32	5	PM	KRAU07
1180	J08374060+1933032	08 37 40.60	+19 33 03.2	Yes	-28	-4	PM	KRAU07
1185	J08374932+1957464 HSHJ181	08 37 49.32	+19 57 46.4	Yes	-24	-18	PM	KRAU07
1190	J08375712+1927499 JS702	08 37 57.12	+19 27 49.9	Yes	-23	-11	PM	KRAU07
1192	J08380048+1940562 HSHJ190	08 38 00.48	+19 40 56.2	Yes	-34	-6	PM	KRAU07
1200	J08380676+1934178 HSHJ194	08 38 06.76	+19 34 17.8	Yes	-29	-9	PM	KRAU07
595	WFC135	08 38 07.96	+19 43 28.6	Yes	-30	-9	PM,PHOT	CHAP05
1204	J08380800+2003505 HSHJ195	08 38 08.00	+20 03 50.5	Yes	-31	-8	PM	KRAU07
1205	J08380809+1844300	08 38 08.09	+18 44 30.0	Yes	-34	-15	PM	KRAU07

Table 6.2 (cont'd)

ID	Other Name(s)	RA ¹	DEC ¹	PM ²	$\mu_{\alpha} \cos(\delta)^3$	μ_{δ}^3	Evidence ⁴	References ⁵
	HSHJ196							
1207	J08381244+2008026	08 38 12.44	+20 08 02.6	Yes	-35	-6	PM	KRAU07
1214	J08382186+2005356	08 38 21.86	+20 05 35.6	Yes	-34	-3	PM	KRAU07
1218	J08382537+2021210	08 38 25.37	+20 21 21.0	No	-57	-62	PM	KRAU07
396	J0838392+194140	08 38 39.29	+19 41 40.2	Yes	-21	-16	SPEC,PM,HA,PHOT	ADAM02,HAMB95
	HSHJ215							
1228	J08384128+1959471	08 38 41.28	+19 59 47.1	Yes	-33	-1	PM	KRAU07
398	J0838415+193418	08 38 41.59	+19 34 18.1	Yes	-35	-5	SPEC,PM,HA,PHOT	ADAM02,HAMB95
	HSHJ218							
562	Prae J083850.6+192317	08 38 50.55	+19 23 16.5	No	-57	37	PHOT	GGAR06
403	J0838510+191833	08 38 51.02	+19 18 33.6	No	-26	-51	SPEC,PM,HA,PHOT	ADAM02,HAMB95
	HSHJ229							
404	J0838530+195136	08 38 53.01	+19 51 36.4	Yes	-35	-4	SPEC,PM,HA,PHOT	ADAM02
1235	J08385420+1951446	08 38 54.20	+19 51 44.6	No	-37	-25	PM	KRAU07
	HSHJ233							
1238	J08385547+1950334	08 38 55.47	+19 50 33.4	Yes	-31	-14	PM	KRAU07
1241	J08385651+1812598	08 38 56.51	+18 12 59.8	Yes	-28	-13	PM	KRAU07
	HSHJ240							
1246	J08390695+1947080	08 39 06.95	+19 47 08.0	Yes	-30	-8	PM	KRAU07

Table 6.2 (cont'd)

ID	Other Name(s)	RA ¹	DEC ¹	PM ²	$\mu_{\alpha} \cos(\delta)^3$	μ_{δ}^3	Evidence ⁴	References ⁵
1248	J08391272+1930169	08 39 12.72	+19 30 16.9	Yes	-36	-8	PM	KRAU07
417	J0839153+191928	08 39 15.37	+19 19 28.5	No	-3	15	SPEC,PM,HA,PHOT	ADAM02
1250	J08391572+1920024 HSHJ256	08 39 15.72	+19 20 02.4	No	12	25	PM	KRAU07
418	J0839167+194742 HSHJ257	08 39 16.79	+19 47 42.6	Yes	-35	-19	SPEC,PM,HA,PHOT	ADAM02,HAMB95
419	J0839184+192244 HSHJ258	08 39 18.50	+19 22 44.3	Yes	-37	-10	SPEC,PM,HA,PHOT	ADAM02,HAMB95
1253	J08391937+1838224 IZ063	08 39 19.37	+18 38 22.4	No	2	15	PM	KRAU07
427	J0839307+185653 HSHJ269	08 39 30.72	+18 56 53.4	Yes	-28	-17	SPEC,PM,HA,PHOT	ADAM02,HAMB95
429	J0839317+192417 HSHJ270	08 39 31.76	+19 24 17.6	Yes	-34	-13	SPEC,PM,HA,PHOT	ADAM02,HAMB95
431	J0839346+194800 HSHJ272	08 39 34.66	+19 48 00.3	Yes	-25	2	SPEC,PM,HA,PHOT	ADAM02,HAMB95
432	J0839361+184049 HSHJ276	08 39 36.16	+18 40 49.0	No	-50	49	SPEC,PM,HA,PHOT	ADAM02,HAMB95
1266	J08393965+1906562	08 39 39.65	+19 06 56.2	No	-30	-28	PM	KRAU07

Table 6.2 (cont'd)

ID	Other Name(s)	RA ¹	DEC ¹	PM ²	$\mu_{\alpha} \cos(\delta)^3$	μ_{δ}^3	Evidence ⁴	References ⁵
434	J0839400+185049 HSHJ280	08 39 40.07	+18 50 49.2	No	34	-39	SPEC,PM,HA,PHOT	ADAM02,HAMB95
436	J0839405+191853 HSHJ279	08 39 40.51	+19 18 53.9	Yes	-38	-3	SPEC,PM,HA,PHOT	ADAM02,HAMB95
1268	J08394166+1929004	08 39 41.66	+19 29 00.4	Yes	-37	-4	PM	KRAU07
1270	J08394255+1918288	08 39 42.55	+19 18 28.8	Yes	-36	1	PM	KRAU07
1273	J08394675+1944126	08 39 46.75	+19 44 12.6	Yes	-31	-10	PM	KRAU07
1274	J08394730+1939344	08 39 47.30	+19 39 34.4	Yes	-33	-13	PM	KRAU07
413	J0839051+194526 HSHJ248	08 39 05.13	+19 45 26.4	Yes	-39	-9	SPEC,PM,HA,PHOT	ADAM02,HAMB95
441	J0839531+192403	08 39 53.16	+19 24 03.7	Yes	-48	-10	SPEC,PM,HA,PHOT	ADAM02
442	J0839544+192737 HSHJ291	08 39 54.41	+19 27 37.2	Yes	-31	-13	SPEC,PM,HA,PHOT	ADAM02,HAMB95
1279	J08400249+1916397 JS717	08 40 02.49	+19 16 39.7	Yes	-26	-1	PM	KRAU07
444	J0840013+202222	08 40 01.35	+20 22 22.7	No	-17	-29	SPEC,PM,HA,PHOT	ADAM02
450	J0840106+202050	08 40 10.61	+20 20 50.5	Yes	-23	-18	SPEC,PM,HA,PHOT	ADAM02
452	J0840115+193911 HSHJ302	08 40 11.59	+19 39 11.8	Yes	-31	-9	SPEC,PM,HA,PHOT	ADAM02,HAMB95

Table 6.2 (cont'd)

ID	Other Name(s)	RA ¹	DEC ¹	PM ²	$\mu_{\alpha} \cos(\delta)^3$	μ_{δ}^3	Evidence ⁴	References ⁵
1287	J08401920+1838025	08 40 19.20	+18 38 02.5	No	-12	-7	PM	KRAU07
1288	J08401923+1812410 AD2740	08 40 19.23	+18 12 41.0	Yes	-28	-9	PM	KRAU07
445	J0840024+194035 HSHJ293	08 40 02.49	+19 40 35.4	Yes	-32	-1	SPEC,PM,HA,PHOT	ADAM02,HAMB95
446	J0840039+185557	08 40 03.92	+18 55 57.5	No	-20	-85	SPEC,PM,HA,PHOT	ADAM02
461	J0840305+195558 JS365	08 40 30.60	+19 55 58.9	Yes	-31	-10	SPEC,PM,HA,PHOT	ADAM02,,JONE91
447	J0840041+192450 HSHJ295	08 40 04.17	+19 24 50.3	No	-8	-18	SPEC,PM,HA,PHOT	ADAM02,HAMB95
470	J0840518+195630 JS390	08 40 51.87	+19 56 30.2	Yes	-44	2	SPEC,PM,HA,PHOT	ADAM02,,JONE91
602	WFC163	08 40 53.59	+19 40 58.3	Yes	-32	-14	PM,PHOT	CHAP05
472	J0840539+200524 HSHJ333	08 40 53.97	+20 05 24.4	Yes	-31	-6	SPEC,PM,HA,PHOT	ADAM02,HAMB95
474	J0840568+194611 HSHJ340	08 40 56.83	+19 46 11.9	Yes	-30	-8	SPEC,PM,HA,PHOT	ADAM02,HAMB95
1303	J08405751+2028414	08 40 57.51	+20 28 41.4	No	-75	-66	PM	KRAU07
1307	J08405890+1914167	08 40 58.90	+19 14 16.7	Yes	-35	-11	PM	KRAU07

Table 6.2 (cont'd)

ID	Other Name(s)	RA ¹	DEC ¹	PM ²	$\mu_{\alpha} \cos(\delta)^3$	μ_{δ}^3	Evidence ⁴	References ⁵
449	J0840081+201306 HSHJ299	08 40 08.16	+20 13 06.6	Yes	-32	-11	SPEC,PM,HA,PHOT	ADAM02,HAMB95
1310	J08410314+1918093	08 41 03.14	+19 18 09.3	Yes	-31	-11	PM	KRAU07
1314	J08411016+1912133	08 41 10.16	+19 12 13.3	No	-17	-31	PM	KRAU07
481	J0841107+190153 JS725	08 41 10.76	+19 01 54.0	No	-37	17	SPEC,PM,HA,PHOT	ADAM02,JONE91
487	J0841152+191149	08 41 15.30	+19 11 49.1	No	4	28	SPEC,PM,HA,PHOT	ADAM02
492	J0841203+185743 HSHJ364	08 41 20.34	+18 57 43.0	No	-57	4	SPEC,PM,HA,PHOT	ADAM02,HAMB95
496	J0841260+195915 HSHJ368	08 41 26.03	+19 59 15.2	Yes	-31	-11	SPEC,PM,HA,PHOT	ADAM02,HAMB95
1327	J08412680+1952367	08 41 26.80	+19 52 36.7	Yes	-44	-12	PM	KRAU07
1329	J08412873+1942490	08 41 28.73	+19 42 49.0	Yes	-31	-6	PM	KRAU07
498	J0841289+184535	08 41 29.00	+18 45 35.2	No	26	-46	SPEC,PM,HA,PHOT	ADAM02
476	J0841031+185555 HSHJ346	08 41 03.14	+18 55 55.2	No	-28	35	SPEC,PM,HA,PHOT	ADAM02,HAMB95
1330	J08413275+1940138	08 41 32.75	+19 40 13.8	Yes	-34	-11	PM	KRAU07
500	J0841335+193300	08 41 33.55	+19 33 00.3	Yes	-34	-8	SPEC,PM,HA,PHOT	ADAM02
506	J0841417+194957	08 41 41.74	+19 49 57.5	No	-45	-23	SPEC,PM,HA,PHOT	ADAM02

Table 6.2 (cont'd)

ID	Other Name(s)	RA ¹	DEC ¹	PM ²	$\mu_{\alpha} \cos(\delta)^3$	μ_{δ}^3	Evidence ⁴	References ⁵
1337	J08414175+2019084	08 41 41.75	+20 19 08.4	Yes	-40	-3	PM	KRAU07
1344	J08414793+1959500	08 41 47.93	+19 59 50.0	Yes	-27	-12	PM	KRAU07
509	J0841494+200436 HSHJ393	08 41 49.46	+20 04 36.3	Yes	-30	-10	SPEC,PM,HA,PHOT	ADAM02,HAMB95
1346	J08415058+1929395	08 41 50.58	+19 29 39.5	Yes	-39	-8	PM	KRAU07
1348	J08415223+1942283	08 41 52.23	+19 42 28.3	Yes	-33	-8	PM	KRAU07
513	J0842016+192646 HSHJ404	08 42 01.60	+19 26 46.1	Yes	-34	-4	SPEC,PM,HA,PHOT	ADAM02,HAMB95
514	J0842016+192701 HSHJ405	08 42 01.67	+19 27 01.5	Yes	-43	-6	SPEC,PM,HA,PHOT	ADAM02,HAMB95
521	J0842238+192312 HSHJ421	08 42 23.83	+19 23 12.6	Yes	-31	-25	SPEC,PM,HA,PHOT	ADAM02,HAMB95
1366	J08422968+1919526	08 42 29.68	+19 19 52.6	Yes	-38	-7	PM	KRAU07
523	J0842394+192452 HSHJ430	08 42 39.44	+19 24 52.0	Yes	-42	3	SPEC,PM,HA,PHOT	ADAM02,HAMB95
1392	J08430637+1923388	08 43 06.37	+19 23 38.8	Yes	-22	-12	PM	KRAU07
525	J0843018+195404	08 43 01.88	+19 54 04.7	Yes	-35	0	SPEC,PM,HA,PHOT	ADAM02
1397	J08431326+2000160	08 43 13.26	+20 00 16.0	Yes	-28	-12	PM	KRAU07
536	J0843337+192424	08 43 33.76	+19 24 24.8	No	4	32	SPEC,PM,HA,PHOT	ADAM02,HAMB95

Table 6.2 (cont'd)

ID	Other Name(s)	RA ¹	DEC ¹	PM ²	$\mu_{\alpha} \cos(\delta)^3$	μ_{δ}^3	Evidence ⁴	References ⁵
	HSHJ459							
539	J0843566+191617	08 43 56.65	+19 16 17.9	Yes	-39	-3	SPEC,PM,HA,PHOT	ADAM02,HAMB95
	HSHJ471							
1413	J08435794+1930592	08 43 57.94	+19 30 59.2	Yes	-44	-20	PM	KRAU07
544	J0844138+192316	08 44 13.83	+19 23 16.5	No	-36	21	SPEC,PM,HA,PHOT	ADAM02
546	J0844265+190720	08 44 26.56	+19 07 20.4	No	-10	-87	SPEC,PM,HA,PHOT	ADAM02
1424	J0844272+1852207	08 44 27.21	+18 52 20.7	No	-13	-17	PM	KRAU07
542	J0844039+190112	08 44 03.90	+19 01 12.7	No	44	-64	SPEC,PM,HA,PHOT	ADAM02,HAMB95
	HSHJ474							
549	J0844364+191717	08 44 36.41	+19 17 17.8	Yes	-38	-22	SPEC,PM,HA,PHOT	ADAM02
550	J0844372+185529	08 44 37.23	+18 55 29.6	No	6	17	SPEC,PM,HA,PHOT	ADAM02,HAMB95
	HSHJ491							

¹Position in J2000 coordinates²Is the object identified by this work as a proper motion candidate of the cluster?³Proper motion in units of mas/yr⁴HA = High $H\alpha$ emission indicative of accretion, PHOT = object selected as a candidate via optical/NIR photometry, PM = Object is consistent with the proper motion of the cluster, SPEC = overall SED fit to that of an intermediate gravity object⁵ADAM02 = Adams et al. (2002), HAMB95 = Hambly et al. (1995), JONE91 = Jones & Stauffer (1991), KRAU07 = Kraus & Hillenbrand (2007)

Table 6.3: Previously Claimed Members of the Pleiades

ID	Other Name(s)	RA ¹	DEC ¹	PM ²	$\mu_{\alpha, \cos(\delta)}^3$	μ_{δ}^3	Evidence ⁴	References ⁵
1908	PLZJ56	03 44 53.51	+25 36 19.46	Yes	25	-42	PM	CASE07
1625		03 45 49.26	+25 24 46.1	Yes	27	-30	PM,PHOT	LODI07
1669		03 46 47.19	+25 20 53.1	Yes	21	-41	PM,PHOT	LODI07
1712	BPL146	03 47 30.66	+25 13 30.6	No	52	-61	PM,PHOT	LODI07
1727	BPL157	03 47 47.87	+25 13 34.3	Yes	16	-43	PM,PHOT	LODI07
1750	BPL170	03 48 15.49	+25 14 36.4	Yes	23	-43	PM,PHOT	LODI07
1765	BPL183	03 48 36.34	+25 15 41.2	Yes	23	-48	PM,PHOT	LODI07
1775	BPL192	03 48 50.45	+25 17 54.7	Yes	13	-45	PM,PHOT	LODI07
1853		03 51 57.12	+24 57 06.4	Yes	19	-39	PM,PHOT	LODI07
1862	BPL252	03 52 04.48	+24 14 39.6	Yes	4	-49	PM,PHOT	LODI07
1864	CFHT23	03 52 18.64	+24 04 28.1	Yes	20	-40	PM,PHOT	LODI07
	CFHTPLIZ15							
1874	BPL268	03 52 44.48	+24 20 59.3	Yes	18	-40	PM,PHOT	LODI07
	BPL269							
341	BRB5	03 52 51.8	+23 33 48.9	Yes	22	-46	PM,PHOT	BIH06,BEJ00,HAM93,BARA98,MORA03
	CFHT-PI-3							
	HHJ 22							
	BPL272							

Table 6.3 (cont'd)

ID	Other Name(s)	RA ¹	DEC ¹	PM ²	$\mu_{\alpha} \cos(\delta)^3$	μ_{δ}^3	Evidence ⁴	References ⁵
	MBSC99							
342	BRB6	03 53 09.6	+23 33 48.3	Yes	31	-49	PM,PHOT	BIH06,BEJ00,BARA98,MORA03
	CFHT-PI-4							
	BPL280							
	MBSC101							
1882	BPL285	03 53 24.12	+23 47 58.4	Yes	22	-41	PM,PHOT	LODI07
1884	BPL293	03 53 49.10	+23 32 49.5	Yes	28	-22	PM,PHOT	LODI07
1886	BPL301	03 54 02.73	+23 35 00.9	Yes	25	-52	PM,PHOT	LODI07
351	BRB15	03 54 05.3	+23 34 00.2	Yes	19	-47	PM,PHOT	BIH06,BEJ00,BARA98,BOU06
	CFHT-PI-25							
	BPL303							
	CFHT-PLIZ-20							
1889	BPL307	03 54 15.60	+24 20 45.7	Yes	17	-39	PM,PHOT	LODI07
	BPL308							
1892	BPL312	03 54 25.03	+24 42 43.5	Yes	20	-44	PM,PHOT	LODI07
1893	BPL313	03 54 28.11	+23 56 36.0	Yes	22	-45	PM,PHOT	LODI07
1896	BPL315	03 54 39.13	+24 35 54.5	Yes	21	-43	PM,PHOT	LODI07
1900	BPL325	03 55 17.17	+23 53 16.7	Yes	5	-43	PM,PHOT	LODI07
1901	BPL326	03 55 18.11	+24 17 05.7	No	16	-8	PM,PHOT	LODI07

Table 6.3 (cont'd)

ID	Other Name(s)	RA ¹	DEC ¹	PM ²	$\mu_{\alpha} \cos(\delta)$ ³	μ_{δ} ³	Evidence ⁴	References ⁵
1902	CFHTPLIZ2 BPL327	03 55 23.08	+24 49 04.9	Yes	23	-43	PM,PHOT	LODI07

¹Position in J2000 coordinates

²Is the object identified by this work as a proper motion candidate of the cluster?

³Proper motion in units of mas/yr

⁴PHOT = object selected as a candidate via optical/NIR photometry, PM = Object is consistent with the proper motion of the cluster

⁵BARA98 = Baraffe et al. (1998), BEJ00 = Béjar (2000), BIH06 = Bihain et al. (2006), BOU06 = Bouy et al. (2006), CASE07 = Casewell et al. (2007), HAM93 = Hambly, Hawkins, & Jameson (1993), MORA03 = Moraux et al. (2003), LODI07 = Lodieu et al. (2007)

Chapter 7

Conclusions

I have taken Megacam i -band imaging of the Taurus, Praesepe, and Pleiades open star clusters in order to conduct a proper motion and color search for new, low-mass members. Combining this new imaging with CFHT archival data and NIR detections from 2MASS, a multi-year baseline was produced from which to extract measurable proper motions. The Pan-STARRS IPP software was used to obtain high-precision astrometric measurements out to cluster distances of $\sim 140 - 200$ pc. Using both proper motion and color selection, 33 new low-mass cluster members have been identified, along with an additional 18 potential cluster members and 4 members recovered from previous cluster searches. The member status of 134 cluster member candidates has been established via low-resolution NIR spectroscopy from the SpeX instrument. The SEDs of the member candidates were fitted to empirical templates of known spectral type and surface gravity, and permitted to be reddened at the typical values expected for younger clusters such as Taurus. The fits were complemented by measured spectral indices known to distinguish objects of high and low surface gravity. The combination of a mean spectral type index and gravity-sensitive Na index is able to separate M-type field dwarfs from M giants and low-mass cluster members across the M3-M9 range. The use of both the SED-fitting and spectral index measurements allows for the classification of followed-up candidates as being bona fide members or galactic field contaminants.

Using a model of the galactic field population by Robin et al. (2003), the greatest contaminants were found to be M-type field dwarfs located $\sim 100 - 1000$ pc behind the clusters. The motion of the Taurus cluster leaves it vulnerable to heavy field contamination, including that of reddened background giants. However, the Praesepe and Pleiades clusters have a very discrepant motion from the majority of the galactic field, and suffer much less kinematic contamination. The earliest M field dwarfs (M0-M2) appear as false positives across most or all of the observed i magnitude range. However, brighter M3 and later type candidates are likely to be bona fide cluster

members, as they must fulfill the proper motion criteria of the cluster whilst also lying close enough to be detected at such magnitudes. This dynamical argument provides greater confidence in the membership status of bright member candidates if they are fit to mid-M spectral types. This is of particular advantage, as such cluster members often share NIR color-space with the bulk of the field population (i.e., M field dwarfs).

The inclusion of proper motion selection reduces the color-selected candidate list by nearly an order-of-magnitude, allowing more effective spectroscopic follow-up. If all the claimed members in this study are in fact genuine, then the follow-up efficiency of the target clusters is 19% for Taurus, 54% for Praesepe, and 29% for the Pleiades. The majority of newly reported members are of spectral type M3-M5, and new Taurus members make up a 10-14% minimum increase in the known cluster IMF across this spectral type range. These results are suggestive that the Taurus IMF may not be as deviant from other young clusters as previously thought. On the other hand, there are previously claimed Taurus and Praesepe members with highly discrepant motions from the mean cluster value. Many of these objects have significant evidence of membership, and further inquiry is needed to determine if the proper motion measurements are inaccurate, or if such objects indeed possess very unusual motions relative to the rest of the cluster population.

This study shows the feasibility of broader and longer-term low-mass cluster member searches using the Pan-STARRS IPP software with high-quality imaging. The Pan-STARRS-1 Survey now in operation will regularly image the entire sky visible from Hawaii down to the extremely red y -band from 2010-2013. Combining this data with more recent NIR surveys such as UKIDSS offers the potential to find low-mass members at even larger distances than the clusters presented here. Such future study will extend the proper motion and color member search down to fainter magnitudes, lower masses, and lead to a more complete census of nearby star-forming regions.

Appendix A

Previously Claimed Low-Mass Cluster Members

The tables listed below are the result of an extensive search of the literature for known low-mass members of the Taurus, Praesepe, and Pleiades clusters. The search was conducted for two primary purposes. First, to minimize the number of cluster members already with published NIR spectra from being unintentionally re-observed during spectroscopic follow-up. In the end, only 4 known members of Taurus were unintentionally recovered by spectroscopy. All other followed-up cluster member candidates (with the exception of one known non-member) had not yet had their membership status determined at the time of this study. The second purpose of this literature search was to match the imaging and proper motion data in this work to known members in order to determine if they pass the PM+Color selection method. While some earlier-type members are listed below (as they were included in some published tables with the lower-mass members), the only attempt to be as comprehensive and complete as possible was for the M-type cluster members, as they are the focus of this work. The criteria for an object to be included in the tables were:

1. The object was claimed as a cluster member as part of study to identify low-mass members of Taurus, Praesepe, or the Pleiades
2. The object possessed evidence for cluster membership, or was quoted in multiple studies as a well-established cluster member

The tables are presented in the following format:

- Column 1: The ID number of the object as given by this work
- Column 2: Other identifiers as given by the associated reference(s)

- Columns 3-4: The reported RA and DEC for the object in J2000 coordinates
- Column 5: The reported J magnitude for the object as given in the associated reference(s)
- Column 6: The spectral type for the object as given in the associated reference(s)
- Columns 7-14: The evidence for membership as given in the associated reference(s); SPEC = Object's SED is fit to a cluster member template, and/or the object has spectral index measurement(s) that correspond to an intermediate surface gravity; PM = Object's proper motion consistent with the bulk cluster motion; LI = Object has lithium detected in absorption; HA = Object has strong H α emission consistent with on-going accretion; UV = Object claimed as a member due to UV excess; MIR = Object selected as a member candidate from multiple color cuts in the mid- and/or far-IR; OPT/NIR = Object is noted as being selected as a member candidate using optical and/or NIR color selection; ARCH = An archival object (i.e., an object is quoted in associated reference(s) as a well-established member of the cluster)
- Columns 15-17: All references associated with the information presented on the object: ADAM02 = Adams et al. (2002), BARA98 = Baraffe et al. (1998), BEJ00 = Béjar (2000), BIH06 = Bihain et al. (2006), BOU06 = Bouy et al. (2006), BRIC02 = , CASE07 = Casewell et al. (2007), CHAP05 = Chappelle et al. (2005), FIND10 = Findeisen & Hillenbrand (2010), GGAR06 = González-García et al. (2006), HAM93 = Hambly, Hawkins, & Jameson (1993), HAMB95 = Hambly et al. (1995), JONE91 = Jones & Stauffer (1991), KLEI27 = Klein Wassink (1927), KRAU07 = Kraus & Hillenbrand (2007), LODI07 = Lodieu et al. (2007), LUHM04 = Luhman (2004), LUHM06a = Luhman (2006), LUHM06b = Luhman et al. (2006), MORA03 = Moraux et al. (2003), QUAN10 = Quanz et al. (2010), REBU10 = Rebull et al. (2010), SLES06 = Slesnick et al. (2006), WICH00 = Wichmann et al. (2000)

Table A.1: Previously Claimed Low-Mass Taurus Members

ID	Other ID(s)	RA	DEC	J	SPT	SPEC	PM	LI	HA	UV	MIR	OPT/NIR	ARCH	Ref1	Ref2	Ref3
918	SCH J03253332+2426581	03 25 33.2	+24 26 58.1	12.34	M4.5	X	SLES06
919	SCH J0359099+2009362	03 59 09.9	+20 09 36.2	13.47	M4.75	X	SLES06
920	SCH J0400220+2232382	04 00 22.0	+22 32 38.2	13.45	M4.75	X	SLES06
921	SCH J0400279+2031593	04 00 27.9	+20 31 59.3	13.14	M5.75	X	SLES06
2148	J04034997+2620382	04 03 49.97	+26 20 38.2	...	M5.25	X	X	...	X	LUHM09
	XEST 06-006
922	SCH J0407246+2332554	04 07 24.6	+23 32 55.4	12.77	M4	X	SLES06
923	SCH J0407350+2237396	04 07 35.0	+22 37 39.6	12.16	M5	X	SLES06
744	J04080782+2807280	04 08 07.82	+28 07 28.0	12.45	M3.75	X	...	X	X	X	LUHM06a	LUHM06b	...
2328	2MASS04110570+2216313	04 11 05.70	+22 16 31.3	...	M4	...	X	X	FIND10
2222	...	04 11 59.7	+29 42 36	X	...	REBU09
924	SCH J0412433+2055306	04 12 43.3	+20 55 30.6	14.24	M8	X	SLES06
2074	LkCa 1	04 13 14.14	+28 19 10.8	9.63	M4	X	BRIC02
2075	Anon 1	04 13 27.21	+28 16 24.9	8.84	M0	X	BRIC02
2223	...	04 13 32.3	+29 17 26	X	REBU09
2224	...	04 13 39.4	+29 21 14	X	...	REBU09
2076	IRAS 04108+2803 A	04 13 53.26	+28 11 23.6	13.61	X	...	X	BRIC02	REBU09	...
2077	IRAS 04108+2803 B	04 13 54.69	+28 11 33.1	16.46	X	...	X	BRIC02	REBU09	...
2195	IRAS041082910	04 13 57.3	+29 18 19	...	K5	X	...	X	REBU09
2126	J04141188+2811535	04 14 11.88	+28 11 53.5	13.16	M6.25	X	X	LUHM04	REBU09	...
2196	IRAS041112800G	04 14 12.2	+28 08 37	X	...	X	REBU09
2078	V773 Tau A+B	04 14 12.91	+28 12 12.4	7.49	K3	X	...	X	BRIC02	REBU09	...
2079	FM Tau	04 14 13.57	+28 12 49.3	10.31	M0	X	...	X	...	X	BRIC02	REBU09	...
2080	FN Tau	04 14 14.58	+28 27 58.1	9.47	M5	X	...	X	BRIC02	REBU09	...
2081	CW Tau	04 14 17.00	+28 10 57.8	9.54	K3	X	...	X	...	X	BRIC02	REBU09	...
2082	CIDA 1	04 14 17.61	+28 06 09.8	11.7	M5.5	X	...	X	BRIC02	REBU09	...
2083	MHO 1	04 14 26.27	+28 06 03.2	12.41	M2.5	BRIC02
2084	MHO 2	04 14 26.40	+28 05 59.7	11.45	M2.5	BRIC02
2225	...	04 14 27.3	+25 51 30	...	G5	X	REBU09
2085	MHO 3	04 14 30.55	+28 05 14.6	11.16	K7	BRIC02
2149	J04144739+2803055	04 14 47.39	+28 03 05.5	...	M5.25	X	X	...	X	BRIC02
	XEST 20-066	LUHM09
2197	FP Tau	04 14 47.3	+26 46 26	...	M4
2198	CX Tau	04 14 47.8	+26 48 11	...	M2.5	X	...	X	REBU09
2086	LkCa 3 A+B	04 14 47.97	+27 52 34.5	8.36	M1	X	...	X	BRIC02
2087	FO Tau A+B	04 14 49.28	+28 12 30.4	9.66	M2	X	...	X	BRIC02	REBU09	...
2150	J04145234+2805598	04 14 52.34	+28 05 59.8	...	M3.25	X	X	...	X	LUHM09
	XEST 20-071
2088	CIDA 2	04 15 05.16	+28 08 46.1	10.1	M4.5	BRIC02
2071	2M J0415147+280009	04 15 14.72	+28 00 09.5	15.09	M8.5	X	X	BRIC02

Table A.1 (cont'd)

ID	Other ID(s)	RA	DEC	J	SpT	SPEC	PM	LI	HA	UV	MIR	OPT/NIR	ARCH	Ref1	Ref2	Ref3
745	J04152409+2910434	04 15 24.09	+29 10 43.4	13.69	M7	X	X	X	LUHM06a	LUHM06b	
2226	...	04 15 35.6	+28 47 41	X	...	REBU09	...	
2151	J04153916+2818586	04 15 39.16	+28 18 58.6	...	M3.75	X	X	...	X	LUHM09	REBU09	
2152	J04154278+2909597	04 15 42.78	+29 09 59.7	...	M1.25	X	X	...	X	...	X	LUHM09	REBU09	
	IRAS 04125+2902	
2153	J04155799+2746175	04 15 57.99	+27 46 17.5	...	M5.5	X	X	...	X	LUHM09	REBU09	
2227	...	04 16 04.8	+26 18 01	X	REBU09	...	
2228	...	04 16 05.8	+28 14 26	X	...	REBU09	...	
2127	J04161210+2756385	04 16 12.10	+27 56 38.6	12.28	M4.75	X	X	LUHM04	REBU09	
746	J04161885+2752155	04 16 18.85	+27 52 15.5	12.55	M6.25	X	X	X	LUHM06a	LUHM06b	
2229	HD281820	04 16 24.5	+29 08 58	...	A2	REBU09	...	
925	SCH J0416272+2053093	04 16 27.2	+20 53 09.3	12.05	M5	X	SLES06	...	
2089	LkCa 4	04 16 28.12	+28 07 35.8	9.21	K7	X	BRIC02	...	
2128	J04163048+3037053	04 16 30.49	+30 37 05.3	13.62	M4.5	X	LUHM04	...	
747	J04163911+2858491	04 16 39.11	+28 58 49.1	12.72	M5.5	X	X	X	X	LUHM06a	LUHM06b	REBU09
2230	...	04 17 06.2	+26 44 13	...	K3	X	...	REBU09	...	
748	J04173372+2820468	04 17 33.72	+28 20 46.8	9.77	M1.5	X	...	X	LUHM06b	BRIC02	REBU09
	CYTau	
2090	LkCa 5	04 17 38.93	+28 33 00.8	9.95	M2	X	BRIC02	...	
749	J04174955+2813318	04 17 49.55	+28 13 31.8	...	M5	X	X	...	X	...	X	LUHM06b	REBU09	
750	KPN010	
	V410X-ray1	04 17 49.65	+28 29 36.2	11	M2	X	...	X	LUHM06b	BRIC02	REBU09
2231	...	04 18 01.1	+28 35 26	...	K1	X	REBU09	...	
2232	...	04 18 03.3	+24 40 09	...	A9	X	...	REBU09	...	
751	J04180796+2826036	04 18 07.96	+28 26 03.6	11.49	M6	X	LUHM06b	BRIC02	
	V410X-ray3	
2233	...	04 18 10.5	+28 44 47	X	REBU09	...	
2154	J04181078+2519574	04 18 10.78	+25 19 57.4	...	M1.5	X	X	...	X	...	X	LUHM09	REBU09	
	V409 Tau	
752	IRAS 04151+2512	
	J04181710+2828419	04 18 17.10	+28 28 41.9	12.9	M5	X	...	X	LUHM06b	BRIC02	REBU09
	V410Anon13	
2234	2MASX041823212519281	04 18 23.2	+25 19 28	X	X	...	REBU09	...	
753	J04182239+2824375	04 18 22.39	+28 24 37.5	15.1	G1	X	LUHM06b	BRIC02	
	V410Anon24	
754	J04182909+2826191	04 18 29.09	+28 26 19.1	14.85	M1	LUHM06b	BRIC02	
	V410Anon25	
755	J04183030+2743208	04 18 30.30	+27 43 20.8	...	M5.5	X	X	LUHM06b	...	
	KPN011	
756	J04183110+2827162	04 18 31.10	+28 27 16.2	8.43	K3	X	LUHM06b	BRIC02	

Table A.1 (cont'd)

ID	Other ID(s)	RA	DEC	J	SpT	SPEC	PM	LI	HA	UV	MIR	OPT/NIR	ARCH	Ref1	Ref2	Ref3
757	V410TauA+B+C J04183112+2816290	04 18 31.12	+28 16 29.0	9.81	M1	X	...	X	LUHM066	BRIC02	REBU09
2235	DDTauA+B ...	04 18 31.2	+28 26 17	X	...	REBU09
758	J04183158+2816585	04 18 31.58	+28 16 58.5	10.51	M1.5	X	...	X	LUHM066	BRIC02	REBU09
759	CZTauA+B J04183203+2831153	04 18 32.03	+28 31 15.3	15.12	M2.5	X	...	X	LUHM066	BRIC02	REBU09
760	PSC04154+2823 J04183444+2830302	04 18 34.44	+28 30 30.2	13.7	M0	X	...	X	LUHM066	BRIC02	REBU09
761	V410X-ray2 J04184023+2824245	04 18 40.23	+28 24 24.5	13.55	M4	X	X	...	X	LUHM066	BRIC02	REBU09
762	V410X-ray4 J04184061+2819155	04 18 40.61	+28 19 15.5	8.71	A6	X	LUHM066	BRIC02	REBU09
763	V892Tau J04184133+2827250	04 18 41.33	+28 27 25.0	16.13	K4.5	X	LUHM066	BRIC02	REBU09
764	LRI J04184250+2818498	04 18 42.50	+28 18 49.8	11.91	M1	X	...	X	LUHM066	BRIC02	REBU09
765	V410X-ray7 J04184505+2820528	04 18 45.05	+28 20 52.8	16.37	K3	X	LUHM066	BRIC02	REBU09
766	V410Anon20 J04184703+2820073	04 18 47.03	+28 20 07.3	8.52	K7	X	LUHM066	BRIC02	REBU09
767	Hubble 4 J04185115+2814332	04 18 51.15	+28 14 33.2	13.89	M7.5	X	X	X	LUHM066	BRIC02	REBU09
768	KPNO2 J04185147+2820264	04 18 51.47	+28 20 26.4	12.89	K7	X	BRIC02	BRIC02	REBU09
2236	CoKuTau/1 ...	04 18 58.0	+23 50 31
769	J04185813+2812234	04 18 58.13	+28 12 23.4	13.78	M6	X	...	X	LUHM066	REBU09	REBU09
2237	PSC04158+2805 IRAS04158+2805
770	J04190110+2819420	04 19 01.10	+28 19 42.0	10.52	M4.5	X	...	X	REBU09	BRIC02	REBU09
771	V410X-ray6 J04190126+2802487	04 19 01.26	+28 02 48.7	...	M9	X	X
772	KPNO12 J04190197+2823332	04 19 01.97	+28 22 33.2	11.99	M5	X	LUHM066	BRIC02	REBU09
773	V410X-ray5a J04191281+2829330	04 19 12.81	+28 29 33.0	10.45	M2	X	...	X	LUHM066	BRIC02	REBU09
2200	FQTauA+B BPTau	04 19 15.8	+29 06 26	...	K7	X	...	X	REBU09

Table A.1 (cont'd)

ID	Other ID(s)	RA	DEC	J	SpT	SPEC	PM	LI	HA	UV	MIR	OPT/NIR	ARCH	Ref1	Ref2	Ref3
774	J04192625+2826142	04 19 26.25	+28 26 14.2	9.49	K7	X	LUHM066	BRIC02	
	V819Tau
775	J04193545+2827218	04 19 35.45	+28 27 21.8	...	M5.25	X	...	X	...	X	LUHM066	REBU09	
	FK1tau
	Haro6-4	LUHM09
	XEST 23-076	LUHM09
	XEST 24-063	LUHM09
2238	...	04 19 36.2	+26 52 56	...	G3	REBU09
2239	...	04 19 40.4	+27 01 00	X	...	REBU09
776	J04194127+2749484	04 19 41.27	+27 49 48.4	9.07	K7	X	...	X	LUHM066	BRIC02	REBU09
	LkCa7A+B
777	J04194148+2716070	04 19 41.48	+27 16 07.0	14.71	X	...	X	LUHM066	REBU09	
	IRAS04166+2706
2201	IRAS041662706	04 19 42.5	+27 13 36	X	...	X	REBU09
2155	J04194657+2712552	04 19 46.57	+27 12 55.2	...	M7.5	X	X	LUHM09	REBU09	
	[GKH94] 41
778	J04195844+2709570	04 19 58.44	+27 09 57.0	...	M6	X	...	X	LUHM066	REBU09	
	IRAS04169+2702
926	SCH J0420068+2432267	04 20 06.8	+24 32 26.7	12.42	M4	X	SLES06
2156	J04201611+2821325	04 20 16.11	+28 21 32.5	...	M6.5	X	X	...	X	LUHM09	REBU09	
2157	J04202144+2813491	04 20 21.44	+28 13 49.1	...	M1	X	X	...	X	LUHM09
2129	J04202555+2700355	04 20 25.55	+27 00 35.5	12.87	M5.25	X	X	LUHM04	REBU09	
2240	...	04 20 25.8	+28 16 41	...	G2	REBU09
2158	J04202583+2819237	04 20 25.83	+28 19 23.7	...	M4	X	X	...	X	LUHM09	REBU09	
	IRAS 04173+2812
2159	J04202606+2804089	04 20 26.06	+28 04 08.9	...	M3.5	X	X	...	X	LUHM09	REBU09	
2160	J04203918+2717317	04 20 39.18	+27 17 31.7	...	M4.5	X	X	...	X	LUHM09
	XEST 16-045
927	SCH J0420491+2327370	04 20 49.1	+23 27 37.0	12.07	M4.25	X	SLES06
2202	CFHT-19	04 21 07.9	+27 02 20	...	M5.25	X	...	X	REBU09
2161	J04210934+2750368	04 21 09.34	+27 50 36.8	...	M5.25	X	X	...	X	LUHM09	REBU09	
2203	IRAS041812654B	04 21 10.3	+27 01 37	X	...	X	REBU09
2241	V412Tau	04 21 10.9	+25 52 59	...	A1	X	...	REBU09
2204	IRAS041812654A	04 21 11.4	+27 01 09	X	...	X	REBU09
2130	J04213459+2701388	04 21 34.60	+27 01 38.9	11.9	M5.5	X	X	LUHM04	REBU09	
2242	...	04 21 35.6	+25 38 35	X	REBU09
2162	J04214013+2814224	04 21 40.13	+28 14 22.4	...	M5.75	X	X	LUHM09
	XEST 21-026
2243	...	04 21 46.3	+24 25 05	...	M3	REBU09
779	J04214631+2659296	04 21 46.31	+26 59 29.6	13.82	M8.5	X	X	...	X	LUHM06a	LUHM06b	REBU09
	CFHT10

Table A.1 (cont'd)

ID	Other ID(s)	RA	DEC	J	SpT	SPEC	PM	LI	HA	UV	MIR	OPT/NIR	ARCH	Ref1	Ref2	Ref3
2244	...	04 21 51.3	+26 57 20	X	...	REBU09
780	J04215450+2652315	04 21 54.50	+26 52 31.5	15.54	K1	X	X	X	LUHM06a	...	LUHM06b
2205	DETau	04 21 55.6	+27 55 06	...	M2	X	...	X	REBU09
781	J04215740+2826355	04 21 57.40	+28 26 35.5	...	M3	X	...	X	...	X	LUHM06b	REBU09	...
	RYTau
782	J04215884+28 18066	04 21 58.84	+28 18 06.6	...	M8	X	LUHM06b
	HD 283572
2206	FSTauB	04 22 00.6	+26 57 32	X	...	X	REBU09
2245	...	04 22 00.9	+23 54 30	...	M3	X	...	REBU09
2207	FSTauAb	04 22 02.1	+26 57 30	...	M0	X	...	X	...	X	REBU09
783	J04220313+2825389	04 22 03.13	+28 25 38.9	...	M7.75	X	LUHM06b
	LKCa 21
2246	...	04 22 12.9	+25 46 59	X	...	REBU09
784	J04221332+1934392	04 22 13.32	+19 34 39.2	12.87	M7.75	X	X	X	LUHM06a	LUHM06b	...
2163	J04221568+2657060	04 22 15.68	+26 57 06.0	...	M1	X	X	...	X	...	X	LUHM09	REBU09	...
	XEST 11-078
	IRAS 04192+2650
785	J04221644+2549118	04 22 16.44	+25 49 11.8	13.07	M1.5	X	X	X	LUHM06a	LUHM06b	...
	CFHT14
786	J04221675+2654570	04 22 16.75	+26 54 57.0	11.58	M1.25	X	X	X	X	LUHM06a	LUHM06b	REBU09
	CFHT21
2247	...	04 22 20.9	+26 42 48	X	X	...	REBU09
2164	J04222404+2646258	04 22 24.04	+26 46 25.8	...	M4.75	X	X	LUHM09
	XEST 11-087
787	J04224786+2645530	04 22 47.86	+26 45 53.0	11.59	M1	X	X	LUHM06b	LUHM06a	REBU09
	IRAS04196+2638
2248	NSV1577	04 22 54.6	+28 23 54	...	A0	X	X	...	X	REBU09
788	J04230607+2801194	04 23 06.07	+28 01 19.4	12.24	M6	X	X	LUHM06b	LUHM06a	REBU09
789	J04230776+2805573	04 23 07.76	+28 05 57.3	...	M2	X	...	X	LUHM06b	REBU09	...
	IRAS04200+2759
790	J04231822+2641156	04 23 18.22	+26 41 15.6	12.66	M3.5	X	X	LUHM06b	LUHM06a	REBU09
2249	...	04 23 25.9	+25 03 54	REBU09
2165	J04233539+2503026	04 23 35.39	+25 03 02.6	...	M7.25	X	X	...	X	...	X	LUHM09	REBU09	...
	FU Tau A
2166	J04233573+2502596	04 23 35.73	+25 02 59.6	...	M9.25	X	X	LUHM09
	FU Tau B
2194	CAHA Tau 6	04 23 35.80	+25 02 59.4	X	X	X	...	QUAN09
2250	...	04 23 39.0	+25 18 55	X	...	REBU09
2208	FTTau	04 23 39.1	+24 56 14	...	M3	X	...	X	REBU09
791	J04242090+2630511	04 24 20.90	+26 30 51.1	13.49	M6.5	X	X	LUHM06b	LUHM06a	REBU09
792	J04242646+2649503	04 24 26.46	+26 49 50.3	12.88	M6	X	X	...	X	LUHM06b	REBU09	...

Table A.1 (cont'd)

ID	Other ID(s)	RA	DEC	J	SpT	SPEC	PM	LI	HA	UV	MIR	OPT/NIR	ARCH	Ref1	Ref2	Ref3
793	CFHT9 J04244457+2610141	04 24 44.57	+26 10 14.1	...	M1	X	...	X	LUHM06b	REBU09	...
794	IRAS04216+2603 J04244506+2701447	04 24 45.06	+27 01 44.7	...	M5	X	LUHM06b
2209	J1-4423 RXJ0424.8	04 24 49.0	+26 43 10	...	K1	X	REBU09
2251	FS116 04 23 50.1	04 23 50.1	+26 40 06	X	REBU09
2252	HD283663 04 23 56.0	04 23 56.0	+24 27 05	...	A1	X	REBU09
2253	... 04 23 58.6	04 23 58.6	+24 47 42	...	K2	X	REBU09
2254	... 04 24 23.2	04 24 23.2	+26 50 08	...	M3	X	X	REBU09
795	J04245708+2711565 04 24 57.08	04 24 57.08	+27 11 56.5	...	M0	X	...	X	LUHM06b	REBU09	...
2255	IPTau 04 25 15.5	04 25 15.5	+28 29 27	...	M6	X	X	REBU09
796	J04251767+2617504 04 25 17.67	04 25 17.67	+26 17 50.4	...	K7	X	LUHM06b
2256	J1-4872B 04 25 18.6	04 25 18.6	+25 55 35	...	M5	REBU09
2257	HD27923 04 25 19.1	04 25 19.1	+23 47 16	...	B9	X	REBU09
2258	HD283637 04 25 58.8	04 25 58.8	+27 37 01	...	B9	X	REBU09
798	J04262939+2624137 04 26 29.39	04 26 29.39	+26 24 13.7	13.32	M6	X	X	...	X	...	X	LUHM06b	BRIC02	REBU09
799	KPNO3 KPNO-Tau.3 04 26 30.55	04 26 30.55	+24 43 55.8	14.66	M8.75	X	BRIC02
928	SCH J04260452+2131408 04 26 45.2	04 26 45.2	+21 31 40.8	13.19	M4.75	X	X	X	LUHM06a	LUHM06b	...
2259	... 04 26 53.3	04 26 53.3	+25 58 58	X	...	SLES06
800	J04265352+2606543 04 26 53.52	04 26 53.52	+26 06 54.3	9.9	K5	X	...	X	LUHM06b	BRIC02	REBU09
801	FVTauA+B 04 26 54.40	04 26 54.40	+26 06 51.0	10.8	M3.5	X	LUHM06b	BRIC02	...
802	FVTauC A+B 04 26 56.29	04 26 56.29	+24 43 35.3	X	LUHM06b
803	IRAS04239+2436 J04265732+2606284	04 26 57.32	+26 06 28.4	...	M5	X	X	...	X	...	X	LUHM06b	REBU09	...
804	KPN013 J04270266+2605304	04 27 02.66	+26 05 30.4	15.56	X	...	X	LUHM06b	BRIC02	REBU09
805	DGTauB J04270280+2542223	04 27 02.80	+25 42 22.3	8.16	M3	X	...	X	LUHM06b	BRIC02	REBU09
806	DFTauA+B J04270469+2606163	04 27 04.69	+26 06 16.3	8.68	K5	X	...	X	...	X	LUHM06b	BRIC02	REBU09
929	DGTau SCH J0427074+2215039	04 27 07.4	+22 15 03.9	12.27	M6.75	X	SLES06
2260	... 04 27 21.0	04 27 21.0	+24 08 29	...	G6	X	...	REBU09

Table A.1 (cont'd)

ID	Other ID(s)	RA	DEC	J	SpT	SPEC	PM	LI	HA	UV	MIR	OPT/NIR	ARCH	Ref1	Ref2	Ref3
807	J04272799+2612052	04 27 27.99	+26 12 05.2	14.98	M9.5	X	X	X	LUHM06b	BRIC02	
	KPNO4
	KPNO-Tau 4
2261	...	04 27 28.1	+26 23 23	...	K1	X	...	BRIC02	...	
2262	2MASX042730232441232	04 27 30.2	+24 41 23	X	REBU09	...	
808	J04274538+2357243	04 27 45.38	+23 57 24.3	14.94	M8.25	X	...	X	REBU09	...	
	CFHT15	LUHM06b	...	
809	J04275730+2619183	04 27 57.30	+26 19 18.3	13.24	M5	X	X	...	X	X	LUHM06a	LUHM06b	REBU09
	IRAS04248+2612
2263	...	04 28 10.4	+24 35 53	X	...	REBU09	...	
2210	LDN1521F-IRS	04 28 38.9	+26 51 35	X	REBU09	...	
810	J04284263+2714039	04 28 42.63	+27 14 03.9	12.11	M5.25	X	...	X	LUHM06b	LUHM04	REBU09
2264	...	04 28 57.4	+24 36 07	X	REBU09	...	
811	J04290068+2755033	04 29 00.68	+27 55 03.3	14.01	M8.25	X	LUHM06b	...	
2265	...	04 29 02.9	+24 31 40	X	...	REBU09	...	
812	J04290498+2649073	04 29 04.98	+26 49 07.3	...	K6	X	...	X	LUHM06b	REBU09	
	IRAS04260+2642
2266	2MASX042905172615358	04 29 05.2	+26 15 35	X	...	REBU09	...	
2267	HD283629	04 29 16.2	+28 56 27	...	G6	X	...	REBU09	...	
813	J04292071+2633406	04 29 20.71	+26 33 40.6	9.8	M4	X	LUHM06b	BRIC02	
	J1-507
2268	IRAS042622735	04 29 20.8	+27 42 07	...	M6	X	X	REBU09	...	
814	J04292165+2701259	04 29 21.65	+27 01 25.9	10.79	M5.5	X	...	X	LUHM06b	REBU09	
	IRAS04263+2654
	CFHT18
815	J04292373+2433002	04 29 23.73	+24 33 00.2	LUHM06b	REBU09	
	GV-TauA+B
2091	FW Tau C	04 29 29.70	+26 16 50.3	BRIC02	...	
816	J04292971+2616532	04 29 29.71	+26 16 53.2	10.3	M4	X	LUHM06b	BRIC02	
	FW-TauA+B
817	J04293008+2439550	04 29 30.08	+24 39 55.0	...	M1	X	...	X	LUHM06b	REBU09	
	IRAS04264+2433
2167	J04293209+2430597	04 29 32.09	+24 30 59.7	X	X	LUHM09	REBU09	
818	J04293606+2435556	04 29 36.06	+24 35 55.6	10.78	M3	X	X	X	...	LUHM06a	REBU09	
819	J04294155+2632582	04 29 41.55	+26 32 58.2	9.76	M1	X	...	X	LUHM06b	BRIC02	REBU09
	DHTau
820	J04294247+2632493	04 29 42.47	+26 32 49.3	9.31	M0	LUHM06b	BRIC02	
	DT-TauA+B
821	J04294568+2630468	04 29 45.68	+26 30 46.8	12.61	M7.5	X	X	LUHM06b	BRIC02	
	KPNO5
	KPNO-Tau 5	BRIC02	...	

Table A.1 (cont'd)

ID	Other ID(s)	RA	DEC	J	SpT	SPEC	PM	LI	HA	UV	MIR	OPT/NIR	ARCH	Ref1	Ref2	Ref3
2269	...	04 29 49.9	+28 42 53	X	...	REBU09
822	J04295156+2606448 IQ1tau	04 29 51.56	+26 06 44.8	9.42	M0.5	X	...	X	LUHM06b	BRIC02	REBU09
823	J04295422+1754041	04 29 54.22	+17 54 04.1	12.65	M4	X	...	X	X	X	LUHM06a	LUHM06b	...
824	J04295950+2433078 CFHT20	04 29 59.50	+24 33 07.8	11.69	M5.5	X	...	X	LUHM06b	REBU09	...
2270	SCH J0429595+2433080	BRIC02
825	J04300724+2608207 KPN06	04 30 04.7	+28 33 06	...	K2	X	...	REBU09
2329	2MASS04301583+2113173 KPN06	04 30 15.83	+21 13 17.3	...	M2.5	X	BRIC02
826	J04302365+2359129 CFHT16	04 30 23.65	+23 59 12.9	14.97	M8.5	X	FIND10
2271	...	04 30 24.1	+28 19 16	...	M5	LUHM06b
827	J04302961+2426450 FXT1tauA+B	04 30 29.61	+24 26 45.0	...	M1	X	...	X	REBU09
2272	...	04 30 34.2	+25 24 27	...	K4.5	REBU09
2273	...	04 30 42.8	+27 43 29	...	M6	REBU09
828	J04304425+2601244 DK1tauA+B	04 30 44.25	+26 01 24.4	8.71	K7	X	LUHM06b	BRIC02	...
2092	DK1tauA+B	04 30 44.41	+26 01 23.8	BRIC02	REBU09	...
2274	DK1tau B	04 30 44.7	+26 33 08	...	K3	X	REBU09
829	J04305028+2300088 IRAS04278+2253	04 30 50.28	+23 00 08.8	...	F1	X	LUHM06b
830	J04305137+2442222 ZZ1tau	04 30 51.37	+24 42 22.2	...	M5	X	...	X	...	X	LUHM06b	REBU09	...
831	J04305171+2441475 ZZ1tauRS	04 30 51.71	+24 41 47.5	...	M4.5	X	...	X	LUHM06b	REBU09	...
832	J04305718+2556394 KPN07	04 30 57.18	+25 56 39.4	14.5	M8.25	X	X	X	LUHM06b	BRIC02	...
833	J04311444+2710179 JH56	04 31 14.44	+27 10 17.9	...	M0.5	BRIC02
2093	MHO 9	04 31 15.94	+18 20 04.7	...	M4.25
834	J04311907+2335047 SCH J0431191+2335048	04 31 19.07	+23 35 04.7	13.51	M7.75	BRIC02
835	J04312382+2410529 V9271tauA+B	04 31 23.82	+24 10 52.9	...	M5.5	X	LUHM06b
2094	MHO 4	04 31 24.08	+18 00 21.6	...	M7
836	J04312669+2703188	04 31 26.69	+27 03 18.8	14.83	M7.5	X	LUHM06b

Table A.1 (cont'd)

ID	Other ID(s)	RA	DEC	J	SpT	SPEC	PM	LI	HA	UV	MIR	OPT/NIR	ARCH	Ref1	Ref2	Ref3
2275	CPHT13
2276	...	04 31 31.4	+23 00 25	...	K2	X	...	REBU09
2095	L1551/RS5	04 31 33.1	+29 28 56	...	B9	X	...	REBU09
2096	LkHa 358	04 31 34.10	+18 08 04.0	13.09	X	BRIC02
2097	LkHa 358	04 31 36.27	+18 13 40.9	12.99	M5.5	X	BRIC02
2098	HL Tau	04 31 37.60	+18 12 22.2	X	BRIC02
2099	XZ Tau A+B	04 31 38.40	+18 13 59.0	10.31	K7	X	BRIC02
2277	...	04 31 40.00	+18 13 58.0	9.91	M3	X	BRIC02
2100	L1551NE	04 31 41.2	+29 39 22	...	K2	X	...	REBU09
2278	...	04 31 44.40	+18 08 32.0	16.2	X	BRIC02
837	J04315056+2424180	04 31 45.0	+28 59 08	...	F0	X	...	REBU09
2102	V710 Tau A	04 31 50.56	+24 24 18.0	10.44	M0.5	X	...	X	LUHM066	BRIC02	REBU09
2103	V710 Tau B
838	J04315844+2543299	04 31 57.70	+18 21 37.0	9.82	M0.5	X	BRIC02
2168	J04315968+1821305	04 31 57.71	+18 21 33.8	10.2	M2	X	BRIC02
839	LkHa 267	04 31 58.44	+25 43 29.9	10.59	M5	X	LUHM066	BRIC02	...
2104	L1551-51
2279	GSCO1833-00754	04 31 59.68	+18 21 30.5	...	M1.5	X	LUHM09
2105	V826 Tau
2280	...	04 32 03.29	+25 28 07.8	11.72	M6.25
2106	V826 Tau A+B	04 32 09.29	+17 57 23.1	9.71	K7	...	X	X	LUHM066
840	J04321540+2428597	04 32 13.6	+25 17 46	...	A9	X	...	REBU09
2107	MHO 5	04 32 14.6	+22 37 42	9.12	K7	X	BRIC02
841	J04321786+2422149	04 32 15.83	+18 01 38.7	9.16	K7	X	REBU09
842	CPHT7	04 32 15.40	+24 28 59.7	11.22	M0	X	...	X	BRIC02	BRIC02	REBU09
2108	MHO 6
843	J04322329+2403013	04 32 16.02	+18 12 43.4	11.16	M6	X	BRIC02
2169	J04322415+2251083	04 32 17.86	+24 22 14.9	11.54	M6	X	LUHM066
2281
2109	MHO 7	04 32 18.85	+24 22 27.1	9.51	M0.5	X	LUHM066	BRIC02	...
2282
844	J04323058+2419572	04 32 22.10	+18 27 35.7	11.76	M4.75	X	BRIC02
845	FY Tau	04 32 23.29	+24 03 01.3	12.33	M7.75	X	LUHM066
	J04323176+2420029	04 32 24.15	+22 51 08.3	...	M4.5	X	X	...	X	LUHM09	REBU09	...
	...	04 32 25.1	+26 47 32	...	K1	REBU09
	...	04 32 26.27	+18 27 45.2	11.08	M5.25	X	BRIC02
	...	04 32 28.1	+27 11 22	...	M6	REBU09
	...	04 32 30.58	+24 19 57.2	9.96	K7	X	...	X	LUHM066	BRIC02	REBU09

	...	04 32 31.76	+24 20 02.9	9.88	M0	X	...	X	LUHM066	BRIC02	REBU09

Table A.1 (cont'd)

ID	Other ID(s)	RA	DEC	J	SpT	SPEC	PM	LI	HA	UV	MIR	OPT/NIR	ARCH	Ref1	Ref2	Ref3
846	FZtau J04323205+2257266	04 32 32.05	+22 57 26.6
	IRAS04295+2251	04 32 32.05	+22 57 26.6	X	...	X	LUHM06b	REBU09	...
847	J04324282+2552314	04 32 42.82	+25 52 31.4	8.96	M2	BRIC02	...
	UZ1tauBb+Bb	04 32 42.82	+25 52 31.4	8.96	M2	X	LUHM06b	BRIC02	...
848	J04324303+2552311	04 32 43.03	+25 52 31.1	8.95	M1	X	...	X	...	X	LUHM06b	BRIC02	REBU09
	UZ1tauA	04 32 43.03	+25 52 31.1	8.95	M1	X	...	X	...	X	LUHM06b	BRIC02	...
2110	L1551+55	04 32 43.74	+18 02 56.4	10.2	K7	BRIC02
849	J04324911+2253027	04 32 49.11	+22 53 02.7	X	...	X	LUHM06b	REBU09	...
	JH 112	04 32 49.11	+22 53 02.7	X	...	X	LUHM06b	REBU09	...
2170	J04324938+2253082	04 32 49.38	+22 53 08.2	...	M4.25	X	X	LUHM09
850	J04325026+2422115	04 32 50.26	+24 22 11.5	13.96	M7.5	X	LUHM06b
	CFHT5	04 32 50.26	+24 22 11.5	13.96	M7.5	X	LUHM06b
2171	J04325119+1730092	04 32 51.19	+17 30 09.2	...	M8.25	X	X	LUHM09
	LH 0429+17	04 32 51.19	+17 30 09.2	...	M8.25	X	X	LUHM09
2283	HD284481	04 32 56.4	+22 23 42	...	A8	REBU09
851	J04330197+2421000	04 33 01.97	+24 21 00.0	10.86	M5.5	X	X	LUHM06b	BRIC02	...
	MHO8	04 33 01.97	+24 21 00.0	10.86	M5.5	X	LUHM06b	BRIC02	...
2284	HD282276	04 33 04.2	+29 21 49	...	B8	X	...	X	REBU09	...	REBU09
852	J04330622+2409339	04 33 06.22	+24 09 33.9	9.12	M2	X	...	X	LUHM06b	BRIC02	...
	GHT1tauA+B	04 33 06.22	+24 09 33.9	9.12	M2	X	...	X	LUHM06b	BRIC02	...
853	J04330664+2409549	04 33 06.64	+24 09 54.9	8.14	K7	X	...	X	LUHM06b	BRIC02	REBU09
	V807tauA+B	04 33 06.64	+24 09 54.9	8.14	K7	X	...	X	LUHM06b	BRIC02	...
854	J04330781+2616066	04 33 07.81	+26 16 06.6	...	M6	X	X	LUHM06b
	KPN014	04 33 07.81	+26 16 06.6	...	M6	X	X	LUHM06b
855	J04330945+2246487	04 33 09.45	+22 46 48.7	13.15	M6	X	X	...	X	LUHM06a	LUHM06b	REBU09
	CFHT12	04 33 09.45	+22 46 48.7	13.15	M6	X	X	...	X	LUHM06a	LUHM06b	...
856	J04331003+2433433	04 33 10.03	+24 33 43.3	9.32	K7	LUHM06b	BRIC02	...
	V830tau	04 33 10.03	+24 33 43.3	9.32	K7	LUHM06b	BRIC02	...
2285	HD282277	04 33 12.6	+29 12 50	...	A7	REBU09
932	SCH J0433131+2025200	04 33 13.1	+20 25 20.0	14.2	M5	X	X	...	SLES06
857	J04331435+2614235	04 33 14.35	+26 14 23.5	14.64	M0	X	...	X	LUHM06b	BRIC02	REBU09
	IRAS04301+2608	04 33 14.35	+26 14 23.5	14.64	M0	X	...	X	LUHM06b	BRIC02	...
2211	IRAS04302247	04 33 16.5	+22 53 20	X	REBU09
2286	...	04 33 16.6	+26 27 24	X	...	REBU09
2212	IRAS043032240	04 33 19.0	+22 46 34	...	M0.5	X	...	X	REBU09
2172	J04332621+2245293	04 33 26.21	+22 45 29.3	...	M4	X	X	...	X	LUHM09	REBU09	...
	XEST J7-036	04 33 26.21	+22 45 29.3	...	M4	X	X	...	X	LUHM09	REBU09	...
858	J04333405+2421170	04 33 34.05	+24 21 17.0	9.33	K6	X	...	X	LUHM06b	BRIC02	REBU09
	G1tau	04 33 34.05	+24 21 17.0	9.33	K6	X	...	X	LUHM06b	BRIC02	...
859	J04333456+2421058	04 33 34.56	+24 21 05.8	9.03	K7	X	...	X	LUHM06b	BRIC02	REBU09

Table A.1 (cont'd)

ID	Other ID(s)	RA	DEC	J	SpT	SPEC	PM	LI	HA	UV	MIR	OPT/NIR	ARCH	Ref1	Ref2	Ref3
860	GK Tau J04333678+2609492	04 33 36.78	+26 09 49.2	10.32	K7	BRIC02	REBU09
2173	ISTau A+B J04333905+2227207	04 33 39.05	+22 27 20.7	...	M1.75	X	X	...	X	LUHM06b
861	J04333906+2520382	04 33 39.06	+25 20 38.2	...	K7	X	...	X	LUHM06b	REBU09	REBU09
2111	DL Tau HN Tau B J04333921+1751498	04 33 39.21	+17 51 49.8	...	M4
2112	HN Tau A J04333934+175152.2	04 33 39.34	+17 51 52.2	10.7	K5	X	BRIC02
2174	J04334171+1750402	04 33 41.71	+17 50 40.2	...	M4	X	LUHM09
2287	...	04 33 41.8	+22 38 36	...	K2	X	...	REBU09
862	J04334291+2526470	04 33 42.91	+25 26 47.0	14.64	M8.75	X	LUHM06b
2175	J04334465+2615005	04 33 44.65	+26 15 00.5	...	M4.75	X	X	...	X	LUHM09	REBU09	...
2113	DM Tau J04334875+181010.2	04 33 48.75	+18 10 10.2	10.45	M1	X	BRIC02
2213	CTau J043352.0	04 33 52.0	+22 50 30	...	K7	X	...	X	REBU09
863	J04335245+2612548	04 33 52.45	+26 12 54.8	15.8	M8.5	X	X	LUHM06b	...	REBU09
2176	J04335252+2256269	04 33 52.52	+22 56 26.9	...	M5.75	X	X	...	X	LUHM09
2114	XEST 17-059 IT Tau B J04335456+261325.5	04 33 54.56	+26 13 25.5
864	J04335470+2613275	04 33 54.70	+26 13 27.5	9.89	K2	X	...	X	LUHM06b	BRIC02	REBU09
2288	IT Tau A ...	04 33 59.2	+29 36 36	...	M3	X
2214	JH108 J043410.9	04 34 10.9	+22 51 44	...	M1	X	REBU09
2215	CFHT-1 J043415.2	04 34 15.2	+22 50 30	X	REBU09
2115	HBC 407 J043418.03	04 34 18.03	+18 30 06.7	10.59	G8	X	BRIC02
2289	...	04 34 19.5	+26 52 10	REBU09
2290	HD284530 J043419.8	04 34 19.8	+23 26 49	...	B8	X	...	REBU09
2291	...	04 34 35.4	+26 44 06	...	M3	X	REBU09
2216	WaTau1 J043439.2	04 34 39.2	+25 01 01	...	K0	X	REBU09
933	SCH J0434454+2308035	04 34 45.4	+23 08 03.5	12.8	M5.25	X	SLES06
2292	...	04 34 52.5	+24 02 44	...	K2	X	...	REBU09
866	J04345542+2428531	04 34 55.42	+24 28 53.1	9.42	K7	X	...	X	LUHM06b	BRIC02	REBU09
2177	AA Tau J04345693+2258358	04 34 56.93	+22 58 35.8	...	M1.5	X	X	X	X	LUHM09
867	XEST 08-003 J04350850+2311398	04 35 08.50	+23 11 39.8	12.53	M6.5
2116	CFHT11 HO Tau J043520.20	04 35 20.20	+22 32 14.7	11.23	M0.5	REBU09	...
2117	FF Tau A+B J043520.89	04 35 20.89	+22 54 24.3	9.82	K7	X	...	X	BRIC02
2118	HBC 412 A+B J043524.51	04 35 24.51	+17 51 43.0	10.02	M2	X	BRIC02
868	J04352737+2414589	04 35 27.37	+24 14 58.9	9.15	M0	X	...	X	LUHM06b	BRIC02	REBU09
	DN Tau

Table A.1 (cont'd)

ID	Other ID(s)	RA	DEC	J	SpT	SPEC	PM	LI	HA	UV	MIR	OPT/NIR	ARCH	Ref1	Ref2	Ref3
2119	IRAS 04325+2402	04 35 35.39	+24 08 19.8	17.1	X	...	X	BRIC02	REBU09	
869	J04354093+2411087 CoKuTau3A+B	04 35 40.93	+24 11 08.7	10.75	M1	X	...	X	LUHM06b	BRIC02	REBU09
2120	CoKu Tau 3B	04 35 40.96	+24 11 07.1	X	BRIC02
2072	2M J0435418+223411	04 35 41.85	+22 34 11.6	12.96	M5.75	X	...	X	BRIC02
2178	J04354203+2252226 XEST 08-033	04 35 42.03	+22 52 22.6	...	M4.75	X	X	X	X	LUHM09
870	XEST 09-023
2179	J04354526+2737130 J04354733+2250216 HQ Tau	04 35 45.26	+27 37 13.0	15.01	M9.25	X	LUHM06b
871	J04355109+2252401 KPN015	04 35 51.09	+22 52 40.1	...	M1.5	X	...	X	X	LUHM06b
2073	2M J0435514+224911	04 35 51.43	+22 49 11.9	15.49	M8.5	X	...	X	BRIC02
2180	J04355209+2255039 XEST 08-047	04 35 52.09	+22 55 03.9	...	M4.5	X	X	X	X	LUHM09
872	J04355277+2254231 HP Tau	04 35 52.77	+22 54 23.1	9.58	K3	X	...	X	...	X	LUHM06b	BRIC02	REBU09
2181	J04355286+2250585 XEST 08-049	04 35 52.86	+22 50 58.5	...	M4.25	X	X	X	X	LUHM09
873	J04355349+2254089 XEST 09-033	04 35 53.49	+22 54 08.9	10.05	K7	LUHM06b	BRIC02	...
874	HP Tau/G3	04 35 54.15	+22 54 13.4	8.11	G0	LUHM06b	BRIC02	...
875	J04355684+2254360 Har06-28 A+B	04 35 56.84	+22 54 36.0	11.16	M5	X	...	X	LUHM06b	BRIC02	REBU09
2293	J04355760+2253574 JH225	04 35 57.6	+22 53 57	...	M5	X	...	X	X	REBU09
2182	J04355892+2238353 XEST 09-042	04 35 58.92	+22 38 35.3	...	M0	X	X	X	X	LUHM09
2294
2189	CAHA Tau 1	04 36 09.00	+24 08 21.2	X	X	...	X	REBU09
876	J04361030+2159364	04 36 10.30	+21 59 36.4	14.85	M8.5	X	X	X	X	QUAN09
877	J04361038+2259560 CFHT2	04 36 10.38	+22 59 56.0	13.76	M7.5	X	LUHM06a	LUHM06b	BRIC02
878	CFHT BD-Tau 2 J04361909+2542589	04 36 19.09	+25 42 58.9	8.84	M0	BRIC02	...	LUHM04

Table A.1 (cont'd)

ID	Other-ID(s)	RA	DEC	J	SpT	SPEC	PM	LI	HA	UV	MIR	OPT/NIR	ARCH	Ref1	Ref2	Ref3
2295	LkCa14
879	J04362151+2351165	04 36 21.4	+27 19 12	...	K2	X	REBU09
880	J04363893+2258119	04 36 21.51	+23 51 16.5	13.16	M5.25	X	LUHM06b	LUHM06a	...
	CFHT3	04 36 38.93	+22 58 11.9	13.7	M7.75	X	LUHM06b	BRIC02	...
	CFHT BD-Tau 3
2296	...	04 36 36.1	+26 59 10	...	K2	X	...	BRIC02
2297	...	04 36 42.0	+26 53 39	X	REBU09
2217	HD283759	04 36 49.1	+24 12 58	...	F2	X	...	X	REBU09
2298	...	04 37 20.8	+25 00 19	...	G0	X	...	REBU09
2183	J04373705+2331080	04 37 37.05	+23 31 08.0	...	L0	X	X	LUHM09
881	J04375670+2546229	04 37 56.70	+25 46 22.9	14.13	...	X	X	LUHM06b	LUHM06a	REBU09
	ITG1
882	J04380083+2558572	04 38 00.83	+25 58 57.2	11.55	M7.25	X	LUHM06b	LUHM04	...
	ITG2
934	SCH J0438001+2327167	04 38 00.1	+23 27 16.7	13.27	M5.25	X	SLES06
2299	...	04 38 01.9	+25 19 26	...	K8	X	X	REBU09
2300	...	04 38 03.6	+22 12 23	...	G0	X	X	...	REBU09
883	J04381486+2611399	04 38 14.86	+26 11 39.9	15.18	M7.25	X	...	X	...	X	LUHM06b	LUHM04	REBU09
2218	RXJ0438.22302	04 38 15.6	+23 02 27	...	M1	X	REBU09
935	SCH J0438163+2326404	04 38 16.3	+23 26 40.4	11.8	M4.75	X	SLES06
2301	...	04 38 16.5	+26 14 50	X	...	REBU09
884	J04382134+2609137	04 38 21.34	+26 09 13.7	12.53	M6.5	X	...	X	LUHM06b	LUHM04	REBU09
	GMTau
2302	...	04 38 26.7	+26 55 01
885	J04382858+2610494	04 38 28.58	+26 10 49.4	9.18	M0	X	...	X	LUHM06b	LUHM04	REBU09
	DOTau
886	J04383528+2610386	04 38 35.28	+26 10 38.6	8.67	M1	X	LUHM06b	LUHM04	...
	HV'TauA+B
936	SCH J0438586+2336352	04 38 58.6	+23 36 35.2	11.97	M4.25	X	SLES06
937	SCH J0438587+2323596	04 38 58.7	+23 23 59.6	12.49	M6.5	X	SLES06
938	SCH J0439016+2336030	04 39 01.6	+23 36 03.0	11.33	M6	X	X	...	X	SLES06	REBU09	...
887	J04390396+2544264	04 39 03.96	+25 44 26.4	12.65	M7.25	X	...	X	LUHM06b	LUHM04	REBU09
	CFHT6
888	J04390525+2337450	04 39 05.25	+23 37 45.0	13.38	K5	X	X	...	X	LUHM06b	LUHM06a	REBU09
939	SCH J0439064+2334179	04 39 06.4	+23 34 17.9	12.09	M7.5	X	SLES06
2141	IRAS 04361+2547	04 39 13.89	+25 53 20.9	15.32	...	X	LUHM04
2219	LkCa15	04 39 17.7	+22 21 03	...	K5	X	...	X	REBU09
889	J04392090+2545021	04 39 20.90	+25 45 02.1	9.72	M2.5	X	...	X	LUHM06b	LUHM04	REBU09
	GNTauA+B
890	J04393364+2359212	04 39 33.64	+23 59 21.2	11.57	M5	X	X	LUHM06b	LUHM06a	REBU09

Table A.1 (cont'd)

ID	Other ID(s)	RA	DEC	J	SpT	SPEC	PM	LI	HA	UV	MIR	OPT/NIR	ARCH	Ref1	Ref2	Ref3
891	J04393519+2541447	04 39 35.19	+25 41 44.7	16.68	X	LUHM06b	LUHM04	
	IRAS043654+2535
2140	HV Tau C	04 38 35.49	+26 10 41.5	...	M4	X	X	...	X	LUHM04	REBU09	
2303	...	04 39 39.9	+25 20 34	...	B9	X	...	REBU09	...	
940	SCH J0439410+2304262	04 39 41.0	+23 04 26.2	14.41	M4.5	X	SLES06	...	
2304	...	04 39 43.8	+27 19 56	...	K1	REBU09	...	
892	J04394488+2601527	04 39 44.88	+26 01 52.7	10.64	M5	X	X	LUHM06b	LUHM06a	REBU09
	ITG15
2190	CAHA Tau 2	04 39 47.20	+25 53 32.2	X	X	QUAN09	...	
893	J04394748+2601407	04 39 47.48	+26 01 40.7	11.69	M7	X	...	X	LUHM06b	LUHM04	REBU09
	CFHT4
941	SCH J0439507+2133564	04 39 50.7	+21 33 56.4	14.43	M6	X	SLES06	...	
2220	IRAS043682557	04 39 53.9	+26 03 09	X	...	X	REBU09	...	
894	J04395574+2545020	04 39 55.74	+25 45 02.0	9.84	K4	X	LUHM06b	LUHM04	
	IC20871R
895	J04400067+2358211	04 40 00.67	+23 58 21.1	12.43	M6	X	X	LUHM06b	LUHM06a	REBU09
896	J04400174+2556292	04 40 01.74	+25 56 29.2	13.22	M5.5	X	LUHM06b	...	
	CFHT17
897	J04400800+2605253	04 40 08.00	+26 05 25.3	12.41	M5.25	X	...	X	LUHM06b	REBU09	
	IRAS043704+2559	LUHM04	
2305	...	04 40 23.0	+25 57 02	...	G0	X	...	REBU09	...	
2191	CAHA Tau 3	04 40 39.30	+25 23 02.0	X	QUAN09	...	
898	J04403979+2519061	04 40 39.79	+25 19 06.1	11.82	M2	X	LUHM06b	LUHM04	
2306	...	04 40 48.4	+23 39 41	...	K0	X	REBU09	...	
899	J04404950+2551191	04 40 49.50	+25 51 19.1	10.35	M5	X	...	X	LUHM06b	LUHM04	REBU09
	JH223
942	SCH J0440534+2055473	04 40 53.4	+20 55 47.3	12.48	M5	X	SLES06	...	
2192	CAHA Tau 4	04 40 57.40	+25 50 07.9	X	X	QUAN09	...	
900	J04410424+2557561	04 41 04.24	+25 57 56.1	10.57	M3	X	LUHM06b	LUHM04	
	Har06-32
2221	IW Tau AB	04 41 04.7	+24 51 06	...	K7	X	REBU09	...	
901	J04410826+2556074	04 41 08.26	+25 56 07.4	13.21	M3	X	...	X	LUHM06b	LUHM04	REBU09
	ITG33A
902	J04411078+2555116	04 41 10.78	+25 55 11.6	13.19	M5.5	X	...	X	LUHM06b	LUHM04	REBU09
	ITG34
	CFHT8
903	J04411267+2546354	04 41 12.67	+25 46 35.4	16.74	M5.5	X	...	X	LUHM06b	LUHM04	REBU09
	IRAS04381+2540
904	J04412464+2543530	04 41 24.64	+25 43 53.0	16.71	M3.5	X	X	LUHM06b	LUHM06a	REBU09
	ITG40
2307	...	04 41 25.7	+25 43 49	X	...	REBU09	...	

Table A.1 (cont'd)

ID	Other ID(s)	RA	DEC	J	SpT	SPEC	PM	LI	HA	UV	MIR	OPT/NIR	ARCH	Ref1	Ref2	Ref3
2193	CAHA Tau 5	04 41 31.60	+25 49 32.2	X	X	...	QUAN09
905	J04413882+2556267	04 41 38.82	+25 56 26.7	11.04	M0	X	...	X	LUHM06b	LUHM04	REBU09
	IRAS04385+2550
906	J04414489+2301513	04 41 44.89	+23 01 51.3	14.41	M8.5	X	X	X	LUHM06a	LUHM06b	...
2184	J04414565+2301580	04 41 45.65	+23 01 58.0	...	M4.5	X	LUHM09
907	J04414825+2534304	04 41 48.25	+25 34 30.4	13.73	M7.75	X	...	X	LUHM06b	LUHM04	REBU09
908	J04420548+2522562	04 42 05.48	+25 22 56.2	9.11	K7	X	LUHM06b	LUHM04	...
	LkHa332/G2A+B
909	J04420732+2523032	04 42 07.32	+25 23 03.2	8.87	M1	X	LUHM06b	LUHM04	...
	LkHa332/G1A+B
910	J04420777+2523118	04 42 07.77	+25 23 11.8	9.26	K5	X	...	X	LUHM06b	LUHM04	REBU09
	V955TauA+B
911	J04422101+2520343	04 42 21.01	+25 20 34.3	11.4	M4.5	X	...	X	LUHM06b	REBU09	...
	CIDA7
912	J04423769+2515374	04 42 37.69	+25 15 37.4	10.99	M0.5	X	...	X	LUHM06b	LUHM04	REBU09
	DPTau
2308	CCDMJ044272441AB	04 42 41.1	+24 41 17	...	A0	X	...	REBU09
2309	...	04 42 53.9	+25 37 09	...	F5	X	...	REBU09
913	J04430309+2520187	04 43 03.09	+25 20 18.7	10.62	M0	X	...	X	LUHM06b	LUHM04	REBU09
	GOTau
2310	...	04 43 15.8	+23 53 58	X	REBU09
2311	...	04 43 25.1	+25 57 06	X	...	REBU09
2312	TYC1834-591-1	04 43 45.3	+24 39 08	X	...	REBU09
2313	...	04 43 58.3	+23 51 03	...	M3	X	...	REBU09
914	J04442713+2512164	04 44 27.13	+25 12 16.4	10.21	M7.25	X	...	X	LUHM06b	LUHM04	REBU09
	IRAS04414+2506
2314	HD30067	04 45 18.2	+24 24 36	...	A4	X	...	REBU09
2315	...	04 45 39.8	+25 17 04	...	M5	X	...	REBU09
2185	J04455134+1555367	04 45 51.34	+15 55 36.7	...	M2.5	X	...	X	LUHM09
	IRAS 04429+1550
	RXJ 0445 8+1556
	T 1267 425
2316	...	04 45 55.7	+26 18 58	...	K4	X	X	WICH00
2317	...	04 45 57.0	+24 40 42	...	K2	X	...	REBU09
2318	...	04 46 09.6	+24 52 37	X	X	REBU09
2319	...	04 46 39.8	+24 25 26	...	M5	REBU09
915	J04464260+2459034	04 46 42.60	+24 59 03.4	12.2	M4	X	LUHM06b	LUHM04	...
	RXJ04467+2459
2320	...	04 46 44.4	+26 23 06	...	M4	REBU09
2321	...	04 46 50.3	+24 38 15	...	K0.5	X	...	REBU09
2322	...	04 48 02.3	+25 33 59	...	K0.5	X	...	REBU09

Table A.1 (cont'd)

ID	Other ID(s)	RA	DEC	J	SpT	SPEC	PM	LI	HA	UV	MIR	OPT/NIR	ARCH	Ref1	Ref2	Ref3
2323	...	04 48 32.3	+23 47 46	X	X	...	REBU09
916	J04484189+1703374	04 48 41.89	+17 03 37.4	13.53	M7	X	X	X	LUHM06a	...	LUHM06b
2324	2MASX04485745258527	04 48 57.4	+25 58 53	X	REBU09
2325	...	04 49 13.7	+25 25 49	...	F6	X	...	REBU09
2326	CCDMJ04932438A	04 49 16.3	+24 38 27	...	K2	X	...	REBU09
2327	...	04 49 41.5	+25 40 10	...	M3	X	...	REBU09
2330	2MASS04503536+2139233	04 50 53.56	+21 39 23.3	...	M2	...	X	X	...	X	FIND10
2142	UY Aur A+B	04 51 47.38	+30 47 13.5	8.74	K7	X	LUHM04
917	J04520668+3047175	04 52 06.68	+30 47 17.5	14.42	M4	X	X	X	LUHM06a	...	LUHM06b
	IRAS04489+3042
2143	GM Aur	04 55 10.98	+30 21 59.5	8.92	K7	X	LUHM04
2131	J04552333+3027366	04 55 23.33	+30 27 36.6	13.07	M6.25	X	LUHM04
2144	LkCa 19	04 55 36.96	+30 17 55.3	8.49	K0	X	LUHM04
2132	J04554046+3039057	04 55 40.46	+30 39 05.7	12.71	M5.25	X	LUHM04
2133	J04554535+3019389	04 55 45.35	+30 19 38.9	11.44	M4.75	X	LUHM04
2145	AB Aur	04 55 45.83	+30 33 04.4	5.89	B9	X	LUHM04
2134	J04554757+3028077	04 55 47.57	+30 28 07.7	11.05	M4.75	X	LUHM04
2135	J04554801+3028050	04 55 48.01	+30 28 05.0	13.17	M5.6	X	LUHM04
2186	J04554820+3030160	04 55 48.20	+30 30 16.0	...	M4.5	X	X	...	X	LUHM09
	XEST 26-052
2136	J04554969+3019400	04 55 49.70	+30 19 40.0	12.81	M6	X	LUHM04
2137	J04555288+3006523	04 55 52.89	+30 06 52.3	11.64	M5.25	X	LUHM04
2187	J04555605+3036209	04 55 56.05	+30 36 20.9	...	M4	X	...	X	LUHM09
	JH433
	XEST 26-062
2138	J04555636+3049374	04 55 56.37	+30 49 37.5	12	M5	X	LUHM04
2146	SU Aur	04 55 59.38	+30 34 01.6	7.13	G2	X	LUHM04
2188	J04560118+3026348	04 56 01.18	+30 26 34.8	...	M3.5	X	X	LUHM09
	XEST 26-071
2147	HBC 427	04 56 02.02	+30 21 03.8	8.51	K5	X	LUHM04
2331	2MAS04565683+2308514	04 56 56.83	+23 08 51.4	...	K3	X	FIND10
2139	J04574903+3015195	04 57 49.03	+30 15 19.5	15.77	M9.25	X	LUHM04
943	SCH J0502377+2154050	05 02 37.7	+21 54 05.0	13.16	M4.25	X	SLES06
2121	CIDA 8	05 04 41.40	+25 09 54.7	10.91	M3.5	X	BRIC02
2122	CIDA 10	05 06 16.74	+24 46 10.1	10.72	M4	X	BRIC02
2123	CIDA 11	05 06 23.32	+24 32 19.9	10.41	M3.5	X	BRIC02
944	SCH J0506466+2104298	05 06 46.6	+21 04 29.8	12.05	M5.25	X	SLES06
2124	RX J05072+2437	05 07 12.07	+24 37 16.4	10.1	K6	X	BRIC02
2125	CIDA 12	05 07 54.96	+25 00 15.6	11.38	M4	X	BRIC02
2332	2MAS05122759+2253492	05 12 27.59	+22 53 49.2	...	M2	...	X	FIND10
945	SCH J0516021+2214530	05 16 02.1	+22 14 53.0	11.67	M5	X	SLES06

Table A.1 (cont'd)

ID	Other ID(s)	RA	DEC	J	SpT	SPEC	PM	LI	HA	UV	MIR	OPT/NIR	ARCH	Ref1	Ref2	Ref3
946	SCH J0516058+2236152	05 16 05.8	+22 36 15.2	13.29	M4	X	SLES06
947	SCH J0518028+2327126	05 18 02.8	+23 27 12.6	12.99	M5	X	SLES06
948	SCH J0522333+2439254	05 22 33.3	+24 39 25.4	12.75	M4.75	X	SLES06
949	SCH J0522335+2439197	05 22 33.5	+24 39 19.7	12.79	M4.5	X	SLES06
950	SCH J0523020+2428087	05 23 02.0	+24 28 08.7	12.6	M4	X	SLES06
951	SCH J0523500+2435237	05 23 50.0	+24 35 23.7	13.81	M6	X	SLES06
952	SCH J0531021+2333579	05 31 02.1	+23 33 57.9	12.28	M4	X	SLES06
953	SCH J0531026+2334022	05 31 02.6	+23 34 02.2	12.26	M4	X	SLES06
954	SCH J0532021+2423030	05 32 02.1	+24 23 03.0	13.69	M5	X	SLES06
955	SCH J0533363+2102276	05 33 36.3	+21 02 27.6	11.93	M4.5	X	SLES06
956	SCH J0534480+2243142	05 34 48.0	+22 43 14.2	12.83	M4.25	X	SLES06
957	SCH J0536190+2242428	05 36 19.0	+22 42 42.8	12.13	M4.75	X	SLES06
958	SCH J0537385+2428518	05 37 38.5	+24 28 51.8	11.66	M5.25	X	SLES06
959	SCH J0539009+2322081	05 39 00.9	+23 22 08.1	12.68	M6	X	SLES06

Table A.2.: Previously Claimed Low-Mass Praesepe Members

ID	Other ID(s)	RA	DEC	J	SpT	SPEC	PM	LJ	HA	UV	MIR	OPT/NIR	ARCH	Ref1
973	J08243324+1917432 AD666	08 24 33.24 ...	+19 17 43.2	M3.1	...	X	KRAU07
974	J08252503+2013177 AD738	08 25 25.03 ...	+20 13 17.7	M1.6	...	X	KRAU07
975	J08253573+2106085 AD755	08 25 35.73 ...	+21 06 08.5	M3.5	...	X	KRAU07
976	J08254162+1930425 AD769	08 25 41.62 ...	+19 30 42.5	M4.1	...	X	KRAU07
977	AD769
977	J08260122+2215200	08 26 01.22	+22 15 20.0	...	M3.7	...	X	KRAU07
978	J08261745+1943357 AD839	08 26 17.45 ...	+19 43 35.7	M3.4	...	X	KRAU07
979	J08263483+1933590 AD867	08 26 34.83 ...	+19 33 59.0	M2.4	...	X	KRAU07
980	J08275060+2014363 AD1025	08 27 50.60 ...	+20 14 36.3	K7.1	...	X	KRAU07
981	J08275096+1948207 AD1026	08 27 50.96 ...	+19 48 20.7	M1.2	...	X	KRAU07
982	J08281588+1812280 AD1081	08 28 15.88 ...	+18 12 28.0	M4.5	...	X	KRAU07
983	J08282020+1915307 AD1098	08 28 20.20 ...	+19 15 30.7	M3.4	...	X	KRAU07
984	J08282693+2006171 AD1121	08 28 26.93 ...	+20 06 17.1	M3.5	...	X	KRAU07
985	J08284865+1858359 AD1164	08 28 48.65 ...	+18 58 35.9	M4.7	...	X	KRAU07
986	J08284992+1959203 AD1166	08 28 49.92 ...	+19 59 20.3	M2.1	...	X	KRAU07
987	J08291780+1742115 AD1215	08 29 17.80 ...	+17 42 11.5	M3.2	...	X	KRAU07
988	J08292058+1810459 AD1223	08 29 20.58 ...	+18 10 45.9	M3.7	...	X	KRAU07
989	J08292796+2108383 AD1240	08 29 27.96 ...	+21 08 38.3	M1.1	...	X	KRAU07
990	J08295083+1823566 AD1282	08 29 50.83 ...	+18 23 56.6	M5.5	...	X	KRAU07
991	J08295706+1834000 AD1296	08 29 57.06 ...	+18 34 00.0	M1.8	...	X	KRAU07
992	J08295869+1928590 HSHU1	08 29 58.69 ...	+19 28 59.0	M4.6	...	X	KRAU07

Table A.2 (cont'd)

ID	Other ID(s)	RA	DEC	J	SpT	SPEC	PM	LI	HA	UV	MIR	OPT/NIR	ARCH	Ref1
993	J08300599+1816463 HSHJ3	08 30 05.99 ...	+18 16 46.3	M4.5	X	KRAU07
994	J08303665+1822380 HSHJ5	08 30 36.65 ...	+18 22 38.0	M5	X	KRAU07
995	J08303865+1728194 HSHJ6	08 30 38.65 ...	+17 28 19.4	M1.1	X	KRAU07
996	J08305102+1921088 HSHJ7	08 30 51.02 ...	+19 21 08.8	K7.4	X	KRAU07
997	J08305140+1853515 HSHJ8	08 30 51.40 ...	+18 53 51.5	M3.4	X	KRAU07
998	J08305580+1708223 ADJ421	08 30 55.80 ...	+17 08 22.3	M2.6	X	KRAU07
999	J08305760+2039448 ADJ423	08 30 57.60 ...	+20 39 44.8	K7.9	X	KRAU07
1000	J08305892+1841410 ADJ427	08 30 58.92 ...	+18 41 41.0	M0.3	X	KRAU07
1001	J08310020+1924160 HSHJ10	08 31 00.20 ...	+19 24 16.0	M4.4	X	KRAU07
1002	J08310603+1807480 HSHJ11	08 31 06.03 ...	+18 07 48.0	M4.4	X	KRAU07
1003	J08310759+1635041 ADJ452	08 31 07.59 ...	+16 35 04.1	M4.2	X	KRAU07
1004	J08311310+2054003 ADJ465	08 31 13.10 ...	+20 54 00.3	M3.3	X	KRAU07
1005	J08311399+2108149 ADJ467	08 31 13.99 ...	+21 08 14.9	M4.2	X	KRAU07
1006	J08312690+1840564 ADJ500	08 31 26.90 ...	+18 40 56.4	M4.8	X	KRAU07
1007	J08312987+2024374 ADJ508	08 31 29.87 ...	+20 24 37.4	M0.1	X	KRAU07
1008	J08313281+2101280 ADJ512	08 31 32.81 ...	+21 01 28.0	K7.1	X	KRAU07
1009	J08313445+1718235 ADJ515	08 31 34.45 ...	+17 18 23.5	M4.3	X	KRAU07
1010	J08314045+1947541 HSHJ15	08 31 40.45 ...	+19 47 54.1	M2	X	KRAU07
1011	J08314090+1829429 HSHJ16	08 31 40.90 ...	+18 29 42.9	M2.8	X	KRAU07
1012	J08314297+1829064 HSHJ17	08 31 42.97 ...	+18 29 06.4	M3.5	X	KRAU07
1013	J08315427+1845361	08 31 54.27	+18 45 36.1	...	M4.1	...	X	KRAU07

Table A.2 (cont'd)

ID	Other ID(s)	RA	DEC	J	SpT	SPEC	PM	LI	HA	UV	MIR	OPT/NIR	ARCH	Ref1
1014	HSHJ18 J08320188+1958471	08 32 01.88	+19 58 47.1	...	M3.6	...	X	KRAU07
1015	HSHJ19 J08320273+2046207 AD1572	08 32 02.73	+20 46 20.7	...	M3.8	...	X	KRAU07
1016	J08321067+2120296 AD1594	08 32 10.67	+21 20 29.6	...	K7.5	...	X	KRAU07
1017	J08321786+1932495 HSHJ22	08 32 17.86	+19 32 49.5	...	M3.2	...	X	KRAU07
1018	J08321889+1903086 HSHJ23	08 32 18.89	+19 03 08.6	...	M3	...	X	KRAU07
1019	J08323244+2050410 JS10	08 32 32.44	+20 50 41.0	...	M2.5	...	X	KRAU07
1020	J08324481+1802101 AD1660	08 32 44.81	+18 02 10.1	...	M3	...	X	KRAU07
1021	J08324679+1959517 HSHJ25	08 32 46.79	+19 59 51.7	...	M3.4	...	X	KRAU07
1022	J08324877+1840407 HSHJ26	08 32 48.77	+18 40 40.7	...	M3.5	...	X	KRAU07
1023	J08325309+1830293 JS16	08 32 53.09	+18 30 29.3	...	M1.6	...	X	KRAU07
1024	J08325808+2212203 AD1693	08 32 58.08	+22 12 20.3	...	M2.3	...	X	KRAU07
1025	J08325907+1718235 AD1695	08 32 59.07	+17 18 23.5	...	M2.6	...	X	KRAU07
1026	J08325958+2007149 AD1696	08 32 59.58	+20 07 14.9	...	M4.3	...	X	KRAU07
1027	J08330040+2043103 JS19	08 33 00.40	+20 43 10.3	...	M3.6	...	X	KRAU07
1028	J08330557+1855487 JS22	08 33 05.57	+18 55 48.7	...	M2.4	...	X	KRAU07
1029	J08330745+2007482 JS23	08 33 07.45	+20 07 48.2	...	K7	...	X	KRAU07
1030	J08330771+1845157 HSHJ33	08 33 07.71	+18 45 15.7	...	M3.5	...	X	KRAU07
1031	J08330845+2026372 J08331098+1929221	08 33 08.45	+20 26 37.2	...	M3.3	...	X	KRAU07
1032	HSHJ34 J08331347+2033011	08 33 10.98	+19 29 22.1	...	M3.9	...	X	KRAU07
1033	J08331347+2033011 AD1727	08 33 13.47	+20 33 01.1	...	M3.5	...	X	KRAU07
1034	J08331393+2042483	08 33 13.93	+20 42 48.3	...	M4.6	...	X	KRAU07

Table A.2 (cont'd)

ID	Other ID(s)	RA	DEC	J	SpT	SPEC	PM	LI	HA	UV	MIR	OPT/NIR	ARCH	Ref1
1035	AD1728 J08331425+2036212	08 33 14.25	+20 36 21.2	...	M4.3	...	X	KRAU07
1036	AD1731 J08331440+1904364	08 33 14.40	+19 04 36.4	...	M1.4	...	X	KRAU07
1037	JS27 J08331576+2309433	08 33 15.76	23 09 43.3	...	M4.1	...	X	KRAU07
1038	AD1734 J08331663+2120204	08 33 16.63	+21 20 20.4	...	M3.5	...	X	KRAU07
1039	AD1737 J08331799+1916328	08 33 17.99	+19 16 32.8	...	M3.7	...	X	KRAU07
1040	JS667 J08332341+1822586	08 33 23.41	+18 22 58.6	...	M4.8	...	X	KRAU07
1041	JS670 J08332348+2018032	08 33 23.48	+20 18 03.2	...	M4.7	...	X	KRAU07
1042	AD1750 J08332462+1952579	08 33 24.62	+19 52 57.9	...	M3.7	...	X	KRAU07
1043	JS669 J08332628+2331122	08 33 26.28	23 31 12.2	...	M2.2	...	X	KRAU07
1044	AD1757 J08332700+1920288	08 33 27.00	+19 20 28.8	...	M1.4	...	X	KRAU07
1045	JS35 J08332821+1843363	08 33 28.21	+18 43 36.3	...	M4.2	...	X	KRAU07
1046	HSH41 J08333385+1824300	08 33 33.85	+18 24 30.0	...	M4.3	...	X	KRAU07
1047	HSH44 J08333394+2004256	08 33 33.94	+20 04 25.6	...	M2.3	...	X	KRAU07
1048	HSH43 J08333450+1957059	08 33 34.50	+19 57 05.9	...	M4.6	...	X	KRAU07
1049	AD1775 J08333802+1857175	08 33 38.02	+18 57 17.5	...	M1.9	...	X	KRAU07
1050	JS41 J08333838+2028525	08 33 38.38	+20 28 52.5	...	M3.6	...	X	KRAU07
1051	AD1786 J08334395+1847508	08 33 43.95	+18 47 50.8	...	M2.5	...	X	KRAU07
1052	JS44 J08334526+1939160	08 33 45.26	+19 39 16.0	...	M3.9	...	X	KRAU07
1053	JS672 J08334697+2126276	08 33 46.97	+21 26 27.6	...	K7.7	...	X	KRAU07
1054	JS45 J08335077+1946586	08 33 50.77	+19 46 58.6	...	M0.5	...	X	KRAU07
	JS46

Table A.2 (cont'd)

ID	Other ID(s)	RA	DEC	J	SpT	SPEC	PM	LI	HA	UV	MIR	OPT/NIR	ARCH	Ref1
1055	J08335224+1926118 HSH150	08 33 52.24 ...	+19 26 11.8	M4.5	...	X	KRAU07
1056	J08335924+1921454 JS48	08 33 59.24 ...	+19 21 45.4	M0.3	...	X	KRAU07
1057	J08340049+1855361 HSH52	08 34 00.49 ...	+18 55 36.1	M3.2	...	X	KRAU07
1058	J08340155+2100390 AD1837	08 34 01.55 ...	+21 00 39.0	M4.2	...	X	KRAU07
1059	J08340246+1919219 JS50	08 34 02.46 ...	+19 19 21.9	M2.3	...	X	KRAU07
1060	J08340314+2020305 AD1841	08 34 03.14 ...	+20 20 30.5	M3	...	X	KRAU07
1061	J08340433+1658247 AD1844	08 34 04.33 ...	+16 58 24.7	M4.1	...	X	KRAU07
1062	J08340489+2040473 JS53	08 34 04.89 ...	+20 40 47.3	M3.1	...	X	KRAU07
1063	J08340669+2049468 AD1852	08 34 06.69 ...	+20 49 46.8	M4	...	X	KRAU07
1064	J08341139+2104148 AD1863	08 34 11.39 ...	+21 04 14.8	M4	...	X	KRAU07
1065	J08341389+2123521 AD1868	08 34 13.89 ...	+21 23 52.1	M3.9	...	X	KRAU07
1066	J08341803+1828154 HSH54	08 34 18.03 ...	+18 28 15.4	M4.3	...	X	KRAU07
1067	J08342092+2031444 AD1887	08 34 20.92 ...	+20 31 44.4	M4.3	...	X	KRAU07
1068	J08342738+1841501 AD1904	08 34 27.38 ...	+18 41 50.1	M4.7	...	X	KRAU07
1069	J08343073+1906003 JS675	08 34 30.73 ...	+19 06 00.3	M2.3	...	X	KRAU07
1070	J08343109+2037456 AD1907	08 34 31.09 ...	+20 37 45.6	M4.6	...	X	KRAU07
1071	J08343429+2122073 AD1915	08 34 34.29 ...	+21 22 07.3	M3.5	...	X	KRAU07
1072	J08343431+1847565 JS62	08 34 34.31 ...	+18 47 56.5	M2.9	...	X	KRAU07
1073	J08343499+1904229 HSH57	08 34 34.99 ...	+19 04 22.9	M4	...	X	KRAU07
1074	J08343646+1823530 JS65	08 34 36.46 ...	+18 23 53.0	M0.7	...	X	KRAU07
1075	J08343970+1908126	08 34 39.70	+19 08 12.6	...	M3	...	X	KRAU07

Table A.2 (cont'd)

ID	Other ID(s)	RA	DEC	J	SpT	SPEC	PM	LI	HA	UV	MIR	OPT/NIR	ARCH	Ref1
1076	HSHJ60 J08344851+1755588	08 34 48.51	+17 55 58.8	...	M4.4	...	X	KRAU07
1077	HSHJ62 J08344931+1725480 AD1940	08 34 49.31	+17 25 48.0	...	M2.9	...	X	KRAU07
1078	J08344967+1847040 JS72	08 34 49.67	+18 47 04.0	...	M1.5	...	X	KRAU07
1079	J08345385+1801055 HSHJ65	08 34 53.85	+18 01 05.5	...	M4	...	X	KRAU07
599	WFC142 J08345495+2138544	08 34 54.28	+19 02 32.7	X	X	...	CHAP05 KRAU07
1080	AD1951 J08345513+2006198	08 34 54.95	+21 38 54.4	...	M3.8	...	X	KRAU07
1081	J08345513+2006198 JS75	08 34 55.13	+20 06 19.8	...	M1	...	X	KRAU07
361	J08345544+201104 HSHJ064	08 34 55.40	+20 11 04.1	13.843	M4.5	X	X	...	X	X	...	ADAM02 HAMB95 KRAU07
1082	J08345733+1729160 HSHJ66	08 34 57.33	+17 29 16.0	...	M4.3	...	X	KRAU07
1083	J08345927+2108373 AD1962	08 34 59.27	+21 08 37.3	...	M4.5	...	X	KRAU07
1084	J08350623+1849246 JS680	08 35 06.23	+18 49 24.6	...	M3.3	...	X	KRAU07
362	J0835063+195648 HSHJ067	08 35 06.34	+19 56 48.0	14.963	M4.5	X	X	...	X	X	...	ADAM02 HAMB95
363	J0835078+202023 J08351477+1916317	08 35 07.89	+20 20 23.3	13.611	M3.5	X	X	...	X	X	...	ADAM02 KRAU07
1085	HSHJ70 J08351521+1922315	08 35 14.77	+19 16 31.7	...	M2.9	...	X	KRAU07
1086	J08351521+1922315 AD1994	08 35 15.21	+19 22 31.5	...	M4.5	...	X	KRAU07
1087	J08351587+1750446 HSHJ73	08 35 15.87	+17 50 44.6	...	M4.8	...	X	KRAU07
1088	J08351605+1912077 HSHJ71	08 35 16.05	+19 12 07.7	...	M3.6	...	X	KRAU07
364	J0835169+195453 JS84	08 35 16.96	+19 54 53.5	13.137	M3	X	X	...	X	X	...	ADAM02 JONE91 KRAU07
1089	J08351703+2058108 AD1999	08 35 17.03	+20 58 10.8	...	M4.7	...	X	KRAU07
1090	J08351705+1736244 HSHJ74	08 35 17.05	+17 36 24.4	...	M4.2	...	X	KRAU07
365	J0835193+194541 HSHJ075	08 35 19.35	+19 45 41.3	14.25	M4.5	X	X	...	X	X	...	ADAM02 HAMB95

Table A.2 (cont'd)

ID	Other ID(s)	RA	DEC	J	SpT	SPEC	PM	LI	HA	UV	MIR	OPT/NIR	ARCH	Ref1
1091	J08352169+1829342 JS87	08 35 21.69 ...	+18 29 34.2	M1.8	...	X	KRAU07
1092	J08352430+1925443	08 35 24.30	+19 25 44.3	...	M5	...	X	KRAU07
1093	J08353194+2101045 IZ024	08 35 31.94 ...	+21 01 04.5	M5.2	...	X	KRAU07
1094	J08353387+1855474 JS91	08 35 33.87 ...	+18 55 47.4	M0.2	...	X	KRAU07
1095	J08353571+1859445 JS92	08 35 35.71 ...	+18 59 44.5	K7.9	...	X	KRAU07
1096	J08353613+1931583 HSHJ78	08 35 36.13 ...	+19 31 58.3	M4.6	...	X	KRAU07
1097	J08353851+1821321 JS93	08 35 38.51 ...	+18 21 32.1	M2.3	...	X	KRAU07
1098	J08353928+2024099 AD2042	08 35 39.28 ...	+20 24 09.9	M4.2	...	X	KRAU07
1099	J08353967+1907364 JS94	08 35 39.67 ...	+19 07 36.4	M3.1	...	X	KRAU07
1100	J08354015+1842283 JS95	08 35 40.15 ...	+18 42 28.3	M3.3	...	X	KRAU07
1101	J08354461+1857382 HSHJ84	08 35 44.61 ...	+18 57 38.2	M4.2	...	X	KRAU07
1102	J08354678+1952153 JS97	08 35 46.78 ...	+19 52 15.3	K7.4	...	X	KRAU07
1103	J08354722+1808300 HSHJ87	08 35 47.22 ...	+18 08 30.0	M3.2	...	X	KRAU07
1104	J08354730+1935227 HSHJ86	08 35 47.30 ...	+19 35 22.7	M3.6	...	X	KRAU07
1105	J08355026+1951001 WFC94	08 35 50.26 ...	+19 51 00.1	M4.1	...	X	KRAU07
366	J0835520+201558 J08355289+1818510 JS686	08 35 51.93 08 35 52.07 ...	+19 20 33.6 +20 15 58.8 ...	14.83	M5 M1.9	X ...	X X	...	X	X	CHAP05 ADAM02 KRAU07
1107	J08355651+2037070 AD2082	08 35 56.51 ...	+20 37 07.0	M4.6	...	X	KRAU07
367	J0835572+192106 HSHJ090	08 35 57.21 ...	+19 21 06.5 ...	15.04	M4.5	X	X	...	X	X	...	ADAM02 HAMB95
1108	J08355919+1818296 HSHJ94	08 35 59.19 ...	+18 18 29.6	M1.9	...	X	KRAU07
368	J0835594+200440 HSHJ091	08 35 59.46 ...	+20 04 40.6 ...	13.885	M4	X	X	...	X	X	...	ADAM02 HAMB95
1109	J08360048+1758333	08 36 00.48	+17 58 33.3	...	M1.9	...	X	KRAU07

Table A.2 (cont'd)

ID	Other ID(s)	RA	DEC	J	SpT	SPEC	PM	LI	HA	UV	MIR	OPT/NIR	ARCH	Ref1
	JS105
1110	J08360107+2117113	08 36 01.07	+21 17 11.3	...	M4.5	...	X	KRAU07
	HSH92
369	J08360164+195731	08 36 01.62	+19 57 31.4	15.192	...	X	X	...	X	X	...	ADAM02 HAMB95 KRAU07
	HSH095
1111	J08360242+1904265	08 36 02.42	+19 04 26.5	...	M4.3	...	X	KRAU07
	HSH99
1112	J08360325+2050157	08 36 03.25	+20 50 15.7	...	M4.1	...	X	KRAU07
	HSH96
370	J08360334+192528	08 36 03.33	+19 25 28.8	14.511	M4	X	X	...	X	X	...	ADAM02 HAMB95 KRAU07
	HSH100
1113	J08360444+1955130	08 36 04.44	+19 55 13.0	...	K7.5	...	X	KRAU07
	JS107
1114	J08360631+2040599	08 36 06.31	+20 40 59.9	...	M0.4	...	X	KRAU07
	JS109
1115	J08360860+1957254	08 36 08.60	+19 57 25.4	...	M4.3	...	X	KRAU07
1116	J08360865+1844509	08 36 08.65	+18 44 50.9	...	K7.4	...	X	KRAU07
	JS112
1117	J08360896+1909309	08 36 08.96	+19 09 30.9	...	M3	...	X	KRAU07
	JS111
1118	J08360898+1913481	08 36 08.98	+19 13 48.1	...	M1.3	...	X	KRAU07
	JS110
1119	J08360991+1917166	08 36 09.91	+19 17 16.6	...	M4.8	...	X	KRAU07
	IZ031
1120	J08361083+1941413	08 36 10.83	+19 41 41.3	...	M4.1	...	X	KRAU07
1121	J08361143+1952403	08 36 11.43	+19 52 40.3	...	M0	...	X	KRAU07
	JS113
1122	J08361204+1752467	08 36 12.04	+17 52 46.7	...	M4.1	...	X	KRAU07
	HSH110
1123	J08361207+1844077	08 36 12.07	+18 44 07.7	...	M3.9	...	X	KRAU07
	JS688
371	J08361424+192530	08 36 14.29	+19 25 30.3	12.78	M3.5	X	X	...	X	X	...	ADAM02 JONE91 KRAU07
	JS689
1124	J08361553+2041098	08 36 15.53	+20 41 09.8	...	M0.2	...	X	KRAU07
	JS117
1125	J08361590+2007129	08 36 15.90	+20 07 12.9	...	M0.9	...	X	KRAU07
	JS119
1126	J08361598+2033112	08 36 15.98	+20 33 11.2	...	K7.6	...	X	KRAU07
	JS118
372	J0836161+192240	08 36 16.16	+19 22 40.7	14.645	...	X	X	...	X	X	...	ADAM02 HAMB95
	HSH113

Table A.2 (cont'd)

ID	Other ID(s)	RA	DEC	J	SpT	SPEC	PM	LI	HA	UV	MIR	OPT/NIR	ARCH	Ref1
1127	J08361902+1855084 JS124	08 36 19.02 ...	+18 55 08.4	M2.3	...	X	KRAU07
373	J0836191+195354 JS123	08 36 19.16 ...	+19 53 55.0 ...	13.489	M4	X	X	...	X	X	...	ADAM02 JONE91 KRAU07
1128	J08361936+2040467 AD2148	08 36 19.36 ...	+20 40 46.7	M5.6	...	X	ADAM02 KRAU07
374	J0836203+200700 HSH118	08 36 20.40 ...	+20 07 00.4 ...	13.758	M3.5	X	X	...	X	X	...	ADAM02 KRAU07
1129	J08362111+1850276 WFC140	08 36 21.11 ...	+18 50 27.6	M4.2	...	X	CHAP05 ADAM02 JONE91 KRAU07
598	J08362118+201219 HSH118	08 36 21.20 ...	+19 38 45.5	M3	X	X	...	X	X	...	CHAP05 ADAM02 JONE91 KRAU07
375	J08362156+2053506 JS126	08 36 21.56 ...	+20 53 50.6	M2.7	...	X	KRAU07
1130	J08362241+2007070 JS125	08 36 22.41 ...	+20 07 07.0	M3.8	...	X	KRAU07
1131	J08362327+1832422 AD2155	08 36 23.27 ...	+18 32 42.2	M5.4	...	X	KRAU07
1132	J08362342+1824210 AD2159	08 36 23.42 ...	+18 24 21.0	M0.9	...	X	KRAU07
1133	J08362515+2108565 JS129	08 36 25.15 ...	+21 08 56.5	M1.2	...	X	KRAU07
1134	J08362712+1951546 JS128	08 36 27.12 ...	+19 51 54.6	M1.4	...	X	KRAU07
1135	J08362943+2103104 JS132	08 36 29.43 ...	+21 03 10.4	M3.1	...	X	KRAU07
1136	J08362990+1938375 HSH125	08 36 29.90 ...	+19 38 37.5	X	KRAU07
607	J08363050+1955139 WFC204	08 36 30.50 ...	+19 55 13.9	M4.5	...	X	X	...	CHAP05 KRAU07
376	J0836312+193533 HSH126	08 36 31.24 ...	+19 35 33.4 ...	13.896	M4	X	X	...	X	X	...	ADAM02 HAMB95 KRAU07
1138	J08363150+1818549 JS694	08 36 31.50 ...	+18 18 54.9	M4.4	...	X	KRAU07
1139	J08363338+1954544 JS136	08 36 33.38 ...	+19 54 54.4	M1.8	...	X	KRAU07
1140	J08363491+2016307 JS139	08 36 34.91 ...	+20 16 30.7	M1.8	...	X	KRAU07
1141	J08363642+1911068 JS140	08 36 36.42 ...	+19 11 06.8	K7.2	...	X	KRAU07
1142	J08363855+2111300 AD2196	08 36 38.55 ...	+21 11 30.0	M4.4	...	X	KRAU07
1143	J08363947+2022339 JS140	08 36 39.47 ...	+20 22 33.9	M3.7	...	X	KRAU07

Table A.2 (cont'd)

ID	Other ID(s)	RA	DEC	J	SpT	SPEC	PM	LI	HA	UV	MIR	OPT/NIR	ARCH	Ref1
1144	JS141 J08364107+1818262	08 36 41.07	+18 18 26.2	...	M1.9	...	X	KRAU07
	JS144
1145	J08364118+2016399	08 36 41.18	+20 16 39.9	...	M3.5	...	X	KRAU07
593	WFC115	08 36 44.74	+19 17 23.9	X	X	...	CHAP05
377	J0836450+200845	08 36 45.02	+20 08 45.8	14,568	M4.5	X	X	...	X	X	...	ADAM02
600	WFC150	08 36 48.06	+19 49 02.2	X	X	...	CHAP05
1146	J08364895+1918593	08 36 48.95	+19 18 59.3	...	M1.8	...	X	KRAU07
	JS148
1147	J08364957+1933230	08 36 49.57	+19 33 23.0	...	M1	...	X	KRAU07
	JS150
1148	J08365052+1840541	08 36 50.52	+18 40 54.1	...	M3.8	...	X	KRAU07
	HSJU135
378	J0836510+190418	08 36 51.08	+19 04 18.6	14,121	M3.5	X	X	...	X	X	...	ADAM02
	HSJU136	HAMB95
379	J0836516+185019	08 36 51.64	+18 50 19.4	14,293	M4.5	X	X	...	X	X	...	ADAM02
	HSJU138	HAMB95
597	WFC138	08 36 52.03	+19 00 42.2	X	X	...	CHAP05
380	J0836540+193701	08 36 54.06	+19 37 01.9	14,644	M4	X	X	...	X	X	...	ADAM02
	HSJU140	HAMB95
590	WFC91	08 36 54.46	+19 54 15.3	X	X	...	CHAP05
	Riz1
603	WFC169	08 36 55.63	+19 36 15.5	X	X	...	CHAP05
381	J0836560+193557	08 36 56.00	+19 35 57.1	13,289	M3.5	X	X	...	X	X	...	ADAM02
	HSJU143	HAMB95
1149	J08365626+1857480	08 36 56.26	+18 57 48.0	...	M0.9	...	X	KRAU07
	JS159
1150	J08365659+2019101	08 36 56.59	+20 19 10.1	...	M1.6	...	X	KRAU07
	JS157
1151	J08365680+1905280	08 36 56.80	+19 05 28.0	...	K7.9	...	X	KRAU07
	JS160
1152	J08365783+2133556	08 36 57.83	+21 33 55.6	...	K7.7	...	X	KRAU07
	JS156
382	J0836586+184952	08 36 58.67	+18 49 52.3	14,159	M4.5	X	X	...	X	X	...	ADAM02
1153	J08365906+1742063	08 36 59.06	+17 42 06.3	...	M5.4	...	X	KRAU07
	AD2249
1154	J08365989+2024234	08 36 59.89	+20 24 23.4	...	K7.7	...	X	KRAU07
	AD2250
1155	J08370146+2053479	08 37 01.46	+20 53 47.9	...	M4.6	...	X	KRAU07
	HSJU146
612	WFC220	08 37 02.23	+19 52 07.6	X	X	...	CHAP05

Table A.2 (cont'd)

ID	Other ID(s)	RA	DEC	J	SpT	SPEC	PM	LI	HA	UV	MIR	OPT/NIR	ARCH	Ref1
383	J0837026+191942	08 37 02.69	+19 19 42.5	13.067	...	X	X	...	X	X	...	ADAM02
	JS163	JONE91
1156	J08370352+1932096	08 37 03.52	+19 32 09.6	...	M1.6	...	X	KRAU07
	JS164
1157	J08370374+1840025	08 37 03.74	+18 40 02.5	...	K7.4	...	X	KRAU07
	JS165
384	J0837058+191658	08 37 05.87	+19 16 58.9	14.226	M4.5	X	X	...	X	X	...	ADAM02
	HSHJ151	HAMB95
1158	J08370714+2046439	08 37 07.14	+20 46 43.9	...	M3.5	...	X	KRAU07
	AD2272
1159	J08370765+1957274	08 37 07.65	+19 57 27.4	...	M4.2	...	X	KRAU07
1160	J08371189+2040473	08 37 11.89	+20 40 47.3	...	M1.9	...	X	KRAU07
	JS166
1161	J08371261+2032414	08 37 12.61	+20 32 41.4	...	K7	...	X	KRAU07
	JS169
385	J0837139+194218	08 37 13.95	+19 42 18.1	15.141	M2	X	X	...	X	X	...	ADAM02
1162	J08371635+1929103	08 37 16.35	+19 29 10.3	...	K7.7	...	X	KRAU07
	JS172
386	J0837178+192917	08 37 17.90	+19 29 17.1	15.28	M5	X	X	...	X	X	...	ADAM02
387	J0837199+190312	08 37 19.91	+19 03 12.0	12.757	M3	X	X	...	X	X	...	ADAM02
	JS174	JONE91
1163	J08372040+2032079	08 37 20.40	+20 32 07.9	...	M4.6	...	X	KRAU07
1164	J08372243+2202003	08 37 22.43	+22 02 00.3	...	M4	...	X	KRAU07
	AD2305
1165	J08372283+1741152	08 37 22.83	+17 41 15.2	...	M3.6	...	X	KRAU07
	AD2306
1166	J08372285+1719597	08 37 22.85	+17 19 59.7	...	M4.7	...	X	KRAU07
	AD2307
1167	J08372419+1925012	08 37 24.19	+19 25 01.2	...	M1.5	...	X	KRAU07
	JS178
388	J0837245+194712	08 37 24.51	+19 47 12.1	14.436	M4.5	X	X	...	X	X	...	ADAM02
	HSHJ158	HAMB95
1168	J08372526+2006350	08 37 25.26	+20 06 35.0	...	M5.1	...	X	KRAU07
	AD2314
1169	J08372639+1907557	08 37 26.39	+19 07 55.7	...	K7.4	...	X	KRAU07
	JS180
389	J0837270+185836	08 37 27.07	+18 58 36.1	13.307	M3.5	X	X	...	X	X	...	ADAM02
	JS183	JONE91
586	WFC76	08 37 27.61	+19 37 33.0	X	CHAP05
390	J0837279+195412	08 37 27.91	+19 54 12.7	13.392	M3.5	X	X	...	X	X	...	ADAM02
1171	J08372845+2036286	08 37 28.45	+20 36 28.6	...	M0.8	...	X	KRAU07

Table A.2 (cont'd)

ID	Other ID(s)	RA	DEC	J	SpT	SPEC	PM	LI	HA	UV	MIR	OPT/NIR	ARCH	Ref1
1172	JS181 J08372941+1841355 HSHJ165	08 37 29.41 +18 41 35.5 M2.6 X	KRAU07
1173	J08373074+2107402	08 37 30.74	+21 07 40.2	...	M2.8	...	X	KRAU07
1174	J08373155+2251596	08 37 31.55	+22 51 59.6	...	M2.3	...	X	KRAU07
1175	J08373222+1853023 JS188	08 37 32.22 ...	+18 53 02.3	M1.4	X	KRAU07
1176	J08373242+1931180 JS187	08 37 32.42 ...	+19 31 18.0	M1.9	X	KRAU07
1177	J08373305+2040100 HSHJ167	08 37 33.05 ...	+20 40 10.0	M3.4	X	KRAU07
1178	J08373371+1918396 JC105	08 37 33.71 ...	+19 18 39.6	M2.1	X	KRAU07
1179	J08373505+2013265 JS191	08 37 35.05 ...	+20 13 26.5	M1.3	X	KRAU07
594	WFC118	08 37 38.73	+19 03 09.6	X	CHAP05
1180	J08374060+1933032	08 37 40.60	+19 33 03.2	...	M2.8	...	X	KRAU07
1181	J08374154+1830478 IZ049	08 37 41.54 ...	+18 30 47.8	M5.1	X	KRAU07
1182	J08374494+1940290 JS195	08 37 44.94 ...	+19 40 29.0	M2.2	X	KRAU07
1183	J08374912+1715180 AD2354	08 37 49.12 ...	+17 15 18.0	M0.8	X	KRAU07
1184	J08374921+2047068	08 37 49.21	+20 47 06.8	...	M4.8	...	X	KRAU07
1185	J08374932+1957464 HSHJ181	08 37 49.32 ...	+19 57 46.4	M5	X	KRAU07
1186	J08374982+1930508 JS200	08 37 49.82 ...	+19 30 50.8	M1.4	X	KRAU07
1187	J08374984+2047407	08 37 49.84	+20 47 40.7	...	M4.2	...	X	KRAU07
1188	J08375456+2008123 JS206	08 37 54.56 ...	+20 08 12.3	M1.3	X	KRAU07
1189	J08375488+1929097	08 37 54.88	+19 29 09.7	...	M3	...	X	KRAU07
1190	J08375712+1927499 JS702	08 37 57.12 ...	+19 27 49.9	M3.5	X	KRAU07
1191	J08375755+1858232 HSHJ189	08 37 57.55 ...	+18 58 23.2	M5	X	KRAU07
1192	J08380048+1940562 HSHJ190	08 38 00.48 ...	+19 40 56.2	M6.1	X	KRAU07
1193	J08380061+1857529 JS208	08 38 00.61 ...	+18 57 52.9	M3.6	X	KRAU07
1194	J08380113+1958430	08 38 01.13	+19 58 43.0	...	M4	...	X	KRAU07

Table A.2 (cont'd)

ID	Other ID(s)	RA	DEC	J	SpT	SPEC	PM	LI	HA	UV	MIR	OPT/NIR	ARCH	Ref1
1195	JS703	KRAU07
588	J08380136+2032295	08 38 01.36	+20 32 29.5	...	M4.8	...	X	CHAP05
1196	WFC87	08 38 02.34	+19 46 09.0	X	X	...	KRAU07
1197	J08380247+2037164	08 38 02.47	+20 37 16.4	...	M4.7	...	X	KRAU07
1198	J08380371+1941512	08 38 03.71	+19 41 51.2	...	M2.2	...	X	KRAU07
	HSJ192	KRAU07
1198	J08380462+2039352	08 38 04.62	+20 39 35.2	...	M3.4	...	X	KRAU07
	JS704	KRAU07
1199	J08380672+2009445	08 38 06.72	+20 09 44.5	...	M4.3	...	X	KRAU07
	HSJ193	KRAU07
1200	J08380676+1934178	08 38 06.76	+19 34 17.8	...	M3.6	...	X	KRAU07
	HSJ194	KRAU07
1201	J08380711+1718381	08 38 07.11	+17 18 38.1	...	M0.7	...	X	KRAU07
	AD2371	KRAU07
1202	J08380716+1746566	08 38 07.16	+17 46 56.6	...	M2.8	...	X	KRAU07
	HSJ197	KRAU07
1203	J08380730+2026556	08 38 07.30	+20 26 55.6	...	M1.5	...	X	KRAU07
595	WFC135	08 38 07.96	+19 43 28.6	X	X	...	CHAP05
1204	J08380800+2003505	08 38 08.00	+20 03 50.5	...	M3.5	...	X	KRAU07
	HSJ195	KRAU07
1205	J08380809+1844300	08 38 08.09	+18 44 30.0	...	M3.8	...	X	KRAU07
	HSJ196	KRAU07
1206	J08380817+2026461	08 38 08.17	+20 26 46.1	...	M1.3	...	X	KRAU07
604	WFC191	08 38 11.96	+19 59 43.5	X	X	...	CHAP05
1207	J08381244+2008026	08 38 12.44	+20 08 02.6	...	M4.1	...	X	KRAU07
1208	J08381365+1715158	08 38 13.65	+17 15 15.8	...	K7.2	...	X	KRAU07
	AD2380	KRAU07
1209	J08381391+2109262	08 38 13.91	+21 09 26.2	...	M1.7	...	X	KRAU07
	JS216	KRAU07
1210	J08381578+2123083	08 38 15.78	+21 23 08.3	...	M0.8	...	X	KRAU07
1211	J08381695+2018353	08 38 16.95	+20 18 35.3	...	M4.3	...	X	KRAU07
1212	J08382150+2008145	08 38 21.50	+20 08 14.5	...	M4.8	...	X	KRAU07
1213	J08382166+1836400	08 38 21.66	+18 36 40.0	...	K7.1	...	X	KRAU07
	JC123	KRAU07
1214	J08382186+2005356	08 38 21.86	+20 05 35.6	...	M4.6	...	X	KRAU07
1215	J08382386+2043409	08 38 23.86	+20 43 40.9	...	K7.2	...	X	KRAU07
	JS227	KRAU07
1216	J08382489+1658360	08 38 24.89	+16 58 36.0	...	M1.9	...	X	KRAU07
	AD2396	KRAU07
1217	J08382537+1856300	08 38 25.37	+18 56 30.0	...	M2.9	...	X	KRAU07
	JS230	KRAU07

Table A.2 (cont'd)

ID	Other ID(s)	RA	DEC	J	SpT	SPEC	PM	LI	HA	UV	MIR	OPT/NIR	ARCH	Ref1
1218	J08382537+2021210	08 38 25.37	+20 21 21.0	...	M4.3	...	X	KRAU07
391	J0838277+194555	08 38 27.73	+19 45 55.8	12.597	M2	X	X	...	X	X	...	ADAM02
	JS232	JONE91
1219	J08382819+2132460	08 38 28.19	+21 32 46.0	...	K7.4	...	X	KRAU07
	JS231
583	WFC24	08 38 32.13	+19 59 27.1	X	X	...	CHAP05
392	J0838323+184652	08 38 32.33	+18 46 52.9	13.45	M3.5	X	X	...	X	X	...	ADAM02
393	J0838328+194625	08 38 32.83	+19 46 25.7	12.875	M2.5	X	X	...	X	X	...	ADAM02
	HSHJ207	HAMB95
	JS237	KRAU07
1220	J08383287+1723380	08 38 32.87	+17 23 38.0	...	M4.3	...	X	KRAU07
	AD2415	KRAU07
1221	J083833349+2240350	08 38 33.49	+22 40 35.0	...	M3.8	...	X	KRAU07
1222	J08383412+2046292	08 38 34.12	+20 46 29.2	...	M3.5	...	X	KRAU07
	AD2420	KRAU07
1223	J08383435+1811171	08 38 34.35	+18 11 17.1	...	M0.4	...	X	KRAU07
	JS240	KRAU07
1224	J08383564+2110381	08 38 35.64	+21 10 38.1	...	M4.7	...	X	KRAU07
	HSHJ209	KRAU07
1225	J08383709+2114488	08 38 37.09	+21 14 48.8	...	M3.8	...	X	KRAU07
	HSHJ210	KRAU07
394	J0838374+191528	08 38 37.47	+19 15 28.8	13.344	M4	X	X	...	X	X	...	ADAM02
	JS241	JONE91
395	J0838390+201014	08 38 39.06	+20 10 14.8	13.183	M3.5	X	X	...	X	X	...	ADAM02
	JS243	JONE91
1226	J08383915+1729485	08 38 39.15	+17 29 48.5	...	M4.3	...	X	KRAU07
	HSHJ217	KRAU07
396	J0838392+194140	08 38 39.29	+19 41 40.2	14.73	M4.5	X	X	...	X	X	...	ADAM02
	HSHJ215	HAMB95
1227	J08383995+1754210	08 38 39.95	+17 54 21.0	...	M4	...	X	KRAU07
	HSHJ220	KRAU07
1228	J08384128+1959471	08 38 41.28	+19 59 47.1	...	M4.6	...	X	KRAU07
397	J0838414+192518	08 38 41.46	+19 25 18.2	12.014	...	X	X	...	X	X	...	ADAM02
	JS244	JONE91
398	J0838415+193418	08 38 41.59	+19 34 18.1	14.831	M4.5	X	X	...	X	X	...	ADAM02
	HSHJ218	HAMB95
601	WFC159	08 37 41.90	+19 09 31.0	X	X	...	CHAP05
399	J0838421+182255	08 38 42.15	+18 22 55.6	14.064	M4.5	X	X	...	X	X	...	ADAM02
	HSHJ222	HAMB95
400	J0838439+191738	08 38 43.92	+19 17 38.4	12.86	M3.5	X	X	...	X	X	...	ADAM02

Table A.2 (cont'd)

ID	Other ID(s)	RA	DEC	J	SpT	SPEC	PM	LI	HA	UV	MIR	OPT/NIR	ARCH	Ref1
	JS246	JONE91
1229	J08384569+2039439	08 38 45.69	+20 39 43.9	...	M4	...	X	KRAU07
1230	J08384582+2054599	08 38 45.82	+20 54 59.9	...	M4.6	...	X	KRAU07
	AD2453
401	J0838460+203436	08 38 46.10	+20 34 36.5	10.864	K6	X	X	...	X	X	...	ADAM02
	KW544	KLEI27
1231	J08384788+2145334	08 38 47.88	+21 45 33.4	...	M4.5	...	X	KRAU07
	HSHU225
1232	J08384798+2117544	08 38 47.98	+21 17 54.4	...	M3.1	...	X	KRAU07
	HSHU226
562	Prae J083850.6+192317	08 38 50.55	+19 23 16.5	X	...	GGAR06
610	WFC210	08 38 50.24	+19 30 18.6	X	X	...	CHAP05
402	J0838507+192454	08 38 50.72	+19 24 54.2	13.228	M3.5	X	X	...	X	X	...	ADAM02
	JS251	JONE91
1233	J08385084+1800525	08 38 50.84	+18 00 52.5	...	M2.7	...	X	KRAU07
	HSHU230
403	J0838510+191833	08 38 51.02	+19 18 33.6	13.961	M4.5	X	X	...	X	X	...	ADAM02
	HSHU229	HAMB95
1234	J08385103+1951021	08 38 51.03	+19 51 02.1	...	M3	...	X	KRAU07
404	J0838530+195136	08 38 53.01	+19 51 36.4	14.952	M4	X	X	...	X	X	...	ADAM02
1235	J08385420+1951446	08 38 54.20	+19 51 44.6	...	M4.3	...	X	KRAU07
	HSHU233
1236	J08385476+2047168	08 38 54.76	+20 47 16.8	...	M4.6	...	X	KRAU07
405	J0838551+201308	08 38 55.17	+20 13 08.9	13.45	M4	X	X	...	X	X	...	ADAM02
	JS255	JONE91
1237	J08385527+1917017	08 38 55.27	+19 17 01.7	...	M0.9	...	X	KRAU07
	JS256
1238	J08385547+1950334	08 38 55.47	+19 50 33.4	...	M3.6	...	X	KRAU07
1239	J08385566+1715095	08 38 55.66	+17 15 09.5	...	M3.1	...	X	KRAU07
	AD2482
1240	J08385616+2156271	08 38 56.16	+21 56 27.1	...	M4.2	...	X	KRAU07
	AD2484
1241	J08385651+1812598	08 38 56.51	+18 12 59.8	...	M4.6	...	X	KRAU07
	HSHU240
1242	J08385659+2051278	08 38 56.59	+20 51 27.8	...	M4.4	...	X	KRAU07
	HSHU236
406	J0838569+185129	08 38 56.94	+18 51 29.4	13.034	M4	X	X	...	X	X	...	ADAM02
	JS260	JONE91
1243	J08385722+2010536	08 38 57.22	+20 10 53.6	...	K7.2	...	X	KRAU07
	KW560
407	J0838577+184630	08 38 57.77	+18 46 31.0	13.55	M4	X	X	...	X	X	...	ADAM02

Table A.2 (cont'd)

ID	Other ID(s)	RA	DEC	J	SpT	SPEC	PM	LI	HA	UV	MIR	OPT/NIR	ARCH	Ref1
1244	HSHJ242 J08390185+1751208	08 39 01.85	+17 51 20.8	...	M1.1	...	X	HAMB95 KRAU07
408	AD2496 J0839029+193157	08 39 02.92	+19 31 57.3	12.844	M3.5	X	X	...	X	X	...	ADAM02 JONE83
409	JC143 J0839030+192415	08 39 03.09	+19 24 15.7	14.276	M4.5	X	X	...	X	X	...	ADAM02 HAMB95
410	HSHJ246 J0839032+200237	08 39 03.22	+20 02 37.6	11.885	K8	X	X	...	X	X	...	ADAM02 HAMB95
411	J0839039+203402	08 39 03.95	+20 34 02.3	13.118	M3.5	X	X	...	X	X	...	ADAM02 JONE91
412	JS266 J0839041+193121	08 39 04.12	+19 31 21.7	11.589	K7	X	X	...	X	X	...	ADAM02 JONE91
579	JS267 Prae J083904.7+194959	08 39 04.72	+19 49 58.6	X	...	GGAR06
413	J0839051+194526	08 39 05.13	+19 45 26.4	14.031	M4	X	X	...	X	X	...	ADAM02 HAMB95
565	HSHJ248 Prae J083905.4+192032	08 39 05.38	+19 20 31.5	X	...	GGAR06 KRAU07
1245	J08390688+2020542	08 39 06.88	+20 20 54.2	...	M1.4	...	X	KRAU07
1246	JS270 J08390695+1947080	08 39 06.95	+19 47 08.0	...	M4.8	...	X	KRAU07
414	J0839098+194658	08 39 09.87	+19 46 58.9	12.205	M2.5	X	X	...	X	X	...	ADAM02 KLEI27
1247	KW563 J08391017+2024301	08 39 10.17	+20 24 30.1	...	K7.1	...	X	KRAU07
577	JS273 Prae J083910.2+195610	08 39 10.20	+19 56 10.1	GGAR06
1248	J08391272+1930169	08 39 12.72	+19 30 16.9	...	M6.3	...	X	X	...	KRAU07
415	J0839145+200119	08 39 14.53	+20 01 19.1	12.628	M1	X	X	...	X	X	...	ADAM02 HAMB95
416	HSHJ252 J0839150+194331	08 39 15.10	+19 43 31.6	12.922	M3.5	X	X	...	X	X	...	ADAM02 JONE91
1249	JS706 J08391526+1917114	08 39 15.26	+19 17 11.4	...	M1.7	...	X	KRAU07
417	JS281 J0839153+191928	08 39 15.37	+19 19 28.6	14.898	M4.5	X	X	...	X	X	...	ADAM02 KRAU07
1250	J08391572+1920024	08 39 15.72	+19 20 02.4	...	M4.5	...	X	KRAU07
1251	HSHJ256 J08391580+2004141	08 39 15.80	+20 04 14.1	...	M1.8	...	X	KRAU07
418	KW566 J0839167+194742	08 39 16.79	+19 47 42.6	13.002	M1	X	X	...	X	X	...	ADAM02 HAMB95
1252	HSHJ257 J08391805+2044214	08 39 18.05	+20 44 21.4	...	M1.3	...	X	KRAU07
419	J0839184+192244	08 39 18.50	+19 22 44.3	15.043	M4.5	X	X	...	X	X	...	ADAM02

Table A.2 (cont'd)

ID	Other ID(s)	RA	DEC	J	SpT	SPEC	PM	LI	HA	UV	MIR	OPT/NIR	ARCH	Ref1
420	HSJ258 J0839188+184836	08 39 18.90	+18 48 36.7	13.737	M4	X	X	...	X	X	...	HAMB95 ADAM02
1253	JS708 J08391937+1838224	08 39 19.37	+18 38 22.4	...	M5	...	X	JONE91 KRAU07
421	IZ063 J0839210+182612	08 39 21.08	+18 26 12.3	14.724	M4.5	X	X	...	X	X	...	ADAM02 HAMB95
1254	HSJ263 J08392131+2205207	08 39 21.31	+22 05 20.7	...	M3.4	...	X	KRAU07
422	HSJ259 J0839215+204529	08 39 21.55	+20 45 29.4	10.487	K6	X	X	...	X	X	...	ADAM02
423	J0839218+195140	08 39 21.85	+19 51 40.2	10.894	K6	X	X	...	X	X	...	ADAM02 KLEI27
1255	KW172 J08392215+2047584	08 39 22.15	+20 47 58.4	...	M4.1	...	X	KRAU07
424	J0839224+200454	08 39 22.45	+20 04 54.8	13.375	M3	X	X	...	X	X	...	ADAM02
1256	J08392614+1848170	08 39 26.14	+18 48 17.0	...	M4.4	...	X	KRAU07
1257	J08392655+2051446	08 39 26.55	+20 51 44.6	...	M4.4	...	X	KRAU07
1258	HSJ264 J08392667+2025523	08 39 26.67	+20 25 52.3	...	M3.4	...	X	KRAU07
425	J0839272+204359	08 39 27.28	+20 43 59.1	15.3	M5	X	X	...	X	X	...	ADAM02
1259	J08392745+1814556	08 39 27.45	+18 14 55.6	...	M3.8	...	X	KRAU07
426	AD2566 J0839285+192825	08 39 28.59	+19 28 25.2	10.054	K6	X	X	...	X	X	...	ADAM02 KLEI27
1260	KW184 J08393066+1758513	08 39 30.66	+17 58 51.3	...	M3.7	...	X	KRAU07
427	HSJ271 J0839307+185653	08 39 30.72	+18 56 53.4	14.686	M4.5	X	X	...	X	X	...	ADAM02 HAMB95
428	HSJ269 J0839309+195801	08 39 30.96	+19 58 01.9	13.537	M4.5	X	X	...	X	X	...	ADAM02 HAMB95
429	HSJ267 J0839317+192417	08 39 31.76	+19 24 17.6	13.606	M3	X	X	...	X	X	...	ADAM02 HAMB95
430	HSJ270 J0839320+203920	08 39 32.04	+20 39 20.4	10.361	K6	X	X	...	X	X	...	ADAM02 HAMB95
1261	JS297 J08393244+2102526	08 39 32.44	+21 02 52.6	...	M3.9	...	X	ADAM02 HAMB95
431	HSJ268 J0839346+194800	08 39 34.66	+19 48 00.3	13.297	M3.5	X	X	...	X	X	...	ADAM02 HAMB95
1262	HSJ272 J08393572+2144214	08 39 35.72	+21 44 21.4	...	M4.9	...	X	KRAU07
432	AD2587 J0839361+184049	08 39 36.16	+18 40 49.0	14.899	M4.5	X	X	...	X	X	...	ADAM02 HAMB95
	HSJ276	ADAM02 HAMB95

Table A.2 (cont'd)

ID	Other ID(s)	RA	DEC	J	SpT	SPEC	PM	LI	HA	UV	MIR	OPT/NIR	ARCH	Ref1
433	J0839364+191537	08 39 36.44	+19 15 37.8	11.843	K8	X	X	...	X	X	...	ADAM02
	JS302	JONE91
1263	J08393645+1929079	08 39 36.45	+19 29 07.9	...	K7.6	...	X	KRAU07
	JS301
1264	J08393704+1747198	08 39 37.04	+17 47 19.8	...	M0.2	...	X	KRAU07
	AD2595
1265	J08393715+1948580	08 39 37.15	+19 48 58.0	...	K7.8	...	X	KRAU07
	KW569
608	WFC207	08 39 39.37	+19 47 54.9	X	X	...	CHAP05
1266	J08393965+1906562	08 39 39.65	+19 06 56.2	...	M4.6	...	X	KRAU07
434	J0839400+185049	08 39 40.07	+18 50 49.2	14.995	M4.5	X	X	...	X	X	...	ADAM02
	HSJ280	HAMB95
435	J0839405+183658	08 39 40.59	+18 36 58.8	13.977	M4.5	X	X	...	X	X	...	ADAM02
	HSJ282	HAMB95
436	J0839405+191853	08 39 40.51	+19 18 53.9	14.123	M4	X	X	...	X	X	...	ADAM02
	HSJ279	HAMB95
1267	J08394103+1959288	08 39 41.03	+19 59 28.8	...	M0.4	...	X	KRAU07
1268	J08394166+1929004	08 39 41.66	+19 29 00.4	...	M5	...	X	KRAU07
1269	J08394174+2001415	08 39 41.74	+20 01 41.5	...	M0.5	...	X	KRAU07
	KW571
437	J0839420+201745	08 39 42.04	+20 17 45.1	14.043	M4	X	X	...	X	X	...	ADAM02
1270	J08394255+1918288	08 39 42.55	+19 18 28.8	...	M4	...	X	KRAU07
1271	J08394360+2029395	08 39 43.60	+20 29 39.5	...	M3.2	...	X	KRAU07
	JS311
438	J0839452+200727	08 39 45.21	+20 07 27.5	13.165	M4	X	X	...	X	X	...	ADAM02
	JS313	JONE91
439	J0839457+185834	08 39 45.73	+18 58 34.0	13.475	M3.5	X	X	...	X	X	...	ADAM02
	HSJ286	HAMB95
1272	J08394656+1913041	08 39 46.56	+19 13 04.1	...	M0.5	...	X	KRAU07
	JS317
1273	J08394675+1944126	08 39 46.75	+19 44 12.6	...	M3.9	...	X	KRAU07
1274	J08394730+1939344	08 39 47.30	+19 39 34.4	...	M3.7	...	X	KRAU07
1275	J08395128+2034499	08 39 51.28	+20 34 49.9	...	M1.6	...	X	KRAU07
	JS318
440	J0839526+203046	08 39 52.64	+20 30 46.4	13.372	M3.5	X	X	...	X	X	...	ADAM02
	JS715	JONE91
1276	J08395276+2001052	08 39 52.76	+20 01 05.2	...	M2.9	...	X	KRAU07
	JS321
441	J0839531+192403	08 39 53.16	+19 24 03.7	13.94	M4	X	X	...	X	X	...	ADAM02
442	J0839544+192737	08 39 54.41	+19 27 37.2	14.268	M4	X	X	...	X	X	...	ADAM02
	HSJ291	HAMB95

Table A.2 (cont'd)

ID	Other ID(s)	RA	DEC	J	SpT	SPEC	PM	LI	HA	UV	MIR	OPT/NIR	ARCH	Ref1
1277	J08395663+1710335 AD2651	08 39 56.63 ...	+17 10 33.5	M6.3	...	X	KRAU07
1278	J08400006+1722060 AD2662	08 40 00.06 ...	+17 22 06.0	M4.5	...	X	KRAU07
443	J0840007+191834 JS329	08 40 00.72 ...	+19 18 34.8 ...	11.757	K9	...	X	...	X	X	...	ADAM02 JONE91
444	J0840013+202222 J08400249+1916397	08 40 01.35 08 40 02.49	+20 22 22.7 +19 16 39.7	15.056	M4.5	X	X	...	X	X	...	ADAM02 KRAU07
445	J0840024+194035 HSH293	08 40 02.49 ...	+19 40 35.4 ...	13.74	M4	X	X	...	X	X	...	ADAM02 HAMB95
1280	J08400351+2317173 AD2675	08 40 03.51 ...	23 17 17.3	M4.5	...	X	KRAU07
1281	J08400367+1954595 J0840039+185557	08 40 03.67 08 40 03.92	+19 54 59.5 +18 55 57.5	...	M3.8	...	X	KRAU07 ADAM02
446	J0840039+185557 J0840041+192450	08 40 03.92 08 40 04.17	+18 55 57.5 +19 24 50.3	15.097 13.834	M5 M4.5	X X	X X	...	X X	X X	...	ADAM02 HAMB95
447	HSH295	HAMB95
448	J0840063+191826 KW257	08 40 06.36 ...	+19 18 26.5 ...	9.732	K6	X	X	...	X	X	...	ADAM02 KLEI27
449	J0840081+201306 HSH299	08 40 08.16 ...	+20 13 06.6 ...	14.662	M5	X	X	...	X	X	...	ADAM02 HAMB95
1282	J08401002+2025083 JS340	08 40 10.02 ...	+20 25 08.3	M1.2	...	X	KRAU07
450	J0840106+202050 J0840108+185857	08 40 10.61 08 40 10.85	+20 20 50.5 +18 58 57.1	15.412 12.907	M5 M3.5	X X	X X	...	X X	X X	...	ADAM02 ADAM02
451	JS344	JONE91
1283	J08401146+2004032 J0840115+193911	08 40 11.46 08 40 11.59	+20 04 03.2 +19 39 11.8	...	M3.4 M4	...	X X	KRAU07 ADAM02
452	HSH302	HAMB95
453	J0840131+200328 HSH303	08 40 13.10 ...	+20 03 28.1 ...	13.135	M4	X	X	...	X	X	...	ADAM02 HAMB95
454	J0840134+194643 KW267	08 40 13.45 ...	+19 46 43.7 ...	11.328	K7	X	X	...	X	X	...	ADAM02 HAMB95
455	J0840137+194455 KW573	08 40 13.79 ...	+19 44 56.0 ...	12.773	M2	X	X	...	X	X	...	ADAM02 KLEI27
1284	J08401520+2005140 J0840157+195454	08 40 15.20 08 40 15.71	+20 05 14.0 +19 54 54.3	...	M4.1 K7	...	X X	KRAU07 ADAM02
456	KW272	10.71	X	X	...	KLEI27
1285	J08401690+2042422 J0840169+204200	08 40 16.90 08 40 16.95	+20 42 42.2 +20 42 00.8	...	M2.9 M4.5	...	X X	KRAU07 ADAM02
457	HSH309	15.153	X	X	...	ADAM02 HAMB95

Table A.2 (cont'd)

ID	Other ID(s)	RA	DEC	J	SpT	SPEC	PM	LI	HA	UV	MIR	OPT/NIR	ARCH	Ref1
458	J0840170+183629	08 40 17.07	+18 36 29.8	14.278	M4	X	X	...	X	X	...	ADAM02
	HSU310	HAMB95
459	J0840224+203827	08 40 22.42	+20 38 27.2	12.108	K9	X	X	...	X	X	...	ADAM02
	JS353	JONE91
1286	J08401909+1821429	08 40 19.09	+18 21 42.9	...	M1.9	...	X	KRAU07
	JS351
1287	J08401920+1838025	08 40 19.20	+18 38 02.5	...	M4.9	...	X	KRAU07
1288	J08401923+1812410	08 40 19.23	+18 12 41.0	...	M4.6	...	X	KRAU07
	AD2740
1289	J08401982+1855382	08 40 19.82	+18 55 38.2	...	M2	...	X	KRAU07
	JS352
1290	J08402217+1807248	08 40 22.17	+18 07 24.8	...	M0.7	...	X	KRAU07
	JS355
460	J0840265+201513	08 40 26.58	+20 15 13.3	13.054	M2.5	X	X	...	X	X	...	ADAM02
1291	J08402823+1856090	08 40 28.23	+18 56 09.0	...	K7.8	...	X	KRAU07
	JS364
461	J0840305+195558	08 40 30.60	+19 55 58.9	13.267	M2.5	X	X	...	X	X	...	ADAM02
	JS365	JONE91
1292	J08403106+1825562	08 40 31.06	+18 25 56.2	...	M2.5	...	X	KRAU07
	HSU322
462	J0840318+201205	08 40 31.85	+20 12 06.0	10.252	K6	X	X	...	X	X	...	ADAM02
	KW304	KLEI27
1293	J08403416+1821331	08 40 34.16	+18 21 33.1	...	M3.9	...	X	KRAU07
	HSU326
463	J0840349+203603	08 40 34.96	+20 36 03.8	14.883	M4.5	X	X	...	X	X	...	ADAM02
1294	J08403626+1757003	08 40 36.26	+17 57 00.3	...	M2.8	...	X	KRAU07
	AD2795
464	J0840378+202017	08 40 37.89	+20 20 17.9	12.2	M0	X	X	...	X	X	...	ADAM02
	JS373	JONE91
571	Prae J084039.3+192840	08 40 39.28	+19 28 39.6	GGAR06
465	J0840393+195623	08 40 39.37	+19 56 23.9	13.575	M4	X	X	...	X	X	...	ADAM02
466	J0840394+194255	08 40 39.42	+19 42 55.5	13.48	M4	X	X	...	X	X	...	ADAM02
1295	J08403952+1849057	08 40 39.52	+18 49 05.7	...	K7	...	X	KRAU07
467	J0840416+193000	08 40 41.66	+19 30 00.9	14.372	M5	X	X	...	X	X	...	ADAM02
	HSU328	HAMB95
468	J0840424+193357	08 40 42.49	+19 33 57.7	10.116	K6	X	X	...	X	X	...	ADAM02
	KW326	KLEI27
589	WFC88	08 40 43.86	+19 06 00.8	X	X	...	CHAP05
1296	J08404426+2028187	08 40 44.26	+20 28 18.7	...	K7.7	...	X	KRAU07
	JS379
575	Prae J084044.9+200025	08 40 44.90	+20 00 25.3	X	...	GGAR06

Table A.2 (cont'd)

ID	Other ID(s)	RA	DEC	J	SpT	SPEC	PM	LI	HA	UV	MIR	OPT/NIR	ARCH	Ref1
576	Prae J084045.2+192532	08 40 45.24	+19 25 32.3	X	...	GGAR06
1297	J08404692+2028291	08 40 46.92	+20 28 29.1	...	M1.2	...	X	KRAU07
	JS384
469	J0840477+202847	08 40 47.78	+20 28 47.9	13.17	M3	X	X	...	X	X	...	ADAM02
574	Prae J084049.1+195913	08 40 49.14	+19 59 12.6	X	...	GGAR06
609	WFC208	08 40 50.31	+18 23 59.8	X	X	...	CHAP05
563	Prae J084051.2+191010	08 40 51.24	+19 10 09.5	X	...	GGAR06
470	J0840518+195630	08 40 51.87	+19 56 30.2	13.312	M3	X	X	...	X	X	...	ADAM02
	JS390	JONE91
1298	J08405231+1910284	08 40 52.31	+19 10 28.4	...	M3.6	...	X	KRAU07
	JS391
572	Prae J084052.5+190504	08 40 52.52	+19 05 03.5	X	...	GGAR06
471	J0840532+184454	08 40 53.26	+18 44 54.2	14.6	M4	X	X	...	X	X	...	ADAM02
602	WFC163	08 40 53.59	+19 40 58.3	X	X	...	CHAP05
1299	J08405382+1922440	08 40 53.82	+19 22 44.0	...	M1.3	...	X	KRAU07
	JS394
472	J0840539+200524	08 40 53.97	+20 05 24.4	13.796	M3.5	X	X	...	X	X	...	ADAM02
	HSJ333	HAMB95
1300	J08405531+1834592	08 40 55.31	+18 34 59.2	...	K7.6	...	X	KRAU07
	JS398
1301	J08405548+1817523	08 40 55.48	+18 17 52.3	...	M3.6	...	X	KRAU07
	AD2853
473	J0840557+184934	08 40 55.72	+18 49 34.5	14.359	M4	X	X	...	X	X	...	ADAM02
	HSJ338	HAMB95
1302	J08405590+1814462	08 40 55.90	+18 14 46.2	...	M3.9	...	X	KRAU07
	HSJ341
474	J0840568+194611	08 40 56.83	+19 46 11.9	15.051	M4.5	X	X	...	X	X	...	ADAM02
	HSJ340	HAMB95
580	Prae J084057.3+190258	08 40 57.37	+19 02 57.7	X	...	GGAR06
1303	J08405751+2028414	08 40 57.51	+20 28 41.4	...	M4.5	...	X	X	...	KRAU07
1304	J08405784+2307169	08 40 57.84	23 07 16.9	...	M4.5	...	X	KRAU07
	AD2860
475	J0840580+201250	08 40 58.08	+20 12 50.3	14.901	M5	X	X	...	X	X	...	ADAM02
	HSJ342	HAMB95
1305	J08405844+1850463	08 40 58.44	+18 50 46.3	...	M3.7	...	X	KRAU07
1306	J08405877+2228499	08 40 58.77	+22 28 49.9	...	M4.9	...	X	KRAU07
	AD2865
1307	J08405890+1914167	08 40 58.90	+19 14 16.7	...	M5	...	X	KRAU07
1308	J08410176+1748515	08 41 01.76	+17 48 51.5	...	M4.2	...	X	KRAU07
	AD2872
1309	J08410264+1810067	08 41 02.64	+18 10 06.7	...	M4.5	...	X	KRAU07

Table A.2 (cont'd)

ID	Other ID(s)	RA	DEC	J	SpT	SPEC	PM	LI	HA	UV	MIR	OPT/NIR	ARCH	Ref1
476	HSHU347 J0841031+185555	08 41 03.14	... +18 55 55.2	... 13.937	M4	X	X	...	X	X	...	ADAM02
	HSHU346	HAMB95
1310	J08410314+1918093	08 41 03.14	+19 18 09.3	...	M4.6	...	X	KRAU07
477	J0841033+183716	08 41 03.34	+18 37 16.0	15.377	M4.5	X	X	...	X	X	...	ADAM02
1311	J08410532+2028245	08 41 05.32	+20 28 24.5	...	K7.7	...	X	KRAU07
	JS405
478	J0841064+190610	08 41 06.47	+19 06 10.7	15.135	M5	X	X	...	X	X	...	ADAM02
	HSHU348	HAMB95
479	J0841068+192637	08 41 06.90	+19 26 37.0	13.748	M4	X	X	...	X	X	...	ADAM02
1312	J08410746+2154566	08 41 07.46	+21 54 56.6	...	M5	...	X	KRAU07
564	Prae J084108.0+191401	08 41 08.00	+19 14 00.6	X	...	GGAR06
570	Prae J084108.1+191111	08 41 08.13	+19 11 10.8	X	...	GGAR06
1313	J08410926+1734170	08 41 09.26	+17 34 17.0	...	M4.4	...	X	KRAU07
	AD2892
1314	J08411016+1912133	08 41 10.16	+19 12 13.3	...	M4.7	...	X	KRAU07
480	J0841103+194907	08 41 10.31	+19 49 07.1	10.204	K6	X	X	...	X	X	...	ADAM02
	KW368	KLEI27
1315	J08411052+1816070	08 41 10.52	+18 16 07.0	...	M1.7	...	X	KRAU07
	JS415
1316	J08411052+1956067	08 41 10.52	+19 56 06.7	...	M2.6	...	X	KRAU07
481	J0841107+190153	08 41 10.76	+19 01 54.0	13.742	M4.5	X	X	...	X	X	...	ADAM02
	JS725	JONE91
482	J0841110+202238	08 41 11.07	+20 22 38.5	12.725	M2	X	X	...	X	X	...	ADAM02
	JS411	JONE91
581	Prae J084111.2+191349	08 41 11.15	+19 13 49.1	GGAR06
483	J0841113+193146	08 41 11.31	+19 31 46.8	12.798	M3	X	X	...	X	X	...	ADAM02
	JS414	JONE91
1317	J08411162+2215516	08 41 11.62	+22 15 51.6	...	M2.4	...	X	KRAU07
	HSHU350
578	Prae J084111.9+192043	08 41 11.90	+19 20 43.3	X	...	GGAR06
484	J0841131+193234	08 41 13.19	+19 32 34.9	11.234	M0	X	X	...	X	X	...	ADAM02
	JS418	JONE91
1318	J08411392+1858090	08 41 13.92	+18 58 09.0	...	M1.8	...	X	KRAU07
	JS419
485	J0841140+204429	08 41 14.06	+20 44 29.8	13.034	M4	X	X	...	X	ADAM02
	JS416	JONE91
486	J0841144+205946	08 41 14.45	+20 59 46.3	14.644	M4.5	X	X	...	X	X	...	ADAM02
	HSHU356	JONE91
568	Prae J084114.5+191110	08 41 14.46	+19 11 10.1	ADAM02
1319	J08411490+1727366	08 41 14.90	+17 27 36.6	...	M4.1	...	X	HAMB95
		GGAR06
		KRAU07

Table A.2 (cont'd)

ID	Other ID(s)	RA	DEC	J	SpT	SPEC	PM	LI	HA	UV	MIR	OPT/NIR	ARCH	Ref1
	AD2919
487	J0841152+191149	08 41 15.30	+19 11 49.1	14.846	M3	X	X	...	X	X	...	ADAM02
488	J0841154+200216	08 41 15.42	+20 02 16.1	11.878	K8	X	X	...	X	X	...	ADAM02 KLEI27
	KW575	KRAU07
1320	J08411543+1905104	08 41 15.43	+19 05 10.4	...	M1.9	...	X	GGAR06
567	Prae J084115.8+191743	08 41 15.79	+19 17 43.0	X	...	ADAM02
489	J0841163+204854	08 41 16.31	+20 48 54.9	15.374	M5	X	X	...	X	X	...	ADAM02
490	J0841174+203233	08 41 17.49	+20 32 33.0	14.055	M4	X	X	...	X	X	...	ADAM02
1321	J08411779+1703206	08 41 17.79	+17 03 20.6	...	M4.1	...	X	KRAU07
	AD2928
491	J0841190+190518	08 41 19.10	+19 05 18.7	13.735	M4.5	X	X	...	X	X	...	ADAM02
	HSH362	HAMB95
1322	J08411969+1905544	08 41 19.69	+19 05 54.4	...	M4.1	...	X	KRAU07
	AD2934
492	J0841203+185743	08 41 20.34	+18 57 43.0	14.112	M4	X	X	...	X	X	...	ADAM02
	HSH364	HAMB95
1323	J08412044+1937224	08 41 20.44	+19 37 22.4	...	M1	...	X	KRAU07
	JS427
493	J0841208+202047	08 41 20.87	+20 20 47.6	13.188	M2.5	X	X	...	X	X	...	ADAM02
	JS426	JONE91
573	Prae J084122.6+192419	08 41 22.58	+19 24 19.0	GGAR06
1324	J08412371+2056221	08 41 23.71	+20 56 22.1	...	M4.6	...	X	KRAU07
	AD2943
494	J0841239+201457	08 41 23.90	+20 14 57.3	11.661	M0	X	X	...	X	X	...	ADAM02
	KW577	KLEI27
1325	J08412417+1814026	08 41 24.17	+18 14 02.6	...	M1	...	X	KRAU07
	JS432
495	J0841244+200749	08 41 24.46	+20 07 49.6	12.549	M3.5	X	X	...	X	X	...	ADAM02
	JS430	JONE91
585	WFC60	08 41 25.03	+19 09 25.0	X	CHAP05
496	J0841260+195915	08 41 26.03	+19 59 15.2	13.9	M4	X	X	...	X	X	...	ADAM02
	HSH368	HAMB95
1326	J08412614+1748127	08 41 26.14	+17 48 12.7	...	M3.4	...	X	KRAU07
	HSH372
569	Prae J084126.5+195200	08 41 26.54	+19 51 59.7	GGAR06
1329	J08412873+1942490	08 41 28.73	+19 42 49.0	...	M4.3	...	X	X	...	KRAU07
1327	J08412680+1952367	08 41 26.80	+19 52 36.7	...	M4.3	...	X	KRAU07
1328	J08412772+2103409	08 41 27.72	+21 03 40.9	...	M3.5	...	X	KRAU07
	JS730
605	WFC193	08 41 27.76	+19 07 19.7	X	CHAP05
497	J0841288+195832	08 41 28.81	+19 58 32.2	13.008	M3.5	X	X	...	X	X	...	ADAM02

Table A.2 (cont'd)

ID	Other ID(s)	RA	DEC	J	SpT	SPEC	PM	LI	HA	UV	MIR	OPT/NIR	ARCH	Ref1
498	JS434 J0841289+184535	08 41 29.00	JONE91
566	Præ J084130.4+190449	08 41 30.43	+19 04 35.2	15.098	M5	X	X	...	X	X	...	ADAM02
499	J084132.5+200606	08 41 32.52	+20 06 07.0	14.572	M4	X	X	...	X	X	...	GGAR06
	HSU376	ADAM02
1330	J084132.75+1940138	08 41 32.75	+19 40 13.8	...	M5.8	...	X	HAMB95
500	J084133.5+193300	08 41 33.55	+19 33 00.3	14.58	M4	X	X	...	X	X	...	KRAU07
1331	J084133.83+2247556	08 41 33.83	+22 47 55.6	...	M3.5	...	X	ADAM02
	AD2970	KRAU07
501	J084133.8+195808	08 41 33.84	+19 58 08.7	10.396	K6	X	X	...	X	X	...	ADAM02
	KW403	KLEI27
502	J084135.6+184435	08 41 35.70	+18 44 35.0	13.179	M3.5	X	X	...	X	X	...	ADAM02
	JS441	JONE91
1332	J084135.86+2117371	08 41 35.86	+21 17 37.1	...	M3.7	...	X	KRAU07
	HSU378
1333	J084135.99+1906255	08 41 35.99	+19 06 25.5	...	K7.1	...	X	KRAU07
	JC259
503	J084136.5+203404	08 41 36.51	+20 34 04.3	14.145	M4	X	X	...	X	X	...	ADAM02
1334	J084136.62+1854155	08 41 36.62	+18 54 15.5	...	M3	...	X	KRAU07
504	J084137.3+201236	08 41 37.37	+20 12 37.0	14.193	M4	X	X	...	X	X	...	ADAM02
	HSU381	HAMB95
1335	J084137.58+2032004	08 41 37.58	+20 32 00.4	...	M4.8	...	X	KRAU07
	AD2991
1336	J084138.48+1738240	08 41 38.48	+17 38 24.0	...	M0.4	...	X	KRAU07
	HSU385
505	J084139.2+194028	08 41 39.22	+19 40 28.2	13.205	M3.5	X	X	...	X	X	...	ADAM02
	JS447	JONE91
506	J084141.7+194957	08 41 41.74	+19 49 57.5	14.54	M4.5	X	X	...	X	X	...	ADAM02
1337	J084141.75+2019084	08 41 41.75	+20 19 08.4	...	M5.7	...	X	KRAU07
1338	J084142.06+2034079	08 41 42.06	+20 34 07.9	...	M4.2	...	X	KRAU07
1339	J084142.34+1812478	08 41 42.34	+18 12 47.8	...	M4.7	...	X	KRAU07
	HSU389
1340	J084143.34+2121422	08 41 43.34	+21 21 42.2	...	M4.2	...	X	KRAU07
	AD3005
1341	J084143.42+2129504	08 41 43.42	+21 29 50.4	...	M5.1	...	X	KRAU07
	HSU386
1342	J084143.88+1918082	08 41 43.88	+19 18 08.2	...	M0	...	X	KRAU07
	JS452
507	J084144.1+203616	08 41 44.14	+20 36 16.0	13.877	M4	X	X	...	X	X	...	ADAM02
592	WFC104	08 41 47.75	+19 48 37.7	X	X	...	CHAP05
1343	J084147.92+2023226	08 41 47.92	+20 23 22.6	...	M4.4	...	X	KRAU07

Table A.2 (cont'd)

ID	Other ID(s)	RA	DEC	J	SpT	SPEC	PM	LI	HA	UV	MIR	OPT/NIR	ARCH	Ref1
1344	J08414793+1959500	08 41 47.93	+19 59 50.0	...	M4.9	...	X	KRAU07
508	J0841481+192731	08 41 48.19	+19 27 31.2	11.442	K7	X	X	...	X	X	...	ADAM02
	JS455	JONE91
1345	J08414934+1911471	08 41 49.34	+19 11 47.1	...	K7.6	...	X	KRAU07
	JS456
509	J0841494+200436	08 41 49.46	+20 04 36.3	12.874	M3.5	X	X	...	X	X	...	ADAM02
	HSH393	HAMB95
510	J0841500+193934	08 41 50.05	+19 39 34.7	12.773	M2	X	X	...	X	X	...	ADAM02
	JS457	JONE91
587	WFC81	08 41 50.21	+19 06 18.4	X	X	...	CHAP05
1346	J08415058+1929395	08 41 50.58	+19 29 39.5	...	M4.4	...	X	KRAU07
1347	J08415192+2020479	08 41 51.92	+20 20 47.9	...	M1.9	...	X	KRAU07
	JS459
1348	J08415223+1942283	08 41 52.23	+19 42 28.3	...	M4.1	...	X	KRAU07
1349	J08415228+1803067	08 41 52.28	+18 03 06.7	...	K7.6	...	X	KRAU07
	JS462
511	J0841533+191555	08 41 53.35	+19 15 55.8	14.796	M4.5	X	X	...	X	X	...	ADAM02
512	J0841535+193630	08 41 53.59	+19 36 30.7	14.577	M4.5	X	X	...	X	X	...	ADAM02
	HSH397	HAMB95
1350	J08415364+2037159	08 41 53.64	+20 37 15.9	...	M4.6	...	X	KRAU07
1351	J08415464+1818102	08 41 54.64	+18 18 10.2	...	M4.3	...	X	KRAU07
	HSH399
1352	J08415476+1937009	08 41 54.76	+19 37 00.9	...	M4.8	...	X	KRAU07
	IZ080
1353	J08415935+1944452	08 41 59.35	+19 44 45.2	...	M1.2	...	X	KRAU07
513	J0842016+192646	08 42 01.60	+19 26 46.1	14.142	M4	X	X	...	X	X	...	ADAM02
	HSH404	HAMB95
514	J0842016+192701	08 42 01.67	+19 27 01.5	14.215	M4.5	X	X	...	X	X	...	ADAM02
	HSH405	HAMB95
1354	J08420327+2110215	08 42 03.27	+21 10 21.5	...	M4.5	...	X	KRAU07
	HSH403
1355	J08420448+1932427	08 42 04.48	+19 32 42.7	...	M4.5	...	X	KRAU07
515	J0842047+193800	08 42 04.71	+19 38 00.9	15.979	...	X	X	...	X	X	...	ADAM02
	AD3051	KRAU07
1356	J08420517+2057565	08 42 05.17	+20 57 56.5	...	M1.5	...	X	KRAU07
	JS470
1357	J08420732+1837169	08 42 07.32	+18 37 16.9	...	M5	...	X	KRAU07
1358	J08420785+2211051	08 42 07.85	+22 11 05.1	...	M3.5	...	X	KRAU07
	HSH406
516	J0842102+184600	08 42 10.28	+18 46 00.5	14.682	M5	X	X	...	X	X	...	ADAM02
517	J0842127+184101	08 42 12.70	+18 41 01.2	14.439	M4	X	X	...	X	X	...	ADAM02

Table A.2 (cont'd)

ID	Other ID(s)	RA	DEC	J	SpT	SPEC	PM	LI	HA	UV	MIR	OPT/NIR	ARCH	Ref1
1359	J08421311+1918529	08 42 13.11	+19 18 52.9	...	M4.7	...	X	KRAU07
518	J08421364+1950008	08 42 13.65	+19 50 08.8	12.97	M2.5	X	X	...	X	X	...	ADAM02
	JS475	JONE91
519	J08421544+194857	08 42 15.50	+19 48 57.8	13.504	M3.5	X	X	...	X	X	...	ADAM02
	HSH414	HAMB95
1360	J08421753+1759148	08 42 17.53	+17 59 14.8	...	M3.5	...	X	KRAU07
	HSH416	KRAU07
1361	J08421833+1823320	08 42 18.33	+18 23 32.0	...	M2.8	...	X	KRAU07
	JS735	KRAU07
1362	J08421923+1902148	08 42 19.23	+19 02 14.8	...	M2.6	...	X	KRAU07
1363	J08422021+2144439	08 42 20.21	+21 44 43.9	...	M4.7	...	X	KRAU07
	AD3077	KRAU07
520	J0842211+200321	08 42 21.10	+20 03 21.0	14.242	M4	X	X	...	X	X	...	ADAM02
	HSH419	HAMB95
1364	J08422203+1846058	08 42 22.03	+18 46 05.8	...	M4.3	...	X	KRAU07
521	J0842238+192312	08 42 23.83	+19 23 12.6	14.357	M4.5	X	X	...	X	X	...	ADAM02
	HSH421	HAMB95
1365	J08422601+2113510	08 42 26.01	+21 13 51.0	...	M3.7	...	X	KRAU07
	AD3085	KRAU07
1366	J08422968+1919526	08 42 29.68	+19 19 52.6	...	M4.2	...	X	KRAU07
1367	J08422988+1958317	08 42 29.88	+19 58 31.7	...	M4.1	...	X	KRAU07
1368	J08423074+1906578	08 42 30.74	+19 06 57.8	...	M4.2	...	X	KRAU07
1369	J08423077+1929310	08 42 30.77	+19 29 31.0	...	M3.3	...	X	KRAU07
1370	J08423205+1835281	08 42 32.05	+18 35 28.1	...	M1	...	X	KRAU07
	JS488	KRAU07
1371	J08423366+1827290	08 42 33.66	+18 27 29.0	...	M5.2	...	X	KRAU07
	AD3101	KRAU07
522	J0842340+193612	08 42 34.03	+19 36 12.4	12.918	M3.5	X	X	...	X	X	...	ADAM02
	JS490	JONE91
1372	J08423486+2059408	08 42 34.86	+20 59 40.8	...	M1	...	X	KRAU07
	JS489	KRAU07
1373	J08423762+1959189	08 42 37.62	+19 59 18.9	...	M3.5	...	X	KRAU07
1374	J08423831+1832279	08 42 38.31	+18 32 27.9	...	M5.1	...	X	KRAU07
	HSH429	KRAU07
523	J0842394+192452	08 42 39.44	+19 24 52.0	14.347	M4.5	X	X	...	X	X	...	ADAM02
	HSH430	HAMB95
1375	J08424097+1931584	08 42 40.97	+19 31 58.4	...	M4.1	...	X	KRAU07
1376	J08424208+1917323	08 42 42.08	+19 17 32.3	...	K7.3	...	X	KRAU07
	JS497	KRAU07
1377	J08424461+1828000	08 42 44.61	+18 28 00.0	...	M4.1	...	X	KRAU07
	AD3127	KRAU07

Table A.2 (cont'd)

ID	Other ID(s)	RA	DEC	J	SpT	SPEC	PM	LI	HA	UV	MIR	OPT/NIR	ARCH	Ref1
1378	J08424538+2035336	08 42 45.38	+20 35 33.6	...	M4.3	...	X	KRAU07
1379	J08424596+2116163	08 42 45.96	+21 16 16.3	...	K7.5	...	X	KRAU07
	AD3128
1380	J08424654+1826189	08 42 46.54	+18 26 18.9	...	M5.9	...	X	KRAU07
	AD3130
1381	J08424968+1851351	08 42 49.68	+18 51 35.1	...	M1.5	...	X	KRAU07
1382	J08425050+1955038	08 42 50.50	+19 55 03.8	...	M2.6	...	X	KRAU07
524	J0842505+202004	08 42 50.52	+20 20 04.1	14.968	M4	X	X	...	X	X	...	ADAM02
1383	J08425228+1951460	08 42 52.28	+19 51 46.0	...	M2.5	...	X	KRAU07
1384	J08425512+2031144	08 42 55.12	+20 31 14.4	...	M5.2	...	X	KRAU07
1385	J08425668+2030422	08 42 56.68	+20 30 42.2	...	M3.6	...	X	KRAU07
1386	J08425674+2004181	08 42 56.74	+20 04 18.1	...	M3.6	...	X	KRAU07
1387	J08430054+2123281	08 43 00.54	+21 23 28.1	...	M5.7	...	X	KRAU07
	AD3155
525	J0843018+195404	08 43 01.88	+19 54 04.7	14.95	M4.5	X	X	...	X	X	...	ADAM02
1388	J08430289+2145136	08 43 02.89	+21 45 13.6	...	M4.6	...	X	KRAU07
	AD3161
1389	J08430528+1927546	08 43 05.28	+19 27 54.6	...	K7.9	...	X	KRAU07
	JS513
1390	J08430557+1855060	08 43 05.57	+18 55 06.0	...	M4.5	...	X	KRAU07
1391	J08430615+1924521	08 43 06.15	+19 24 52.1	...	M3.6	...	X	KRAU07
	JS514
1392	J08430637+1923388	08 43 06.37	+19 23 38.8	...	M6.3	...	X	KRAU07
526	J0843084+192806	08 43 08.40	+19 28 06.1	13.256	M4.5	X	X	...	X	X	...	ADAM02
	HSU442	HAMB95
1393	J08430905+1943119	08 43 09.05	+19 43 11.9	...	M5.8	...	X	KRAU07
1394	J08431012+1928360	08 43 10.12	+19 28 36.0	...	M4	...	X	KRAU07
	JS523
527	J0843103+194237	08 43 10.33	+19 42 37.4	15.68	M5.5	X	X	...	X	X	...	ADAM02
1395	J08431205+1841451	08 43 12.05	+18 41 45.1	...	M4.3	...	X	KRAU07
	AD3178
528	J0843126+193428	08 43 12.66	+19 34 29.0	14.299	M4.5	X	X	...	X	X	...	ADAM02
	HSU445	HAMB95
1396	J08431292+1831509	08 43 12.92	+18 31 50.9	...	M1.9	...	X	KRAU07
	JS525
1397	J08431326+2000160	08 43 13.26	+20 00 16.0	...	M4.8	...	X	KRAU07
1398	J08431467+1742301	08 43 14.67	+17 42 30.1	...	M4.3	...	X	KRAU07
	HSU449
529	J0843158+190633	08 43 15.87	+19 06 33.2	14.203	M4.5	X	X	...	X	X	...	ADAM02
530	J0843184+193107	08 43 18.43	+19 31 07.8	13.568	M3.5	X	X	...	X	X	...	ADAM02
	HSU450	HAMB95

Table A.2 (cont'd)

ID	Other ID(s)	RA	DEC	J	SpT	SPEC	PM	LI	HA	UV	MIR	OPT/NIR	ARCH	Ref1
1399	J08432013+2004258	08 43 20.13	+20 04 25.8	...	M4.4	...	X	KRAU07
	HSHU451
531	J0843202+200445	08 43 20.30	+20 04 45.6	14.479	M4.5	X	X	...	X	X	...	ADAM02
	HSHU452	HAMB95
532	J0843224+191200	08 43 22.41	+19 12 00.8	13.578	M4	X	X	...	X	X	...	ADAM02
533	J0843224+205425	08 43 22.46	+20 54 25.3	15.302	M5	X	X	...	X	X	...	ADAM02
	HSHU453	HAMB95
1400	J08432392+1840451	08 43 23.92	+18 40 45.1	...	M1.5	...	X	KRAU07
	JSS34
1401	J08432501+2033552	08 43 25.01	+20 33 55.2	...	K7.8	...	X	KRAU07
	JSS33
534	J0843275+194940	08 43 27.59	+19 49 40.5	13.788	M4	X	X	...	X	X	...	ADAM02
	HSHU455	HAMB95
1402	J08433105+1832547	08 43 31.05	+18 32 54.7	...	K7.2	...	X	KRAU07
	JSS36
535	J0843326+195932	08 43 32.63	+19 59 33.0	13.762	M4	X	X	...	X	X	...	ADAM02
	HSHU458	HAMB95
536	J0843337+192424	08 43 33.76	+19 24 24.8	14.106	M4.5	X	X	...	X	X	...	ADAM02
	HSHU459	HAMB95
1403	J08433462+1845138	08 43 34.62	+18 45 13.8	...	M3.8	...	X	KRAU07
	AD3218
537	J0843353+190014	08 43 35.36	+19 00 14.1	12.638	M4	X	X	...	X	X	...	ADAM02
	JSS41	JONE91
538	J0843355+192723	08 43 35.51	+19 27 23.4	14.498	...	X	X	...	X	X	...	ADAM02
	AD3221	KRAU07
1404	J08433659+2119097	08 43 36.59	+21 19 09.7	...	M3.5	...	X	KRAU07
	JSS39
1405	J0843368+2032244	08 43 36.84	+20 32 24.4	...	M3.1	...	X	KRAU07
1406	J08433689+2032140	08 43 36.89	+20 32 14.0	...	M1.3	...	X	KRAU07
	JSS42
1407	J08434306+1754298	08 43 43.06	+17 54 29.8	...	M0.3	...	X	KRAU07
	JSS48
1408	J08434473+1903588	08 43 44.73	+19 03 58.8	...	M1.1	...	X	KRAU07
	JSS50
1409	J08434474+2112343	08 43 44.74	+21 12 34.3	...	M0.8	...	X	KRAU07
	JSS45
1410	J08434736+1803001	08 43 47.36	+18 03 00.1	...	M4.2	...	X	KRAU07
	HSHU466
1411	J08435085+2021567	08 43 50.85	+20 21 56.7	...	M0.7	...	X	KRAU07
	JSS52
1412	J08435181+1954490	08 43 51.81	+19 54 49.0	...	K7.9	...	X	KRAU07

Table A.2 (cont'd)

ID	Other ID(s)	RA	DEC	J	SpT	SPEC	PM	LI	HA	UV	MIR	OPT/NIR	ARCH	Ref1
539	JSS54 J0843566+191617	08 43 56.65	+19 16 17.9	15.428	M5	X	X	...	X	X	...	ADAM02
	HSU471	HAMB95
1413	J08435794+1930592	08 43 57.94	+19 30 59.2	...	M4.6	...	X	KRAU07
540	J0843592+191858	08 43 59.26	+19 18 58.1	13.07	M3	X	X	...	X	X	...	ADAM02
	JSS57	JONE91
1414	J08440067+2038454	08 44 00.67	+20 38 45.4	...	M4.3	...	X	KRAU07
541	J0844033+203137	08 44 03.39	+20 31 37.9	16.251	M5	X	X	...	X	X	...	ADAM02
542	J0844039+190112	08 44 03.90	+19 01 12.7	14.644	M5	X	X	...	X	X	...	ADAM02
	HSU474	HAMB95
1415	J08440699+1947301	08 44 06.99	+19 47 30.1	...	M3.5	...	X	KRAU07
1416	J08441093+2147383	08 44 10.93	+21 47 38.3	...	M2.9	...	X	KRAU07
	HSU475
543	J0844116+201300	08 44 11.64	+20 13 00.2	13.787	M4.5	X	X	...	X	X	...	ADAM02
1417	J08441232+2043010	08 44 12.32	+20 43 01.0	...	M4.4	...	X	KRAU07
	AD3283
1418	J08441324+1849114	08 44 13.24	+18 49 11.4	...	K7.1	...	X	KRAU07
	JSS61
544	J0844138+192316	08 44 13.83	+19 23 16.5	15.187	M2.5	X	X	...	X	X	...	ADAM02
545	J0844191+185609	08 44 19.13	+18 56 10.0	12.955	M4	X	X	...	X	X	...	ADAM02
	JSS64	JONE91
1419	J08442124+1956117	08 44 21.24	+19 56 11.7	...	M4.1	...	X	KRAU07
1420	J08442259+1823093	08 44 22.59	+18 23 09.3	...	M3.2	...	X	KRAU07
	JS744
1421	J08442321+2013557	08 44 23.21	+20 13 55.7	...	M3.9	...	X	KRAU07
1422	J08442555+2235591	08 44 25.55	+22 35 59.1	...	M3.5	...	X	KRAU07
	HSU482
1423	J08442652+1947359	08 44 26.52	+19 47 35.9	...	K7.2	...	X	KRAU07
	JSS66
546	J0844265+190720	08 44 26.56	+19 07 20.5	15.562	M3.5	X	X	...	X	X	...	ADAM02
1424	J08442721+1852207	08 44 27.21	+18 52 20.7	...	M4.2	...	X	KRAU07
547	J0844276+185809	08 44 27.69	+18 58 09.7	13.761	M4	X	X	...	X	X	...	ADAM02
	JS745	JONE91
548	J0844318+193317	08 44 31.86	+19 33 17.4	13.827	M4	X	X	...	X	X	...	ADAM02
	HSU488	HAMB95
1425	J08443259+2140592	08 44 32.59	+21 40 59.2	...	M3.2	...	X	KRAU07
	AD3327
1426	J08443290+1857506	08 44 32.90	+18 57 50.6	...	M3	...	X	KRAU07
	JS568
1427	J08443449+2020295	08 44 34.49	+20 20 29.5	...	M2.9	...	X	KRAU07
	AD3329

Table A.2 (cont'd)

ID	Other ID(s)	RA	DEC	J	SpT	SPEC	PM	LI	HA	UV	MIR	OPT/NIR	ARCH	Ref1
1428	J08443613+1835570	08 44 36.13	+18 35 57.0	...	M0.6	...	X	KRAU07
	JS571
549	J0844364+191717	08 44 36.41	+19 17 17.8	15.51	M4.5	X	X	...	X	X	...	ADAM02
550	J0844372+185529	08 44 37.23	+18 55 29.6	14.244	M4	X	X	...	X	X	...	ADAM02
	HSH491	HAMB95
1429	J08444049+2145537	08 44 40.49	+21 45 53.7	...	M2.3	...	X	KRAU07
	AD3337
1430	J08444075+2011371	08 44 40.75	+20 11 37.1	...	K7.5	...	X	KRAU07
	JS572
1431	J08444277+2057468	08 44 42.77	+20 57 46.8	...	M4	...	X	KRAU07
1432	J08444422+2107134	08 44 44.22	+21 07 13.4	...	M3.9	...	X	KRAU07
	JS750
551	J0844448+192422	08 44 44.81	+19 24 22.2	13.286	M4	X	X	...	X	X	...	ADAM02
	JS574	JONE91
1433	J08445387+2137065	08 44 53.87	+21 37 06.5	...	M1.6	...	X	KRAU07
	AD3349
1434	J08445643+1822171	08 44 56.43	+18 22 17.1	...	M1.3	...	X	KRAU07
	JS582
1435	J08450264+2030438	08 45 02.64	+20 30 43.8	...	M1.1	...	X	KRAU07
	JS586
1436	J08450384+2128181	08 45 03.84	+21 28 18.1	...	M4.4	...	X	KRAU07
	AD3366
1437	J08450450+1700170	08 45 04.50	+17 00 17.0	...	M4.8	...	X	KRAU07
1438	J08450590+1917575	08 45 05.90	+19 17 57.5	...	M3.7	...	X	KRAU07
	AD3369
1439	J08450611+2027133	08 45 06.11	+20 27 13.3	...	M5.2	...	X	KRAU07
	AD3370
1440	J08450854+1909082	08 45 08.54	+19 09 08.2	...	M4.2	...	X	KRAU07
552	J0845123+191824	08 45 12.36	+19 18 24.9	14.644	M4.5	X	X	...	X	X	...	ADAM02
553	J0845144+193320	08 45 14.46	+19 33 20.7	14.792	M5	X	X	...	X	X	...	ADAM02
1441	J08451494+1845399	08 45 14.94	+18 45 39.9	...	M3.6	...	X	KRAU07
	AD3392
1442	J08451557+2103359	08 45 15.57	+21 03 35.9	...	M2.9	...	X	KRAU07
	HSH496
1443	J08452106+1849327	08 45 21.06	+18 49 32.7	...	M4.3	...	X	KRAU07
	AD3400
1444	J08452116+1853035	08 45 21.16	+18 53 03.5	...	M3.7	...	X	KRAU07
	AD3401
1445	J08452235+1949401	08 45 22.35	+19 49 40.1	...	M4.1	...	X	KRAU07
	JS753
554	J0845224+190208	08 45 22.40	+19 02 08.3	13.721	M4.5	X	X	...	X	X	...	ADAM02

Table A.2 (cont'd)

ID	Other ID(s)	RA	DEC	J	SpT	SPEC	PM	LI	HA	UV	MIR	OPT/NIR	ARCH	Ref1
1446	J08452598+2025385 JS594	08 45 25.98 ...	+20 25 38.5	K7.4	...	X	KRAU07
1447	J08452599+2025225 JS595	08 45 25.99 ...	+20 25 22.5	M1.1	...	X	KRAU07
1448	J08452605+1941544	08 45 26.05	+19 41 54.4	...	M1.6	...	X	KRAU07
1449	J08452630+1947040 AD3411	08 45 26.30 ...	+19 47 04.0	M2.2	...	X	KRAU07
555	J0845266+191412	08 45 26.64	+19 14 12.9	13.909	M4.5	X	X	...	X	X	...	ADAM02
556	J0845285+185948	08 45 28.60	+18 59 48.1	15.32	M4.5	X	X	...	X	X	...	ADAM02
596	WFC136	08 45 39.10	+19 38 04.2	X	X	...	CHAP05
1450	J08453218+1857521	08 45 32.18	+18 57 52.1	...	M3.4	...	X	KRAU07
1451	J08453429+1654396 AD3423	08 45 34.29 ...	+16 54 39.6	M4.4	...	X	KRAU07
1452	J08453624+2115211 JS604	08 45 36.24 ...	+21 15 21.1	M1.7	...	X	KRAU07
1453	J08453685+1835553 AD3428	08 45 36.85 ...	+18 35 55.3	M3.4	...	X	KRAU07
1454	J08453688+1843251 AD3429	08 45 36.88 ...	+18 43 25.1	M4	...	X	KRAU07
1455	J08454049+2010255 JS607	08 45 40.49 ...	+20 10 25.5	M2.3	...	X	KRAU07
582	WFC11	08 45 41.05	+19 38 02.6	X	X	...	CHAP05
1456	J08454448+1940324 JS608	08 45 44.48 ...	+19 40 32.4	M3	...	X	KRAU07
1457	J08454589+2029410 JS609	08 45 45.89 ...	+20 29 41.0	M1.8	...	X	KRAU07
557	J0845479+193618	08 45 47.97	+19 36 18.8	13.916	M4.5	X	X	...	X	X	...	ADAM02
1458	J08454868+2131565 JS756	08 45 48.68 ...	+21 31 56.5	M3.6	...	X	KRAU07
1459	J08455142+1925272	08 45 51.42	+19 25 27.2	...	M1.9	...	X	KRAU07
558	J0845528+1919000	08 45 52.81	+19 19 00.8	12.947	M3	X	X	...	X	X	...	ADAM02
559	J0845591+191512	08 45 59.18	+19 15 12.8	13.755	M4	X	X	...	X	X	...	ADAM02
1460	J08460002+1749387 AD3472	08 46 00.02 ...	+17 49 38.7	M3.8	...	X	KRAU07
1461	J08460196+2032031 AD3475	08 46 01.96 ...	+20 32 03.1	M4.4	...	X	KRAU07
560	J0846022+190659 JS617	08 46 02.24 ...	+19 06 59.6 ...	13.287	M3.5	X	X	...	X	X	...	ADAM02
1462	J08460273+1701176 AD3477	08 46 02.73 ...	+17 01 17.6	M2.7	...	X	JONE91 KRAU07
561	J0846031+193147	08 46 03.20	+19 31 47.2	13.418	M3.5	X	X	...	X	X	...	ADAM02

Table A.2 (cont'd)

ID	Other ID(s)	RA	DEC	J	SpT	SPEC	PM	LI	HA	UV	MIR	OPT/NIR	ARCH	Ref1
1463	JSG18 J08460817+1802272 AD3484	08 46 08.17 +18 02 27.2 M3.6 X	JONE91 KRAU07
1464	J08460851+1953527 AD3485	08 46 08.51 ...	+19 53 52.7	M4.5	X	KRAU07
1465	J08460919+2136288 HSHU498	08 46 09.19 ...	+21 36 28.8	M4.2	X	KRAU07
1466	J08461010+1931438 JSG20	08 46 10.10 ...	+19 31 43.8	M0.9	X	KRAU07
1467	J08461381+2051247 JSG23	08 46 13.81 ...	+20 51 24.7	K7.1	X	KRAU07
1468	J08461572+1805500 AD3497	08 46 15.72 ...	+18 05 50.0	M4.3	X	KRAU07
606	WFC200	08 46 16.82	+19 52 30.2	X	X	...	CHAP05
1469	J08461827+1843092 JSG757	08 46 18.27 ...	+18 43 09.2	M3.6	X	KRAU07
1470	J08462006+1841007 AD3505	08 46 20.06 ...	+18 41 00.7	M3.4	X	KRAU07
1471	J08462006+2100321 HSHU499	08 46 20.06 ...	+21 00 32.1	M4.4	X	KRAU07
1472	J08462388+1958043 AD3511	08 46 23.88 ...	+19 58 04.3	M3.2	X	KRAU07
1473	J08462594+1953356 AD3516	08 46 25.94 ...	+19 53 35.6	M6.1	X	KRAU07
1474	J08462632+1750445 AD3517	08 46 26.32 ...	+17 50 44.5	M4.2	X	KRAU07
1475	J08462741+1912325 AD3518	08 46 27.41 ...	+19 12 32.5	M4.6	X	KRAU07
1476	J08463042+1938553 AD3525	08 46 30.42 ...	+19 38 55.3	M4.4	X	KRAU07
1477	J08463198+1858257 AD3527	08 46 31.98 ...	+18 58 25.7	M4.9	X	KRAU07
1478	J08463486+1915260 AD3534	08 46 34.86 ...	+19 15 26.0	M3.3	X	KRAU07
1479	J08463894+1937088 AD3547	08 46 38.94 ...	+19 37 08.8	M3.1	X	KRAU07
584	WFC53	08 46 39.19	+19 27 37.0	X	CHAP05
1480	J08464001+2134295 AD3548	08 46 40.01 ...	+21 34 29.5	M6.2	X	KRAU07
1481	J08464032+1916304	08 46 40.32	+19 16 30.4	...	M4	...	X	KRAU07
1482	J08464281+1925343	08 46 42.81	+19 25 34.3	...	M4	...	X	KRAU07

Table A.2 (cont'd)

ID	Other ID(s)	RA	DEC	J	SpT	SPEC	PM	LI	HA	UV	MIR	OPT/NIR	ARCH	Ref1
611	WFC216	08 46 48.87	+19 32 09.4	X	X	...	CHAP05
1483	J08465370+1902569	08 46 53.70	+19 02 56.9	...	M4.3	...	X	KRAU07
1484	J08465563+1802010	08 46 55.63	+18 02 01.0	...	M5.5	...	X	KRAU07
	IZ131
1485	J08465945+1954595	08 46 59.45	+19 54 59.5	...	M4.4	...	X	KRAU07
1486	J08470424+2216256	08 47 04.24	+22 16 25.6	...	K7.8	...	X	KRAU07
1487	J08470496+1855428	08 47 04.96	+18 55 42.8	...	M4.1	...	X	KRAU07
1488	J08470524+1902099	08 47 05.24	+19 02 09.9	...	M4.6	...	X	KRAU07
1489	J08470910+1811372	08 47 09.10	+18 11 37.2	...	M2.7	...	X	KRAU07
	JS644
1490	J08471193+2107485	08 47 11.93	+21 07 48.5	...	M4.4	...	X	KRAU07
	HSH501
1491	J08471907+2111021	08 47 19.07	+21 11 02.1	...	M4	...	X	KRAU07
1492	J08472162+2039220	08 47 21.62	+20 39 22.0	...	M1.1	...	X	KRAU07
	JS647
1493	J08473450+1737507	08 47 34.50	+17 37 50.7	...	M2.9	...	X	KRAU07
	AD3595
1494	J08473468+1908179	08 47 34.68	+19 08 17.9	...	M1.3	...	X	KRAU07
	JS649
1495	J08474029+2143248	08 47 40.29	+21 43 24.8	...	M4.5	...	X	KRAU07
	HSH502
1496	J08474180+1856287	08 47 41.80	+18 56 28.7	...	M3.3	...	X	KRAU07
1497	J08474511+1821239	08 47 45.11	+18 21 23.9	...	M2.3	...	X	KRAU07
	JS651
1498	J08474886+1836195	08 47 48.86	+18 36 19.5	...	M3.8	...	X	KRAU07
	JS761
1499	J08475052+1909110	08 47 50.52	+19 09 11.0	...	M3.5	...	X	KRAU07
1500	J08475073+2227038	08 47 50.73	+22 27 03.8	...	M2.7	...	X	KRAU07
1501	J08475472+2003428	08 47 54.72	+20 03 42.8	...	M1.4	...	X	KRAU07
	JS653
1502	J08480023+2024068	08 48 00.23	+20 24 06.8	...	M4.1	...	X	KRAU07
1503	J08480129+1949391	08 48 01.29	+19 49 39.1	...	M3.6	...	X	KRAU07
1504	J08480495+1928137	08 48 04.95	+19 28 13.7	...	M2	...	X	KRAU07
	JS656
1505	J08480745+1954592	08 48 07.45	+19 54 59.2	...	M3.7	...	X	KRAU07
1506	J08481021+1908599	08 48 10.21	+19 08 59.9	...	M6.1	...	X	KRAU07
1507	J08481071+1937332	08 48 10.71	+19 37 33.2	...	M4.7	...	X	KRAU07
1508	J08481148+1811280	08 48 11.48	+18 11 28.0	...	M4.4	...	X	KRAU07
1509	J08481155+2126351	08 48 11.55	+21 26 35.1	...	M4.3	...	X	KRAU07
1510	J08481476+2233323	08 48 14.76	+22 33 32.3	...	M0.8	...	X	KRAU07
1511	J08482253+1836448	08 48 22.53	+18 36 44.8	...	M1.8	...	X	KRAU07

Table A.2 (cont'd)

ID	Other ID(s)	RA	DEC	J	SpT	SPEC	PM	LI	HA	UV	MIR	OPT/NIR	ARCH	Ref1
1512	J08482357+1950117	08 48 23.57	+19 50 11.7	...	M2.9	...	X	KRAU07
1513	J08483007+1857034	08 48 30.07	+18 57 03.4	...	M4.9	...	X	KRAU07
1514	J08483057+1945072	08 48 30.57	+19 45 07.2	...	M5	...	X	KRAU07
1515	J08483271+1656236	08 48 32.71	+16 56 23.6	...	M1.5	...	X	KRAU07
	AD3663
1516	J08483450+1955575	08 48 34.50	+19 55 57.5	...	M1.9	...	X	KRAU07
1517	J08484913+2013271	08 48 49.13	+20 13 27.1	...	M0.8	...	X	KRAU07
1518	J08484997+2026359	08 48 49.97	+20 26 35.9	...	M1	...	X	KRAU07
1519	J08485140+2054153	08 48 51.40	+20 54 15.3	...	M4.4	...	X	KRAU07
	HSHU508
1520	J08485990+2041555	08 48 59.90	+20 41 55.5	...	M4.5	...	X	KRAU07
1521	J08491651+2135121	08 49 16.51	+21 35 12.1	...	M3.2	...	X	KRAU07
	HSHU510
1522	J08492404+2014065	08 49 24.04	+20 14 06.5	...	M4.5	...	X	KRAU07
1523	J08492676+1831195	08 49 26.76	+18 31 19.5	...	M0.5	...	X	KRAU07
1524	J08495937+1910010	08 49 59.37	+19 10 01.0	...	M3.4	...	X	KRAU07
1525	J08501368+1941240	08 50 13.68	+19 41 24.0	...	M5.2	...	X	KRAU07
	AD3755
1526	J08503527+2042376	08 50 35.27	+20 42 37.6	...	M4	...	X	KRAU07
	AD3788
1527	J08505613+1957067	08 50 36.13	+19 57 06.7	...	M4.5	...	X	KRAU07
	AD3792
1528	J08504984+1948364	08 50 49.84	+19 48 36.4	...	M3.4	...	X	KRAU07
	AD3814
1529	J08505687+1936578	08 50 56.87	+19 36 57.8	...	M2.5	...	X	KRAU07
1530	J08505988+1900355	08 50 59.88	+19 00 35.5	...	M4.3	...	X	KRAU07
	AD3836
1531	J08510040+1803038	08 51 00.40	+18 03 03.8	...	M2.9	...	X	KRAU07
	AD3840
1532	J08512322+1951183	08 51 23.22	+19 51 18.3	...	M4.4	...	X	KRAU07
	AD3873
1533	J08512584+1918564	08 51 25.84	+19 18 56.4	...	M2.9	...	X	KRAU07
	AD3875
1534	J08513391+1742243	08 51 33.91	+17 42 24.3	...	M4.2	...	X	KRAU07
	AD3886
1535	J08521452+1903391	08 52 14.52	+19 03 39.1	...	M0.7	...	X	KRAU07
	AD3954
1536	J08522025+1822174	08 52 20.25	+18 22 17.4	...	M0.1	...	X	KRAU07
	AD3962
1537	J08532748+1758335	08 53 27.48	+17 58 33.5	...	M2.9	...	X	KRAU07
	AD4089

Table A.2 (cont'd)

ID	Other ID(s)	RA	DEC	J	SpT	SPEC	PM	LI	HA	UV	MIR	OPT/NIR	ARCH	Ref1
1538	J08534667+1918142 AD4129	08 53 46.67 ...	+19 18 14.2	K7.7	X	KRAU07
1539	J08554365+1937424	08 55 43.65	+19 37 42.4	...	M3	...	X	KRAU07
1540	J08575230+1850070	08 57 52.30	+18 50 07.0	...	M5	...	X	KRAU07
1541	J08580519+2152462 AD4529	08 58 05.19 ...	+21 52 46.2	M2.8	X	KRAU07

Table A.3: Previously Claimed Low-Mass Pleiades Members

ID	Other ID(s)	RA	DEC	J	SpT	SPEC	PM	LI	HA	UV	MIR	OPT/NIR	ARCH	Ref1	Ref2
1542	...	03 40 39.46	+23 26 34.8	15.02	X	X	...	LODI07	
1543	...	03 40 40.32	+25 50 48.2	13.033	X	X	...	LODI07	
1544	...	03 40 43.20	+22 49 53.8	13.728	X	X	...	LODI07	
1545	...	03 40 51.82	+23 13 50.6	13.198	X	X	...	LODI07	
1546	...	03 40 54.48	+22 54 25.6	13.849	X	X	...	LODI07	
1547	...	03 41 10.27	+25 45 56.0	13.004	X	X	...	LODI07	
1548	...	03 41 26.36	+23 08 02.7	13.501	X	X	...	LODI07	
1549	UGCS-PI-4	03 41 30.36	+25 17 06.0	15.24	X	X	...	LODI07	
1550	CFHTPLIZ4	03 41 40.90	+25 54 24.1	15.173	X	X	...	LODI07	
1551	...	03 41 58.66	+22 57 01.7	12.759	X	X	...	LODI07	
1552	...	03 42 03.41	+25 22 39.1	13.315	X	X	...	LODI07	
1553	...	03 42 08.29	+25 37 00.0	13.017	X	X	...	LODI07	
1554	...	03 42 29.43	+22 47 25.9	11.737	X	X	...	LODI07	
1555	...	03 42 36.27	+23 22 04.7	13.101	X	X	...	LODI07	
1556	...	03 42 43.80	+25 32 06.2	12.692	X	X	...	LODI07	
1557	...	03 42 44.37	+23 06 16.1	13.795	X	X	...	LODI07	
1558	...	03 42 54.00	+26 08 16.1	13.658	X	X	...	LODI07	
1559	UGCS-PI-9	03 42 59.92	+22 42 51.5	14.666	X	X	...	LODI07	
1560	...	03 43 04.20	+22 48 03.3	11.613	X	X	...	LODI07	
1561	...	03 43 07.57	+25 34 28.0	13.048	X	X	...	LODI07	
1562	...	03 43 19.01	+22 47 10.5	13.578	X	X	...	LODI07	
1563	...	03 43 19.06	+26 04 44.0	13.171	X	X	...	LODI07	
1564	...	03 43 25.16	+22 53 44.4	13.753	X	X	...	LODI07	
1565	...	03 43 26.20	+26 02 30.7	12.791	X	X	...	LODI07	
1566	...	03 43 26.44	+22 42 42.5	13.134	X	X	...	LODI07	
1567	...	03 43 34.14	+25 35 25.8	12.822	X	X	...	LODI07	
1568	...	03 43 35.22	+25 24 30.9	12.719	X	X	...	LODI07	
1569	...	03 43 36.57	+23 12 34.2	13.182	X	X	...	LODI07	
1570	...	03 43 36.67	+25 47 00.6	12.82	X	X	...	LODI07	
1571	...	03 43 37.32	+25 24 32.1	12.506	X	X	...	LODI07	
1572	...	03 43 44.97	+23 03 21.1	12.579	X	X	...	LODI07	
1573	...	03 43 47.08	+26 04 35.4	12.878	X	X	...	LODI07	
1574	...	03 43 52.79	+25 28 30.3	13.393	X	X	...	LODI07	
1575	...	03 43 53.88	+25 28 30.0	12.248	X	X	...	LODI07	
1907	PLZJ323	03 43 55.27	+25 43 26.2	19.613	X	CASE07	
1576	UGCS-PI-13	03 43 56.00	+25 36 25.3	15.3	X	X	...	LODI07	
1577	...	03 44 08.81	+23 04 47.5	11.987	X	X	...	LODI07	
1578	...	03 44 09.32	+23 08 46.8	13.377	X	X	...	LODI07	
1579	...	03 44 10.76	+25 37 38.2	13.297	X	X	...	LODI07	
1580	...	03 44 22.14	+23 10 54.8	14.495	X	X	...	LODI07	

Table A.3 (cont'd)

ID	Other ID(s)	RA	DEC	J	SpT	SPEC	PM	LI	HA	UV	MIR	OPT/NIR	ARCH	Ref1	Ref2
1581	Roque5	03 44 22.44	+23 39 01.4	16.885	X	X	...	LODI07	
1582	BRB4	03 44 23.24	+25 38 44.9	14.692	X	X	...	LODI07	
1583	...	03 44 23.40	+25 21 29.9	12.403	X	X	...	LODI07	
1584	UGCS-PI-14	03 44 25.58	+22 40 07.9	14.944	X	X	...	LODI07	
358	BRB27	03 44 27.24	+25 44 41.9	18.871	X	X	...	BIHA06	CASE07
	CFHT-PLIZ1262	BOU06	
1585	...	03 44 27.50	+24 14 17.1	13.508	X	X	...	LODI07	
1586	...	03 44 27.91	+23 59 59.7	14.437	X	X	...	LODI07	
356	BRB22	03 44 31.27	+25 35 15.1	18.298	X	X	...	BIHA06	CASE07
	CFHT-PLIZ2141	BOU06	
1587	...	03 44 31.72	+23 35 26.1	13.069	X	X	...	LODI07	
1588	CFHT10	03 44 32.33	+25 25 18.0	15.46	X	X	...	LODI07	
1589	...	03 44 33.08	+25 45 09.6	13.307	X	X	...	LODI07	
1590	CFHT16	03 44 35.16	+25 13 42.8	15.651	X	X	...	LODI07	
	CFHTPLIZ9
1591	CFHT-PLIZ9	03 44 35.16	+25 13 42.8	15.651	X	X	...	LODI07	
	CFHT-PI-16
1592	HHJ5	03 44 35.90	+23 34 42.0	14.991	X	X	...	LODI07	
1593	...	03 44 36.28	+23 30 11.0	12.485	X	X	...	LODI07	
1594	...	03 44 47.33	+24 00 37.7	13.131	X	X	...	LODI07	
1595	...	03 44 47.84	+24 12 52.6	13.296	X	X	...	LODI07	
1596	UGCS-PI-16	03 44 53.12	+23 34 22.9	15.74	X	X	...	LODI07	
1908	PLZ156	03 44 53.51	+25 36 19.5	15.25	X	CASE07	
1597	...	03 44 56.69	+23 36 23.5	13.151	X	X	...	LODI07	
1598	...	03 44 58.02	+23 24 31.0	13.183	X	X	...	LODI07	
1599	...	03 44 58.97	+23 23 20.0	11.261	X	X	...	LODI07	
1600	...	03 44 59.48	+23 21 18.1	14.217	X	X	...	LODI07	
1601	...	03 45 01.14	+24 46 41.0	13.404	X	X	...	LODI07	
1602	...	03 45 01.21	+25 21 05.6	13.964	X	X	...	LODI07	
1603	...	03 45 02.88	+25 05 19.7	13.741	X	X	...	LODI07	
1604	...	03 45 04.99	+23 46 06.4	13.707	X	X	...	LODI07	
1605	...	03 45 05.32	+25 28 11.0	12.302	X	X	...	LODI07	
1606	BPL70	03 45 08.69	+22 38 30.5	13.327	X	X	...	LODI07	
1607	...	03 45 09.04	+25 32 49.1	13.605	X	X	...	LODI07	
1608	...	03 45 11.73	+23 41 43.7	17.596	X	X	...	LODI07	
1609	...	03 45 12.16	+23 21 53.0	13.06	X	X	...	LODI07	
1610	BPL71	03 45 12.44	+22 41 50.9	13.138	X	X	...	LODI07	
1611	...	03 45 13.14	+24 15 23.6	13.951	X	X	...	LODI07	
1612	...	03 45 16.13	+24 07 16.1	12.402	X	X	...	LODI07	
1613	...	03 45 16.42	+23 34 01.7	14.426	X	X	...	LODI07	
1614	...	03 45 16.99	+25 15 47.5	11.968	X	X	...	LODI07	

Table A.3 (cont'd)

ID	Other ID(s)	RA	DEC	J	SpT	SPEC	PM	LI	HA	UV	MIR	OPT/NIR	ARCH	Ref1	Ref2
1615	...	03 45 24.78	+24 20 45.3	13.097	X	X	...	LODI07	
1616	BPL73	03 45 26.56	+22 31 32.0	13.093	X	X	...	LODI07	
1617	IPMBD29	03 45 31.37	+24 52 47.5	15.471	X	X	...	LODI07	
1618	...	03 45 36.72	+24 39 06.5	12.216	X	X	...	LODI07	
1619	UGCS-Pt-20	03 45 37.76	+23 43 50.1	14.71	X	X	...	LODI07	
1620	BPL75	03 45 39.12	+22 04 23.1	14.03	X	X	...	LODI07	
1621	...	03 45 39.29	+24 08 20.4	13.903	X	X	...	LODI07	
1622	Roque15	03 45 41.27	+23 54 09.8	15.345	X	X	...	LODI07	
1623	UGCS-Pt-21	03 45 42.33	+24 04 11.2	15.203	X	X	...	LODI07	
1624	...	03 45 43.17	+26 02 26.6	13.157	X	X	...	LODI07	
1625	...	03 45 49.26	+25 24 46.1	15.712	X	X	...	LODI07	
1626	BPL77	03 45 49.36	+24 25 07.1	12.647	X	X	...	LODI07	
1627	BPL78	03 45 50.42	+22 36 05.6	16.039	X	X	...	LODI07	
1628	...	03 45 50.62	+23 44 36.9	16.377	X	X	...	LODI07	
1629	Roque13	03 45 50.66	+24 09 03.5	15.692	X	X	...	LODI07	
	BPL79
1630	BPL80	03 45 51.95	+25 10 01.7	13.605	X	X	...	LODI07	
1631	...	03 45 52.60	+25 54 59.9	12.734	X	X	...	LODI07	
1632	...	03 45 52.76	+23 27 54.0	13.149	X	X	...	LODI07	
1633	UGCS-Pt-22	03 45 54.96	+23 33 57.9	15.56	X	X	...	LODI07	
1634	BPL82	03 45 54.99	+24 13 26.0	12.649	X	X	...	LODI07	
1635	ini42	03 45 55.17	+22 51 31.1	15.634	X	X	...	LODI07	
1636	...	03 45 56.97	+23 01 29.0	13.37	X	X	...	LODI07	
1637	BPL83	03 45 57.28	+25 11 12.7	12.272	X	X	...	LODI07	
1638	...	03 45 57.91	+24 08 40.9	14.526	X	X	...	LODI07	
1639	BPL84	03 46 00.93	+22 12 29.4	14.729	X	X	...	LODI07	
1640	BPL85	03 46 02.96	+24 40 55.7	14.078	X	X	...	LODI07	
1641	BPL86	03 46 03.45	+24 20 57.0	13.415	X	X	...	LODI07	
1642	...	03 46 03.67	+25 52 28.8	13.492	X	X	...	LODI07	
1643	BPL88	03 46 04.57	+24 09 55.8	13.997	X	X	...	LODI07	
1644	BPL90	03 46 08.70	+24 40 33.1	13.532	X	X	...	LODI07	
1645	...	03 46 12.87	+24 03 15.6	11.377	X	X	...	LODI07	
1646	BPL95	03 46 17.94	+24 41 09.4	12.519	X	X	...	LODI07	
1647	BPL96	03 46 19.41	+23 00 55.7	14.022	X	X	...	LODI07	
1648	...	03 46 19.43	+26 02 35.6	11.723	X	X	...	LODI07	
1649	BPL97	03 46 19.86	+24 59 01.4	12.769	X	X	...	LODI07	
1650	...	03 46 22.20	+23 52 41.1	12.979	X	X	...	LODI07	
1651	UGCS-Pt-28	03 46 22.25	+23 52 26.6	15.526	X	X	...	LODI07	
1652	BPL99	03 46 23.03	+24 36 17.9	13.556	X	X	...	LODI07	
1653	...	03 46 23.47	+24 01 51.3	13.633	X	X	...	LODI07	
1654	BPL101	03 46 24.12	+24 30 12.7	14.697	X	X	...	LODI07	

Table A.3 (cont'd)

ID	Other ID(s)	RA	DEC	J	SpT	SPEC	PM	LI	HA	UV	MIR	OPT/NIR	ARCH	Ref1	Ref2
1655	BPL102	03 46 24.64	+24 28 46.3	13.378	X	X	...	LOD107	
1656	IPMBD25	03 46 26.09	+24 05 09.5	15.127	X	X	...	LOD107	
1657	BPL103	03 46 27.01	+24 27 13.9	12.91	X	X	...	LOD107	
1658	...	03 46 31.02	+23 01 34.7	14.579	X	X	...	LOD107	
1659	BPL105	03 46 31.32	+22 18 19.6	13.329	X	X	...	LOD107	
1660	UGCS-PI-31	03 46 34.25	+23 50 03.7	17.483	X	X	...	LOD107	
1661	UGCS-PI-33	03 46 35.36	+23 57 07.4	15.346	X	X	...	LOD107	
1662	...	03 46 35.53	+24 01 35.4	13.626	X	X	...	LOD107	
1663	...	03 46 36.07	+23 04 17.3	12.861	X	X	...	LOD107	
1664	...	03 46 40.27	+25 43 53.4	12.86	X	X	...	LOD107	
1665	...	03 46 43.19	+23 37 21.9	14.073	X	X	...	LOD107	
1666	...	03 46 43.60	+23 59 42.4	12.413	X	X	...	LOD107	
1667	BPL109	03 46 44.79	+24 44 58.3	14.198	X	X	...	LOD107	
1668	...	03 46 45.78	+25 27 30.3	12.715	X	X	...	LOD107	
1669	...	03 46 47.19	+25 20 53.1	13.323	X	X	...	LOD107	
1670	...	03 46 48.79	+23 04 07.3	12.264	X	X	...	LOD107	
1671	UGCS-PI-36	03 46 50.03	+24 00 23.6	15.594	X	X	...	LOD107	
1672	...	03 46 50.09	+23 31 56.1	13.233	X	X	...	LOD107	
1673	BPL110	03 46 50.19	+22 12 42.4	14.375	X	X	...	LOD107	
1674	...	03 46 52.61	+23 38 43.1	13.152	X	X	...	LOD107	
1675	BPL112	03 46 52.97	+24 15 07.8	15.058	X	X	...	LOD107	
1676	BPL113	03 46 53.61	+24 17 14.8	12.015	X	X	...	LOD107	
1677	BPL114	03 46 54.03	+25 14 44.8	12.345	X	X	...	LOD107	
1678	...	03 46 55.32	+23 22 49.3	14.162	X	X	...	LOD107	
1679	BPL116	03 46 55.32	+24 11 16.6	13.705	X	X	...	LOD107	
1680	...	03 46 55.78	+23 56 24.1	13.169	X	X	...	LOD107	
1681	...	03 46 57.10	+23 15 02.2	11.98	X	X	...	LOD107	
1682	...	03 46 58.17	+23 33 38.8	13.681	X	X	...	LOD107	
1683	...	03 46 59.32	+24 01 42.8	12.942	X	X	...	LOD107	
1684	BPL122	03 47 01.85	+24 13 28.1	14.931	X	X	...	LOD107	
1685	...	03 47 02.35	+23 32 36.0	14.294	X	X	...	LOD107	
1686	...	03 47 03.78	+23 36 58.6	11.504	X	X	...	LOD107	
1687	...	03 47 04.75	+25 22 50.0	12.068	X	X	...	LOD107	
1688	BPL124	03 47 05.71	+24 40 03.6	15.447	X	X	...	LOD107	
1689	UGCS-PI-40	03 47 05.79	+23 45 34.7	14.883	X	X	...	LOD107	
1690	BPL126	03 47 08.15	+24 18 24.5	12.734	X	X	...	LOD107	
1691	BPL128	03 47 09.42	+24 15 34.8	14.45	X	X	...	LOD107	
1692	...	03 47 09.52	+23 25 56.3	13.896	X	X	...	LOD107	
1693	UGCS-PI-41	03 47 10.65	+23 58 16.4	14.887	X	X	...	LOD107	
1694	BPL129	03 47 11.02	+24 13 51.6	14.241	X	X	...	LOD107	
1695	BPL130	03 47 11.79	+24 13 31.3	14.805	X	X	...	LOD107	

Table A.3 (cont'd)

ID	Other ID(s)	RA	DEC	J	SpT	SPEC	PM	LI	HA	UV	MIR	OPT/NIR	ARCH	Ref1	Ref2
1696	BPL131	03 47 11.86	+24 13 53.8	14.027	X	X	...	LODI07	
1697	...	03 47 13.67	+23 49 53.2	11.89	X	X	...	LODI07	
1698	BPL133	03 47 15.29	+25 06 55.3	12.348	X	X	...	LODI07	
1699	...	03 47 15.38	+23 26 05.9	13.368	X	X	...	LODI07	
1700	BPL134	03 47 15.45	+24 23 30.9	13.644	X	X	...	LODI07	
1701	BPL135	03 47 15.75	+22 21 16.9	13.127	X	X	...	LODI07	
1702	BPL136	03 47 16.45	+24 44 50.2	13.398	X	X	...	LODI07	
1909	PLZJ100	03 47 19.19	+25 50 53.3	20.254	X	CASE07	
1703	...	03 47 20.84	+25 05 12.1	12.02	X	X	...	LODI07	
1704	...	03 47 21.84	+25 53 52.3	11.892	X	X	...	LODI07	
1705	BPL140	03 47 22.46	+22 31 10.8	14.19	X	X	...	LODI07	
1706	...	03 47 22.68	+23 44 06.8	13.203	X	X	...	LODI07	
1707	BPL141	03 47 22.98	+24 50 56.1	12.628	X	X	...	LODI07	
1708	BPL144	03 47 25.80	+25 08 32.8	12.284	X	X	...	LODI07	
1709	...	03 47 26.77	+23 38 02.4	13.13	X	X	...	LODI07	
1710	...	03 47 28.12	+23 26 53.4	12.76	X	X	...	LODI07	
1711	BPL145	03 47 28.43	+24 40 33.1	13.722	X	X	...	LODI07	
1712	BPL146	03 47 30.66	+25 13 30.6	14.978	X	X	...	LODI07	
1713	BPL147	03 47 32.00	+24 10 24.8	13.649	X	X	...	LODI07	
1714	...	03 47 33.46	+23 41 32.8	11.703	X	X	...	LODI07	
1715	...	03 47 34.17	+25 43 06.0	13.191	X	X	...	LODI07	
1716	BPL149	03 47 35.86	+24 52 26.7	13.606	X	X	...	LODI07	
1717	...	03 47 36.04	+23 28 26.7	14.112	X	X	...	LODI07	
1718	BPL150	03 47 37.66	+24 24 23.1	13.677	X	X	...	LODI07	
1719	BPL151	03 47 38.05	+24 49 10.9	12.525	X	X	...	LODI07	
348	BRB12	03 47 39.0	+24 36 22.1	15.537	X	X	...	BIHA06	LODI07
	CFHT-PL11	BEJ00	
	Roque16	ZAP97	
	BPL152	BARA98	
1720	BPL153	03 47 39.36	+24 27 32.0	13.048	X	X	...	LODI07	
1721	...	03 47 41.19	+23 44 24.9	11.389	X	X	...	LODI07	
1722	...	03 47 44.05	+24 03 56.4	15.051	X	X	...	LODI07	
1723	HHJ152	03 47 44.66	+23 42 03.1	13.501	X	X	...	LODI07	
1724	BPL154	03 47 44.67	+22 12 44.0	14.692	X	X	...	LODI07	
1725	BPL155	03 47 44.68	+22 23 53.0	13.412	X	X	...	LODI07	
1726	BPL156	03 47 45.92	+24 38 01.3	13.464	X	X	...	LODI07	
1727	BPL157	03 47 47.87	+25 13 34.3	12.934	X	X	...	LODI07	
1728	BPL158	03 47 49.78	+24 25 43.2	13.534	X	X	...	LODI07	
1729	BPL159	03 47 50.95	+24 30 18.6	12.322	X	X	...	LODI07	
1730	...	03 47 51.97	+23 39 48.0	13.896	X	X	...	LODI07	
1731	BPL160	03 47 52.88	+22 59 33.9	12.999	X	X	...	LODI07	

Table A.3 (cont'd)

ID	Other ID(s)	RA	DEC	J	SpT	SPEC	PM	LI	HA	UV	MIR	OPT/NIR	ARCH	Ref1	Ref2
1732	...	03 47 55.28	+23 19 05.8	12.91	X	X	...	LODI07	
1733	BPL162	03 47 56.64	+24 15 31.7	14.138	X	X	...	LODI07	
1734	BPL163	03 47 58.03	+22 06 50.9	15.282	X	X	...	LODI07	
1735	BPL164	03 47 59.38	+24 35 37.1	14.487	X	X	...	LODI07	
1736	BPL165	03 47 59.77	+22 38 30.2	11.821	X	X	...	LODI07	
1737	NOT1	03 48 03.68	+23 44 10.6	14.326	X	X	...	LODI07	
1738	PP15	03 48 04.67	+23 39 30.2	15.294	X	X	...	LODI07	
1739	...	03 48 04.98	+23 24 13.5	14.787	X	X	...	LODI07	
1740	...	03 48 05.72	+22 38 09.3	13.201	X	X	...	LODI07	
1741	BPL166	03 48 05.83	+23 02 02.8	12.365	X	X	...	LODI07	
1742	HHJ240	03 48 06.64	+24 00 06.7	13.364	X	X	...	LODI07	
1743	HHJ156	03 48 08.95	+23 42 23.3	13.567	X	X	...	LODI07	
1744	...	03 48 09.22	+23 58 40.6	13.459	X	X	...	LODI07	
1745	...	03 48 10.18	+23 59 20.2	14.359	X	X	...	LODI07	
1746	...	03 48 13.31	+23 58 46.8	13.177	X	X	...	LODI07	
1747	...	03 48 13.78	+23 37 59.3	12.981	X	X	...	LODI07	
1748	BPL169	03 48 14.30	+24 15 50.6	15.226	X	X	...	LODI07	
1749	...	03 48 15.27	+23 42 03.4	12.586	X	X	...	LODI07	
1750	BPL170	03 48 15.49	+25 14 36.4	13.891	X	X	...	LODI07	
1751	...	03 48 16.09	+23 35 15.3	13.528	X	X	...	LODI07	
1752	...	03 48 17.30	+24 30 15.7	11.54	X	X	...	LODI07	
1753	BPL171	03 48 17.61	+22 04 01.0	13.397	X	X	...	LODI07	
1754	...	03 48 19.84	+23 36 11.9	12.334	X	X	...	LODI07	
1755	BPL173	03 48 20.29	+24 54 55.0	12.46	X	X	...	LODI07	
1756	BPL174	03 48 21.54	+24 34 43.4	13.8	X	X	...	LODI07	
1757	BPL176	03 48 22.81	+24 48 53.5	12.847	X	X	...	LODI07	
1758	BPL178	03 48 25.24	+24 14 25.9	12.795	X	X	...	LODI07	
1759	...	03 48 26.05	+25 14 40.8	11.942	X	X	...	LODI07	
1760	BPL180	03 48 31.06	+24 16 53.2	12.18	X	X	...	LODI07	
1761	BRB16	03 48 31.52	+24 34 37.3	16.727	X	X	...	LODI07	
1762	...	03 48 31.84	+24 01 58.7	13.616	X	X	...	LODI07	
1763	...	03 48 33.78	+24 01 58.8	13.693	X	X	...	LODI07	
1764	HHJ96	03 48 35.49	+24 12 03.1	14.045	X	X	...	LODI07	
1765	BPL182
1766	BPL183	03 48 36.34	+25 15 41.2	14.792	X	X	...	LODI07	
1767	...	03 48 39.31	+24 50 20.0	14.268	X	X	...	LODI07	
1768	BPL184	03 48 39.91	+24 12 42.8	12.638	X	X	...	LODI07	
1769	BPL185	03 48 40.43	+24 36 34.1	13.152	X	X	...	LODI07	
1769	BPL186	03 48 40.60	+25 01 19.8	14.553	X	X	...	LODI07	
1770	BPL187	03 48 42.15	+25 00 28.3	12.556	X	X	...	LODI07	
1771	HHJ44	03 48 42.69	+24 27 19.4	14.372	X	X	...	LODI07	

Table A.3 (cont'd)

ID	Other ID(s)	RA	DEC	J	SpT	SPEC	PM	LI	HA	UV	MIR	OPT/NIR	ARCH	Ref1	Ref2
	WILL6
	BPL188
1772	BPL189	03 48 44.05	+25 06 22.4	13.472	X	X	...	LODI07	...
343	BRB7	03 48 44.7	+24 37 22.7	14.916	X	X	...	BIHA06	LODI07
	CFHT-PL5	BEJ00	...
	DH 590	DEA04	...
1773	BPL190	03 48 45.35	+24 37 26.3	13.977	X	X	...	LODI07	...
1774	HHI207	03 48 46.02	+24 10 12.5	13.453	X	X	...	LODI07	...
1775	BPL192	03 48 50.45	+25 17 54.7	15.121	X	X	...	LODI07	...
1776	...	03 48 50.50	+24 08 27.2	15.492	X	X	...	LODI07	...
1777	HHI8	03 48 55.65	+24 21 40.2	14.953	X	X	...	LODI07	...
1778	BPL195	03 49 00.99	+24 54 10.0	12.674	X	X	...	LODI07	...
1779	...	03 49 01.16	+23 38 15.5	14.419	X	X	...	LODI07	...
1780	...	03 49 02.34	+25 43 24.1	12.359	X	X	...	LODI07	...
1781	BPL197	03 49 02.97	21 54 46.9	14.168	X	X	...	LODI07	...
1782	Roque47	03 49 04.86	+23 33 39.3	15.593	X	X	...	LODI07	...
1783	...	03 49 08.84	+25 53 48.6	12.172	X	X	...	LODI07	...
346	BRB10	03 49 15.1	+24 36 22.4	15.367	X	X	...	BIHA06	LODI07
	CFHT-PL9	BEJ00	...
	BPL202	BARA98	...
	MHOBD6	STA98	...
1784	...	03 49 20.31	+25 25 42.3	13.16	X	X	...	LODI07	...
1785	BPL204	03 49 21.25	+24 41 40.8	14.358	X	X	...	LODI07	...
1786	...	03 49 21.50	+23 39 06.3	12.819	X	X	...	LODI07	...
1787	BPL205	03 49 21.93	+24 54 43.3	13.543	X	X	...	LODI07	...
1788	...	03 49 22.15	+25 47 37.8	13.395	X	X	...	LODI07	...
1789	BPL207	03 49 25.61	+23 02 50.0	14.018	X	X	...	LODI07	...
1790	BPL208	03 49 26.63	+22 50 54.6	13.324	X	X	...	LODI07	...
1791	...	03 49 29.81	+23 38 55.3	13.526	X	X	...	LODI07	...
1792	...	03 49 31.22	+23 41 19.7	13.577	X	X	...	LODI07	...
1793	...	03 49 32.16	+23 16 18.0	14.28	X	X	...	LODI07	...
1794	...	03 49 32.81	+25 47 46.9	13.463	X	X	...	LODI07	...
1795	BPL209	03 49 33.04	+24 32 02.5	12.529	X	X	...	LODI07	...
1796	...	03 49 35.29	+25 59 34.7	13.534	X	X	...	LODI07	...
1797	...	03 49 36.31	+26 02 16.3	14.341	X	X	...	LODI07	...
1798	BPL213	03 49 41.21	+22 56 40.6	15.008	X	X	...	LODI07	...
1799	...	03 49 41.34	+26 08 53.3	12.815	X	X	...	LODI07	...
1800	BPL215	03 49 43.17	+24 39 46.5	15.067	X	X	...	LODI07	...
1801	...	03 49 47.04	+25 42 36.8	12.866	X	X	...	LODI07	...
1802	...	03 49 55.49	+24 06 05.0	13.448	X	X	...	LODI07	...
1803	BPL217	03 49 55.79	+24 44 31.4	12.358	X	X	...	LODI07	...

Table A.3 (cont'd)

ID	Other ID(s)	RA	DEC	J	SpT	SPEC	PM	LI	HA	UV	MIR	OPT/NIR	ARCH	Ref1	Ref2
1804	...	03 49 56.77	+25 22 22.6	13.387	X	X	...	LODI07	
1805	KPNO5	03 49 56.81	+24 59 07.1	15.142	X	X	...	LODI07	
	BPL218	
1806	...	03 49 57.64	+23 43 28.2	14.237	X	X	...	LODI07	
1807	BPL219	03 49 58.33	+25 06 21.0	14.222	X	X	...	LODI07	
1808	BPL220	03 49 59.54	+24 11 45.6	14.346	X	X	...	LODI07	
1809	...	03 50 01.57	+25 24 01.6	12.192	X	X	...	LODI07	
1810	BPL222	03 50 01.87	+25 12 40.9	13.219	X	X	...	LODI07	
1811	...	03 50 02.18	+23 51 44.7	12.814	X	X	...	LODI07	
1812	...	03 50 04.25	+23 10 44.5	13.183	X	X	...	LODI07	
1813	BPL224	03 50 06.56	+24 59 46.3	12.796	X	X	...	LODI07	
1814	...	03 50 08.42	+25 32 55.7	13.175	X	X	...	LODI07	
1815	...	03 50 08.62	+24 40 17.7	14.228	X	X	...	LODI07	
1816	BPL225	03 50 10.77	+24 28 41.4	13.695	X	X	...	LODI07	
1817	...	03 50 12.46	+23 55 36.0	12.952	X	X	...	LODI07	
1818	...	03 50 12.60	+23 48 48.9	14.467	X	X	...	LODI07	
1819	...	03 50 14.76	+25 25 29.8	13.692	X	X	...	LODI07	
1820	BPL226	03 50 15.27	+24 13 36.1	13.129	X	X	...	LODI07	
1821	Roque30	03 50 16.09	+24 08 34.8	17.338	X	X	...	LODI07	
1822	BPL227	03 50 18.22	+24 35 15.3	13.671	X	X	...	LODI07	
1823	BPL228	03 50 19.15	+24 16 34.0	15.081	X	X	...	LODI07	
1824	BPL228	03 50 19.15	+24 16 34.0	15.081	X	X	...	LODI07	
1825	...	03 50 25.16	+23 55 41.8	13.598	X	X	...	LODI07	
1826	BPL229	03 50 29.30	+24 56 34.6	13.556	X	X	...	LODI07	
1827	BPL230	03 50 29.96	+25 03 06.7	12.535	X	X	...	LODI07	
1828	BPL231	03 50 33.08	+24 20 21.7	13.355	X	X	...	LODI07	
357	BRB23	03 50 39.53	+25 02 54.5	18.55	X	X	...	BIHA06	
1829	...	03 50 40.83	+24 40 02.7	14.248	X	X	...	LODI07	
1830	...	03 50 42.44	+24 12 55.4	13.992	X	X	...	LODI07	
1831	...	03 50 54.65	+24 21 55.8	13.587	X	X	...	LODI07	
1832	...	03 50 57.42	+24 06 30.8	12.65	X	X	...	LODI07	
1833	...	03 51 03.61	+24 32 35.2	13.277	X	X	...	LODI07	
1834	...	03 51 05.58	+24 44 12.2	11.374	X	X	...	LODI07	
1835	CFHT-PLIZ1	03 51 05.97	+24 36 16.9	15.654	X	X	...	LODI07	
1836	...	03 51 07.10	+23 20 57.6	13.661	X	X	...	LODI07	
1837	BPL232	03 51 11.88	+23 44 43.3	14.243	X	X	...	LODI07	
1838	...	03 51 17.95	+26 01 22.1	13.71	X	X	...	LODI07	
1839	BPL233	03 51 19.07	+24 10 13.1	12.219	X	X	...	LODI07	
1840	...	03 51 19.48	+23 09 49.5	13.002	X	X	...	LODI07	
1841	...	03 51 19.77	+23 04 04.1	14.183	X	X	...	LODI07	
1842	...	03 51 23.89	+25 05 52.6	12.545	X	X	...	LODI07	

Table A.3 (cont'd)

ID	Other ID(s)	RA	DEC	J	SpT	SPEC	PM	LI	HA	UV	MIR	OPT/NIR	ARCH	Ref1	Ref2
1843	...	03 51 24.17	+26 03 11.4	12.517	X	X	...	LODI07	
350	BRB14	03 51 25.6	+23 45 20.6	16.13	X	X	X	...	BIHA06	
	CFHT-PL121	BEJ00	
	Calar3	MART96	
	BPL235	BARA98	
	CFHT-PL1Z-12	BOU06	
1844	...	03 51 25.88	+24 47 38.7	11.988	X	X	...	LODI07	
1845	UGCS-PI-56	03 51 38.96	+24 30 44.8	16.408	X	X	...	LODI07	
1846	BPL237	03 51 39.08	+23 22 04.4	13.92	X	X	...	LODI07	
1847	...	03 51 39.12	+24 35 29.1	13.42	X	X	...	LODI07	
1848	CFHT-PL-IZ-10	03 51 44.94	+23 26 39.3	16.031	X	X	...	LODI07	
	BPL240
1849	CFHTPL1Z31	03 51 47.65	+24 39 59.0	17.555	X	X	...	LODI07	
1850	...	03 51 50.59	+22 53 44.4	12.917	X	X	...	LODI07	
338	BRB1	03 51 51.6	+23 34 50.2	14.29	X	X	...	BIHA06	LODI07
	CFHT-PI-1	BEJ00	
	BPL242	BARA98	
	MBSC91	MORA03	
1910	PL1Z123	03 51 53.38	+24 38 12.1	19.96	X	CASE07	
1851	BPL244	03 51 54.52	+23 33 31.4	12.651	X	X	...	LODI07	
1852	BPL245	03 51 55.05	+23 57 42.1	13.489	X	X	...	LODI07	
1853	...	03 51 57.12	+24 57 06.4	15.301	X	X	...	LODI07	
1854	...	03 51 57.53	+25 48 31.2	13.115	X	X	...	LODI07	
1855	BPL246	03 51 58.35	+23 58 19.3	13.55	X	X	...	LODI07	
1856	UGCS-PI-58	03 51 59.27	+23 17 17.8	15.811	X	X	...	LODI07	
1857	BPL248	03 52 01.65	+25 01 29.2	13.409	X	X	...	LODI07	
1858	BPL249	03 52 02.10	+23 15 45.4	16.7	X	X	...	LODI07	
1859	...	03 52 02.27	+24 21 47.9	12.17	X	X	...	LODI07	
1860	BPL250	03 52 02.64	+25 06 14.9	13.668	X	X	...	LODI07	
1861	BPL251	03 52 03.58	+25 01 13.6	13.76	X	X	...	LODI07	
1862	BPL252	03 52 04.48	+24 14 39.6	13.788	X	X	...	LODI07	
344	BRB8	03 52 05.8	+24 17 31.7	15.186	X	X	...	BIHA06	LODI07
	CFHT-PI-7	BEJ00	
	BPL253	BARA98	
	MBSC108	MORA03	
347	BRB11	03 52 06.7	+24 16 01.4	15.523	X	X	...	BIHA06	LODI07
	CFHT-PI-13	BEJ00	
	Teide2	MART98	
	BPL254	BARA98	
	CFHT-PL1Z-3	BOU06	
340	BRB3	03 52 07.9	+23 59 14.6	14.62	X	X	...	BIHA06	LODI07

Table A.3 (cont'd)

ID	Other ID(s)	RA	DEC	J	SpT	SPEC	PM	LI	HA	UV	MIR	OPT/NIR	ARCH	Ref1	Ref2
1863	CFHT-PL-6	BEJ00	
1864	...	03 52 13.32	+26 08 36.9	12.684	X	X	...	LODI07	
1864	CFHT23	03 52 18.64	+24 04 28.1	16.394	X	X	...	LODI07	
1865	CFHTPLIZ15
1865	BPL260	03 52 18.71	+23 52 36.6	14.002	X	X	...	LODI07	
1866	...	03 52 20.66	+24 33 55.6	11.982	X	X	...	LODI07	
1867	...	03 52 24.00	+23 55 15.8	14.05	X	X	...	LODI07	
1868	BPL261	03 52 30.91	+24 32 39.5	12.399	X	X	...	LODI07	
1911	PLZJ10	03 52 31.19	+24 46 29.6	18.181	X	CASE07	
1911	PLIZ35
1869	BRB15
1869	BPL262	03 52 31.37	+25 15 07.5	12.732	X	X	...	LODI07	
1912	PLZJ235	03 52 32.57	+24 44 36.6	20.039	X	CASE07	
1870	BPL264	03 52 33.34	+23 51 06.7	13.383	X	X	...	LODI07	
1871	BPL265	03 52 35.32	+25 01 04.6	13.583	X	X	...	LODI07	
354	BRB20	03 52 39.16	+24 46 29.7	18.06	X	X	...	BIHA06	
1872	CFHT-PLIZ-35	BOU06	
1872	...	03 52 42.21	+25 10 42.2	14.525	X	X	...	LODI07	
1873	BPL266	03 52 43.24	+24 27 58.5	13.703	X	X	...	LODI07	
339	BRB2	03 52 44.3	+23 54 15.2	14.546	X	X	...	BIHA06	LODI07
1874	CFHT-PL-2	BEJ00	
1874	BPL267	BARA98	
1874	DH 765	DEA04	
1874	BPL268	03 52 44.48	+24 20 59.3	13.932	X	X	...	LODI07	
1875	BPL269
1875	BPL270	03 52 46.44	+24 33 41.0	13.49	X	X	...	LODI07	
341	BRB5	03 52 51.8	+23 33 48.9	14.807	X	X	...	BIHA06	LODI07
1877	CFHT-PL-3	BEJ00	
1877	HJI 22	HAM93	
1877	BPL272	BARA98	
359	MBC99	MORA03	
359	BRB28	03 52 54.92	+24 37 18.6	18.839	X	X	...	BIHA06	CASE07
1876	BPL275	03 52 55.92	+24 57 41.8	15.099	X	X	...	LODI07	
1913	PLZJ45	03 52 58.20	+24 17 31.6	15.247	X	CASE07	
1877	BRB8
1877	CFHT-PL-7
1877	...	03 53 01.63	+22 58 48.2	13.411	X	X	...	LODI07	
1878	BPL278	03 53 05.13	+25 04 15.6	14.74	X	X	...	LODI07	
342	BRB6	03 53 09.6	+23 33 48.3	14.96	X	X	...	BIHA06	
1878	CFHT-PL-4	BEJ00	
1878	BPL280	BARA98	

Table A.3 (cont'd)

ID	Other ID(s)	RA	DEC	J	SpT	SPEC	PM	LI	HA	UV	MIR	OPT/NIR	ARCH	Ref1	Ref2
1879	MBCS101	MORA03	
1880	...	03 53 10.16	+23 03 10.7	12.555	X	X	...	LODI07	
1881	BPL281	03 53 15.71	+22 52 14.3	12.638	X	X	...	LODI07	
1914	PLZJ112	03 53 16.44	+23 20 58.1	14.093	X	X	...	LODI07	
1882	BPL285	03 53 19.37	+24 53 31.9	20.281	X	CASE07	
1883	HHI28	03 53 24.12	+23 47 58.4	13.399	X	X	...	LODI07	
1884	BPL293	03 53 48.04	+23 49 09.7	14.344	X	X	...	LODI07	
345	BRB9	X	LODI07
1885	BPL298	03 53 49.10	+23 32 49.5	15.23	X	X	...	LODI07	
360	BRB29	03 53 55.1	+23 23 37.4	15.155	X	X	...	BIHA06	LODI07
1886	BPL301	BEJ00	
1887	BPL302	BARA98	
351	BRB15	BOU06	
1888	BPL303	LODI07	
352	BRB17	03 54 00.70	+23 58 59.8	12.667	X	X	...	LODI07	
1915	PLZJ77	03 54 01.43	+23 49 58.1	19.05	X	X	...	BIHA06	
353	BRB18	03 54 02.73	+23 35 00.9	13.88	X	X	...	LODI07	
1889	BPL307	03 54 04.89	+25 05 06.2	13.833	X	X	...	LODI07	
1890	BPL310	03 54 05.3	+23 34 00.2	16.666	X	X	...	BIHA06	LODI07
1891	BPL311	BEJ00	
1892	BPL312	BARA98	
1893	BPL313	BOU06	
1894	UGCS-Pl-60	03 54 08.31	+23 54 33.4	17.42	X	X	...	BIHA06	CASE07
1895	...	03 54 10.04	+23 17 52.3	17.647	X	X	...	BIHA06	
1896	BPL315	CASE07	
1897
1898	BPL318
1899	BPL321
355	BRB21	03 54 10.27	+23 41 40.3	18.171
1888	BPL305	03 54 13.02	+23 20 50.8	12.596	X	X	...	BIHA06	CASE07
353	BRB18	03 54 14.08	+23 17 52.2	17.586	X	X	...	BIHA06	LODI07
1889	BPL307	BOU06	
1890	BPL308	03 54 15.60	+24 20 45.7	14.667	X	X	...	LODI07	
1891	BPL311
1892	BPL312	03 54 21.23	+23 23 49.0	12.938	X	X	...	LODI07	
1893	BPL313	03 54 22.49	+23 38 11.9	13.391	X	X	...	LODI07	
1894	UGCS-Pl-60	03 54 25.03	+24 42 43.5	13.661	X	X	...	LODI07	
1895	...	03 54 28.11	+23 56 36.0	14.512	X	X	...	LODI07	
1896	BPL315	03 54 31.48	+22 39 01.6	15.173	X	X	...	LODI07	
1897	...	03 54 37.36	+23 13 32.5	13.408	X	X	...	LODI07	
1898	BPL318	03 54 39.13	+24 35 54.5	14.549	X	X	...	LODI07	
1899	BPL321	03 54 45.87	+22 53 54.8	16.452	X	X	...	LODI07	
		03 54 48.00	+25 12 30.2	12.56	X	X	...	LODI07	
		03 54 58.03	+25 14 29.1	12.82	X	X	...	LODI07	

Table A.3 (cont'd)

ID	Other ID(s)	RA	DEC	J	SpT	SPEC	PM	LI	HA	UV	MIR	OPT/NIR	ARCH	Ref1	Ref2
1916	PLZ1721	03 55 07.14	+24 57 22.3	20.248	X	CASE07	
349	BRB13	03 55 12.5	+23 17 38.0	15.99	X	X	...	BIHA06	
	CFHT-PL-15	BEJ00	
1917	PLZ193	03 55 13.00	+24 36 15.8	19.968	X	CASE07	
1900	BPL325	03 55 17.17	+23 53 16.7	15.229	X	X	...	LOD107	
1901	BPL326	03 55 18.11	+24 17 05.7	15.1	X	X	...	LOD107	
1902	CFHTPL122	03 55 23.08	+24 49 04.9	15.507	X	X	...	LOD107	
	BPL327
1903	BPL328	03 55 27.06	+25 14 45.8	14.643	X	X	...	LOD107	
1904	BPL329	03 55 30.90	+23 23 50.9	13.003	X	X	...	LOD107	
1905	...	03 55 32.83	+23 19 08.0	11.993	X	X	...	LOD107	
1906	BPL334	03 56 11.38	+25 03 36.5	15.229	X	X	...	LOD107	

Appendix B

SED Fitting Results of Member Candidates

The figures below display the entire, best-fit results from the SED fitting technique applied to the cluster member candidates described in Chapter 4. For the sake of visual clarity, the spectra have been gaussian smoothed, normalized, and shifted by a constant value. Also for ease of viewing, spectra with especially high J -band flux have been edited so as to not overlap other candidate spectra within the figure. Each candidate's caption lists (from top to bottom): the ID of the member candidate as given in this work, the spectral and luminosity types of the best fit template to the candidates, the amount of reddening applied to the template to achieve the best fit in visual magnitudes of extinction, and the "status" of the fit as a result of visual inspection. The status is given in the three broad categories of "GOOD", "OK", and "POOR", and these status values were taken into account when assigning the final membership status of each candidate.

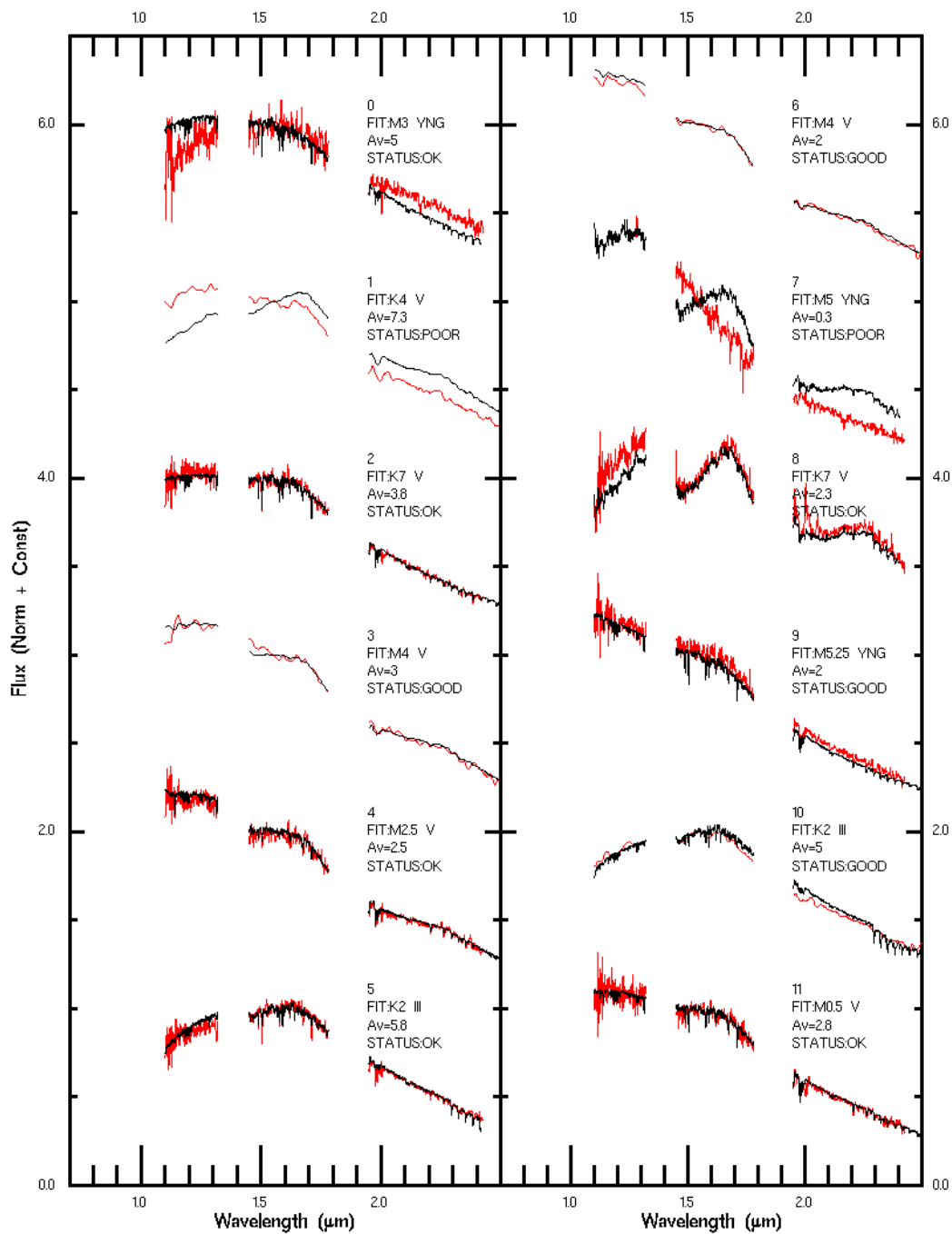


Figure B.1 The best-fit results for Taurus member candidates #000-011. The candidate spectra (red) are normalized and compared with the reddened, best-fit template (black). Each pair of spectra have been gaussian smoothed with $\sigma = 2$ data points and shifted by a constant for reasons of visual clarity.

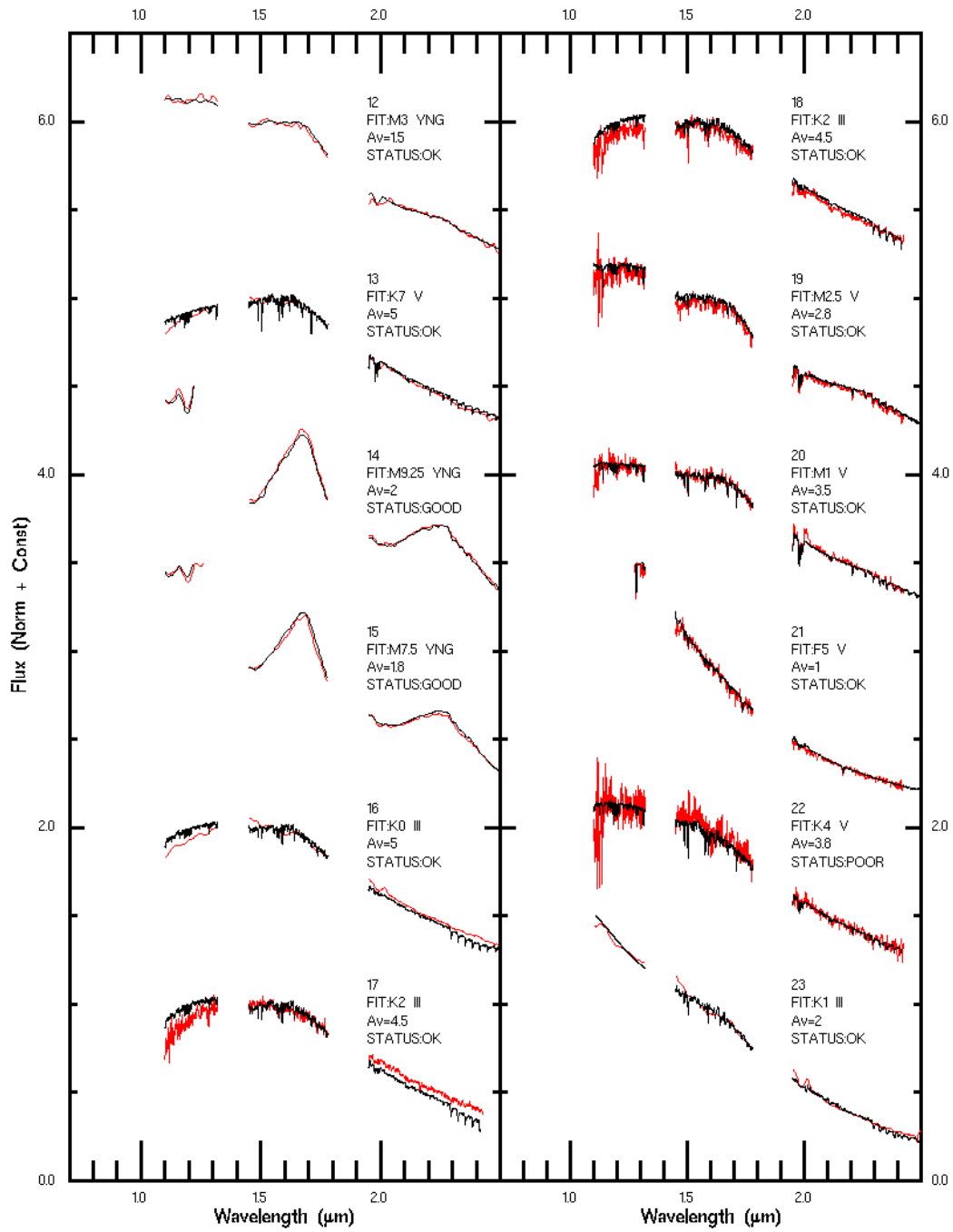


Figure B.2 The best-fit results for Taurus member candidates #012-023. Colors are the same as in Figure B.1

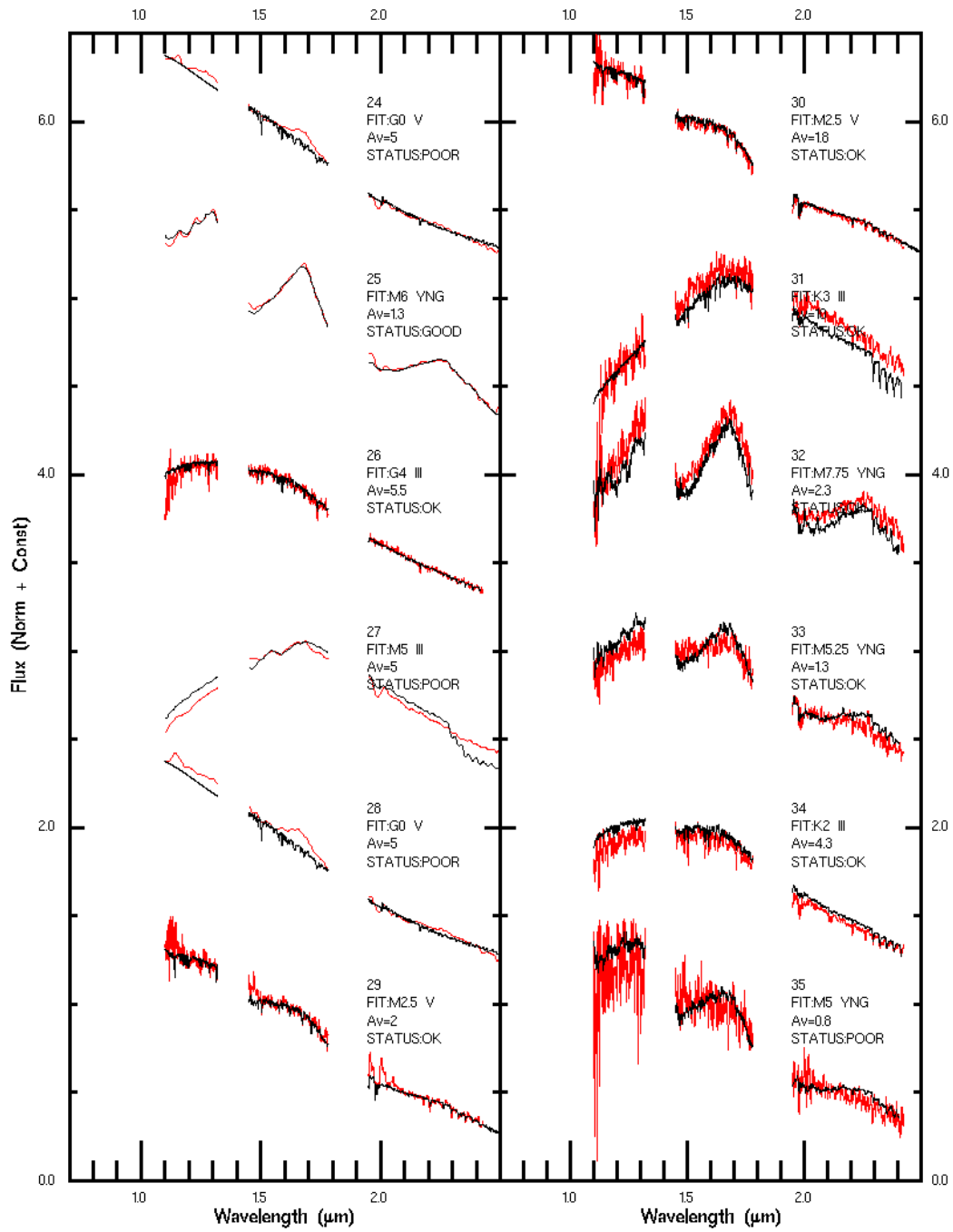


Figure B.3 The best-fit results for Taurus member candidates #024-035. Colors are the same as in Figure B.1

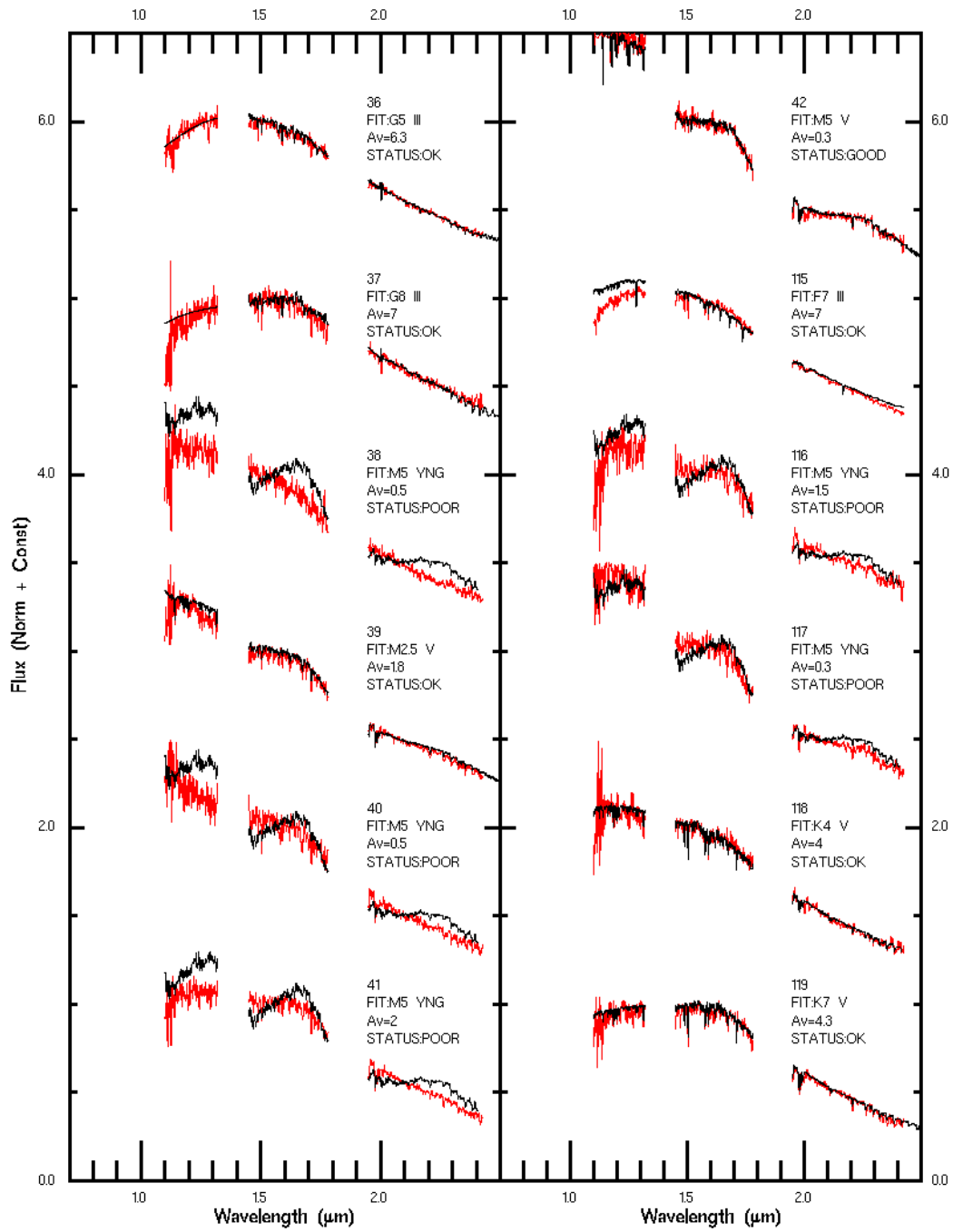


Figure B.4 The best-fit results for Taurus member candidates #036-119. Colors are the same as in Figure B.1

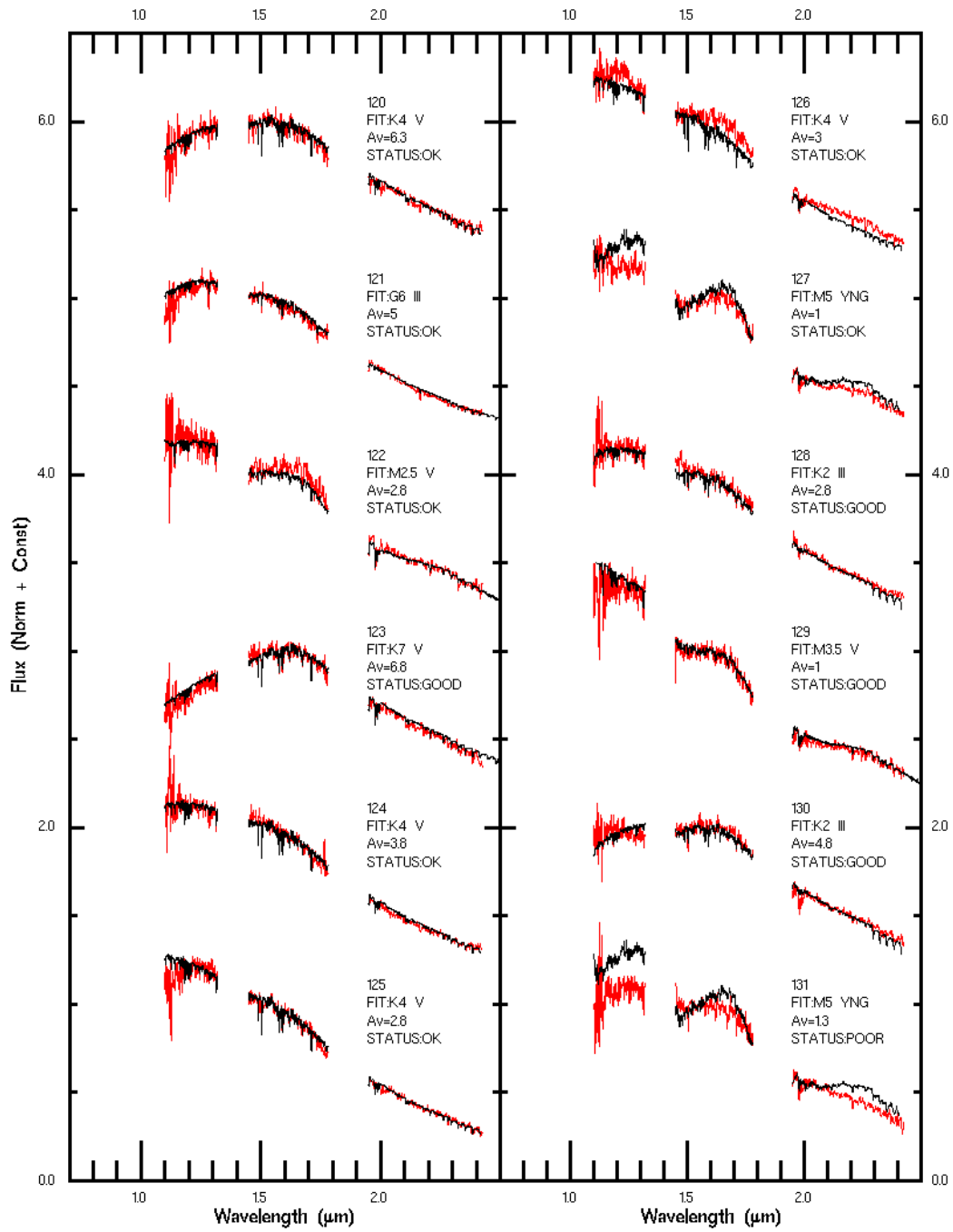


Figure B.5 The best-fit results for Taurus member candidates #120-131. Colors are the same as in Figure B.1

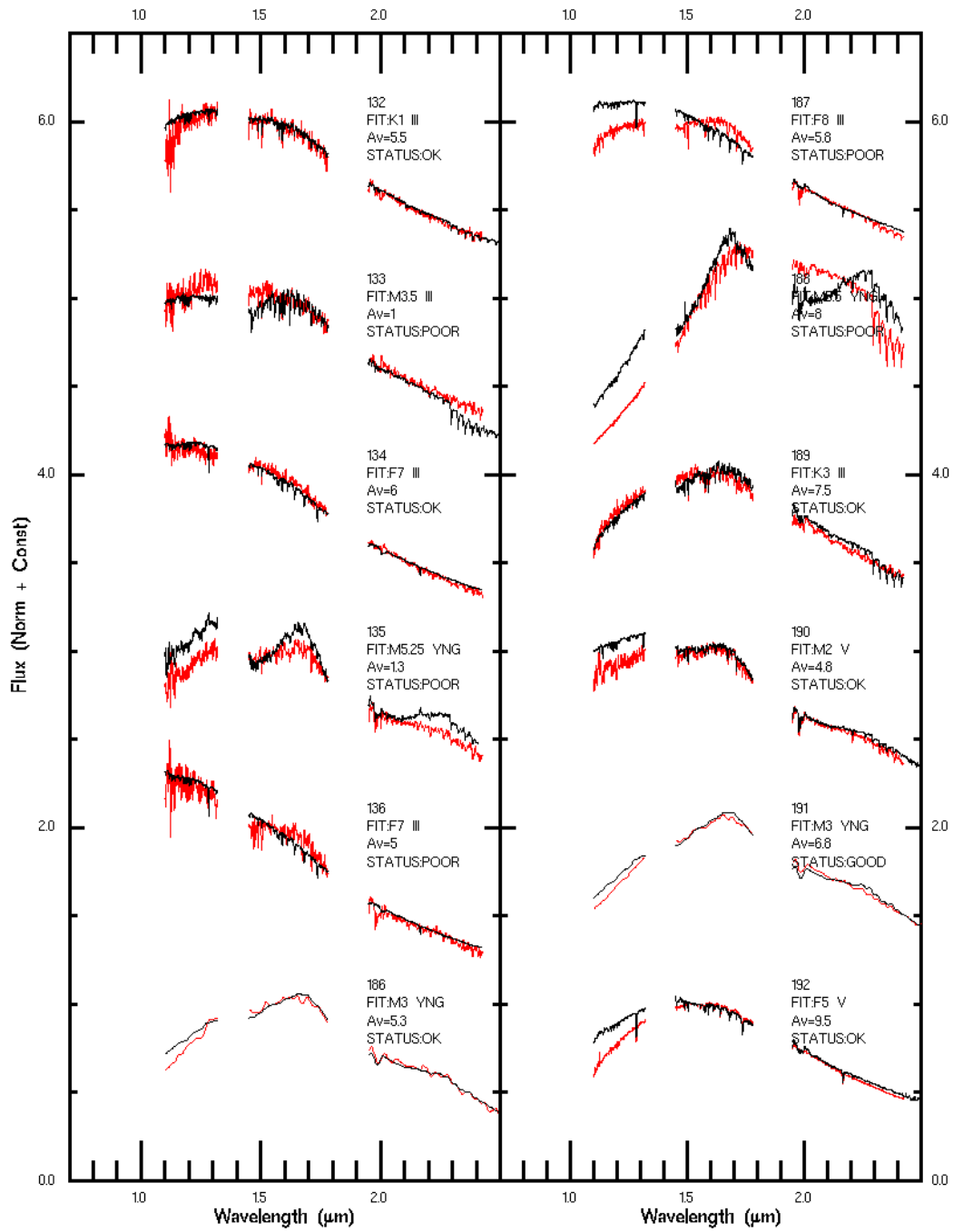


Figure B.6 The best-fit results for Taurus member candidates #132-192. Colors are the same as in Figure B.1

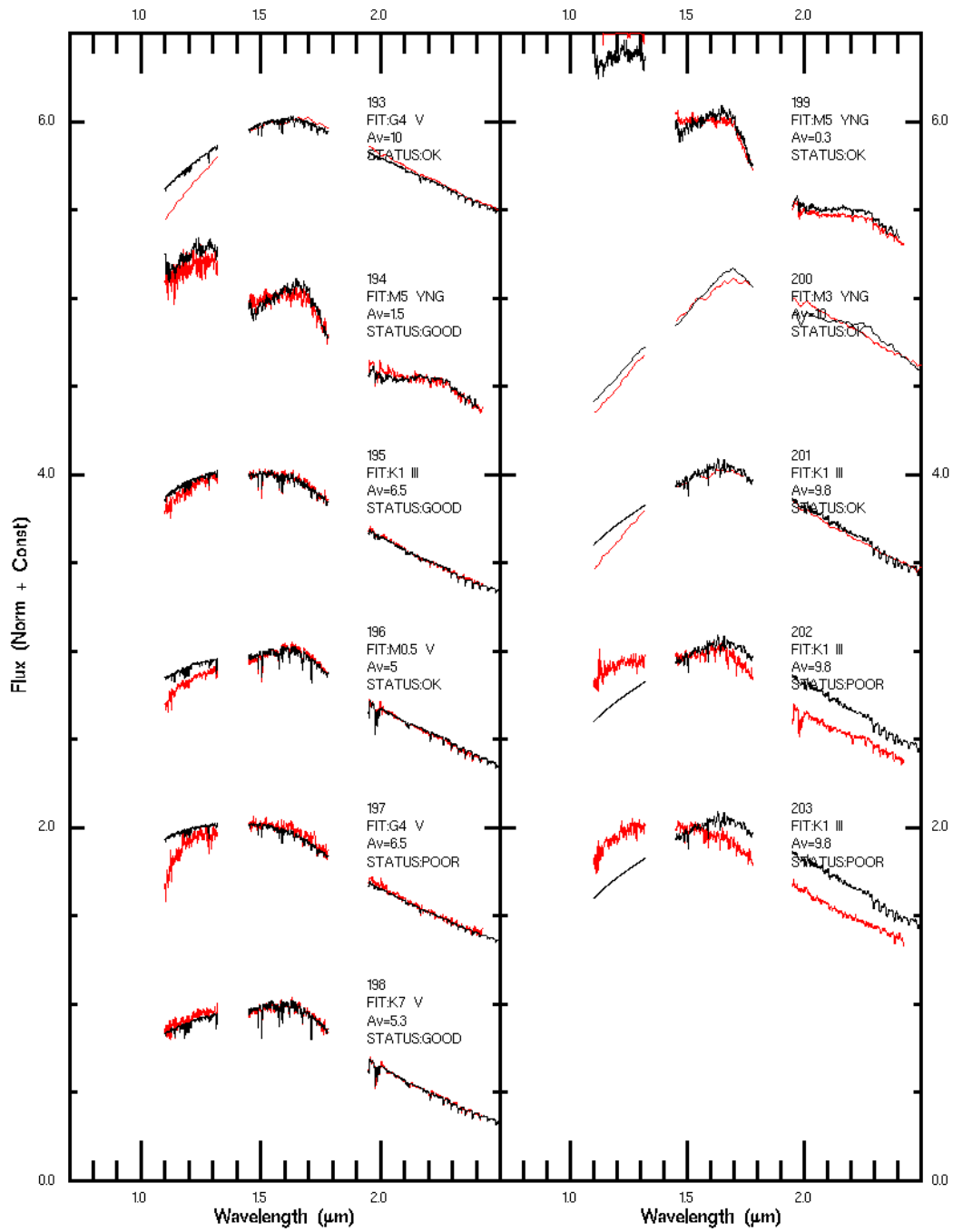


Figure B.7 The best-fit results for Taurus member candidates #193-203. Colors are the same as in Figure B.1

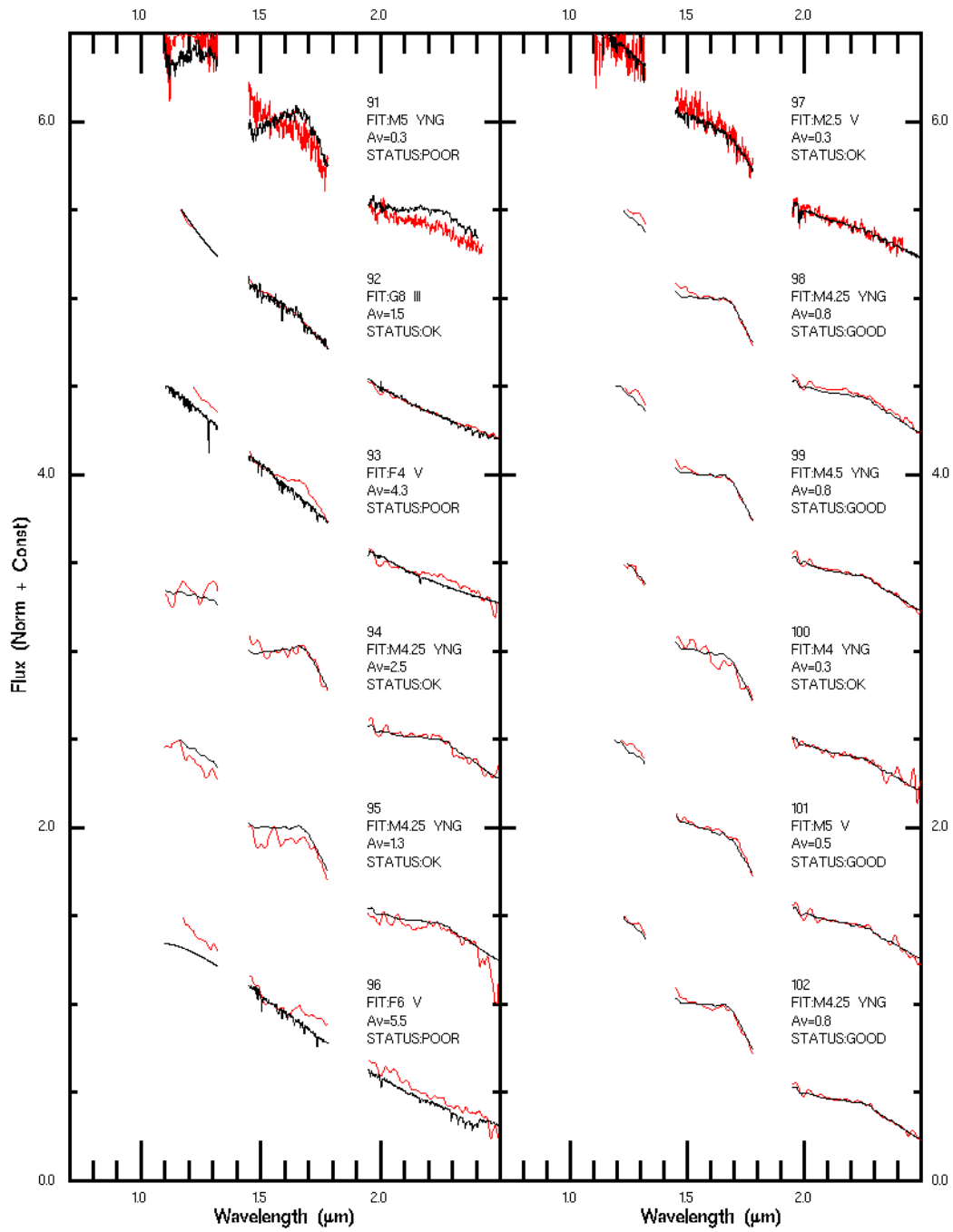


Figure B.8 The best-fit results for Praesepe member candidates #091-102. Colors are the same as in Figure B.1

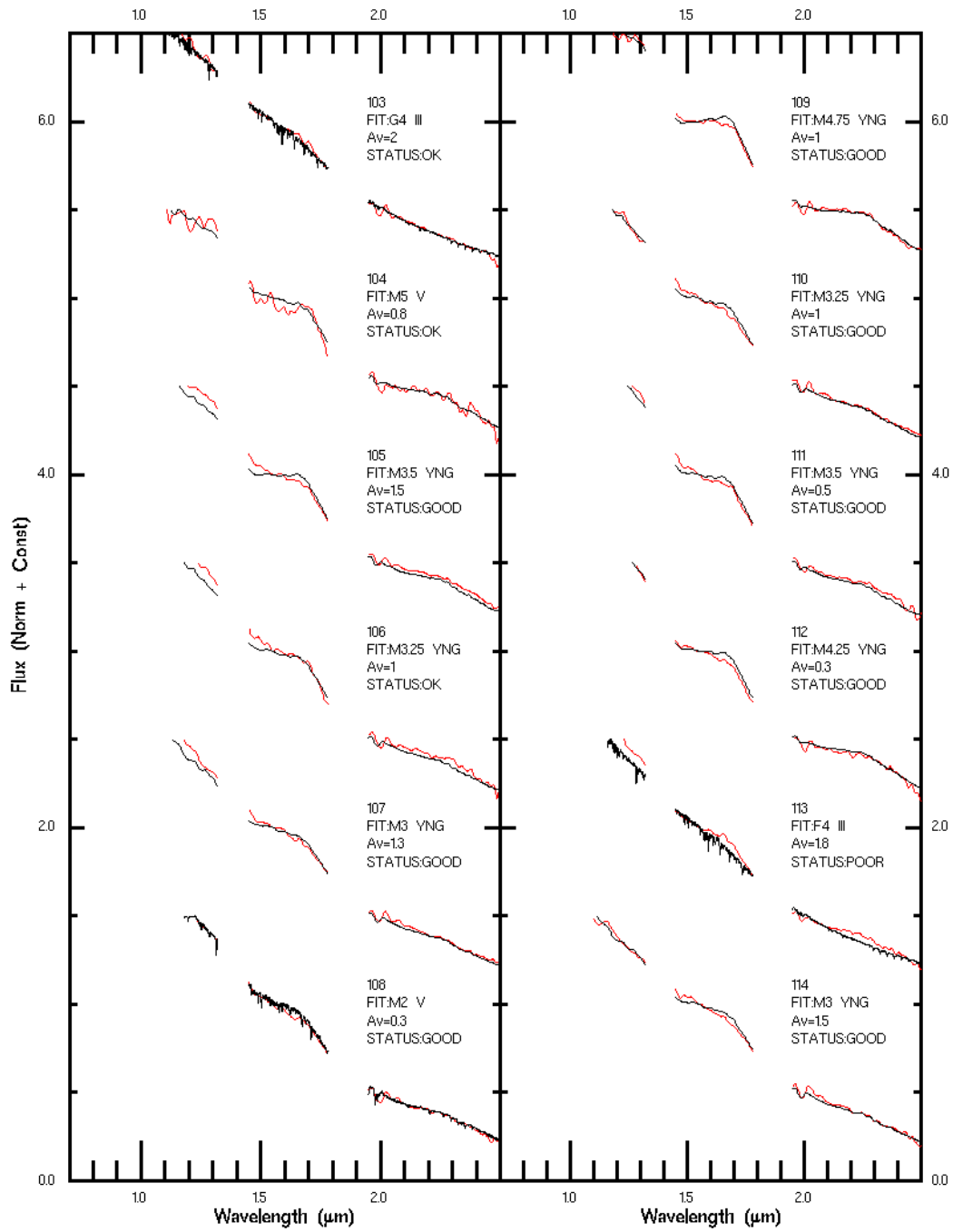


Figure B.9 The best-fit results for Praesepe member candidates #103-114. Colors are the same as in Figure B.1

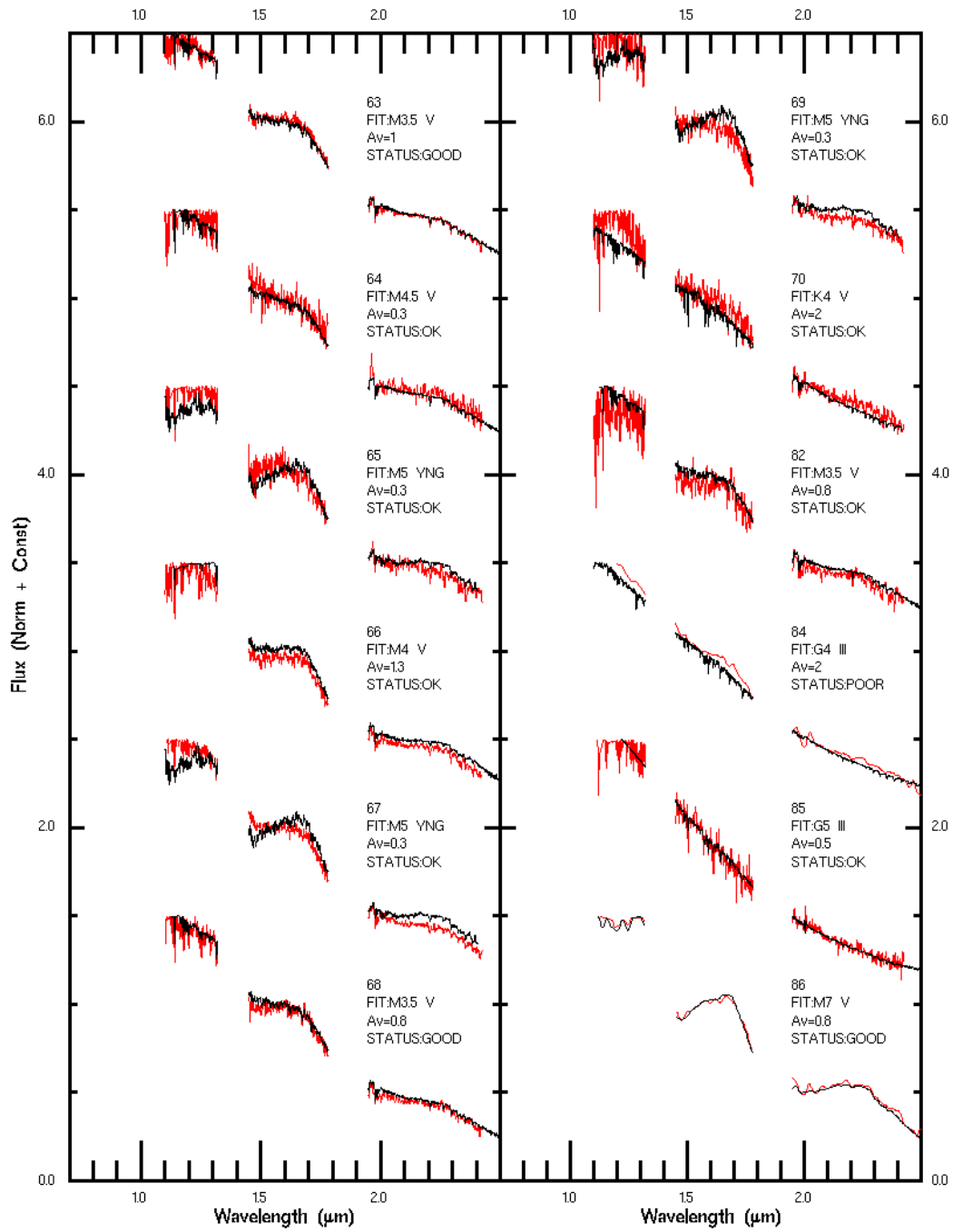


Figure B.10 The best-fit results for Pleiades member candidates #063-086. Colors are the same as in Figure B.1

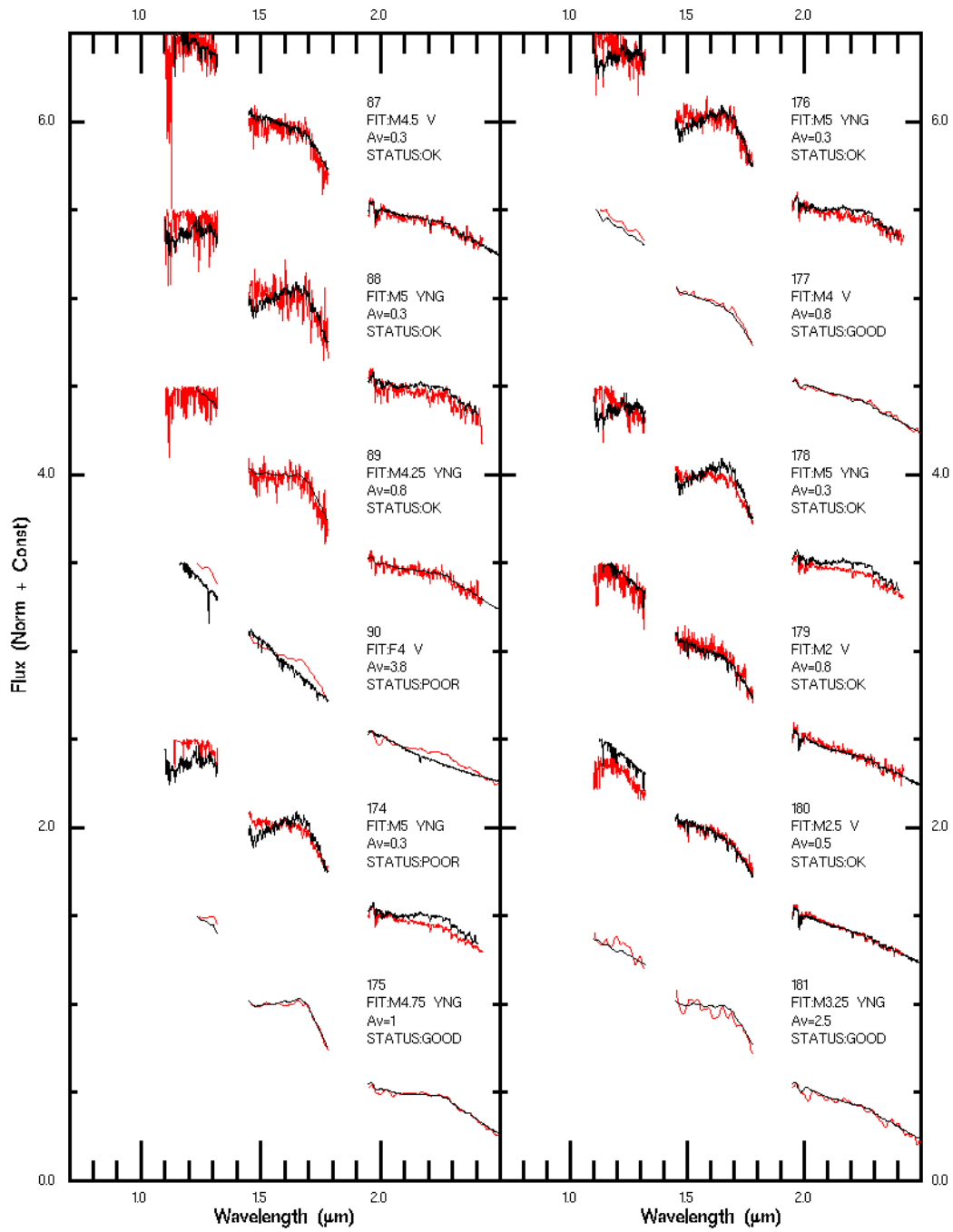


Figure B.11 The best-fit results for Pleiades member candidates #087-181. Colors are the same as in Figure B.1

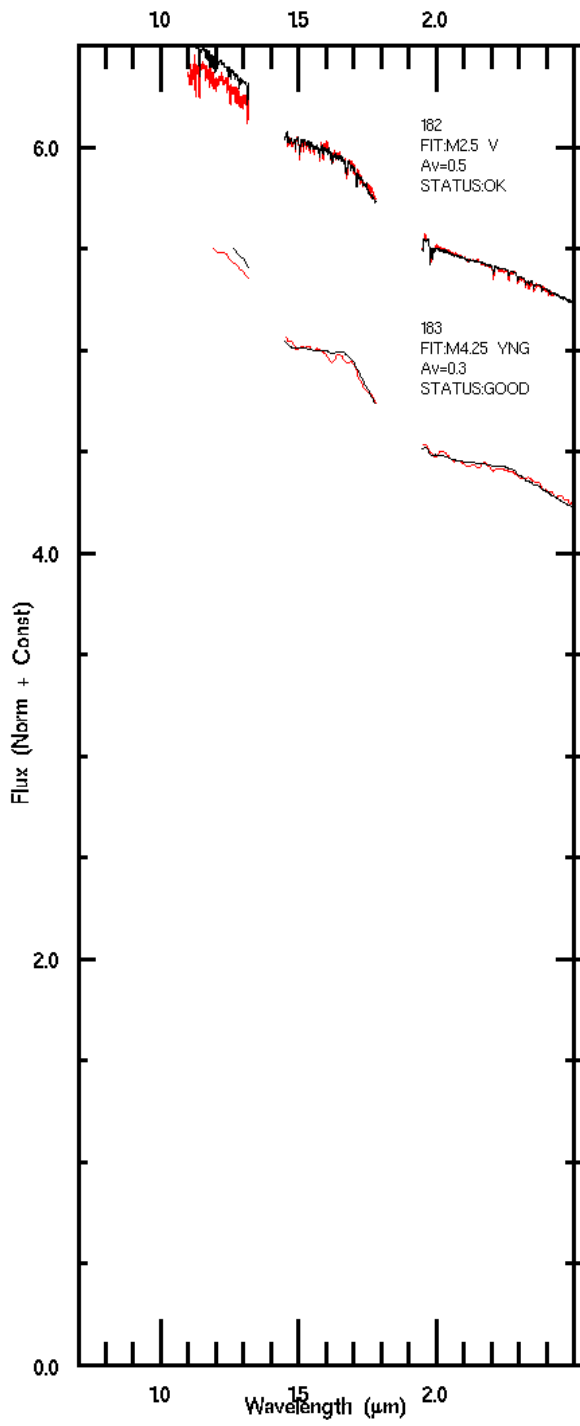


Figure B.12 The best-fit results for Pleiades member candidates #182-183. Colors are the same as in Figure B.1

Appendix C

Spectroscopic Follow-Up Observing Logs

Table C.1: Taurus Follow-Up Observations

ID	Date	Mode ¹	Weather ²
000	Nov-07	SXD	High Humidity
001	Nov-07	Prism	Clear
002	Nov-07	SXD	Clear
003	Nov-07	Prism	High Humidity
004	Nov-07	SXD	Clear
005	Nov-07	SXD	Clear
006	Nov-07	Prism	High Humidity
007	Nov-07	SXD	Clear
008	Nov-07	SXD	Clear
009	Nov-07	SXD	Incoming Fog
010	Nov-07	Prism	High Humidity
011	Nov-07	SXD	Clear
012	Nov-07	Prism	High Humidity
013	Nov-07	Prism	High Humidity
014	Nov-07	Prism	High Humidity

Table C.1 (cont'd)

ID	Date	Mode ¹	Weather ²
015	Nov-07	Prism	High Humidity
016	Nov-07	Prism	High Humidity
017	Nov-07	SXD	Clear
018	Nov-07	SXD	Clear
019	Nov-07	SXD	Clear
020	Nov-07	SXD	Clear
021	Nov-07	SXD	Clear
022	Nov-07	SXD	Clear
023	Nov-07	Prism	High Humidity
024	Nov-07	Prism	High Humidity
025	Nov-07	Prism	High Humidity
026	Nov-07	SXD	Clear
027	Nov-07	Prism	High Humidity
028	Nov-07	Prism	High Humidity
029	Nov-07	SXD	Clear
030	Nov-07	SXD	Clear
031	Nov-07	SXD	Clear
032	Nov-07	SXD	Clear
033	Nov-07	SXD	Clear
034	Nov-07	SXD	Clear
035	Nov-07	SXD	Clear
036	Nov-07	SXD	Clear
037	Nov-07	SXD	Clear
038	Nov-07	SXD	Clear
039	Nov-07	SXD	Clear
040	Nov-07	SXD	Clear
041	Nov-07	SXD	Clear
042	Nov-07	SXD	Clear
115	Jan-09	SXD	High Humidity

Table C.1 (cont'd)

ID	Date	Mode ¹	Weather ²
116	Jan-09	SXD	High Humidity
117	Jan-09	SXD	High Humidity
118	Jan-09	SXD	Clear
119	Jan-09	SXD	Clear
120	Jan-09	SXD	Clear
121	Jan-09	SXD	Clear
122	Jan-09	SXD	Clear
123	Jan-09	SXD	Clear
124	Jan-09	SXD	Clear
125	Jan-09	SXD	High Humidity
126	Jan-09	SXD	Cloudy
127	Jan-09	SXD	Cloudy
128	Jan-09	SXD	Clear
129	Jan-09	SXD	Clear
130	Jan-09	SXD	Clear
131	Jan-09	SXD	Clear
132	Jan-09	SXD	Clear
133	Jan-09	SXD	Clear
134	Jan-09	SXD	Clear
135	Jan-09	SXD	Clear
136	Jan-09	SXD	Clear
186	Nov-09	Prism	Clear
187	Nov-09	SXD	Clear
188	Nov-09	SXD	Clear
189	Nov-09	SXD	Clear
190	Nov-09	SXD	Clear
191	Nov-09	Prism	Clear
192	Nov-09	SXD	Clear
193	Nov-09	Prism	Clear

Table C.1 (cont'd)

ID	Date	Mode ¹	Weather ²
194	Nov-09	SXD	Clear
195	Nov-09	SXD	Clear
196	Nov-09	SXD	Clear
197	Nov-09	SXD	Clear
198	Nov-09	SXD	Clear
199	Nov-09	SXD	Clear
200	Nov-09	Prism	Clear
201	Nov-09	Prism	Clear
202	Nov-09	SXD	Clear
203	Nov-09	SXD	Clear

¹Prism = Prism mode ($R \sim 100$); SXD = Short Cross-Dispersed mode ($R \sim 1000$)

²Weather conditions at the time of observation

Table C.2: Praesepe Follow-Up Observations

ID	Date	Mode ¹	Weather ²
091	Jan-09	SXD	High Humidity
092	Jan-09	Prism	High Humidity
093	Jan-09	Prism	Clear
094	Jan-09	Prism	Clear
095	Jan-09	Prism	Clear
096	Jan-09	Prism	High Humidity
097	Jan-09	SXD	High Humidity
098	Jan-09	Prism	Clear
099	Jan-09	Prism	Clear
100	Jan-09	Prism	High Humidity
101	Jan-09	Prism	High Humidity
102	Jan-09	Prism	Clear
103	Jan-09	Prism	Clear
104	Jan-09	Prism	Clear
105	Jan-09	Prism	High Humidity
106	Jan-09	Prism	Clear
107	Jan-09	Prism	Clear
108	Jan-09	Prism	Clear
109	Jan-09	Prism	Clear
110	Jan-09	Prism	Clear
111	Jan-09	Prism	Clear
112	Jan-09	Prism	High Humidity
113	Jan-09	Prism	Clear
114	Jan-09	Prism	High Humidity

¹Prism = Prism mode ($R \sim 100$); SXD = Short Cross-Dispersed mode ($R \sim 1000$)

²Weather conditions at the time of observation

Table C.3: Pleiades Follow-Up Observations

ID	Date	Mode ¹	Weather ²
063	Aug-08	SXD	Clear
064	Aug-08	SXD	Clear
065	Aug-08	SXD	Clear
066	Aug-08	SXD	Clear
067	Aug-08	SXD	Clear
068	Aug-08	SXD	Clear
069	Aug-08	SXD	Clear
070	Aug-08	SXD	Clear
082	Jan-09	SXD	Clear
084	Jan-09	Prism	High Humidity
085	Jan-09	SXD	High Humidity
086	Jan-09	Prism	High Humidity
087	Jan-09	SXD	High Humidity
088	Jan-09	SXD	Clear
089	Jan-09	SXD	Clear
090	Jan-09	Prism	Clear
174	Nov-09	SXD	Clear
175	Nov-09	Prism	Clear
176	Nov-09	SXD	Clear
177	Nov-09	Prism	Clear
178	Nov-09	SXD	Clear
179	Nov-09	SXD	Clear
180	Nov-09	SXD	Clear
181	Nov-09	Prism	Clear
182	Nov-09	SXD	Clear
183	Nov-09	Prism	Clear

Table C.3 (cont'd)

ID	Date	Mode ¹	Weather ²
----	------	-------------------	----------------------

¹Prism = Prism mode ($R \sim 100$); SXD = Short Cross-Dispersed mode ($R \sim 1000$)

²Weather conditions at the time of observation

References

- Adams, J. D., Stauffer, J. R., Skrutskie, M. F., Monet, D. G., Zwart, S. F. P. et al. 2002, *AJ*, 124, 1570
- Allers, K. N., Jaffe, D. T., Luhman, K. L., Liu, M. C., Wilson, J. C. et al. 2007, *ApJ*, 657, 511
- Béjar, V. J. S. 2000, PhD Thesis, Universidad de La Laguna
- Baraffe, I., Chabrier, G., Allard, F., & Hauschildt, P. H. 1998, *A&A*, 337, 403
- Bate, M. R. 2009, *MNRAS*, 392, 590
- Bertout, C. & Genova, F. 2006, *A&A*, 460, 499
- Bihain, G., Rebolo, R., Béjar, V. J. S., et al. 2005, *AN*, 326, 1057
- Bihain, G., Rebolo, R., Béjar, V. J. S., Caballero, J. A., Bailer-Jones, C. A. L. et al. 2006, *A&A*, 458, 805
- Bonnell, I. A., Clark, P., & Bate, M. R. 2008, *MNRAS*, 389, 1556
- Boudreault, S. & Bailer-Jones, C. A. L. 2009, *ApJ*, 706, 1484
- Boudreault, S., Bailer-Jones, C. A. L., Goldman, B., Henning, T., & Caballero, J. A. 2010, *A&A*, 510, 27B
- Bouy, H., Moraux, E., Bouvier, J., Brandner, W., Martín, E. L. et al. 2006, *ApJ*, 637, 1056
- Briceño, C., Luhman, K. L., Hartmann, L., Stauffer, J. R., & Kirkpatrick, J. D. 2002, *ApJ*, 580, 317
- Casewell, S. L., Dobbie, P. D., Hodgkin, S. T., Moraux, E., Jameson, R. F., et al. 2007, *MNRAS*, 378, 1131
- Chabrier, G., Baraffe, I., Allard, F., & Hauschildt, P. 2000, *ApJ*, 542, 464

Chabrier, G. 2003, PASP, 115, 763

Chappelle, R. J., Pinfield, D. J., Steele, I. A., Dobbie, P. D., & Magazzu, A. 2005, MNRAS, 361, 1323

Cruz, K. L., Reid, I. N., Kirkpatrick, J. D., Burgasser, A. J., Liebert, J., Solomon, A. R., Schmidt, S. J., Allen, P. R., Hawley, S. L., & Covey, K. R. 2007, AJ, 133, 439

Cushing, M. C., Vacca, W. D., & Rayner, J. T. 2004, PASP, 116, 362

Findeisen, K. & Hillenbrand, L. 2010, AJ, 139, 1338

Fitzpatrick, E. L. 1985, ApJ, 299, 219

González-García, B. M., Zapatero Osorio, M. R., Bejár, V. J. S., Bihain, G., Barrado y Navascués, D. et al. 2006, A&A, 460, 799

Guieu, S., Dougados, C., Monin J.-L., Magnier, E., & Martín E. L. 2006, A&A, 446, 485

Hambly, N. C., Hawkins, M. R. S., & Jameson, R. F. 1993, A&AS, 100, 607

Hambly, N. C., Steele, I. A., Hawkins, M. R. S., & Jameson, R. F. 1995, A&AS, 109, 29

Hartmann, L., Jones, B. F., Stauffer, J. R., & Kenyon, S. J. 1991, AJ, 101, 1050

Jones, B. F. & Herbig, G. H. 1979, AJ, 84, 1872

Jones, B. F. & Stauffer, J. R. 1991, AJ, 102, 1080

Kaiser, N., Tonry, J. L., & Luppino, G. A. 2000, PASP, 112, 768

Kaiser, N., Burgett, W., Chambers, K., Denneau, L., Jedicke, R. et al. 2010, SPIE, 7733, 77330E

Kirkpatrick, J. D. 2005, ARAA, 43, 6.1

Klein Wassink, W. J. 1927, Publ. Kapteyn Astron. Lab. Groningen, No. 41

Kraus, A. L. & Hillenbrand, L. A. 2007, AJ, 134, 2340

Kraus, A. L. & Hillenbrand, L. A. 2009, ApJ, 704, 531

Kroupa, P. 2001, MNRAS, 322, 231

- Lodieu, N., Dobbie, P. D., Deacon, N. R., Hodgkin, S. T., Hambly, N. C. et al. 2007, MNRAS, 380, 712
- Loinard, L., Mioduszewski, A. J., Rodriguez, L. F., Gonzalez, R. A., Rodriguez, M. I., & Torres, R. M. 2005, ApJ, 619, L179
- Luhman, K. L., Stauffer, J. R., Muench, A. A., Rieke, G. H., Lada, E. A. et al. 2003, ApJ, 593, 1093
- Luhman, K. L. 2004, ApJ, 617, 1216
- Luhman, K. L. 2006a, ApJ, 645, 676
- Luhman, K. L., Whitney, B. A., Meade, M. R., Babler, B. L., Indebetouw, R. et al. 2006, ApJ, 647, 1180
- Luhman, K. L., Mamajek, E. E., Allen, P. R., & Cruz, K. L. 2009, ApJ, 703, 399
- Luhman, K. L. & Mamejek, E. E. 2010, ApJ, 716, L120
- Magnier, E. A., & Cuillandre, J.-C. 2004, PASP, 166, 449
- Magnier, E., Kaiser, N., & Chambers, K. 2006, *Adv. Maui Optical & Space Surveillance Technologies Conf.*
- Martín, E. L., Douglas, C., Magnier, E., Ménard, F., Magazzù, A., Cuillandre, J.-C., & Delefosse, X. 2001, ApJ, 561, L195
- Moraux, E., Bouvier, J., Stauffer, J. R., & Cuillandre, J.-C. 2003, A&A, 400, 891
- Moraux, E. & Clarke, C. 2005, A&A, 429, 895
- Muzerolle, J., Luhman, K. L., Briceño, C., Hartmann, L., & Calvet, N. 2005, ApJ, 625, 906
- Pickles, A. J. 1998, PASP, 110, 863
- Quanz, S. P., Goldman, B., Henning, T., Bradner, W., Burrows, A. et al. 2010, ApJ, 708, 770
- Rayner, J. T., Toomey, D. W., Onaka, P. M., Denault, A. J., Stahlberger, W. E. et al. 2003, PASP, 115, 362
- Rayner, J. T., Cushing, M. C., & Vacca, W. D. 2009, ApJS, 185, 289

- Rebull, L. M., Padgett, D. L., McCabe, C.-E., Hillenbrand, L. A., Stapelfeldt, K. R. et al. 2010, ApJS, 186, 259
- Reipurth, B. & Clarke, C. 2001, AJ, 122, 432
- Robin, A. C., Reyl , C., Derri re, S., Picaud, S. 2003, A&A, 409, 523
- Rowles, J. & Froebirch, D. 2009, MNRAS, 395, 1640
- Salpeter, E. E. 1955, ApJ, 121, 161
- Scelsi, L., Sacco, G., Affer, L., Argiroffi, Pillitteri, I. et al. 2008, A&A, 490, 601
- Schlegel, D. J., Finkbeiner, D. P., & Davis, M. 1998, ApJ, 500, 525
- Sestito, P., Palla, F., & Randich, S. 2008, A&A, 487, 965
- Shenoy, S. S., Whittet, D. C. B., Ives, J. A., & Watson, D. M. 2008, ApJSS, 176, 457
- Slesnick, C. L., Hillenbrand, L. A., & Carpenter, J. M. 2004, ApJ, 610, 1045
- Slesnick, C. L., Carpenter, J. M., Hillenbrand, L. A., & Mamajek, E. E. 2006, AJ, 132, 2665
- Stamatellos, D., Hubber, D. A., & Whitworth, A. P. 2007, MNRAS, 382, L30
- Thies, I. & Kroupa, P. 2007, ApJ, 671, 767
- Vacca, W. D., Cushing, M. C., & Rayner, J. T. 2003, PASP, 115, 389
- van Leeuwen, F. 2009, A&A, 497, 209
- Wichmann, R., Torres, G., Melo, C. H. F., Frink, S., Allain, S. et al. 2000, A&A, 359, 181